

BORON IN DISGUISE: TOWARDS BN BIOMIMICS

by

ERIC RYAN ABBEY

A DISSERTATION

Presented to the Department of Chemistry  
and the Graduate School of the University of Oregon  
in partial fulfillment of the requirements  
for the degree of  
Doctor of Philosophy

September 2011

## DISSERTATION APPROVAL PAGE

Student: Eric Ryan Abbey

Title: Boron in Disguise: Towards BN Biomimics

This dissertation has been accepted and approved in partial fulfillment of the requirements for the Doctor of Philosophy degree in the Department of Chemistry by:

Professor Kenneth M. Doxsee	Chair
Professor Shih-Yuan Liu	Advisor
Professor Victoria J. DeRose	Member
Professor Michael M. Haley	Member
Professor Janis Weeks	Outside Member

and

Kimberly Andrews Espy	Vice President for Research & Innovation/Dean of the Graduate School
-----------------------	---

Original approval signatures are on file with the University of Oregon Graduate School

Degree awarded September 2011

© 2011 Eric Ryan Abbey

## DISSERTATION ABSTRACT

Eric R. Abbey

Doctor of Philosophy

Department of Chemistry

September 2011

Title: Boron in Disguise: Towards BN Biomimics

Approved: \_\_\_\_\_  
Professor Shih-Yuan Liu

Chemists have long recognized the potential of the BN bond to mimic CC double bonds in aromatic systems. Phenyl and indole are two of the most important arenes in natural systems, as well as medicine, applied chemistry, and materials science. Despite the potential of BN arenes as phenyl and indole mimics in biomolecules, few isoelectronic and isostructural BN biomolecules have been synthesized. Substitution of BN for C=C imparts tunability to aromatic systems, giving new and potentially valuable properties to the resulting molecules. Our group has sought to expand the utility of BN arenes by developing the synthetic arsenal available to chemists seeking to incorporate the BN bond into biological and other organic molecules of importance.

The scope of this dissertation is twofold: 1) development of the first “fused” BN indole, including a survey of its reactivity towards electrophiles, synthesis of the parent N-H compound with complete characterization, and a comparison to natural indole and 2) expansion of the synthetic methodologies for constructing 1,2-dihydro-1,2-azaborine derivatives, including complete structural characterization of a family of “pre-aromatic”

and aromatic compounds and a protection-free synthesis of azaborines. The contributions outlined in this dissertation expand both the fundamental understanding of BN isosterism in aromatic molecules and the synthetic toolbox for chemists seeking to incorporate BN arenes into biological and other organic motifs. This dissertation includes previously published and unpublished coauthored material.

## CURRICULUM VITAE

NAME OF AUTHOR: Eric Ryan Abbey

### GRADUATE AND UNDERGRADUATE SCHOOLS ATTENDED:

University of Oregon, Eugene, OR  
Whitman College, Walla Walla, WA

### DEGREES AWARDED

Doctor of Philosophy in Chemistry, September 2011, University of Oregon  
Master of Science in Chemistry, June 2007, University of Oregon  
Bachelor of Arts, May, 2002, Whitman College

### AREAS OF SPECIAL INTEREST:

Synthetic Organic Chemistry  
Airfree Transformations

### PROFESSIONAL EXPREIENCE:

Research Assistant, University of Oregon, 2005-2011

Laboratory Technician, Hewlett Packard, 2002-2005

Research Assistant, Whitman College, 2000-2002

### GRANTS, AWARDS, AND HONORS:

National Science Foundation IGERT Fellow 2010-2011

National Science Foundation GK-12 Fellow 2008-2010

### PUBLICATIONS:

**Abbey, E. R.**; Zakharov, L. N.; Liu, S. -Y. "Boron in Disguise: the Parent "Fused" BN Indole *manuscript submitted*.

Campbell, P. G; **Abbey, E. R.**; Neiner, D.; Grant, D. J.; Dixon, D. A.; Liu, S.-Y. "Resonance Stabilization Energy of 1,2-Azaborines: A Quantitative Experimental

Study by Reaction Calorimetry.” *J. Am. Chem. Soc.* **2010**, *132*, 18048-1805.

**Abbey, E. R.**; Zakharov, L. N.; Liu, S.-Y. “Electrophilic Aromatic Substitution Reactions of a BN Indole.” *J. Am. Chem. Soc.* **2010**, *132*, 16340-16342.

- Featured in *Chemical and Engineering News*, “Science and Technology Concentrates” section, **2010**, *88*, 36.

**Abbey, E. R.**; Zakharov, L. N.; Liu, S.-Y. “Crystal Clear Structural Evidence for Electron Delocalization in 1,2-Dihydro-1,2-azaborines.” *J. Am. Chem. Soc.* **2008**, *130*, 7250-7252.

- Featured in *Chemical and Engineering News*, “News of the Week” section, **2008**, *86*, 12.

Marwitz, J. V.; **Abbey, E. R.**; Jenkins, J. T.; Zakharov, L. N.; Liu, S.-Y. “Diversity through Isosterism: the Case of Boron-Substituted 1,2-Dihydro-1,2-azaborines.” *Org. Lett.* **2007**, *9*, 4905-4908.

## ACKNOWLEDGEMENTS

I would like to sincerely thank my research advisor Professor Shih-Yuan Liu for his guidance over the past five years. I would also like to thank my committee member Professor Victoria DeRose for advice and mentorship. Thank you to my committee member Professor Mike Haley for guidance, and to my committee chair Professor Kenneth Doxsee for interesting questions and input. I would also like to acknowledge my outside committee member Professor Janis Weeks. Thanks to Professors Darren Johnson, David Tyler, and Jim Hutchison for hosting me during my rotations, and to Professor John Keana for valuable discussions and input. Thank you Professor Deborah Exton for career advice. Dr. Lev Zakharov and Dr. Mike Strain provided invaluable instrumentation support. I would like to thank Dr. Adam Marwitz for his early mentorship and camaraderie in our nascent project. Dr. Adam Glass, Patrick Campbell and Ashley Lamm provided great insight and collaboration in the lab and were great friends to have. Ben Morris, Jesse Jenkins, and Sam Klonoski, all contributed to this research project. Thanks to Calden Carroll for friendship and fluorimetry, and Chris Weber for CV measurements. I would like to thank my parents Rick and Nancy for their love and support and for instilling curiosity and drive. Thanks to my brother and best friend Lucas for countless adventures. I would like to thank all of my other great friends in life, too many to enumerate, for love, inspiration, and support. Thank you to the National Science Foundation GK-12 and IGERT programs for three years of financial support.

To my loving family, for their unwavering support

## TABLE OF CONTENTS

Chapter		Page
I.	INTRODUCTION: ELEMENTAL ISOSTERISM AND BN INDOLES	
	1.1. Introduction.....	1
	1.2. Early Explorations of 1,3,2-Diazaborole Chemistry.....	3
	1.3. Functionalization at Nitrogen .....	7
	1.4. Functionalization at Boron.....	8
	1.5. Development of Boryl Ligands for Organometallic Chemistry .....	11
	1.6. Benzodiazaboroles as Optoelectronic Materials.....	13
	1.7. Conclusion .....	16
	1.8 Bridge to Chapter II .....	17
II	STRUCTURAL EVIDENCE FOR ELECTRON DELOCALIZATION IN 1,2-DIHYDRO-1,2-AZABORINES	
	2.1. General Overview .....	18
	2.2. Introduction.....	18
	2.3. Synthesis and Characterization of Reference Compounds.....	21
	2.4. Conclusion .....	27
	2.5 Bridge to Chapter III.....	27
III.	PROTECTION-FREE 1,2-AZABORINE SYNTHESIS	
	3.1. General Overview .....	30
	3.2. Introduction.....	30
	3.3. Synthesis and Characterization of a New 1,2-Dihydro-1,2-Azaborine Synthon.....	31

Chapter		Page
	3.4. Conclusion .....	34
	3.5. Bridge to Chapter IV.....	35
<b>IV</b>	<b>ELECTROPHILLIC AROMATIC SUBSTITUTION OF A BN INDOLE</b>	
	4.1. General Overview .....	36
	4.2. Introduction.....	36
	4.3. Synthesis and Reactivity Studies on “Fused” BN Indole.....	37
	4.4. Conclusion .....	43
	4.5. Bridge to Chapter V .....	44
<b>V.</b>	<b>BORON IN DISGUISE: THE PARENT “FUSED” BN INDOLE</b>	
	5.1. General Overview .....	45
	5.2 Introduction.....	45
	5.3. Synthesis and Characterization of the Parent “Fused” BN Indole.....	47
	5.4. Conclusion .....	53
<b>APPENDICES</b>		
A:	SUPPORTING INFORMATION FOR CHAPTER II .....	54
B:	SUPPORTING INFORMATION FOR CHAPTER III .....	130
C:	SUPPORTING INFORMATION FOR CHAPTER IV .....	138
D:	SUPPORTING INFORMATION FOR CHAPTER V .....	170
	REFERENCES CITED.....	211

## LIST OF FIGURES

Figure	Page
1.1. Isoelectronic and isostructural relationship between BN and CC bonds .....	1
1.2. Organic indole vs. BN indoles .....	2
1.3. X-ray crystal structure of benzodiazaboryllithium complex ....	11
2.1. Strategy for determining electron delocalization in 1,2-azaborines: direct structural comparison .....	21
2.2. ORTEP illustrations, with thermal ellipsoids drawn at the 35% probability level, of heterocycles <b>1-5</b> .....	26
3.1. Previous 1,2-azaborine synthons and the parent 1,2-azaborine..	32
4.1. A novel biomimetic BN indole .....	39
4.2. ORTEP illustrations, with thermal ellipsoids drawn at the 35% probability level, of <b>7</b> and <b>6e</b> .....	44
5.1. Indole, “external” and “fused” BN indoles.....	49
5.2. CV Measurements of BN indole <b>3a</b> and indole <b>1a</b> (0.8 M TBAOTf in CH <sub>3</sub> CN at glassy carbon electrode).....	53
5.3. Optical Data for <b>3a</b> and <b>1a</b> .....	54

## LIST OF TABLES

Table	Page
2.1. Selected bond distances and deviations from planarity (Å) for BN-heterocycles <b>1-5</b> .....	27
4.1. EAS reactions of <b>2</b> .....	42
5.1. Bond lengths of <b>3c•Fnap</b> , <b>3a•Ar</b> , and <b>1a•Pic</b> .....	52
5.2. pK <sub>a</sub> Bracketing experiment for <b>3a</b> .....	55

## LIST OF SCHEMES

Scheme	Page
1.1. General strategy for benzodiazaborole construction, and the first examples.....	4
1.2. Early studies of benzodiazaboroles by Letsinger.....	5
1.3. Early routes to benzodiazaboroles .....	6
1.4. Functionalization at nitrogen .....	7
1.5. Boron functionalization before heterocycle formation .....	8
1.6. Boron functionalization after heterocycle formation .....	9
1.7. Synthesis of benzodiazaboryl lithium <b>35</b> .....	10
1.8. Oxidative addition of a BBr bond to platinum complex <b>38</b> .....	12
1.9. Hydroboration (1), cycanoboration (2), and carboboration (3) using benzodiazaboroles .....	12
1.10. Synthesis of boryl iridium pincer complex <b>47</b> .....	13
1.11. Benzodiazaborole-containing fluorophores prepared by Weber et al.....	14
1.12. Synthesis of chromophores from phenylenediboronic acids ....	15
1.13. Synthesis of benzodiazaborole cavitand <b>54</b> .....	16
2.1. Synthesis of diene precursor <b>1</b> .....	22
2.2. Catalytic transformations of <b>1</b> .....	24
Scheme	Page

3.1. Synthesis of synthon <b>5</b> .....	33
3.2. Dewar's near miss.....	34
3.3. Derivatization of synthon <b>5</b> .....	36
4.1. Synthesis of <i>N-t</i> -Bu-BN-indole <b>2</b> .....	39
4.2. Regioselectivity in EAS reactions of <i>N-t</i> -Bu-BN-indole <b>2</b> .....	41
4.3. EAS competition experiment with dimethyliminium chloride as the electrophile.....	45
5.1. Synthesis of <b>3a</b> .....	51

# CHAPTER I

## INTRODUCTION: ELEMENTAL ISOSTERISM AND BN INDOLES

### 1.1. Introduction

BN/CC elemental isosterism is emerging as a strategy for altering the properties of classic organic motifs with minimal disruption to the shape of the structure being mimicked. The past half century has witnessed a slow but continuous development of isoelectronic BN analogs of CC bonds found in  $sp^3$ ,  $sp^2$  olefin, and  $sp^2$  aromatic skeletons, with renewed attention in the past two decades.<sup>1</sup> Of particular interest to our lab are the phenyl mimics, the 1,2-dihydro-1,2-azaborines (from now on abbreviated as 1,2-azaborines) and derivatives thereof (Figure 1.1). 1,2-Azaborines are phenyl analogs in which a C=C bond has been replaced by an isoelectronic BN bond, where the nitrogen lone pair donates into the empty  $p$  orbital of boron. Marwitz has extensively reviewed the chemistry of 1,2-azaborines,<sup>2</sup> which will not be discussed further in this section, except in their role as a mimic of the phenyl fragment contained in a newly developed class of indole mimics, the “fused” BN indoles.

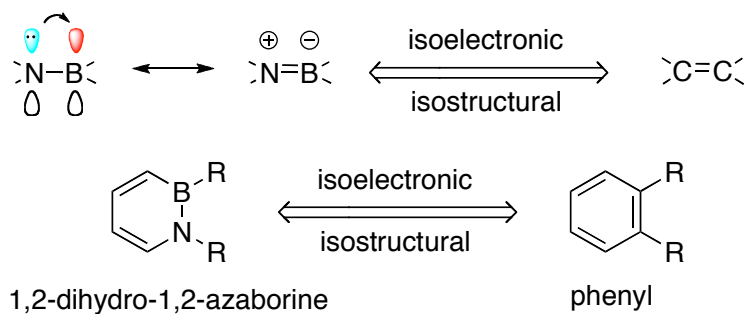


**Figure 1.1.** Isoelectronic and isostructural relationship between BN and CC bonds.

Indole (i.e., benzopyrrole) consists of a pyrrole ring fused to a phenyl ring, resulting in a  $10\pi$ -aromatic system in which the nitrogen lone pair is delocalized into the bicyclic ring current (Figure 1.2). To date, two classes of BN-substituted indoles have been synthesized. The “external” BN indoles, more commonly known as 1,3,2-benzodiazaboroles (from now on abbreviated as benzodiazaboroles), are bicyclic aromatic heterocycles in which a BN pyrrole (better known as a 1,3,2-diazaborole) is fused to a benzene ring. Benzodiazaboroles were first reported by Goubeau in 1957<sup>3</sup> and are the first example of a CBN arene. The second class of BN indoles is the recently reported “fused” BN indoles, first synthesized by our lab in 2010.<sup>4</sup>

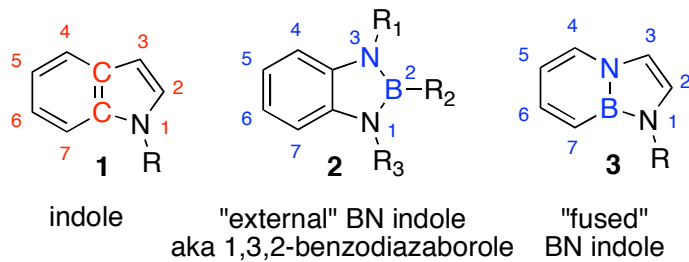


**Figure 1.2.** Organic indole vs. BN indoles.

Indole is one of the most ubiquitous heterocycles in biology and medicine. Indole-based molecular systems have been incorporated into traditional and fluorescent dyes, opto-electronics, and hydrogen storage materials. “The synthesis and functionalization of indoles has been the object of research for over 100 years.”<sup>5</sup> Not surprisingly, chemists have pursued BN indoles as an avenue for expanding the chemical space of indole-based structures through “elemental isosterism.” Generally speaking, CBN aromatics have similar structural features to their CC analogs, with altered and sometimes tunable properties. Our lab has initiated a program to develop the synthesis and functionalization

of monocyclic 1,2-azaborines as described by Marwitz, and use the 1,2-azaborine core as the basis of for a new BN indole analog, the “fused” BN indole. Before describing our work on 1,2-azaborines and “fused” BN indoles in later chapters, the remainder of Chapter I will be devoted to a tutorial review of “external” BN-substituted indoles, or benzodiazaboroles as they are referred to in the literature. The great body of work concerning CBN arenes other than BN indoles is beyond the scope of this introduction. Furthermore, polycyclic aromatic compounds containing a BN indole motif, as well as polymeric materials containing this structure will not be discussed in this work.

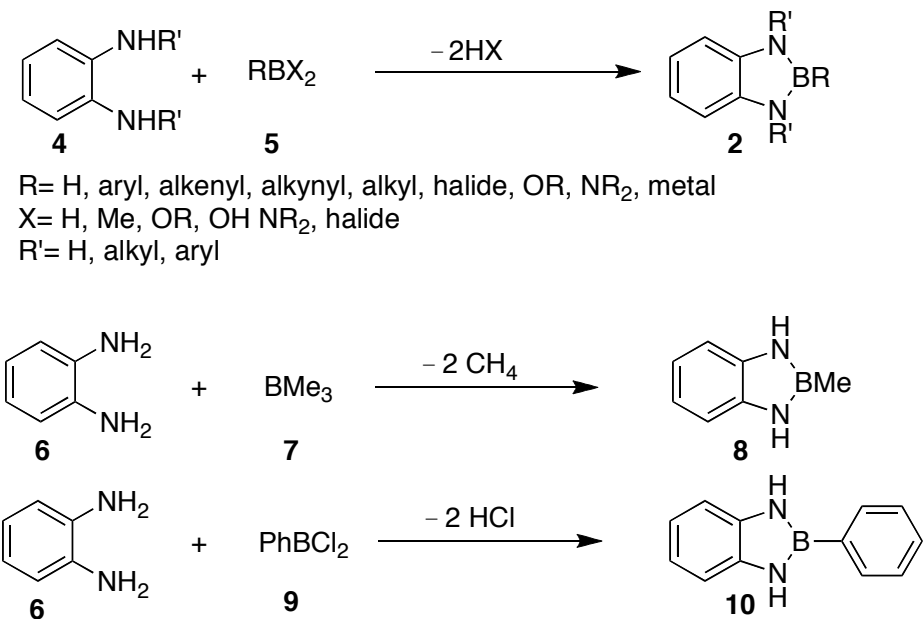
The past two decades have witnessed a resurgence in the chemistry of benzodiazaboroles. The early contributions to the chemistry of benzodiazaboroles will first be reviewed, followed by sections devoted an exploration of the common methods of synthesis and functionalization of these heterocycles, and finally a review of the modern applications. The applications can be divided into two categories: 1) development of boryl ligands for organometallic chemistry and 2) exploration of the optical properties of derivatives of **2**.

## 1.2. Early Explorations of 1,3,2-Diazaborole Chemistry

Almost every synthesis of benzodiazaboroles proceeds by condensation of a 1,2-phenylenediamine **4** with a borane **5**, including the initial synthesis by Goubeau<sup>3</sup>. Reaction of phenylenediamine with trimethylborane provided the first benzodiazaborole **8**, the B-Me derivative in 60% yield (Scheme 1.1).

A year later, Dewar reported the synthesis of the *B*-Ph derivative **10** by condensing 1,2-phenylenediamine **6** with phenylboron dichloride **9** (*R*= Ph, *X*=Cl.)

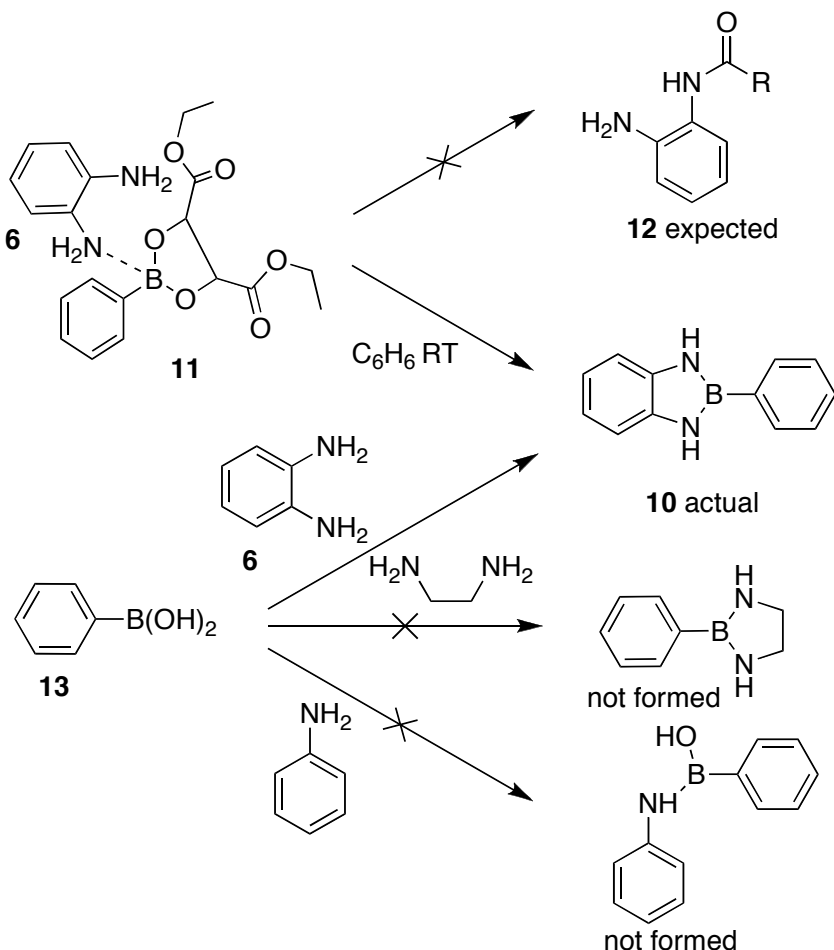
Dewar was one of the first to recognize the potential of elemental isosterism as a means to access new aromatic heterocycles. In the same report, BN isosteres of benzofuran and benzothiophene were synthesized in a similar manner.<sup>6</sup>



**Scheme 1.1.** General strategy for benzodiazaborole construction, and the first examples.

Soloway prepared a variety of derivatives by condensing aryl and alkylboronic acids **5** (R=alkyl, aryl X=OMe, Scheme 1.1) with substituted 1,2-phenylenediamines **4** in refluxing xylenes. Even then, the potential of BN derivatives of natural arenes was recognized. Soloway stated: “the preparation of a boron-containing purine antimetabolite might extend this (cancer) treatment to other neoplasms.”<sup>7</sup> Letsinger accidentally prepared the same BPh benzodiazaborole in an attempt to accelerate amide formation using a BPh tartrate **11** and phenylenediamine **6** (Scheme 1.2).<sup>8</sup> Probing the reaction further, they noted that attempts to form BN bonds from phenylboronic acid **13** and either ethylenediamine or aniline did not yield the expected BN compound at high

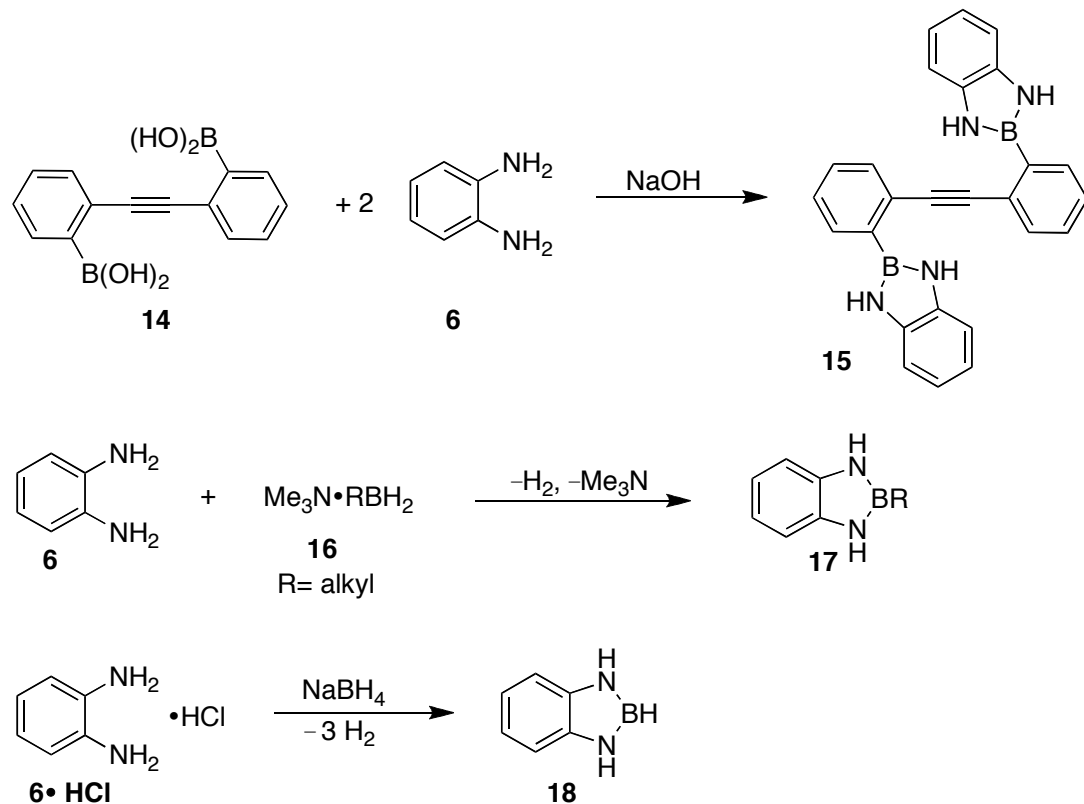
temperatures, whereas the reaction with phenylenediamine proceeds even at room temperature. They conclude that the “unusual reactivity of phenylenediamine is related to its particular geometry and the stability of the ring system which is formed.” This is one of the earliest observations of the aromatic stabilization in CBN arenes. Letsinger used this observation as a way to characterize boronic acids in further work, by preparing stable derivatives of sensitive boronic acids such as **14** (Scheme 1.3).<sup>9</sup> This led to the first example of a conjugated polycyclic BN indole **15** connected by a phenylethyynyl linkage, a common motif utilized in optical materials.



**Scheme 1.2.** Early studies of benzodiazaboroles by Letsinger.

Because of the inexact characterization methods (IR, and elemental analysis) of the time, Hawthorne sought to prepare these compounds via a different route to make sure there had been no rearrangement of substitutents. In 1960, he demonstrated the synthesis of alkyl benzodiazaboroles **17** from phenylenediamine **6** and trimethylaminealkylboranes **16** (Scheme 1.3), releasing H<sub>2</sub> and trimethylamine.<sup>10</sup>

The parent benzodiazaborole **18** was synthesized by Goubeau in 1964 by condensation of phenylenediamine hydrochloride **6•HCl** with sodium borohydride<sup>11</sup> (Scheme 1.3). Many other examples of benzodiazaboroles with various boron and nitrogen substituents were synthesized using the strategy of condensing a phenylenediamine **4** with a substituted borane **5**.

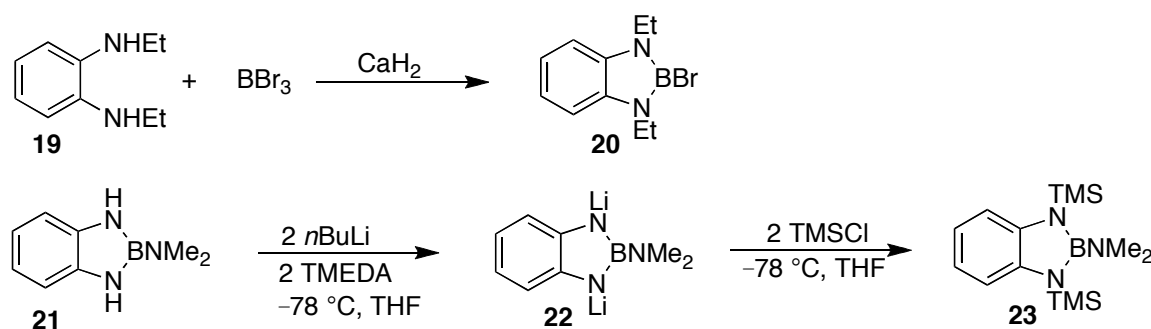


**Scheme 1.3.** Early routes to benzodiazaboroles.

A lull in the development of benzodiazaboroles occurred from the late 1960's until the late 1980's, when interest was renewed in these compounds. With the early contributions outlined, this introduction will now focus on general strategies of functionalization of benzodiazaboroles, with noteworthy examples being provided

### 1.3. Functionalization at Nitrogen

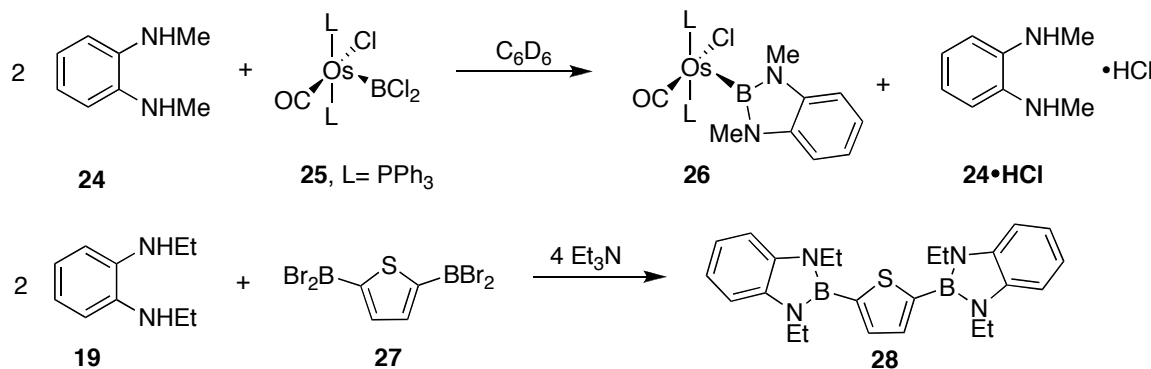
Two primary strategies for functionalization at nitrogen are utilized: 1) begin with an *N*-substituted *o*-phenylenediamine, such as the diethyl *o*-phenylenediamine **19** used in the synthesis of **20**<sup>12</sup> (Scheme 1.4). This seems to be the preferred method, as it avoids the use of harsh conditions on sensitive boron-containing structures. 2) functionalize nitrogen after condensation with boron, such as the lithiation/silylation sequence employed in the synthesis of **23**<sup>13</sup> (Scheme 1.4). The second strategy is viable if the transformations are compatible with the BN motif, and is employed if the nitrogen substituent is not compatible with the Lewis acidic borane being used.



**Scheme 1.4.** Functionalization at nitrogen.

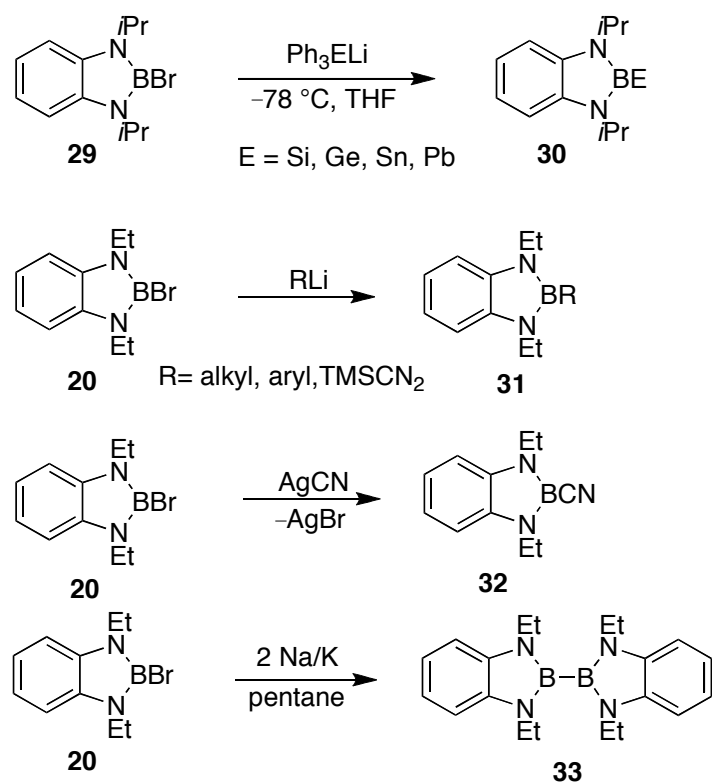
## 1.4. Functionalization at Boron

More attention has been given to boron functionalization, perhaps because this is where the unique properties of benzodiazaboroles are derived from. The strategies available for boron functionalization are similar to those for used for substitution at nitrogen: either functionalize before heterocycle formation, or after. A variety of monofunctional boranes **5** can be condensed with phenylenediamines **4**, provided they have compatible leaving groups, which include halides, amides, alkoxides, hydroxides and even methyl groups. Boranes can be functionalized with aryl, alkyl, alkenyl, alkynyl, and metallo groups, or one of the aforementioned leaving groups for further functionalization. One interesting example is the condensation of the *N,N'*-dimethylphenylenediamine **24** with the boryl osmium complex **25** to afford the osmium-bound benzodiazaborole **26**<sup>14</sup> (Scheme 1.5). A bis-substituted thiophene **28** derivative can be synthesized from the bis-dibromoborylthiophene **27** with *N,N'*-diethylphenylenediamine **19** in the presence of triethylamine.



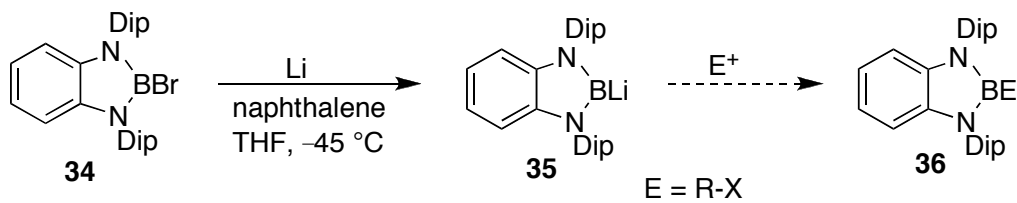
**Scheme 1.5.** Boron functionalization before heterocycle formation.

Boron substitution after heterocycle formation is also a widely used strategy. With a labile group such as bromide on benzodiazaborole **20**, nucleophiles such as group 14<sup>15</sup> and carbon-based<sup>16</sup> lithiates and can be added to boron (Scheme 1.6). If the leaving group on boron is a halide, silver-based nucleophiles like silver cyanide<sup>12</sup> are useful for creating cyanide-substituted heterocycles **32**. Additionally, bromide substituted benzodiazaboroles **20** can be reduced with alkali metals such as Na/K<sup>12</sup> to afford the diboryl species **33** (Scheme 1.6). Attempts to further reduce **33** to the anion with Na/K were unsuccessful.



**Scheme 1.6.** Boron functionalization after heterocycle formation.

The first boryllithiums **35** were created from diazaboroles and benzodiazaboroles,<sup>17</sup> which are capable of acting as boron nucleophiles (Scheme 1.7).



**Scheme 1.7.** Synthesis of benzodiazaboryl lithium **35**.

Boryl anions are currently a subject of great interest, due to their unusual electronic structure. All other first row lithiates (i.e., LiF, LiOR, LiNR<sub>2</sub>, LiCR<sub>3</sub>) have a complete octet, whereas boryl lithiates only have six valence electrons, making them isoelectronic with carbenes. The diazaboryl lithiates were found to have a similar polarity to alkyl lithiates, making them strong nucleophiles. Presumably, benzodiazaboryl lithiates will also react as in a similar fashion to diazaboryl lithiates, though this has not yet been reported. In addition to their theoretical novelty, stable boron nucleophiles have the potential to be extremely useful synthons for chemists. Boron moieties traditionally have electrophilic character, and rely on nucleophilic substitution for functionalization. Nucleophilic boron centers open the door to a much wider array of benzodiazaborole-containing structures.

The benzodiazaboryllithium complex **35•2 THF** containing two THF solvent molecules was characterized by X-ray crystallography (Figure 1.3). The structural characteristics of **35•2 THF** are very similar to an analogous carbene **37**, with almost identical bond angles at the nucleophilic center (NBN **35•2 THF** = 100.0(3)<sup>°</sup> vs. NCN **37** = 103.8(2)<sup>°</sup>) and an elongated BN bond (~0.1 Å) resulting from boron's larger atomic radius.

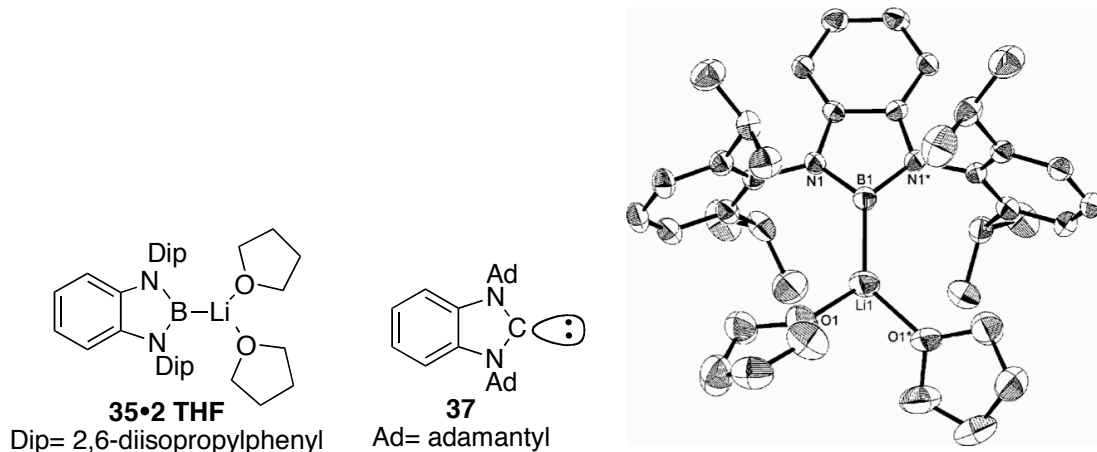
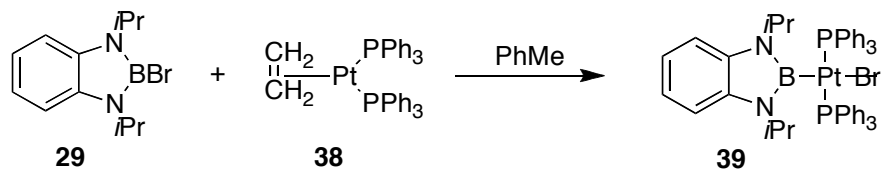


**Figure 1.3.** X-ray crystal structure of benzodiazaboryllithium complex.

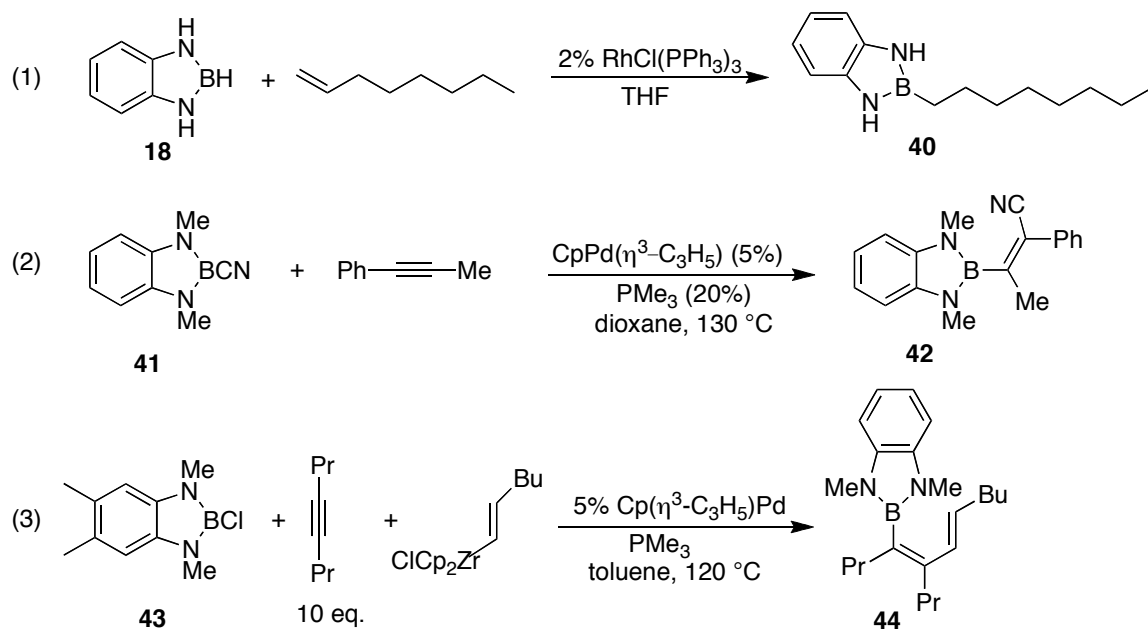
## 1.5. Development of Boryl Ligands for Organometallic Chemistry

The interactions of benzodiazaboroles with transition metals is a burgeoning field, with new ligands based on this scaffold currently under investigation. Construction of benzodiazaborole-metal complexes follows the aforementioned strategies for boron functionalization: form the B-M bond before heterocycle formation as in the synthesis of osmium complex **26** (Scheme 1.5), or more frequently, form the B-M bond from the benzodiazaborole with a labile group on boron, such as H, halo, or cyano ligands via oxidative addition, such as the addition of BBr benzodiazaborole **29** to platinum complex **38** (Scheme 1.8).<sup>15</sup>



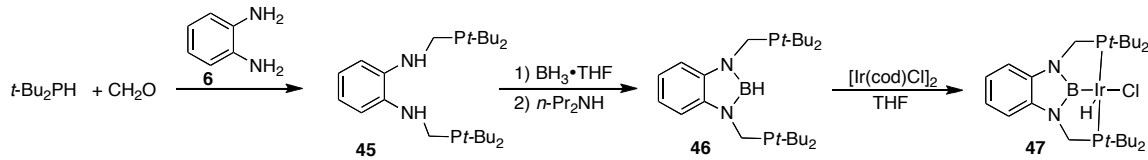
**Scheme 1.8.** Oxidative addition of a BBr bond to platinum complex **38**.

Boron-based ligands are strong  $\sigma$ -donors, with better electron-releasing character than the other first row elements (e.g. C, N, O, F). Organometallic transformations using benzodiazaboroles have mostly been limited to borylation-type reactions. Examples include hydroboration<sup>18</sup> (1) (Scheme 1.9), cyanoboration<sup>19</sup> (2), and carboboration<sup>20</sup> (3), in which the benzodiazaborole is a stoichiometric reagent forming a B-C bond via a transition metal catalyst. All of these examples require a catalyst, whereas many other boron-based reagents do not, which is perhaps a testament to the aromatic stabilization provided by the benzodiazaborole system.



**Scheme 1.9.** Hydroboration (1), cyanoboration (2), and carboboration (3) using benzodiazaboroles.

Just recently, the scope of organometallic chemistry involving benzodiazaboroles began to be broadened. Nozaki recently reported an iridium complex **47** using a tridentate PBP ligand **46** containing a benzodiazaborole core (Scheme 1.10). The authors speculate that “if the boryl ligand is stabilized and acts as a ‘supporting’ ligand, the strong electron-releasing property of the boryl ligand can be applied to functionalization reactions other than borylations.”<sup>21</sup> Complex **47** has a longer Ir-Cl bond than does the corresponding PCP complex, indicative of the stronger σ-donor ability of the boryl ligand compared to carbon. Such boryl complexes may soon begin to find broader application in organometallic chemistry due to their unique properties.

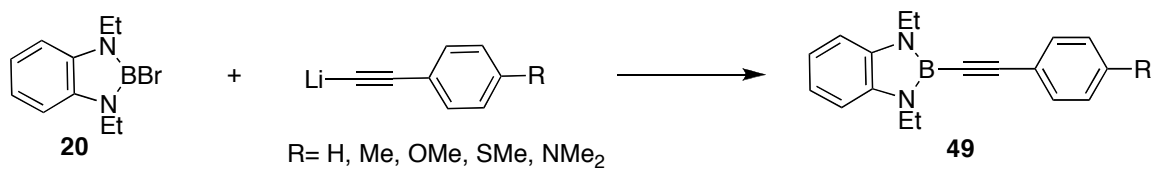
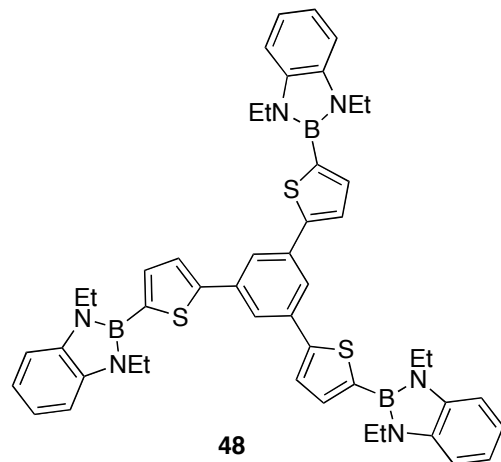


**Scheme 1.10.** Synthesis of boryl iridium pincer complex **47**.

## 1.6. Benzodiazaboroles as Optoelectronic Materials

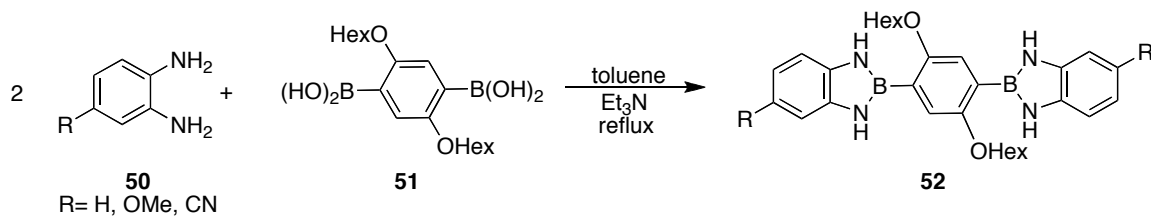
The vacant *p*-orbital of boron is known to participate in aromatic systems by accepting π-electrons from neighboring atoms. The resulting structures can have interesting consequences on charge transfer within conjugated systems. Benzodiazaboroles have received much recent attention as new building blocks for optical materials. By incorporating benzodiazaboroles into common conjugated structures

using the previously discussed functionalization strategies, Weber et al. were able to make blue fluorescent chromophores such as **48**. Such chromophores had good quantum yields, high extinction coefficients, second and third order non-linear optical properties and were all analyzed structurally by XRD<sup>22</sup> (Scheme 1.11). The authors report shorter B-C bond lengths for thiophene-substituted chromophores compared to phenylene spacers, resulting in better  $\pi$ -overlap, but the phenyl-based molecules had higher quantum yields. The same authors performed a similar study on arylethynyl systems containing benzodiazaboroles (Scheme 1.11). These compounds were all highly fluorescent, with quantum yields ranging from 0.89-0.99 in the violet-blue region, with the SMe derivative being the least fluorescent. In contrast to other systems with  $sp^2$  boron centers, such as  $-BAr_2$ , benzodiazaboroles appear to act as  $\pi$ -electron donors.<sup>23</sup>



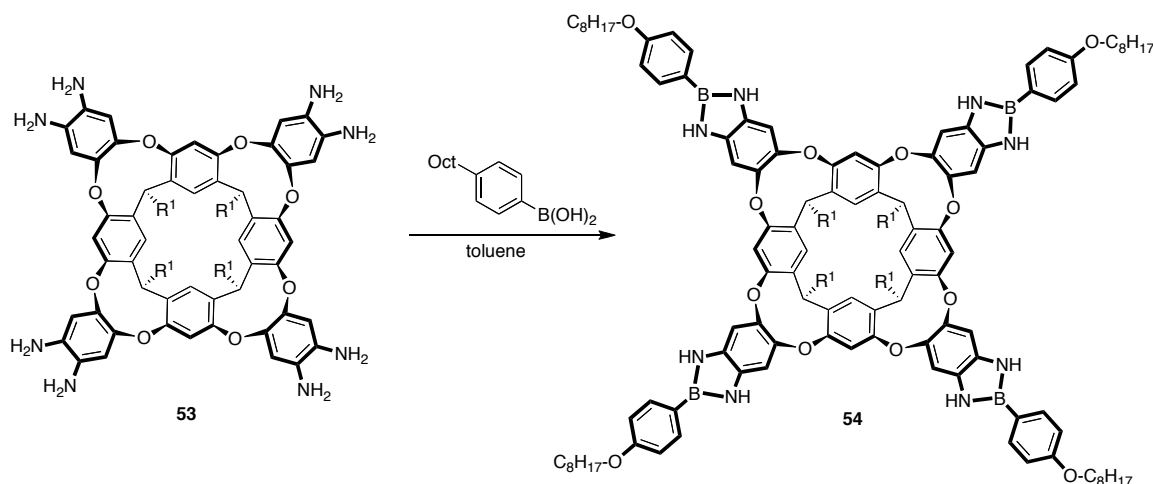
**Scheme 1.11.** Benzodiazaborole-containing fluorophores prepared by Weber et al.

Maruyama et al. reported similar compounds by condensing phenylenediboronic acids **51** with prefunctionalized phenylenediamines **50** to yield benzo-substituted benzodiazaboroles **52** linked by a phenylene spacer<sup>24</sup> (Scheme 1.12). The authors point out that benzodiazaboroles are well suited to application in optoelectronic materials because in contrast to many other boron-containing molecules, benzodiazaboroles are quite stable to air and water and are readily prepared. Like Weber's fluorophores, these compounds emit in the blue region and have high quantum yields ( $\phi = 0.66\text{--}0.99$ ).



**Scheme 1.12.** Synthesis of chromophores from phenylenediboronic acids.

One novel application of benzodiazaboroles that takes advantage of their optical properties is the construction of resorcin[4]arene cavitands **54** with benzodiazaborole walls (Scheme 1.13).<sup>25</sup> Encapsulation of a quaternary ammonium cationic guest causes a dramatic blue shift in the fluorescence emission of the capsule (from 404 to 357 nm), imparting sensing abilities to this assembly that differ from the normal Lewis base-sensing abilities usually associated with boron-containing compounds. The authors report association constants as high as  $K_a > 10^9 \text{ M}^{-1}$ . Given the abundance of desirable optical properties as well as facile assembly and stability, benzodiazaboroles may become a staple for chemists seeking to create new optoelectronic materials.



**Scheme 1.13.** Synthesis of benzodiazaborole cavitand **54**.

## 1.7. Conclusion

Benzodiazaboroles are a well-studied class of BN-substituted indole analogs with a rich history dating back to 1957. After roughly two decades of relative inactivity, these heterocycles are receiving renewed interest. Benzodiazaboroles have evolved from a chemical curiosity to a building block of optical materials and a ligand with unique properties that are just beginning to be unlocked. Despite their isolectronic and isostructural relationship to indoles, benzodiazaboroles bear only a cursory resemblance to indole. These heterocycles behave more like a stabilized chelated boron, which makes them useful for the aforementioned applications, but quite different from indole. Benzodiazaboroles lack a C=C bonds on the five-membered ring, and therefore cannot participate in electrophilic aromatic substitution (EAS) reactions. EAS reactions are a hallmark of indole chemistry, especially within biological systems. Benzodiazaboroles are more symmetric than indole, with two N-H functionalities instead of one. Despite the differences, they also share some similarities. Both systems are fluorescent in the same region of the spectrum, and both have a high degree of stabilization provided by

aromaticity. Chapters 4 and 5 of this manuscript will be devoted to our explorations of another BN indole isomer, the “fused” BN indoles. Complete characterization of these new indole analogs will be provided and evidence highlighting the similarities between “fused” BN indoles and natural indoles will be discussed

### **1.8. Bridge to Chapter II**

Chapters II-V of this dissertation contain co-authored material. Chapters II, IV, and V contain previously published material. With the history of BN indoles now reviewed, and the history of 1,2-azaborines review by Marwitz, the contributions I have made to both avenues will now be discussed. Chapters II and III will be devoted to 1,2-azaborine chemistry, and chapters IV and V will be devoted to “fused” BN indoles containing the 1,2-azaborine core. All five chapters have the unifying theme of understanding and developing BN isosterism of fundamental aromatic molecules. Chapter II is the first and most fundamental in nature. In this study, a family of aromatic and “pre-aromatic” 1,2-azaborine derivatives were synthesized and characterized by X-ray crystallography, illustrating the structural differences between aromatic rings and those that are merely conjugated.

# CHAPTER II

## STRUCTURAL EVIDENCE FOR ELECTRON DELOCALIZATION IN 1,2-DIHYDRO-1,2-AZABORINES

### **2.1. General Overview**

This chapter describes the synthesis and structural characterization of a family of aromatic and “pre-aromatic” 1,2-azaborine derivatives, showing with detail the structural changes that occur when a ring becomes aromatic. This chapter is based on previously published material: Abbey, E. R.; Zakharov, L. N.; Liu, S. -Y. *J. Am. Chem. Soc.* **2008**, *130*, 7250-7252. All of the lab work with the exception of X-ray crystallography (performed by Lev N. Zakharov) was performed by me. The manuscript was drafted by me. Professor Shih-Yuan Liu provided editorial assistance and scientific guidance for all material in this chapter.

### **2.2. Introduction**

The isolation and structural description of benzene marked the birth of the concept of aromaticity.<sup>1,2</sup> Since this important discovery more than a century ago, derivatives of benzene, i.e., arenes, have been playing a pivotal role not only in the field of chemistry but also in other scientific disciplines.<sup>3,4</sup> 1,2-Dihydro-1,2-azaborine (from now on abbreviated as 1,2-azaborine) is related to benzene by substitution of a single CC bond unit of benzene with an isoelectronic BN bond.<sup>5</sup>

Despite its seemingly simple structure, relatively little is known about this family of heterocycles compared to their isoelectronic analogues. Dewar<sup>6,7</sup> and White<sup>8</sup> pioneered

the chemistry of 1,2-azaborine and its ring-fused *polycyclic* derivatives in the 1960s.<sup>9</sup> Recent contributions by Ashe,<sup>10-17</sup> Piers,<sup>18-23</sup> and Paetzold<sup>24</sup> have facilitated the preparation of novel BN-heterocycles and sparked a renewed interest in these compounds. As part of a program directed toward the development and application of 1,2-azaborines as versatile arene surrogates, we recently addressed a limitation associated with existing synthetic methods for *monocyclic* 1,2-azaborines, i.e., the narrow scope with respect to the boron substituent, by presenting the first general solution for the synthesis of *B*-substituted 1,2-azaborines.<sup>25</sup>

Because of the similarity between 1,2-azaborine and the quintessential aromatic compound, benzene, the characterization of its aromaticity has been of substantial interest. In the past, assertions of aromaticity of 1,2-azaborines have heavily relied on computational studies.<sup>26-29</sup> Recent synthetic achievements have provided experimental data to supplement the theoretical calculations. For instance, Ashe has demonstrated that 1,2-azaborines can undergo electrophilic aromatic substitutions.<sup>16</sup> The <sup>1</sup>H NMR chemical shifts of 1,2-azaborines are consistent with the presence of aromatic ring current effects.<sup>9b</sup>

The geometrical structure of conjugated compounds (i.e., their bond length equalization due to delocalization) provides another crucial criteria of aromaticity.<sup>30</sup> For instance, geometry-based indices of aromaticity have been developed to quantify the extent of aromaticity in carbo- and heterocycles.<sup>31</sup> To date, only five X-ray crystal structures of non π-bound 1,2-azaborines have been reported.<sup>13,16,17,25</sup> All of these structures exhibit a planar geometry, with intra-ring C–C, C–B, C–N, and B–N bond lengths ranging from 1.35-1.41 Å, 1.50-1.53 Å, 1.37-1.39 Å, and 1.43-1.45 Å, respectively. While these bond distances are consistent with a delocalized picture of this

six-membered heterocycle, the lack of structural data of directly comparable reference compounds renders this description somewhat arbitrary and ambiguous. We envisioned that the synthesis of reference heterocycles **A-D** (Figure 1) and their direct structural comparison with the presumed delocalized structure **E** would provide an unambiguous picture of electron delocalization in 1,2-azaborines.

To the best of our knowledge, no structural data are currently available for monocyclic aminoboranes **A-D** illustrated in Figure 2.1.<sup>32</sup> Furthermore, there are no examples of heterocycles **C** and **D** in the literature. In this communication, we present the synthesis and structural characterization of a complete set of compounds described in Figure 2.1 (**A-E**; R<sup>1</sup>=*t*-Bu, R<sup>2</sup>=NPh<sub>2</sub>). Direct comparison of these structures unambiguously reveals localized bonding in heterocycles **A-D** and delocalized bond distances in the aromatic molecule **E**.

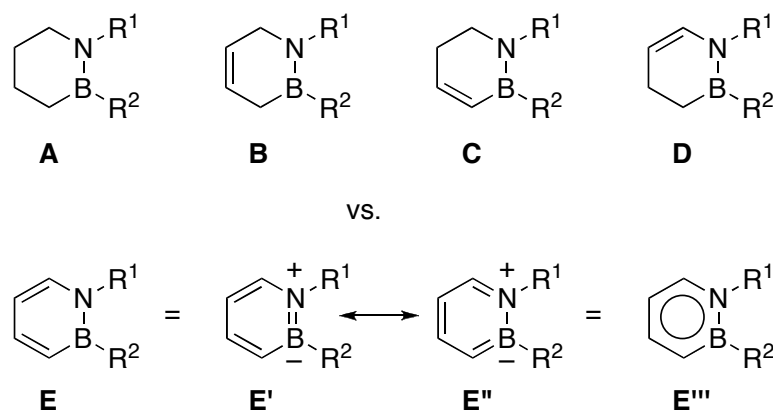


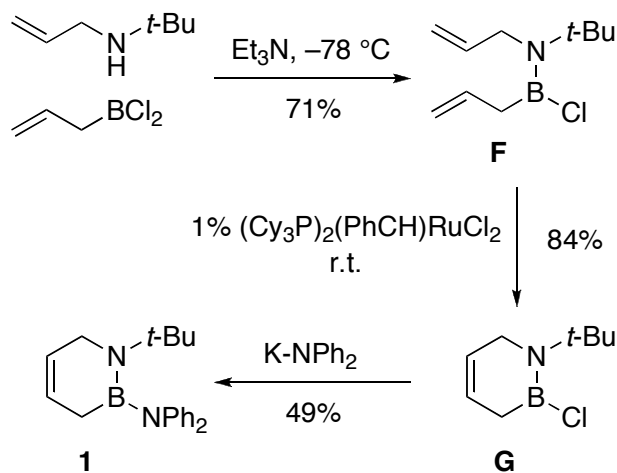
**Figure 2.1.** Strategy for determining electron delocalization in 1,2-azaborines: direct structural comparison.

In our early work on *B*-substituted 1,2-azaborines, we noticed that heterocycle **1** containing *N-t*-Bu and *B*-NPh<sub>2</sub> substituents furnishes highly crystalline solids suitable for

single crystal X-ray diffraction. Thus we chose this substitution pattern for our comparative structural investigation.

### 2.3. Synthesis and Characterization of Reference Compounds

The synthesis of **1** is described in Scheme 2.1. Condensation of *t*-butylallylamine with allylboron dichloride produced the diene precursor **F**. Ring-closing metathesis<sup>33</sup> of this intermediate using the first generation Grubbs catalyst gave product **G** in 84% isolated yield. Nucleophilic attack at the *B*-Cl bond in **G** with potassium diphenylamide furnished the desired heterocycle **1**.

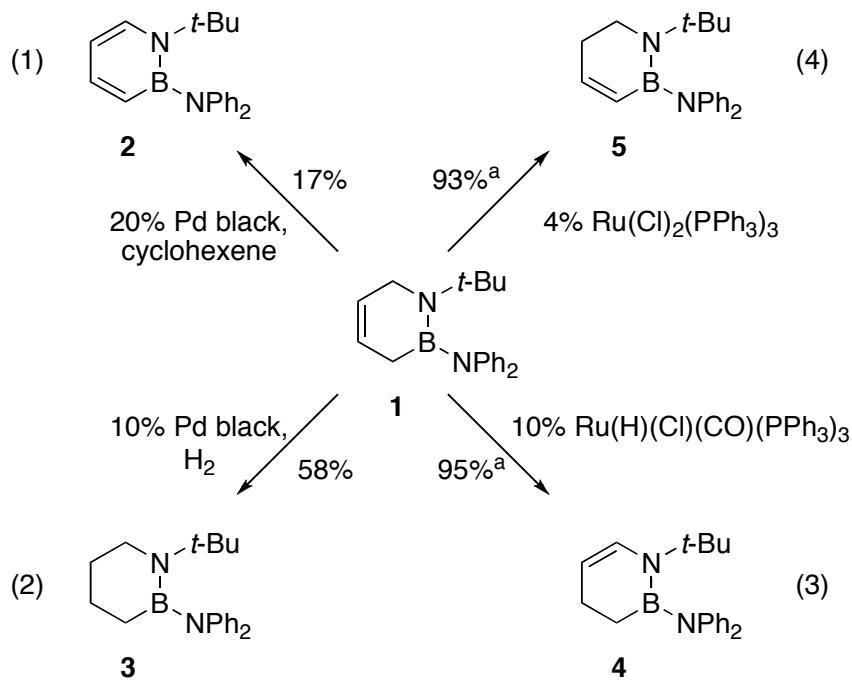


**Scheme 2.1.** Synthesis of diene precursor **1**.

We envisioned that heterocycle **1** could serve as a universal precursor toward the four remaining target structures (**2-5** in Scheme 2.2). Indeed, dehydrogenation of **1** using Pd black<sup>25</sup> generated structure **2** (eq 1). Conversely, compound **1** could be hydrogenated using the same catalyst to furnish **3** (eq 2). Prior to our studies, no methods were

available to synthesize heterocycle **4** and **5**. Recognizing that precursor **1** contains an allylamine fragment, we thought that we could take advantage of existing isomerization methods to produce the enamine isomer **4**. Ruthenium complexes have been shown to transform *N*-allylamines and *N*-allylamides into their corresponding isomers in a catalytic fashion.<sup>34-36</sup> Thus, we began to investigate the use of commercially available ruthenium catalysts for the synthesis of **4**. We were surprised to discover a striking difference in reactivity between two of the surveyed ruthenium complexes. While Ru(H)(Cl)(CO)(PPh<sub>3</sub>)<sub>3</sub> generated the desired *N*-vinyl isomer **4** selectively (eq 3), we were delighted to observe that attempts at the same transformation with Ru(Cl)<sub>2</sub>(PPh<sub>3</sub>)<sub>3</sub> provided the *B*-vinyl isomer **5**, also with high selectivity (eq 4).

The synthetic access to compounds **1-5** in Scheme 2.2 paves the road for their structural analysis. Gratifyingly, we were able to obtain structural data for all five heterocycles via single crystal X-ray diffraction. Selected structural parameters are summarized in Figure 2.2 and Table 2.1. Analysis of the data reveals the following trends without exception: 1) all non-aromatic structures (i.e., **1**, **3**, **4**, and **5**) have B–N bond distances consistent with significant double bond character (~1.41 Å), which lengthen to 1.45 Å after oxidation to **2** (red entries, Table 1); 2) formal C=C double bonds in **1**, **4**, **5** lengthen significantly upon aromatization (blue entries, Table 2.1); 3) all formal single bonds shorten upon delocalization (Table 2.1); 4) the puckered conformations in non-aromatic heterocycles **1**, **3**, **4**, and **5** become planar upon formation of 1,2-azaborine **2** (Figure 2.2, and Table 2.1, entry planarity).



<sup>a</sup> Determined by <sup>1</sup>H NMR analysis versus a calibrated internal standard. See Supporting Information for details.

**Scheme 2.2.** Catalytic transformations of **1**.

Heterocycle **3** serves as a good reference point for structural comparisons. The C–C, C–B, and C–N bond distances in **3** are consistent with formal single bonds (Figure 2.2, and Table 2.1).<sup>37</sup> The B–N bond distance of 1.403(2) Å is consistent with a strong double bond character (sum of covalent radii = 1.56 Å). Thus, **3** is isoelectronic and isostructural with a 1,2-disubstituted cyclohexene. Structural comparisons in the Cambridge Crystallographic Database (CCD) indicate that the half-chair conformation of **3** is also adopted by many 1,2-disubstituted cyclohexenes.<sup>38</sup>

Compound **1** is analogous to a 1,2-disubstituted 1,4-cyclohexadiene. It is more planar than **3**, with a root mean square deviation from planarity of 0.164 Å compared to 0.226 Å in **3** (Table 2.1). However, it is less planar than 1,2-disubstituted 1,4-cyclohexadiene structures, which are almost completely planar.<sup>39</sup> The twisting observed in **1** might be due to steric interactions between the relatively bulky *N*-*t*-Bu and the *B*-NPh<sub>2</sub> substituents. The bond lengths in **1** (in Å) N(1)–B = 1.405(2), and C(4)–C(5) = 1.319(2) are consistent with localized double bonds. The slight shortening of the formal single bonds C(3)–C(4) and C(5)–C(6) in **1** compared to **3** (1.493 Å vs. 1.511 and 1.508, respectively) is consistent with a contraction due to a change in hybridization from sp<sup>3</sup> to sp<sup>2</sup>.

Partially conjugated **4** and **5** represent the two possible BN-heterocyclic isomers equivalent to 1,3-cyclohexadiene. The bond distances in **5** (in Å) N(1)–B = 1.407(2), B–C(3) = 1.559(2), C(3)–C(4) = 1.338(2) indicate a localized short-long-short “diene” bond sequence. The torsion angle between the double bonds of this “diene”  $\angle$ N(1)–B–C(3)–C(4) is  $-30.9(2)^\circ$ , indicating a non-planar geometry. Similarly, the structural parameters in **4** (in Å) C(5)–C(6) = 1.319(3), C(6)–N(1) = 1.432(3), N(1)–B = 1.417(3), are also consistent with a localized “diene” moiety. The value of the torsion angle of  $-25.2(3)^\circ$  shows that the C(5)–C(6)–N(1)–B fragment in **4** is non-planar as well.

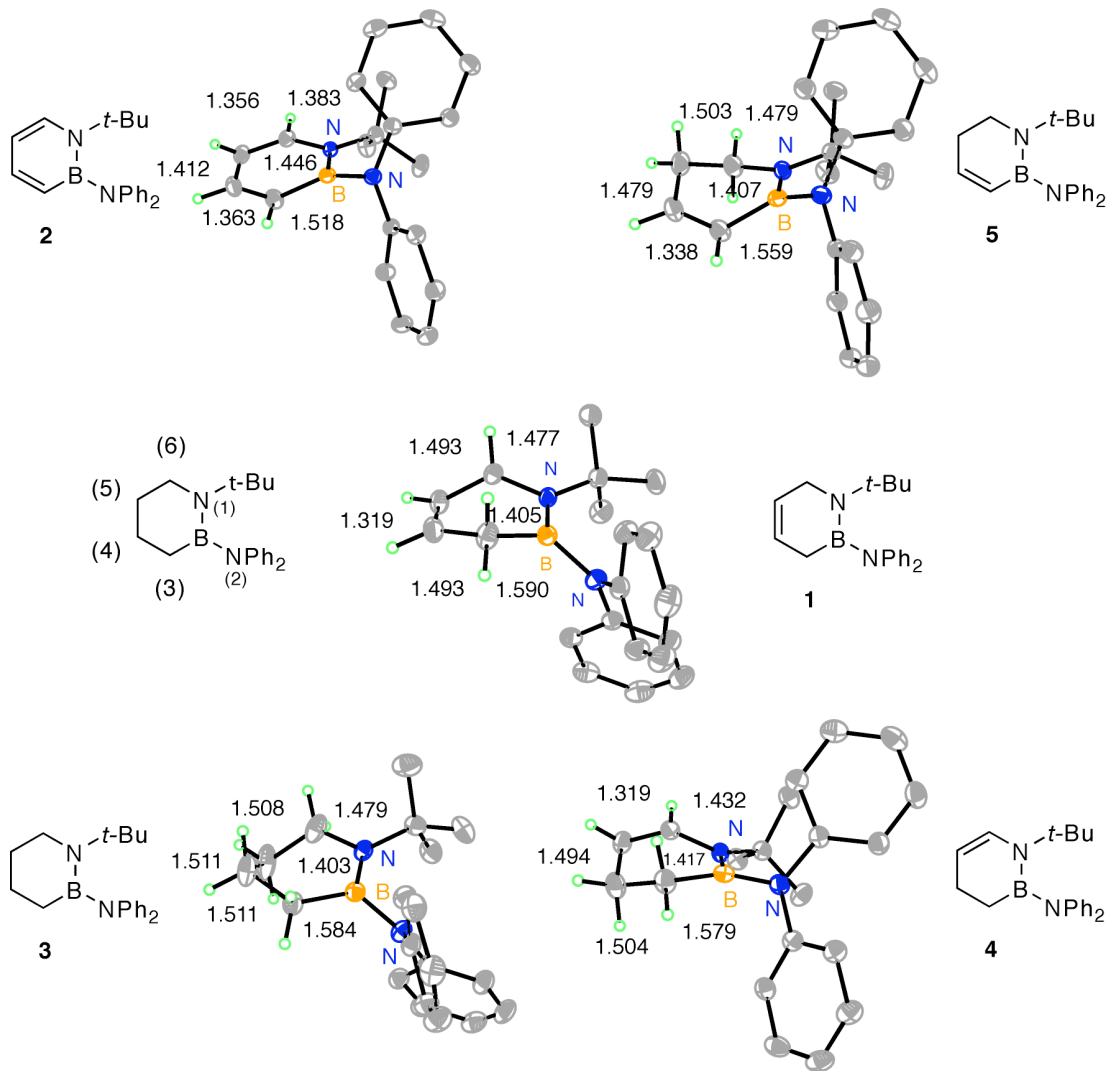


**Figure 2.2.** ORTEP illustrations, with thermal ellipsoids drawn at the 35% probability level, of heterocycles **1-5**.

Direct comparison of partially conjugated “dienes” **4** and **5** with fully delocalized 1,2-azaborine **2** highlights the clear contrast between *localized* bonding in “dienes” **4** and **5** and *delocalized* bonding in **2** (Table 2.1, bold entries). Upon forming the six π-electron species **2**, the N(1)–B bond lengthens, and both the B–C(3) and C(6)–N(1) bonds shorten. This observation is consistent with both resonance structures **E'** and **E''** (Figure 2.1)

contributing to the overall structure of 1,2-azaborine **E**, which is indicative of aromatic delocalization (**E'''**).

**Table 2.1.** Selected Bond Distances and Deviations from Planarity (Å) for BN-Heterocycles **1-5**

		(6)				
		(5)	(4)	(3)	(2)	
N(1)-B		1.403(2)	1.405(2)	1.407(2)	1.417(3)	1.446(2)
B-C(3)		1.584(3)	1.590(2)	1.559(2)	1.579(4)	1.518(2)
C(3)-C(4)		1.511(3)	1.493(2)	1.338(2)	1.504(4)	1.363(2)
C(4)-C(5)		1.511(3)	1.319(2)	1.479(2)	1.494(4)	1.412(2)
C(5)-C(6)		1.508(3)	1.493(2)	1.503(2)	1.319(3)	1.356(2)
C(6)-N(1)		1.479(2)	1.477(2)	1.479(2)	1.432(3)	1.383(2)
B-N(2)		1.488(2)	1.478(2)	1.483(2)	1.480(3)	1.486(2)
planarity <sup>a</sup>		0.226	0.164	0.199	0.183	0.048

<sup>a</sup> Root mean square deviation of intra-ring atoms from the least-square plane (in Å).

Structures **1-5** reveal with unprecedented detail the geometrical changes that occur from saturated **3** on its transition to the aromatic heterocycle **2** via partially unsaturated **1**, **4** and **5**. The trends described above are consistent with those seen when comparing non-aromatic cyclohexene, and cyclohexadiene structures with the delocalized aromatic benzene structure.

The boron in boron-containing heterocycles has been shown to accept  $\pi$ -electrons from exocyclic amine substituents to varying degrees, depending on the electronic properties of the heterocycle.<sup>40</sup> The exocyclic nitrogen atom N(2) in **1-5** adopts a trigonal

planar structure (sum of the angles =  $360 \pm 1^\circ$ ). The B–N(2) bond distances in **1–5** remain constantly  $\sim 1.48$  Å (Table 2.1), consistent with some  $\pi$ -bonding.<sup>41</sup> However, as illustrated in Figure 2.2, the orientation of the nitrogen lone pair in **1–5** permits only minimal interaction with the boron atom. We believe that this distortion from co-planarity results from unfavorable steric interactions between the bulky *N*-*t*-Bu and *B*-NPh<sub>2</sub> substituents.

#### 2.4. Conclusion

In summary, we have successfully structurally characterized the first examples of “pre-aromatic” 1,2-azaborine heterocycles, enabling the direct comparison of delocalized bonds of 1,2-azaborines to their corresponding formal double and single bonds in non-aromatic systems. The comprehensive data presented in this study provide an unprecedented look into the structural changes that occur in six-membered BN-heterocycles on their road to aromaticity, and they establish with little ambiguity that 1,2-azaborines such as **2** possess delocalized structures consistent with aromaticity.

#### 2.5. Bridge to Chapter III

Chapter II explored the aromatic character of 1,2-azaborines using X-ray crystallography. A coherent picture is beginning to emerge of the fundamental character of 1,2-azaborines, yet significant synthetic hurdles still remain before they can be incorporated into complex molecular structures at will. Chapter III describes the development of a new 1,2-azaborine synthon that does not require the use of protecting groups. This new method allows rapid construction of 1,2-azaborines that previously required a tedious synthesis or were entirely unavailable. This route cuts out the need for stoichiometric amounts of metal reagents, resulting in a cheaper, greener method.

## CHAPTER III

### PROTECTION-FREE 1,2-AZABORINE SYNTHESIS

#### **3.1. General Overview**

This excerpt is based on material that is not yet published. The bulk of the lab work was performed by me, including the development of the protocols, early derivatizations including parent 1,2-azaborine synthesis and *B*-Cl substitution, and synthesis of a large quantity of starting material **5** that I provided to my collaborators. Ashley Lamm performed the work on the carbon-based derivatization and Patrick Campbell worked on the methoxy and amino substitutions on the new synthon I developed. The idea for protection-free synthesis was conceived entirely by me. This chapter was written entirely by me. Professor Shih-Yuan Liu provided editorial assistance and scientific guidance for all material in this chapter.

#### **3.2. Introduction**

Strategic substitution of the BN bond pair into classic arene scaffolds has provided new perspectives on concepts related to aromaticity, such as resonance stabilization,<sup>1</sup> aromatic substitution reactions,<sup>2,3</sup> and the structural consequences of  $\pi$ -bonding.<sup>4</sup> Deliberate tuning of electronic and reactivity profiles can be achieved from BN-substitution into established material and biological systems, allowing access to properties unavailable to their organic and inorganic relatives. 1,2-dihydro-1,2-azaborines (abbreviated as 1,2-azaborines) have attracted recent attention for their unique optical properties,<sup>5</sup> favorable hydrogen storage parameters,<sup>6</sup> and for examples of substitution into

biological<sup>7</sup> and pharmaceutical motifs.<sup>8</sup> Dewar<sup>9</sup> and White<sup>10</sup> were the pioneers of 1,2-azaborine chemistry, creating the first examples in the 1960s. After a period of relative inactivity, many synthetic milestones have been reached in the past 20 years; notably the developments by Ashe,<sup>11</sup> Piers,<sup>12</sup> and Liu.<sup>13</sup> But before the potential of this heterocycle can be fully realized, significant synthetic hurdles must still be overcome which allow more efficient construction of 1,2-azaborine cores, combined with the ability to incorporate them into complex molecular scaffolds at will.

### 3.3. Synthesis and Characterization of a New 1,2-Dihydro-1,2-Azaborine Synthon

In the past, chemists had to choose between 1,2-azaborine synthons containing labile groups on either nitrogen, such as Ashe's *N*-TMS 1,2-azaborine **1**,<sup>14</sup> or boron such as our *B*-Cl 1,2-azaborine **2**<sup>8</sup> (Figure 3.1). In both cases, the syntheses required that a non-labile group be attached to neighboring boron or nitrogen atoms, respectively. Our group recently synthesized the parent 1,2-dihydro-1,2-azaborine **4**,<sup>15</sup> from *N*-TBS *B*-Cl-1,2-azaborine **3**, which is the first example of a 1,2-azaborine synthon that can be functionalized at both nitrogen and boron positions. However, creating the parent **4** from **3** requires four additional synthetic steps, one to install the *B*-H and three subsequent steps to remove the *N*-TBS protecting group. Fluoridic deprotection of *N*-TBS with HF•pyridine in the parent 1,2-azaborine synthesis proceeds in 76% yield, but requires complexation with stoichiometric chromium (0) in 71% yield, followed by a costly demetallation step with only a 10% isolated yield. The synthesis of precursor **3** also requires the use of stoichiometric organotin reagents, which are expensive and toxic.

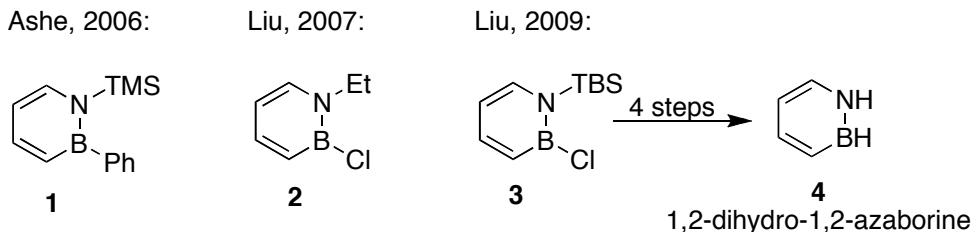
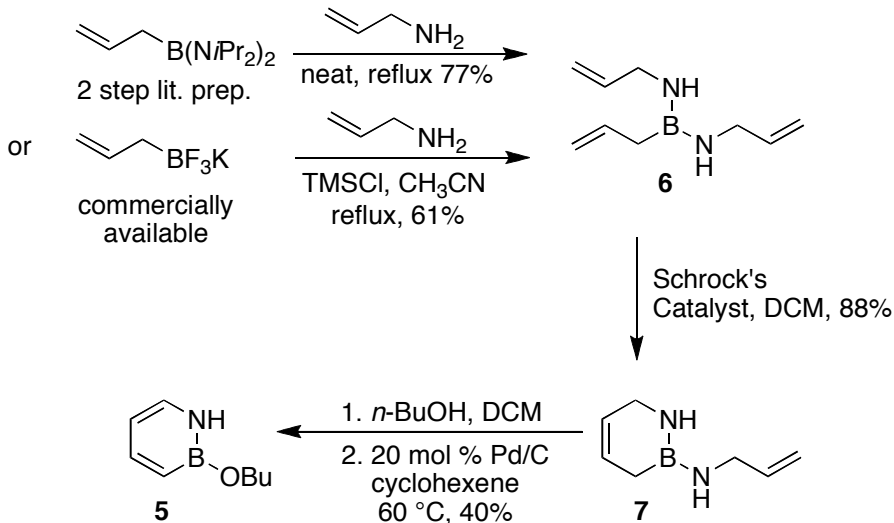


**Figure 3.1.** Previous 1,2-azaborine synthons and the parent 1,2-azaborine.

Herein we report the protection-free synthesis of a new 1,2-azaborine synthon **5**, which can be readily functionalized at boron and nitrogen. By rethinking our starting materials, we have eliminated the need for an *N*-protecting group, resulting in a higher yielding, greener<sup>16</sup> and more cost-effective route to BN-substituted phenyl analogs that more accurately mimic their organic relatives. The new synthon **5** is available in three synthetic steps from commercially available materials and requires only catalytic amounts of metals.

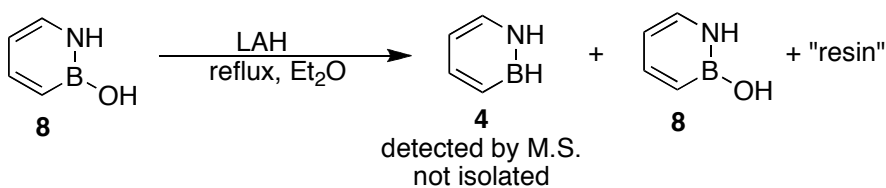
By generating allylboron dichloride *in situ* from the commercially available potassium allyltrifluoroborate, we eliminate the need for tin. Instead of keeping one of the *B*-Cl bonds intact as in our previous syntheses, we quench both *B*-Cl bonds at once with allylamine to afford a the much less reactive **6** in 61% yield (Scheme 3.1). Alternatively, **6** can be synthesized from *bis*-diisopropylaminoallylborane<sup>17</sup> in refluxing allylamine in 77% yield. By eliminating the reactive *B*-Cl bond, we negate the need for an *N*-protecting group. Ring-closing metathesis with Schrock's Mo catalyst allows access to heterocycle **7** in 88% yield with the *N*-H bond intact. Substitution of the *B*-allyl amino fragment with *n*-butanol followed by Pd/C oxidation in cyclohexene and affords the chromatographable **5** in 40% yield.



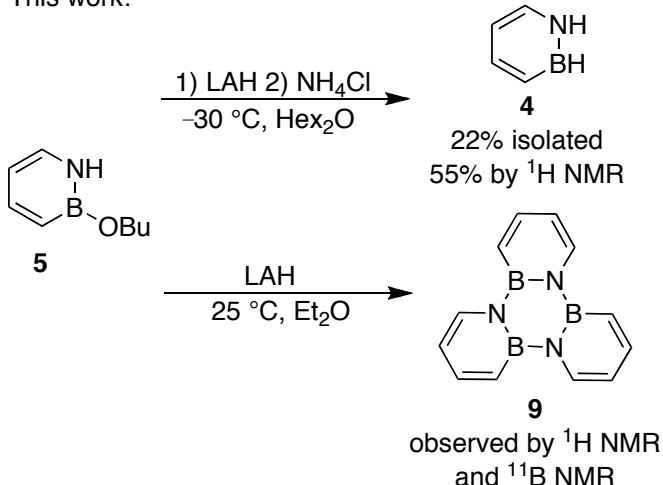
**Scheme 3.1.** Synthesis of synthon **5**.

Our new azaborine synthon **5** allows for synthesis of the parent 1,2-azaborine **4** in 4 steps instead of the 8 steps used in Marwitz's original synthesis (Scheme 3.2). Treatment of **5** with LAH followed by solid  $\text{NH}_4\text{Cl}$  in high-boiling dihexyl ether at  $-30^\circ\text{C}$  allows isolation of clean parent **4** via vacuum transfer in 22% yield (55% by  $^1\text{H}$  NMR.) Dewar's original attempts at synthesizing **4** started with precursor **8** that is remarkably similar to our synthon **5**. Dewar treated **8** with LAH, detecting parent **4** by mass spectrometry, but the material "resinified quickly".<sup>18</sup> He concluded that 1,2-azaborines are too reactive and ceased work on this scaffold. Indeed, treatment of our synthon **5** with LAH without protic workup leads to trimer **9** observed by Dewar. Had he used a protic workup, he would have probably have succeeded in isolation of the parent **4** almost 50 years earlier.

Dewar 1967:



This work:



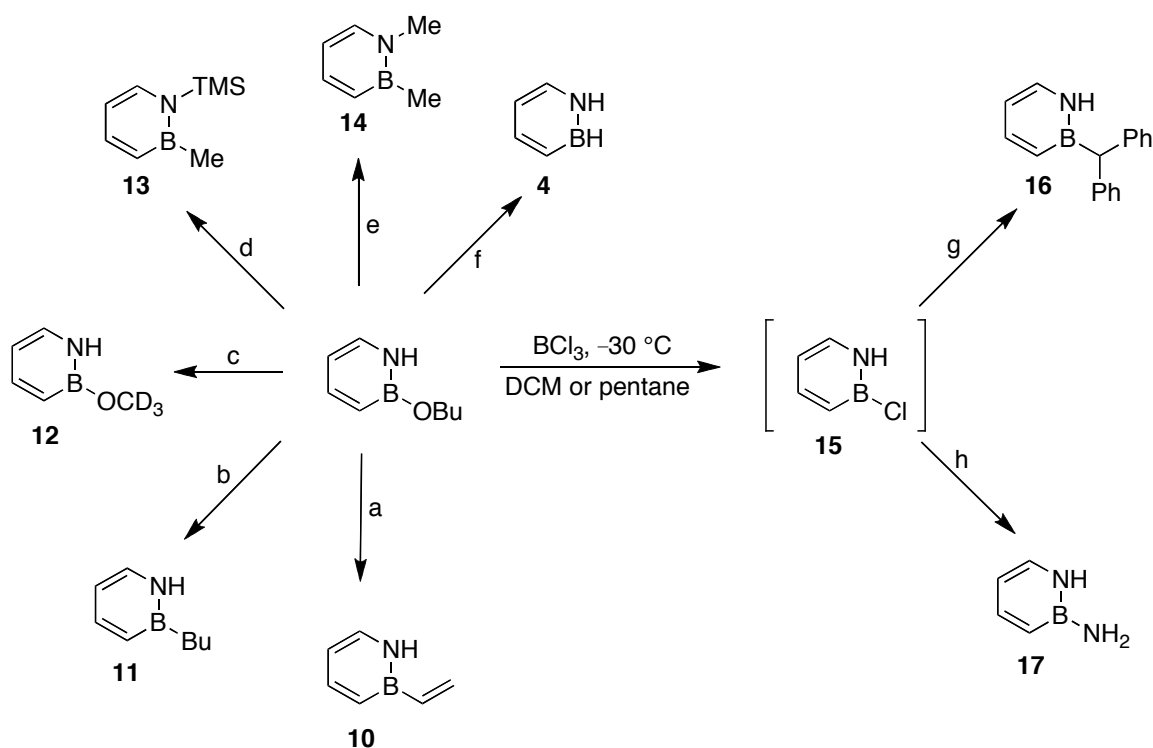
**Scheme 3.2.** Dewar's near miss.

The parent **4** can be derivatized to provide other simple benzenoid mimics containing a free *N*-H group using nucleophilic aromatic substitution reactions,<sup>3</sup> but the starting material requires eight synthetic steps to create. Using the new synthon **5**, many of the same BN analogs of important benzenoids can be accessed in five fewer steps if **5** is substituted directly. This newfound economy provides access to many unprecedented BN isosteres of phenyl-based molecules containing a free *N*-H, the exploration of which was cost-prohibitive using existing protocols.

The derivatization of **5** is still in-progress, but initial results demonstrate the promise of the new route. Addition of vinylmagnesium bromide followed by acidic workup affords the previously reported BN styrene analog **10**<sup>19</sup> in 53% yield (Scheme

3.3.) Treatment with *n*-BuLi followed by acidic workup affords the *B-n*-Bu derivative **11** in 83% yield. Treatment of **5** with excess alcohol at elevated temperatures effects metathesis of the BO bond. Refluxing **5** in methanol *d*4 eliminates *n*-butanol, yielding BN anisole **12** as the major product by <sup>1</sup>H NMR and as confirmed by HRMS. Unfortunately, **12** is unstable on silica and its volatility hinders isolation by other means. As was previously demonstrated with the parent 1,2-azaborine **4**, functionalization of both nitrogen and boron can be achieved in one step. The addition of MeLi to **5** installs a methyl group on boron, which can be quenched with TMSCl to afford the *B*-Me *N*-TMS derivative **13** in 63% yield or with MeI to afford the BN *o*-xylene analog **14** in 49% yield.

Other nucleophiles incapable of displacing the strong BO bond can still be added to **5**. Pretreatment with of **5** with BCl<sub>3</sub> generates a much more electrophilic boron center. *In situ* generation of *B*-Cl *N*-H azaborine **15** at -30 °C allows less reactive nucleophiles to be added to **15** without the need to protect the nitrogen (Scheme 3.3). Intermediate **15** trimerizes readily, and must be kept cold and used immediately. Treatment of **15** with diphenylmethyl lithium followed by acidic workup affords the theoretically interesting BN triphenylmethane analog **16** in 75% yield. Initial studies suggest that amides will also add to **15**. <sup>11</sup>B NMR data suggests formation of the BN aniline analog **17** by treatment of **15** with potassium amide followed by workup with NH<sub>4</sub>Cl, yet isolation remains challenging. Exploration of the functionalization possibilities of **5** are just beginning, but the first glimpses into the reactivity demonstrate the wider range of substitution patterns made available by this intermediate.



**Scheme 3.3.** Derivatization of synthon **5**. Conditions: a) vinylMgBr, -30 °C Et<sub>2</sub>O; HCl, 53%; b) *n*-BuLi, -30 °C Et<sub>2</sub>O; HCl, 83%; c) xs. CD<sub>3</sub>OD, 70 °C, not isolated; d) MeLi, -30 °C Et<sub>2</sub>O; TMSCl, 63%; e) MeLi, -30 °C Et<sub>2</sub>O; MeI, 49%; f) LAH, -30 °C Hex<sub>2</sub>O; NH<sub>4</sub>Cl, 22%; (55% by <sup>1</sup>H NMR) g) Ph<sub>2</sub>CHLi, -30 °C pentane; HCl, 75%; h) NaNH<sub>2</sub>, -30 °C, pentane; NH<sub>4</sub>Cl, not isolated.

### 3.4. Conclusion

Though still incomplete, the initial progress towards easily-synthesized BN analogs of fundamentally-interesting benzenoids, as well as more complex scaffolds desired for possible application, is promising. The synthetic economy gained by circumventing protection/deprotection protocols enables chemists to access 1,2-azaborine structures previously regarded as cost/labor prohibitive. With less time and resources required for the synthesis of 1,2-azaborine structures, efforts can be redirected towards studying the properties of these heterocycles and exploring possible applications derived thereof.

### **3.5. Bridge to Chapter IV**

Chapter III discussed the development of a versatile 1,2-azaborine synthon that does not require the use of protecting groups and greatly improves the efficiency of constructing these rings. Chapters IV and V will be devoted to the development of the first “fused” BN indoles, which are indole analogs containing a 1,2-azaborine core, where the BN bond is substituted for the bridgehead CC bond in the indole ring system. Chapter IV outlines the synthesis of *N-t*-Bu BN indole and surveys the aptitude of this molecule to undergo electrophilic aromatic substitutions (EAS) at the 3-position, a hallmark of indole chemistry. These studies reveal a similar but enhanced EAS reactivity of BN “fused” indole compared to its organic analog indole.

## CHAPTER IV

### ELECTROPHILIC AROMATIC SUBSTITUTION OF A BN INDOLE

#### **4.1. General Overview**

In this chapter, the synthesis of the first “fused” BN indole is presented and the reactivity towards electrophiles is surveyed. This chapter is based on previously published material see: Abbey, E.R.; Zakharov, L. N.; Liu, S. -Y. *J. Am. Chem. Soc.* **2010**, *132*, 16340-16342. All of the lab work, with the exception of X-ray crystallography (performed by Lev N. Zakharov), was performed by me. The manuscript was drafted by me. Professor Shih-Yuan Liu provided editorial assistance and scientific guidance for all material in this chapter.

#### **4.2. Introduction**

Indole<sup>1</sup> is one of the most ubiquitous heterocyclic motifs in nature. Due to the abundance of biologically active indole derivatives,<sup>2</sup> the indole ring system has become an important structural component in drug discovery efforts. Consequently, the synthesis and functionalization of indoles has been a major focus in research, the expansion of the chemical space of accessible indole structures being one of the goals.<sup>3</sup> An alternative approach to expand structural diversity is “elemental isosterism”. To this end, the BN/CC isosterism has recently emerged as a viable strategy to create biomimetic analogues of common structural units in organic molecules (e.g., olefin,<sup>4</sup> benzene,<sup>5</sup> and indene<sup>6</sup>). Despite the recent advances in this area, the elemental isosterism of the biologically important indole has remained virtually unexplored. To date, the only BN-substituted

indoles are phenylenediamine-type heterocycles containing an external BN unit as illustrated in **1** (Scheme 4.1).<sup>7,8</sup> To the best of our knowledge, electrophilic aromatic substitution (EAS), a crucial reaction of the biochemistry of indoles<sup>9</sup> has not been demonstrated with these phenylenediamine-type BN indoles. Herein we report the first example of a “BN-fused” indole (e.g., heterocycle **2** in Figure 4.1), and we demonstrate that this new BN indole undergoes EAS reactions with the same regioselectivity as its organic analogue, *N*-*t*-Bu-indole **3**.<sup>10</sup>

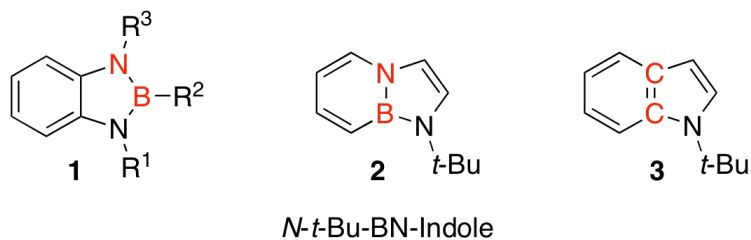
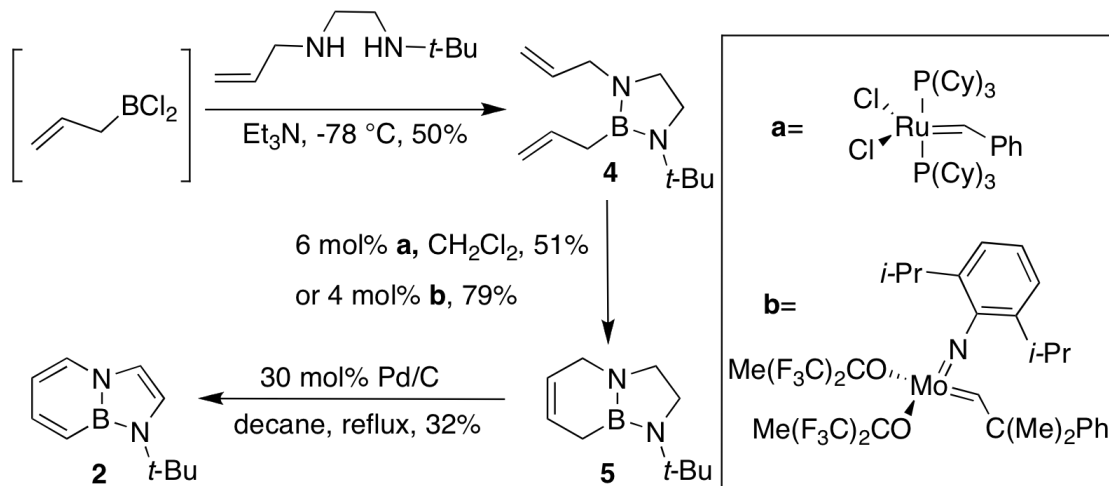


**Figure 4.1.** A novel biomimetic BN indole.

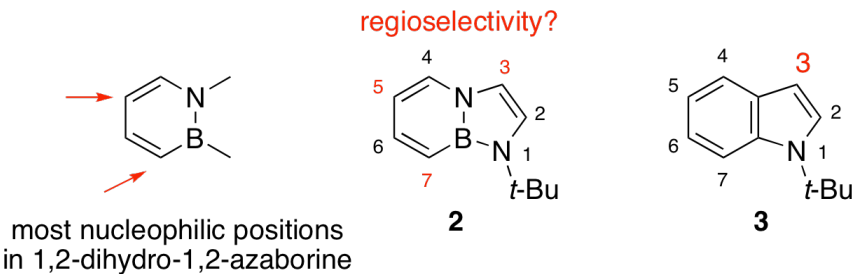
### 4.3. Synthesis and Reactivity Studies on “Fused” BN Indole

Synthesis of *N*-*t*-Bu-BN-indole **2** begins with the condensation of *N*-*t*-Bu-*N'*-allylenediamine with *in situ*-generated allylboron dichloride (Scheme 4.1), affording heterocycle **4** in 50% yield. Ring-closing metathesis (RCM) with Grubbs first generation catalyst provides the bicyclic **5** in 51% yield.<sup>11</sup> The yield of the RCM step can be improved to 79% using Schrock’s catalyst. Dehydrogenation of precursor **5** to furnish the target compound **2** is accomplished in the presence of Pd/C in refluxing decane.<sup>12</sup>



**Scheme 4.1.** Synthesis of *N*-*t*-Bu-BN-indole **2**.

With *N*-*t*-Bu-BN-indole **2** in hand, we then investigated its reactivity toward EAS. Indole itself displays high EAS reactivity, which is estimated to be orders of magnitude greater than benzene.<sup>13</sup> This is due to indole's electron-rich nature, and the high electron density at its 3-position is responsible for indole's regioselectivity toward EAS reactions. The bicyclic *N*-*t*-Bu-BN-indole **2** consists of a 6-membered 1,2-dihydro-1,2-azaborine heterocycle<sup>14,15</sup> and a 5-membered 2,3-dihydro-1*H*-1,3,2-diazaborole core (Scheme 4.2).<sup>16</sup> Thus, we were particularly interested in whether unnatural *N*-*t*-Bu-BN-indole **2** would display the classical indole-type regioselectivity in EAS reactions (i.e., at the 3-position) or substitution at the 7- and 5-positions,<sup>17</sup> which have been demonstrated to be most nucleophilic in monocyclic 1,2-azaborine structures.



**Scheme 4.2.** Regioselectivity in EAS reactions of *N*-*t*-Bu-BN-indole **2**.

We surveyed the EAS reaction of *N*-*t*-Bu-BN-indole **2** with a variety of electrophiles. As can be seen from Table 4.1, bromination of **2** occurred at the 3-position, yielding the brominated product **6a** (Table 4.1, entry 1). The Mannich reaction of **2** with dimethyliminium chloride provided our first BN indole alkaloid, *N*-*t*-Bu-BN-gramine **6b** in 53% yield (Table 4.1, entry 2). Lewis acid-mediated Michael addition of **2** to cyclohexenone with zirconium tetrachloride<sup>18</sup> furnished **6c** in 57% yield (Table 4.1, entry 3). Deuterium exchange occurred in degassed 1:1 CD<sub>3</sub>OD/D<sub>2</sub>O at 100 °C providing **6d** in 39% isolated yield<sup>19</sup> (Table 4.1, entry 4). Friedel-Crafts acylation of **2** with acetyl chloride was accomplished in the presence of Et<sub>2</sub>AlCl<sup>20</sup> to yield **6e** (Table 4.1, entry 5). In each case, we observed substitution at the 3-position of **2**. The H(2) and H(3) proton signals of **2** appear as one singlet in <sup>1</sup>H NMR (in CD<sub>2</sub>Cl<sub>2</sub>) integrating for two protons. Thus, we determined the substitution pattern of EAS products by either single crystal X-ray diffraction (e.g., for **6e**), or NOESY experiments (e.g., for **6a** and **6c**).

**Table 4.1.** EAS Reactions of **2**

entry	electrophile ( $E^+$ )	catalyst	3-substituent (E)	product	yield (%)
1	$\text{Br}_2$	-		<b>6a</b>	39
2		-		<b>6b</b>	53
3		$\text{ZrCl}_4$		<b>6c</b>	57
4	$\text{CD}_3\text{OD}/\text{D}_2\text{O}$	-		<b>6d</b>	39 <sup>a</sup>
5		$\text{Et}_2\text{AlCl}$		<b>6e</b>	23

<sup>a</sup>  $^1\text{H}$  NMR indicates ~80% deuterium enrichment.

The modest yields of these reactions are likely due to side reactions associated with the relatively acidic reaction conditions. Indoles are known to undergo self-condensation reactions in the presence of acids.<sup>21</sup> We determined that *N*-*t*-Bu-BN-indole **2** forms the *B*-methoxy-substituted trimer **7** (Figure 4.2) in acidic methanol solution among other by-products.<sup>22</sup> In one instance, we were able to isolate a single crystal of **7** and determine its structure by X-ray crystallography. Although substituted at the nitrogen and at the C(3) position, the structure of **7** provides us with the first glimpse into the bonding of BN indoles fused at the BN unit. Comparing the intra-ring bond distances of the 6-membered ring of **7** and a *B*-diphenylamino-substituted 1,2-azaborine **A** (Figure

4.2),<sup>23</sup> the most noticeable difference is observed in the B–N bond distances. In the fused bicyclic BN indole **7** the B(1)–N(2) distance (1.463(2) Å) is longer than the corresponding B–N bond in a monocyclic 1,2-azaborine (1.446(2) Å). This is likely due to the better  $\pi$ -overlap between the “exocyclic” nitrogen atom in **7** (i.e., N(1)) versus in **A**. It is also consistent with the shorter N(1)–B(1) distance in **7** (1.440(2) Å) compared to the B–N(exocyclic) bond length of 1.486(2) Å in **A**. We are also interested in comparing the BN indole structure **7** with its carbonaceous counterpart. The typical bond distances of a 1,3-dialkylsubstituted indole are illustrated in the bottom right corner of Figure 4.1 (structure **B**).<sup>24</sup> The most significant differences in bond distances are directly associated with the replacement of the C=C bond in **B** with a B–N unit. Due to the larger covalent radius of boron,<sup>25</sup> the B(1)–C(7) (1.509(2) Å) and B(1)–N(1) (1.440(2) Å) bond lengths are significantly longer (by ~0.1 Å) than those in indole **B**. On the other hand, presumably due to the slightly smaller covalent radius of the nitrogen (vs. carbon),<sup>25</sup> the N(2)–C(4) (1.370(2) Å) and N(2)–C(3) (1.404(2) Å) distances are shorter than the corresponding bonds in **B**, although this difference is less pronounced (i.e., shorter by only ~0.02 Å). Thus, while BN indoles are geometrically similar in shape compared to natural indoles, the differences in bonding (e.g., bond lengths and electronic structure) could potentially lead to significantly different biological activity.

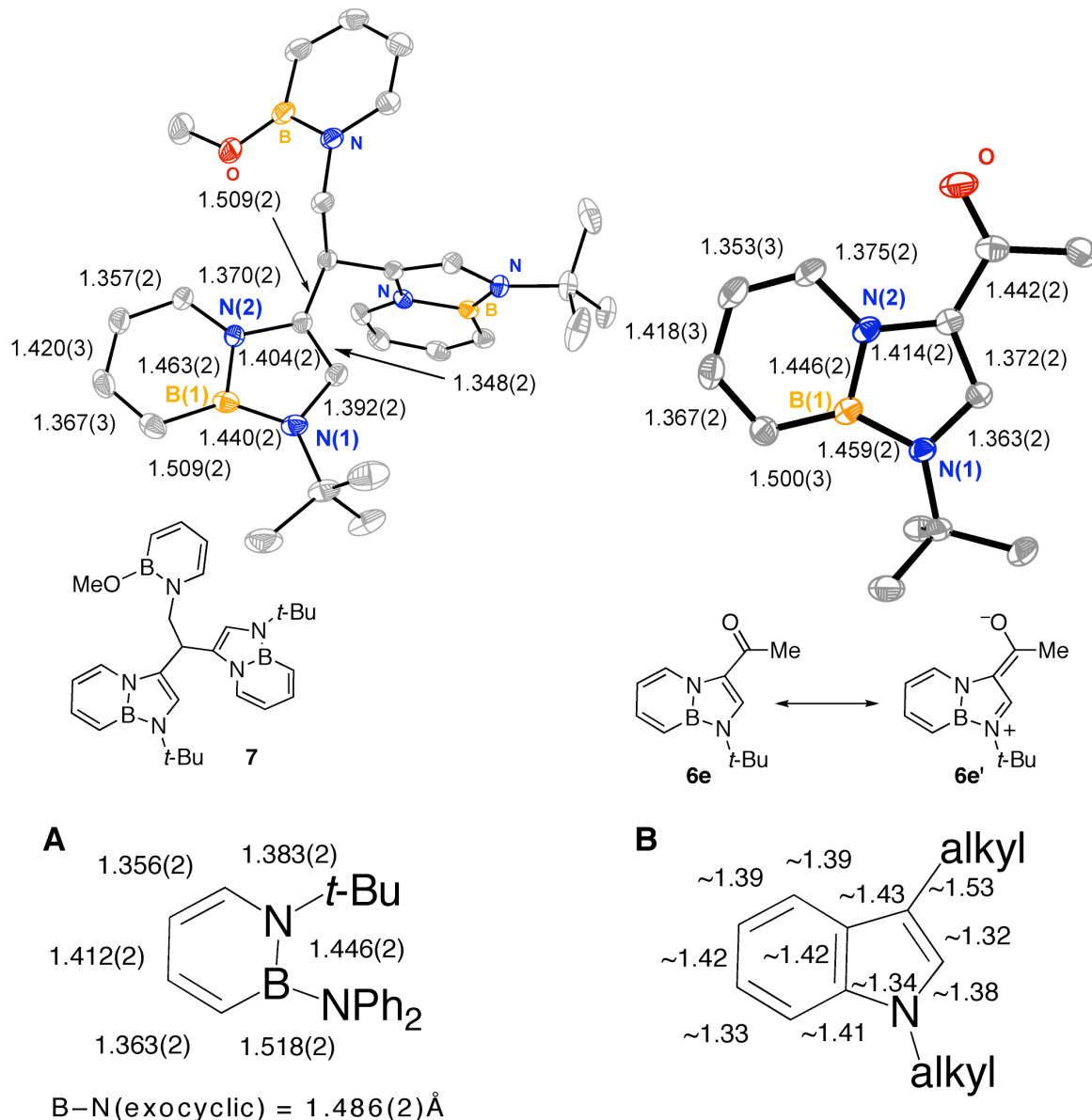
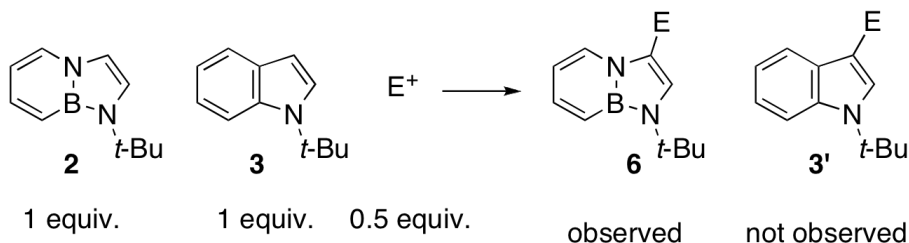


**Figure 4.2.** ORTEP illustrations, with thermal ellipsoids drawn at the 35% probability level, of **7** and **6e**.

We were also very pleased to discover that acylated BN indole **6e** forms crystalline solids suitable for single crystal X-ray diffraction analysis. The structure of **6e** is illustrated in Figure 4.2 (top right). Because of the electronic impact of the acetyl substituent at the C(3) position, significant changes in bond distances are observed

compared to **7**. The N(1)–C(2) (1.363(2) Å), C(2)–C(3) (1.372(2) Å), and the B(1)–N(2) bond distances in **6e** are consistent with a significant contribution of structure **6e'**.

In order to probe the effect of BN/CC isosterism of indoles on the reactivity in EAS reactions, we performed competition experiments between *N*-*t*-Bu-BN-indole **2** and its corresponding carbonaceous analogue **3**. Protection of the pyrrolic nitrogen with an *N*-*t*-butyl group allows the reactivity of the 3-position to be evaluated without the influence of an indole N-H. Using one equivalent of each indole **2** and **3** and 0.5 equivalent of electrophile ( $E^+$  = dimethyliminium chloride) in  $CD_2Cl_2$ , we observed only EAS products associated with *N*-*t*-Bu-BN-indole **2**, with indole **3** remaining intact (Scheme 4.3). We hypothesize that *N*-*t*-Bu-BN-indole **2** exhibits greater enamine character in the pyrrolic ring and is therefore more nucleophilic than indole **3**.



**Scheme 4.3.** EAS competition experiment with dimethyliminium chloride as the electrophile.

#### 4.4. Conclusion

In summary, we synthesized the first examples of BN-fused indole derivatives. We also demonstrated that this new family of BN indoles undergoes EAS reaction with classical indole-type regioselectivity at the 3-position. Competition experiments revealed that *N*-*t*-Bu-BN-indole **2** is more nucleophilic in EAS reactions than its carbonaceous counterpart. Single crystal X-ray structure analysis showed that while BN indoles are

similar in shape compared to classical indoles, significant differences in bond distances, in particular those associated with the boron atom, are observed. Our work lays the synthetic foundation for BN-substituted unnatural products containing the indole motif and highlights the potential of BN/CC isosterism as a general strategy in expanding the chemical space of biologically active molecules.

#### **4.5. Bridge to Chapter V**

Chapter IV discussed the development of the first BN “fused” indole, the *N-t*-Bu derivative. Chapters V will be devoted to the synthesis of the parent “fused” BN indole, with the *N*-H intact and a comparison of the physical properties to its organic analog, indole. These studies reveal similar but properties of BN “fused” indole compared to its organic analog indole, with important differences. The excitation and emission of BN indole are red-shifted, as with many BN arenes, and the *N*-H is significantly less acidic.

## CHAPTER V

### BORON IN DISGUISE: THE PARENT “FUSED” BN INDOLE

#### 5.1. General Overview

This chapter describes the synthesis of the parent “fused” BN indole, a new BN isostere of the biologically important indole. All of the work described in this chapter, with the exception of the cyclic voltammetry (performed by Chris Weber) and the X-ray crystallography (performed by Lev Zakharov) was performed entirely by me. The manuscript was drafted by me. Professor Shih-Yuan Liu provided editorial assistance and scientific guidance for all material in this chapter.

#### 5.2. Introduction

Indole **1** is a heterocycle of great importance to biological systems. Within proteins, the redox-active indole side-chain of tryptophan is one of the primary charge carriers involved in through-space electron transfer.<sup>1</sup> The optical properties of indole make tryptophan one of the principal intrinsic fluorophores in protein fluorescence microscopy.<sup>2</sup> Indole is the biosynthetic parent to the essential amino acid tryptophan, the neurotransmitters serotonin<sup>3</sup> and melatonin,<sup>4</sup> the auxin plant hormones,<sup>5</sup> and remains a prominent structural feature in drug design.<sup>6</sup> Expansion of the diversity available to indole-based structures through BN isosterism has produced the phenylenediamine family of “external” BN indoles **2**,<sup>7,8</sup> (Figure 5.1). and the recently reported “fused” BN indoles **3** containing the 1,2-dihydro-1,2-azaborine **4** core. Our group recently found that the “fused” BN indole **3b** displays similar reactivity to indole **1b** in electrophilic aromatic

substitution (EAS) reactions.<sup>9</sup> While *N-t*-Bu-BN indole **3b** closely mimics indole's chemistry at the C2-C3 bond, it does not contain a free *N*-H fragment, an important feature in the biochemistry of indole and its derivatives.<sup>10</sup> We now wish to report the synthesis of the parent *N*-H BN indole **3a**, with an in-depth comparison to its carbonaceous counterpart.

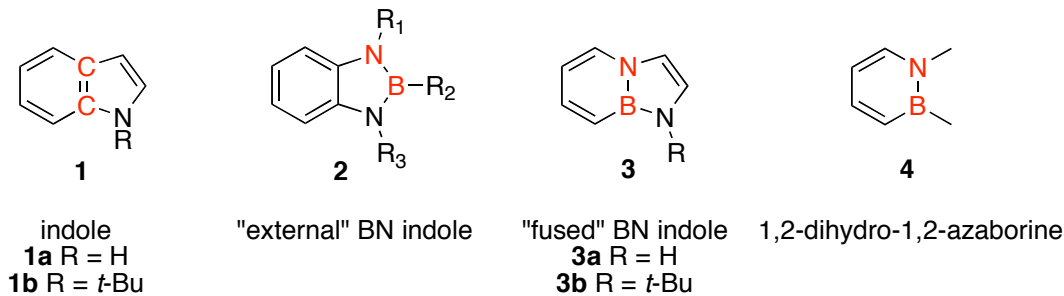


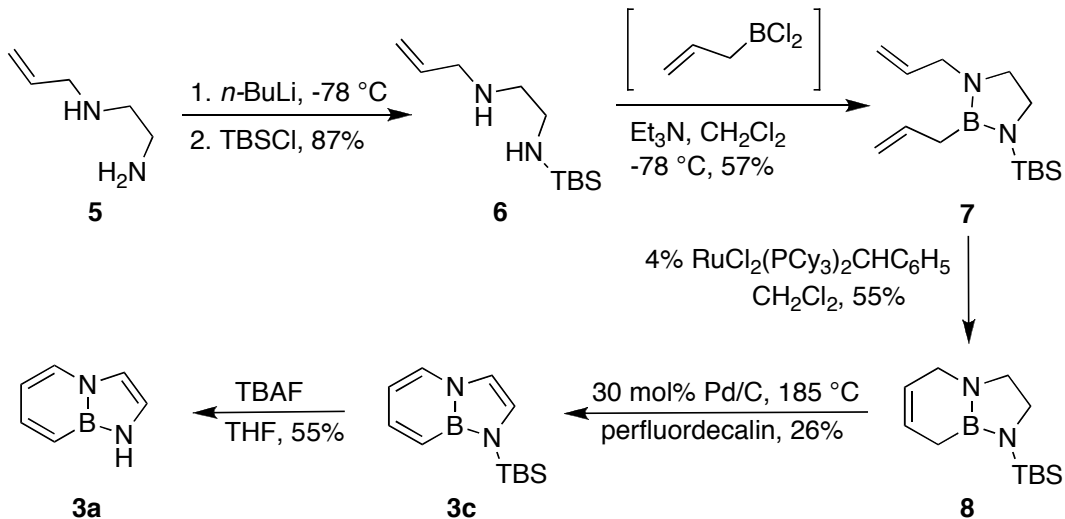
**Figure 5.1.** Indole, "external" and "fused" BN indoles.

Substitution of  $sp^3$  and  $sp^2$  CC bonds with their respective BN bond pair in biological motifs has the potential to yield isostructural and isoelectronic BN unnatural products. The concealment of boron in biological structures is driven by potential therapeutic and analytical motives. Spielvogel and others have synthesized BN glycine<sup>11</sup> and other BN amino acid analogs with  $sp^3$  BN bonds. Similarly shaped but not truly isostructural  $sp^2$  BN nucleosides have received a great deal of attention in recent decades.<sup>12</sup> Despite the wealth of boron-containing compounds investigated for biomedical applications, few examples of completely isostructural and isoelectronic BN analogs of natural products have been synthesized. Within this small family of BN biomolecules, there are no examples containing an  $sp^2$  BN bond pair, to the best of our knowledge. The "external" BN indole **2** is isoelectronic and isostructural with indole, but is not isosymmetric and therefore cannot accurately mimic indole's rich chemistry. The

dearth of  $sp^2$  BN biomimetics is likely the result of high reactivity and air/water-sensitivity of the resulting compounds. Incorporation of the  $sp^2$  BN bond pair into an aromatic system such as 1,2-dihydro-1,2-azaborine **4** greatly enhances stability towards water.<sup>13</sup>

### 5.3. Synthesis and Characterization of the Parent “Fused” BN Indole

Synthesis of **3a** begins with protection of *N*-allylethylenediamine **5** with *n*-BuLi/TBSCl to provide **6** in 87% yield (Scheme 5.1.) Condensation of **6** with *in-situ* generated allylboron dichloride affords heterocycle **7** in 55% yield. Ring-closing metathesis (RCM) with Grubbs' first-generation catalyst catalyst provides the bicyclic product **8** in 58% yield. Oxidative dehydrogenation with catalytic Pd/C in perfluorodecalin affords the fully aromatic *N*-TBS BN indole **3c** in 26% yield. Perfluorodecalin was found to be a more convenient solvent to the decane used in the synthesis of **3b**, because the product can be isolated via biphasic extraction with cold THF. Interestingly, XRD studies of crystals isolated from the crude reaction mixture revealed an almost parallel ( $3.7^\circ$ )  $\pi$ -complex (**3c**•**Fnap**) of the product **3c** with perfluoronaphthalene **Fnap** (Table 5.1.) with an interplanar distance of 3.524 Å. Silica gel chromatography allowed isolation of clean **3c**. Deprotection with TBAF afforded the parent BN indole **3a** in 55% yield.



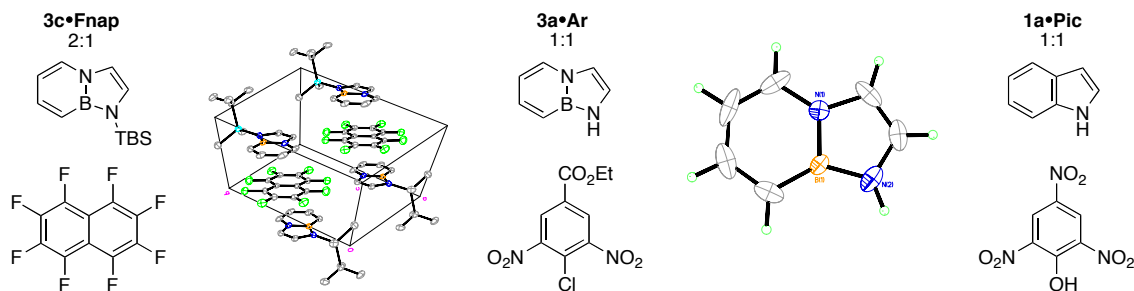
**Scheme 5.1.** Synthesis of **3a**.

With **3a** in hand, we began characterization of the structural, optical, and physical features of the new heterocycle. X-ray quality crystals of **3a** had a disordered structure, with an identical unit cell (cell volume  $662.42 \text{ \AA}^3$ , space group  $\text{Pna}2_1$ ) to the similarly disordered indole XRD data.<sup>14</sup> Given our fortuitous discovery of the crystalline  $\pi$ -complex (**3c**•**Fnap**), we attempted cocrystallization of the parent **3a** with perfluoronaphthalene. X-ray quality crystals of (**3a**•**Fnap**) were obtained though slow evaporation from  $\text{CH}_2\text{Cl}_2$ , but were unfortunately also disordered. Screening other electron deficient aromatics, we successfully obtained an ordered XRD structure by complexation with **Ar**. The orange 1:1 complex **3a**•**Ar** shows evidence of  $\pi$ - $\pi$  stacking in the solid state, with an interplanar distance of  $3.2684 \text{ \AA}$  and an almost parallel ( $1.2^\circ$ ) relationship. These structural features are consistent with charge-transfer and are slightly shorter than the range of spacings found in indole-picrate  $\pi$ -complexes ( $3.3$ - $3.5 \text{ \AA}$ ) such as **1a**•**Pic**.<sup>15</sup> Comparison of the structures of the parent “fused” BN indole with a similar natural indole  $\pi$ -complex reveals striking similarities. With the exception of the bonds 4,6

and 9, all other bond lengths of **3a** are within similar regimes as the structure of natural indole **1a** (Table 5.1.) A shortened bond ( $\sim 0.07 \text{ \AA}$ ) 4 in BN indole **3a** is consistent with a smaller atomic radius of nitrogen versus carbon. A longer ( $\sim 0.1 \text{ \AA}$ ) bond 9 in **3a** compared to **1a** is likely the consequence of the larger atomic radius of boron compared to carbon. It is unclear the reason for the shorter bond 6 in **3a**. All three structures are highly planar, with bond lengths consistent with aromatic delocalization. All three indoles have a shortened C(2)-C(3) bond length (bond 3), which shows significant double bond character and is responsible for much of indole's unique chemistry.

**Table 5.1.** Bond lengths of **3c•Fnap**, **3a•Ar**, and **1a•Pic**.

Bond	Complex		
	<b>3c•Fnap</b>	<b>3a•Ar</b>	<b>1a•Pic</b>
1	1.444(8)	1.417(7)	1.401(7)
2	1.408(7)	1.369(8)	1.354(9)
3	1.304(9)	1.339(9)	1.304(9)
4	1.403(8)	<b>1.402(7)</b>	<b>1.468(9)</b>
5	1.349(8)	1.367(7)	1.36(1)
6	1.384(10)	1.357(10)	1.42(1)
7	1.392(11)	1.395(11)	1.37(1)
8	1.343(9)	1.361(10)	1.361(9)
9	1.525(9)	<b>1.487(8)</b>	<b>1.378(7)</b>
Bridgehead	1.442(8)	1.423(7)	1.392(7)



Cyclic voltammetry reveals some of the electronic differences between these two heterocycles. BN indole **3a** has an irreversible oxidation wave, peaking at 1.04 V compared to 1.18 V measured for indole **1a** vs. SCE (Figure 5.2). Both oxidations are irreversible and show evidence of polymerization at the electrode, consistent with previous CV measurements of indole.<sup>16</sup> The lower oxidation potential measured for **3a** is consistent with a higher energy HOMO compared to indole, and has been observed in comparisons of other BN arenes to their organic analogs.<sup>17</sup>

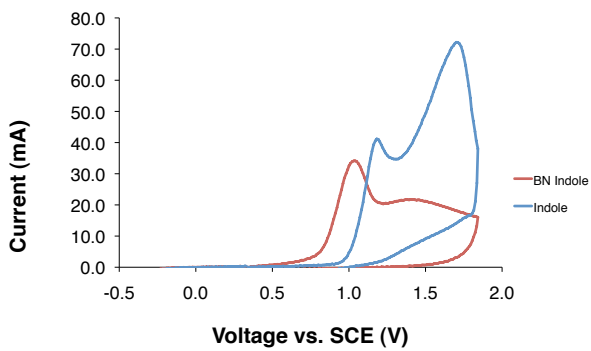
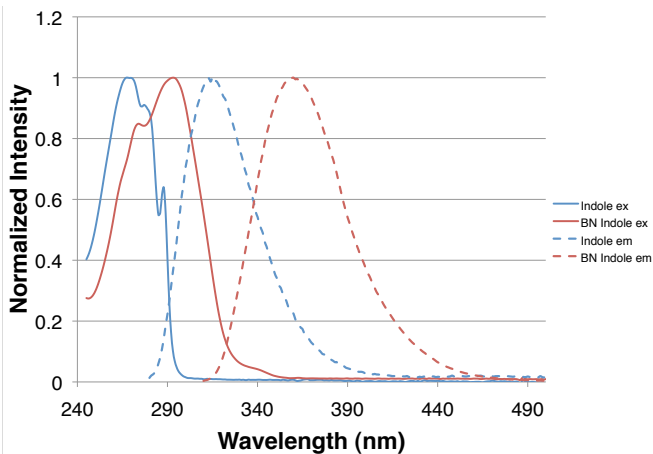


**Figure 5.2.** CV Measurements of BN indole **3a** and indole **1a** (0.8 M TBAOTf in CH<sub>3</sub>CN at glassy carbon electrode)

Like indole, “fused” BN indole **3a** is fluorescent. The absorbance and emission wavelengths of many BN-substituted arenes are red-shifted with respect to their organic analogs.<sup>17,18</sup> Indole’s absorbance  $\lambda_{\text{max}}$  is 265 nm, whereas BN indole’s  $\lambda_{\text{max}}$  is red-shifted to 293 nm (Figure 5.3). The emission  $\lambda_{\text{max}}$  of indole is 315 nm, and BN indole  $\lambda_{\text{max}}$  is red-shifted to 360 nm. As with many BN arenes, BN indole **3a** displays a larger Stokes shift than its carbonaceous counterpart<sup>19</sup> indole **1a** at 6350 and 5570 cm<sup>-1</sup>, respectively. The red-shifted absorbance and greater Stokes shift of **3a** are consistent with a lower HOMO/LUMO bandgap. The quantum yield of **3a** ( $\Phi= 0.08$ ) is significantly lower than

indole<sup>20</sup> **1a** ( $\Phi = 0.32$ ), as is the molar absorbitivity ( $\epsilon = 6400$  vs.  $8200 \text{ M}^{-1} \text{ cm}^{-1}$ , respectively).



	$\lambda_{\text{ex}}$	$\lambda_{\text{em}}$	$\epsilon (\text{M}^{-1} \text{ cm}^{-1})$	$\Phi (\text{CH}_3\text{CN})$	Stokes Shift ( $\text{cm}^{-1}$ )
<b>BN Indole <b>3a</b></b>	293	360	6400	$0.083 \pm 0.011$	6350
<b>Indole <b>1a</b></b>	268	315	8200 <sup>a</sup>	0.32 <sup>b</sup>	5570

<sup>a</sup> Literature value, reference 19

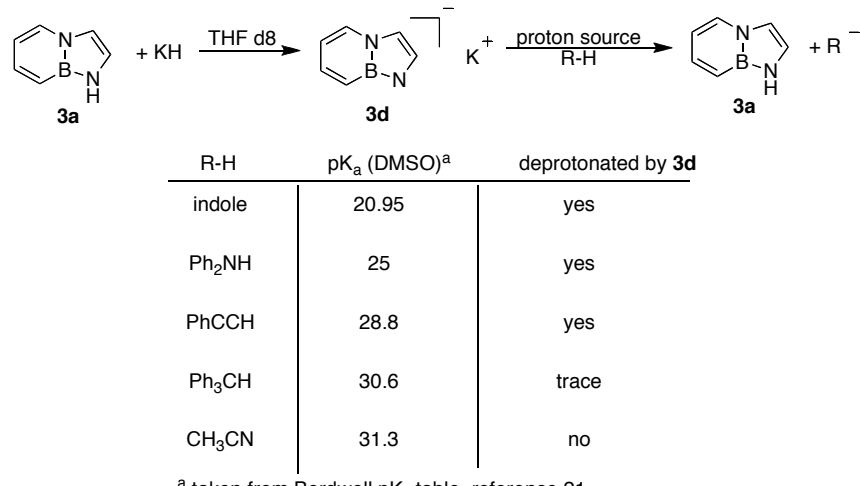
<sup>b</sup> Literature value, reference 20

**Figure 5.3.** Optical Data for **3a** and **1a**.

The *N*-H functionality is a critical component of indole-containing biomolecules. While we previously established that *N*-*t*-Bu-BN indole **3b** displays the same regioselectivity as indole in EAS reactions, the chemistry of the *N*-H of BN indole **3a** is completely unexplored. We sought to estimate the pK<sub>a</sub> of the *N*-H proton through a series of <sup>1</sup>H NMR bracketing experiments. Deprotonation with potassium hydride in THF *d*8 occurs cleanly, yielding anion **3d**. By adding one equivalent of a proton source R-H of known pK<sub>a</sub> to a solution of anion **3d**, we were able to observe whether the pK<sub>a</sub> standard was deprotonated, indicating the relative acidity of **3a**. This bracketing strategy

demonstrated that the *N*-H proton of BN indole is roughly nine orders of magnitude more basic than natural indole, with a  $pK_a$  around 30, compared to the literature value of indole at 20.95<sup>21</sup> (Table 5.2). Indeed, addition of one equivalent of indole **1a** to anion **3d** cleanly yields the starting BN indole **3a**. The greater basicity of **3a** may result from inductive effects from the neighboring boron atom.

**Table 5.2.**  $pK_a$  Bracketing Experiment for **3a**



We also investigated the water and air stability of BN indole **3a**. Using the previously reported methods for measuring the air and water stability of 1,2-azaborines,<sup>13</sup> we found that **3a** was significantly more resistant to degradation than any monocyclic 1,2-azaborine measured. **3a** shows <5% degradation when exposed to ten equivalents of water in DMSO *d*6 solution for 96 hrs, and benzene *d*6 solutions exposed to pure O<sub>2</sub> at 50 °C degrade <5% over 4 hours by <sup>1</sup>H NMR compared to internal standards. Neat material degrades over the course of hours in the presence of air.

#### **5.4. Conclusion**

“Fused” BN indoles **3** are emerging as fascinating mimics of the classic indole **1** motif, with structures and reactivity that mirror indole’s, but with notable differences. With a few exceptions, the structures of BN indoles and their carbonaceous analogs are nearly identical. BN indoles display similar reactivity patterns to indoles, but with enhanced basicity and nucleophilicity. Optical and electronic measurements of the parent **3a** are consistent with a smaller bandgap and higher HOMO energy levels compared to natural indole, following the trends seen in other BN arenes. The similarities between the two classes of indoles will continue to inspire investigations into how classic indole-based chemical systems can be tuned through substitution of a BN bond pair at the bridgehead position.

APPENDIX A  
SUPPORTING INFORMATION FOR CHAPTER II

***General***

All oxygen- and moisture-sensitive manipulations were carried out under an inert atmosphere using either standard Schlenk techniques or a glove box.

THF, Et<sub>2</sub>O, CH<sub>2</sub>Cl<sub>2</sub>, and pentane were purified by passing through a neutral alumina column under argon. Cyclohexene was dried over CaH<sub>2</sub> and distilled under N<sub>2</sub> prior to use. Diphenylamine was dried using a Dean-Stark apparatus with anhydrous benzene as the solvent.

Potassium hydride (Strem) was washed with pentane three times and pumped dry under vacuum prior to use. All other chemicals and solvents were purchased (Aldrich or Strem) and used as received.

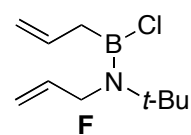
Preparative TLC (1000 µm thickness) plates were purchased from Silicycle and heated to 120° C for 2 h in an oven before being brought into the glove box.

<sup>11</sup>B NMR spectra were recorded on a Varian Unity/Inova 600 spectrometer at ambient temperature. <sup>1</sup>H NMR spectra were recorded on a Varian Unity/Inova 300 or Varian Unity/Inova 600 spectrometer<sup>13</sup>C NMR spectra were recorded on a Varian Unity/Inova 300 or Varian Unity/Inova 500 spectrometer. All chemical shifts are externally referenced: <sup>11</sup>B NMR to BF<sub>3</sub>•Et<sub>2</sub>O ( $\delta$  0).

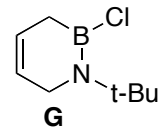
IR spectra were recorded on a Nicolet Magna 550 FT-IR instrument with OMNIC software.

High-resolution mass spectroscopy data were obtained at the Mass Spectroscopy Facilities and Services Core of the Environmental Health Sciences Center at Oregon State University. Financial support for this facility has been furnished in part by the National Institute of Environmental Health Sciences, NIH (P30 ES00210).

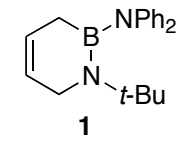
**N-tert-butylallylaminooallylborane chloride (F):** Allyltriphenyltin (16.1g, 41.2 mmol) was dissolved in anhydrous CH<sub>2</sub>Cl<sub>2</sub> (74 mL) in a dry box pressurized with N<sub>2</sub>. The solution was cooled to -78° C in a dry ice/acetone bath. A 1.0 M solution of boron trichloride (41.2 mL, 41.2 mmol) in hexanes was added dropwise via syringe while stirring vigorously under N<sub>2</sub>, causing a white precipitate to form. The mixture was stirred for 4 h at -78° C, followed by the addition a solution of *N*-allyl-*N*-tert-butylamine (4.90 g, 43.3 mmol) and anhydrous triethylamine (6.04 ml, 43.3 mmol) in anhydrous pentane (4.0 mL) dropwise via syringe. The reaction mixture was allowed to slowly warm to 25° C for 18 h, followed by solvent removal *in vacuo*, and filtration through a glass frit. The solid was washed with anhydrous pentane (60 mL), and the solvent was again removed *in vacuo*. The resulting cloudy liquid was transferred to a 25 mL round bottom flask containing a stir bar, and purified via fractional distillation (38° C, 70 mTorr) to afford the clear colorless liquid product (5.9 g, 71%). The <sup>1</sup>H NMR and <sup>11</sup>B NMR spectra were consistent with 1 existing as two B-N rotomers in the ratio of 1:1. Spectral data for F: <sup>1</sup>H NMR (C<sub>6</sub>D<sub>6</sub>, 600MHz): δ 6.18 (m, 2H), δ 5.72 (m, 1H), δ 5.55 (1H), δ 5.03 (m, 4H), δ 3.94 (br s, 2H), δ 3.53 (br s, 2H), δ 2.27 (br s, 2H), δ 1.99 (br s, 2H), δ 1.31 (s, 9H), δ 1.08 (s, 9H). <sup>13</sup>C NMR (CD<sub>2</sub>Cl<sub>2</sub>, 125 MHz): δ 139.3, 139.1, 115.1, 114.7, 57.6, 51.1, 50.0, 32.3, 31.3, 31.0 (br). <sup>11</sup>B NMR (C<sub>6</sub>D<sub>6</sub>, 192.5 MHz): δ 39.5 (d, *J*=174 Hz). FTIR (thin film) 3078, 2975, 2965, 1634, 1405, 1367, 1261, 1242, 1194, 1115, 1089, 1026, 991, 916, 903, 809, 735, 648, 563, 435 cm<sup>-1</sup>.



**1-*t*-Butyl-2-chloro-3,6-dihydro-1,2-azaborine (**G**):** Grubbs gen. 1 catalyst (0.381 g, 0.345 mmol) was dissolved in anhydrous CH<sub>2</sub>Cl<sub>2</sub> (150 mL) under N<sub>2</sub> in a 500 mL Schlenk flask. A solution of **F** (6.88 g, 34.5 mmol) in anhydrous CH<sub>2</sub>Cl<sub>2</sub> (35 mL) was added via pipet while stirring. The reaction mixture was allowed to stir for 45 min. at 25° C, in which time the color changed from purple to brownish red and evolved ethylene gas bubbles. The flask was then sealed and heated to 50° C for 2 h before cooling to 25° C. The solvent was removed *in vacuo*, and the reddish oil was purified via fractional distillation (34° C, 80 mTorr) to afford the clear colorless product (4.98 g, 84%). Spectral data for **G**: <sup>1</sup>H NMR (C<sub>6</sub>D<sub>6</sub>, 600MHz): δ 5.58 (m, 1H), δ 5.27 (m, 1H), δ 3.38 (m, 2H), δ 1.82 (br s, 2H), δ 1.27 (s, 9H). <sup>13</sup>C NMR (CD<sub>2</sub>Cl<sub>2</sub>, 125 MHz): δ 125.3, 124.5, 57.5, 47.8, 30.8, 22.4 (br). <sup>11</sup>B NMR (C<sub>6</sub>D<sub>6</sub>, 192.5 MHz): δ 37.9. FTIR (thin film) 3029, 2978, 2922, 2876, 1494, 1478, 1455, 1435, 1399, 1367, 1326, 1304, 1201, 1180, 1094, 986, 959, 702, 666 cm<sup>-1</sup>. HRMS (EI) calcd. for C<sub>8</sub>H<sub>15</sub>BClN (M<sup>+</sup>) 171.09861, found 171.09796.



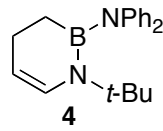
**N-*t*-Butyl-2-diphenylamino-3,6-dihydro-1,2-azaborine (**I**):** In a glove box, a 50 mL RBF containing a stir bar was charged with potassium hydride (0.370 g, 9.19 mmol) and diphenylamine (1.50 g, 8.84 mmol). Cold THF (25 mL) was added, and the slurry was stirred for 2.5 h, in which time it bubbled vigorously and turned from colorless to light green. When the bubbling ceased, the resulting solution was filtered through an Acrodisc, and added dropwise to a solution of **2** (1.50 g, 8.75 mmol) in cold THF (15 mL) in a 100 ml RBF. The mixture was stirred at 25 °C for 16 h, and <sup>11</sup>B NMR showed the reaction was incomplete. A similarly prepared solution of KNPh<sub>2</sub> (0.056 g, 1.40 mmol KH) and (0.225 g, 1.30 mmol HNPh<sub>2</sub>) in cold THF (5.0 mL) was added dropwise to the mixture while stirring. The solution was stirred for an additional 16 h and <sup>11</sup>B NMR showed the reaction was complete. The



solvent was removed *in vacuo*, redissolved in Et<sub>2</sub>O (10 mL), and filtered through an Acrodisc to remove residual salts. The Et<sub>2</sub>O was removed *in vacuo*, and the crude product was dissolved in CH<sub>2</sub>Cl<sub>2</sub> (5.0 mL) and filtered through an Acrodisc. The solvent was removed *in vacuo*, and again redissolved in CH<sub>2</sub>Cl<sub>2</sub> (5.0 mL) and filtered through an Acrodisc. The solvent volume was reduced *in vacuo* to approximately 1 mL, transferred to a 20 mL scintillation vial, and cold pentane (6 mL) was layered on top. The vial was carefully placed in the freezer, and large X-ray quality crystals were repeatedly grown, harvested, and washed with cold pentane to afford the clear, light yellow crystalline product (0.882 g, 34%). Spectral data for **1**: <sup>1</sup>H NMR (CD<sub>2</sub>Cl<sub>2</sub>, 300MHz): δ 7.22 (t, <sup>3</sup>J<sub>HH</sub> = 8.1 Hz, 4H), δ 6.93 (t, <sup>3</sup>J<sub>HH</sub> = 7.8 Hz, 6H), δ 5.83 (m, 1H), δ 5.75 (m, 1H) δ 3.71 (m, 2H), δ 1.49 (m, 2H), δ 1.11 (s, 9H). <sup>13</sup>C NMR (CD<sub>2</sub>Cl<sub>2</sub>, 75 MHz): δ 148.9, 129.4, 127.7, 126.1, 123.8, 121.8, 56.3, 46.4, 29.4, 20.4 (br). <sup>11</sup>B NMR (C<sub>6</sub>D<sub>6</sub>, 192.5 MHz): δ 36.1. FTIR (thin film) 3020, 3008, 2979, 2958, 2939, 2881, 2830, 1587, 1487, 1466, 1429, 1328, 1284, 1263, 1234, 1200, 1146, 1029, 757, 730, 696 cm<sup>-1</sup>.

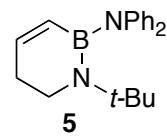
### *Transformations of 1-t-Bu-2-diphenylamino-3,6-dihydro-1,2-azaborine*

**1-t-Bu-2-diphenylamino-5,6-dihydro-1,2-azaborine (4)**: In a glove box, a 20 mL scintillation vial containing a stir bar was added **1** (0.200 g, 0.667 mmol) and Ru(H)(Cl)(CO)(PPh<sub>3</sub>)<sub>3</sub> (0.0760 g, 0.0797 mmol). The vial was charged with benzene (8.0 mL) and heated to 80° C for 16 h, dissolving the catalyst and turning the color red. The solvent was removed *in vacuo* and the remaining product was dissolved in pentane (3.0 mL), then filtered through an Acrodisc to remove the majority of the catalyst. This process was repeated (3x) and the remaining pentane was reduced in volume (~1 mL) and placed in the freezer to yield X-ray quality crystals, which were washed in cold pentane, affording the clear, light yellow product. The impurities visible



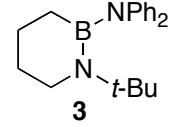
in the spectra are the isomer **4**. Spectral data for **4**:  $^1\text{H}$  NMR ( $\text{CD}_2\text{Cl}_2$ , 500MHz):  $\delta$  7.23 (t,  $^3J_{\text{HH}} = 7.5$  Hz, 4H),  $\delta$  7.00 (t,  $^3J_{\text{HH}} = 7.5$  Hz, 2H),  $\delta$  6.93 (d,  $^3J_{\text{HH}} = 1.0$  Hz, 4H),  $\delta$  6.16 (d,  $^3J_{\text{HH}} = 8.0$  Hz, 1H),  $\delta$  4.95 (dt,  $^3J_{\text{HH}} = 8.0$  Hz,  $^3J_{\text{HH}} = 4.2$  Hz, 1H),  $\delta$  2.05 (m, 2H),  $\delta$  1.06 (s, 9H)  $\delta$  0.97 (t,  $^3J_{\text{HH}} = 8.0$  Hz).  $^{13}\text{C}$  NMR ( $\text{CD}_2\text{Cl}_2$ , 125 MHz):  $\delta$  149.8, 133.1, 129.4, 125.6, 123.1, 107.9, 55.7, 30.0, 21.5, 17.7 (br).  $^{11}\text{B}$  NMR (192.5 MHz,  $\text{CD}_2\text{Cl}_2$ ):  $\delta$  39.2. FTIR (thin film) 3057, 3031, 2971, 2933, 1588, 1491, 1457, 1337, 1319, 1286, 1076, 755, 695, 514,  $\text{cm}^{-1}$ .

**1-t-Bu-2-diphenylamino-3,4-dihydro-1,2-azaborine (5):** In a glove box, a 20 mL scintillation vial containing a stir bar was added **1** (0.198 g, 0.660 mmol) and  $\text{Rh}(\text{H})(\text{CO}) (\text{PPh}_3)_3$  (0.067g, 0.0729 mmol). The vial was charged with benzene (6.0 mL), sealed, and was heated to 80° C for 20 h, changing the solution from yellow to green. The solvent was removed *in vacuo* and the remaining product was dissolved in pentane (3.0 mL) and filtered through an Acrodisc to remove the majority of the catalyst. This process was repeated (3x) and the remaining pentane was allowed to evaporate to yield X-ray quality crystals, which were washed in cold pentane, and dried *in vacuo*, affording the clear, light yellow product **5** (0.041 g, 21%). Spectral data for **5**:  $^1\text{H}$  NMR ( $\text{CD}_2\text{Cl}_2$ , 600MHz):  $\delta$  7.20 (t,  $^3J_{\text{HH}} = 9.6$  Hz, 4H)  $\delta$  6.93 (m, 6H),  $\delta$  6.60 (dt,  $^3J_{\text{HH}} = 11.7$  Hz,  $^3J_{\text{HH}} = 3.7$  Hz, 1H),  $\delta$  5.42 (dd,  $^3J_{\text{HH}} = 11.5$  Hz,  $^4J_{\text{HH}} = 1.4$  Hz, 1H),  $\delta$  3.21 (t,  $^3J_{\text{HH}} = 5.5$  Hz, 2H),  $\delta$  2.26 (m, 2H), 1.11 (s, 9H).  $^{13}\text{C}$  NMR ( $\text{CD}_2\text{Cl}_2$ , 125 MHz):  $\delta$  149.1, 144.9, 132.7 (br), 129.4, 123.8, 121.9, 56.5, 44.5, 30.7, 29.5.  $^{11}\text{B}$  NMR (192.5 MHz,  $\text{CD}_2\text{Cl}_2$ ):  $\delta$  31.7. FTIR (thin film) 3003, 2971, 2926, 2874, 1597, 1589, 1489, 1393, 1330, 1287, 1242, 1147, 1137, 883, 754, 695  $\text{cm}^{-1}$ .



**1-t-Bu-2-diphenylamino-3,4,5,6-tetrahydro-1,2-azaborine (3):**

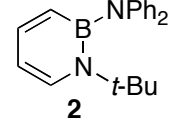
In a glove box, a 500 mL Fischer-Porter tube was charged with **1** (0.150 g, 0.492 mmol), Pd black (0.0053 g, 0.050 mmol), and benzene (3.0 mL).



The vessel was pressurized with 1 atm H<sub>2</sub> and heated to 65° C for 15 h while stirring. The catalyst was removed by filtration through an Acrodisc, followed by *in vacuo* solvent removal. The crude mixture was dissolved in pentane (1.0 ml) and transferred to a 20 mL scintillation vial, which was placed in the freezer. The x-ray quality crystals were washed with cold pentane, and dried *in vacuo* to yield the clear, light yellow product **3** (0.087 g, 58%). Spectral data for **3**: <sup>1</sup>H NMR (CD<sub>2</sub>Cl<sub>2</sub>, 500MHz): δ 7.19 (t, <sup>3</sup>J<sub>HH</sub> = 7.5 Hz, 4H), δ 6.94 (d, <sup>3</sup>J<sub>HH</sub> = 8.0 Hz, 4H), δ 6.90 (t, <sup>3</sup>J<sub>HH</sub> = 7.5Hz, 2H), δ 3.11 (t, <sup>3</sup>J<sub>HH</sub> = 5.5 Hz, 2H), δ 1.69 (m, 2H), δ 1.50 (m, 2H), δ 1.08 (s, 9H), δ 0.98 (t, <sup>3</sup>J<sub>HH</sub> = 7 Hz, 2H). <sup>13</sup>C NMR (CD<sub>2</sub>Cl<sub>2</sub>, 125 MHz): δ 149.4, 129.3, 123.6, 121.4, 56.4, 46.9, 29.8, 29.4, 22.6, 18.9 (br). <sup>11</sup>B NMR (192.5 MHz, CD<sub>2</sub>Cl<sub>2</sub>): δ 37.5. FTIR (thin film) 3060, 3021, 2960, 2921, 1586, 1487, 1429, 1282, 755, 694 cm<sup>-1</sup>.

**1-t-Bu-2-diphenylamino-1,2-azaborine (2):**

In a glove box, a 100 mL Schlenk flask containing a stir bar was charged with **1** (0.150 g, 0.492 mmol), Pd black (0.0106 g, 0.100 mmol), and cyclohexene (10 mL). The vessel was sealed and heated to 80° C for 20 h, then cooled and filtered through an Acrodisc. The solvent was removed *in vacuo* and the crude material was purified via prep TLC (5% Et<sub>2</sub>O/pentane) followed by a second prep TLC plate (pentane) to afford the white solid product **2** (0.025 g, 17%). X-ray quality crystals were grown by slow evaporation from pentane. Spectral data for **2**: <sup>1</sup>H NMR (CD<sub>2</sub>Cl<sub>2</sub>, 600MHz): δ 7.49 (d, <sup>3</sup>J<sub>HH</sub> = 7.2 Hz), δ 7.45 (m, 1H), δ 7.19 (t, <sup>3</sup>J<sub>HH</sub> = 7.8 Hz, 4H), δ 6.90 (m, 6 H), δ 6.28 (d, <sup>3</sup>J<sub>HH</sub> = 10.8 Hz, 1H), δ 6.21 (t, <sup>3</sup>J<sub>HH</sub> = 7.2 Hz, 1H), δ 6.22 (t, <sup>3</sup>J<sub>HH</sub> = 6.6 Hz, 1H), δ 1.38 (s, 9H). <sup>13</sup>C NMR (CD<sub>2</sub>Cl<sub>2</sub>, 125 MHz): δ 149.6, 143.4, 137.3, 132.1 (br), 129.4, 123.5,



121.5, 110.0, 60.2, 31.4.  $^{11}\text{B}$  NMR (192.5 MHz,  $\text{CD}_2\text{Cl}_2$ ):  $\delta$  32.7. FTIR (thin film) 3066, 3033, 2975, 1607, 1585, 1515, 1487, 1394, 1293, 1247, 1197, 900, 753, 696, 594.

### X-ray Crystal Structure Determination.

Diffraction intensity data were collected with a Bruker Smart Apex CCD diffractometer at 173(2) K using  $\text{MoK}\alpha$  - radiation ( $0.71073 \text{ \AA}$ ). The structure was solved using direct methods, completed by subsequent difference Fourier syntheses, and refined by full matrix least-squares procedures on  $\text{F}^2$ . All non-H atoms were refined with anisotropic thermal parameters. H atoms were found on the residual density map and refined with isotropic thermal parameters. The Flack parameter is 0.00(8). All software and sources scattering factors are contained in the SHELXTL (6.10) program package (G.Sheldrick, Bruker XRD, Madison, WI). Crystallographic data and some details of data collection and crystal structure refinement for  $\text{C}_{18}\text{H}_{19}\text{N}_3\text{BNP}$  are given in the following tables.

### Crystallographic data for I.

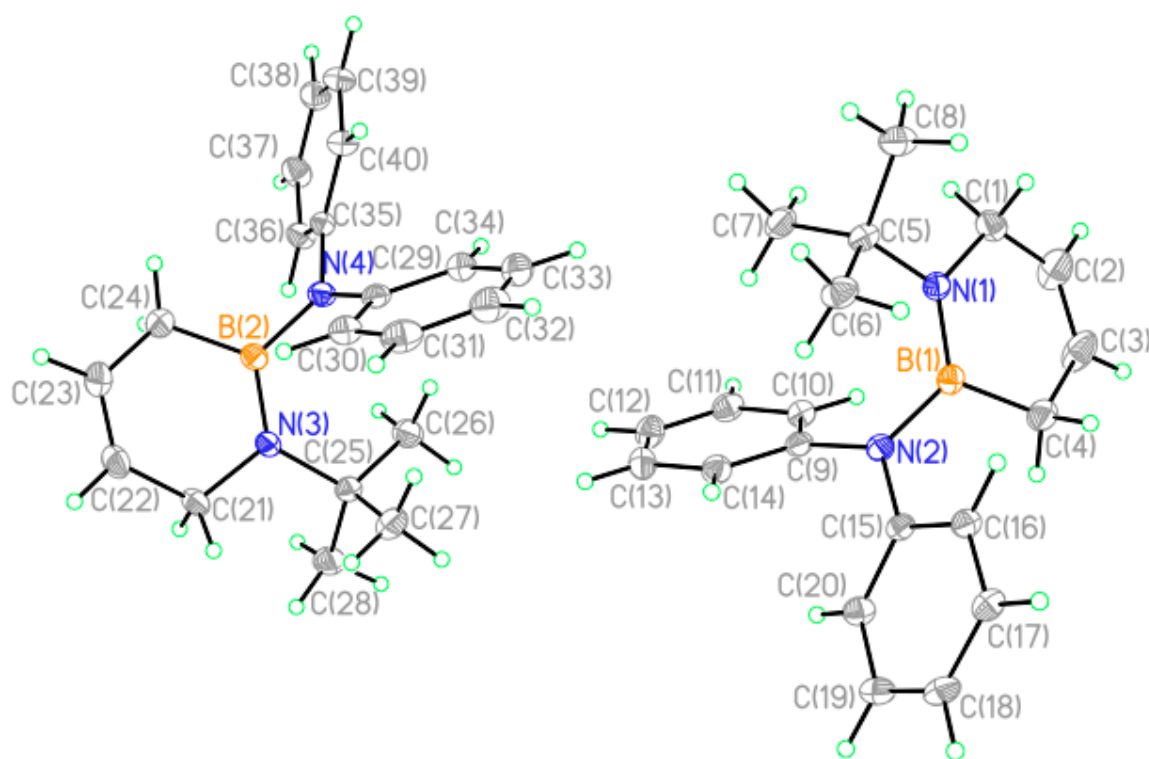


**Table 1. Crystal data and structure refinement for liu14.**

Identification code	liu14	
Empirical formula	C20 H25 B N2	
Formula weight	304.23	
Temperature	173(2) K	
Wavelength	0.71073 Å	
Crystal system	Monoclinic	
Space group	P2(1)/c	
Unit cell dimensions	a = 17.7457(13) Å b = 11.4680(8) Å c = 18.6032(14) Å	a= 90°. b= 113.4510(10)°. g = 90°.
Volume	3473.2(4) Å <sup>3</sup>	
Z	8	
Density (calculated)	1.164 Mg/m <sup>3</sup>	
Absorption coefficient	0.067 mm <sup>-1</sup>	
F(000)	1312	
Crystal size	0.42 x 0.38 x 0.27 mm <sup>3</sup>	
Theta range for data collection	2.14 to 26.99°.	
Index ranges	-22<=h<=22, -14<=k<=14, -23<=l<=23	
Reflections collected	31574	
Independent reflections	7554 [R(int) = 0.0296]	
Completeness to theta = 26.99°	99.8 %	
Absorption correction	Semi-empirical from equivalents	
Max. and min. transmission	0.9821 and 0.9724	
Refinement method	Full-matrix least-squares on F <sup>2</sup>	
Data / restraints / parameters	7554 / 0 / 615	
Goodness-of-fit on F <sup>2</sup>	1.061	
Final R indices [I>2sigma(I)]	R1 = 0.0452, wR2 = 0.1058	
R indices (all data)	R1 = 0.0559, wR2 = 0.1146	
Largest diff. peak and hole	0.249 and -0.219 e.Å <sup>-3</sup>	

**Table 2.** Atomic coordinates ( $\times 10^4$ ) and equivalent isotropic displacement parameters ( $\text{\AA}^2 \times 10^3$ ) for liu14. U(eq) is defined as one third of the trace of the orthogonalized  $U_{ij}$  tensor.

	x	y	z	U(eq)
N(1)	4936(1)	848(1)	1250(1)	25(1)
N(2)	4321(1)	2784(1)	1410(1)	25(1)
N(3)	376(1)	1197(1)	3860(1)	25(1)
N(4)	915(1)	-703(1)	3541(1)	27(1)
B(1)	5002(1)	2060(1)	1382(1)	25(1)
B(2)	328(1)	-18(1)	3753(1)	26(1)
C(1)	5686(1)	125(1)	1522(1)	33(1)
C(2)	6464(1)	760(2)	1935(1)	53(1)
C(3)	6554(1)	1899(2)	1946(1)	51(1)
C(4)	5849(1)	2693(1)	1556(1)	37(1)
C(5)	4157(1)	144(1)	885(1)	29(1)
C(6)	3487(1)	892(1)	282(1)	37(1)
C(7)	3880(1)	-326(1)	1514(1)	38(1)
C(8)	4284(1)	-914(1)	438(1)	38(1)
C(9)	3997(1)	2524(1)	1979(1)	25(1)
C(10)	4511(1)	2061(1)	2701(1)	27(1)
C(11)	4205(1)	1758(1)	3255(1)	33(1)
C(12)	3387(1)	1943(1)	3107(1)	38(1)
C(13)	2871(1)	2414(1)	2393(1)	37(1)
C(14)	3168(1)	2696(1)	1829(1)	30(1)
C(15)	4102(1)	3851(1)	995(1)	24(1)
C(16)	4168(1)	3958(1)	274(1)	27(1)
C(17)	3937(1)	4983(1)	-157(1)	30(1)
C(18)	3626(1)	5913(1)	113(1)	31(1)
C(19)	3572(1)	5822(1)	834(1)	32(1)
C(20)	3816(1)	4812(1)	1276(1)	29(1)
C(21)	-372(1)	1844(1)	3781(1)	31(1)
C(22)	-1152(1)	1168(1)	3415(1)	36(1)

C(23)	-1190(1)	20(1)	3432(1)	40(1)
C(24)	-430(1)	-694(1)	3807(1)	38(1)
C(25)	1116(1)	1974(1)	4060(1)	31(1)
C(26)	1912(1)	1285(1)	4443(1)	43(1)
C(27)	1106(1)	2602(1)	3332(1)	43(1)
C(28)	1117(1)	2884(1)	4671(1)	42(1)
C(29)	1068(1)	-432(1)	2868(1)	27(1)
C(30)	451(1)	82(1)	2220(1)	33(1)
C(31)	595(1)	385(1)	1563(1)	42(1)
C(32)	1347(1)	159(1)	1537(1)	48(1)
C(33)	1960(1)	-363(1)	2173(1)	44(1)
C(34)	1831(1)	-647(1)	2838(1)	34(1)
C(35)	1208(1)	-1766(1)	3940(1)	26(1)
C(36)	1362(1)	-1832(1)	4736(1)	32(1)
C(37)	1604(1)	-2873(1)	5140(1)	37(1)
C(38)	1720(1)	-3855(1)	4768(1)	40(1)
C(39)	1590(1)	-3793(1)	3985(1)	39(1)
C(40)	1328(1)	-2764(1)	3567(1)	32(1)

---

---

**Table 3.** Bond lengths [Å] and angles [°] for liu14.

N(1)-B(1)	1.4079(18)
N(1)-C(1)	1.4755(16)
N(1)-C(5)	1.5097(17)
N(2)-C(15)	1.4161(15)
N(2)-C(9)	1.4224(15)
N(2)-B(1)	1.4846(17)
N(3)-B(2)	1.4047(18)
N(3)-C(21)	1.4767(16)
N(3)-C(25)	1.5056(16)
N(4)-C(35)	1.4142(16)
N(4)-C(29)	1.4178(16)
N(4)-B(2)	1.4780(17)
B(1)-C(4)	1.582(2)
B(2)-C(24)	1.590(2)
C(1)-C(2)	1.477(2)
C(1)-H(1A)	0.987(17)
C(1)-H(1B)	1.004(16)
C(2)-C(3)	1.316(2)
C(2)-H(2)	0.99(2)
C(3)-C(4)	1.482(2)
C(3)-H(3)	0.99(2)
C(4)-H(4A)	1.002(19)
C(4)-H(4B)	0.98(2)
C(5)-C(6)	1.531(2)
C(5)-C(7)	1.5353(19)
C(5)-C(8)	1.5384(19)
C(6)-H(6A)	0.990(18)
C(6)-H(6B)	1.012(17)
C(6)-H(6C)	0.986(17)
C(7)-H(7A)	1.013(19)
C(7)-H(7B)	0.994(18)
C(7)-H(7C)	0.974(17)

C(8)-H(8A)	0.994(19)
C(8)-H(8B)	1.009(18)
C(8)-H(8C)	0.987(16)
C(9)-C(10)	1.3947(18)
C(9)-C(14)	1.3982(18)
C(10)-C(11)	1.3864(18)
C(10)-H(10)	0.989(14)
C(11)-C(12)	1.383(2)
C(11)-H(11)	0.967(16)
C(12)-C(13)	1.387(2)
C(12)-H(12)	0.966(16)
C(13)-C(14)	1.3861(19)
C(13)-H(13)	0.974(16)
C(14)-H(14)	0.996(16)
C(15)-C(16)	1.3957(18)
C(15)-C(20)	1.3992(18)
C(16)-C(17)	1.3888(18)
C(16)-H(16)	0.975(15)
C(17)-C(18)	1.3836(19)
C(17)-H(17)	0.994(14)
C(18)-C(19)	1.387(2)
C(18)-H(18)	0.987(16)
C(19)-C(20)	1.3859(19)
C(19)-H(19)	0.989(16)
C(20)-H(20)	0.985(14)
C(21)-C(22)	1.493(2)
C(21)-H(21A)	0.997(15)
C(21)-H(21B)	1.004(16)
C(22)-C(23)	1.319(2)
C(22)-H(22)	0.967(17)
C(23)-C(24)	1.493(2)
C(23)-H(23)	0.996(19)
C(24)-H(24A)	1.014(19)
C(24)-H(24B)	0.987(19)

C(25)-C(26)	1.526(2)
C(25)-C(27)	1.529(2)
C(25)-C(28)	1.5415(19)
C(26)-H(26A)	1.016(19)
C(26)-H(26B)	0.980(19)
C(26)-H(26C)	1.000(19)
C(27)-H(27A)	1.02(2)
C(27)-H(27B)	0.986(18)
C(27)-H(27C)	1.01(2)
C(28)-H(28A)	1.009(18)
C(28)-H(28B)	0.990(18)
C(28)-H(28C)	1.000(18)
C(29)-C(30)	1.395(2)
C(29)-C(34)	1.3988(19)
C(30)-C(31)	1.389(2)
C(30)-H(30)	0.974(15)
C(31)-C(32)	1.379(2)
C(31)-H(31)	0.996(18)
C(32)-C(33)	1.383(3)
C(32)-H(32)	0.962(18)
C(33)-C(34)	1.384(2)
C(33)-H(33)	0.968(18)
C(34)-H(34)	0.992(16)
C(35)-C(36)	1.3953(19)
C(35)-C(40)	1.3980(18)
C(36)-C(37)	1.3851(19)
C(36)-H(36)	0.981(16)
C(37)-C(38)	1.380(2)
C(37)-H(37)	0.997(17)
C(38)-C(39)	1.383(2)
C(38)-H(38)	0.995(16)
C(39)-C(40)	1.387(2)
C(39)-H(39)	0.964(17)
C(40)-H(40)	0.975(15)

B(1)-N(1)-C(1)	119.60(11)
B(1)-N(1)-C(5)	127.08(11)
C(1)-N(1)-C(5)	113.23(10)
C(15)-N(2)-C(9)	118.89(10)
C(15)-N(2)-B(1)	120.95(10)
C(9)-N(2)-B(1)	118.97(10)
B(2)-N(3)-C(21)	118.87(11)
B(2)-N(3)-C(25)	128.29(11)
C(21)-N(3)-C(25)	112.83(10)
C(35)-N(4)-C(29)	119.58(10)
C(35)-N(4)-B(2)	118.00(10)
C(29)-N(4)-B(2)	121.41(11)
N(1)-B(1)-N(2)	123.16(12)
N(1)-B(1)-C(4)	119.62(12)
N(2)-B(1)-C(4)	117.14(12)
N(3)-B(2)-N(4)	123.75(12)
N(3)-B(2)-C(24)	118.66(12)
N(4)-B(2)-C(24)	117.48(12)
N(1)-C(1)-C(2)	115.51(12)
N(1)-C(1)-H(1A)	110.2(10)
C(2)-C(1)-H(1A)	107.5(9)
N(1)-C(1)-H(1B)	109.2(9)
C(2)-C(1)-H(1B)	108.6(9)
H(1A)-C(1)-H(1B)	105.3(12)
C(3)-C(2)-C(1)	125.43(15)
C(3)-C(2)-H(2)	120.3(13)
C(1)-C(2)-H(2)	114.3(13)
C(2)-C(3)-C(4)	121.91(15)
C(2)-C(3)-H(3)	118.6(12)
C(4)-C(3)-H(3)	119.5(12)
C(3)-C(4)-B(1)	111.52(12)
C(3)-C(4)-H(4A)	105.7(10)
B(1)-C(4)-H(4A)	110.2(11)

C(3)-C(4)-H(4B)	111.6(12)
B(1)-C(4)-H(4B)	113.4(11)
H(4A)-C(4)-H(4B)	103.9(15)
N(1)-C(5)-C(6)	109.57(10)
N(1)-C(5)-C(7)	111.01(11)
C(6)-C(5)-C(7)	111.47(13)
N(1)-C(5)-C(8)	111.04(11)
C(6)-C(5)-C(8)	106.47(12)
C(7)-C(5)-C(8)	107.17(11)
C(5)-C(6)-H(6A)	110.9(10)
C(5)-C(6)-H(6B)	110.1(10)
H(6A)-C(6)-H(6B)	109.8(13)
C(5)-C(6)-H(6C)	108.1(9)
H(6A)-C(6)-H(6C)	109.3(13)
H(6B)-C(6)-H(6C)	108.6(13)
C(5)-C(7)-H(7A)	111.3(10)
C(5)-C(7)-H(7B)	108.6(10)
H(7A)-C(7)-H(7B)	108.4(14)
C(5)-C(7)-H(7C)	113.3(9)
H(7A)-C(7)-H(7C)	107.3(13)
H(7B)-C(7)-H(7C)	107.8(13)
C(5)-C(8)-H(8A)	108.9(10)
C(5)-C(8)-H(8B)	112.6(10)
H(8A)-C(8)-H(8B)	106.4(14)
C(5)-C(8)-H(8C)	112.6(9)
H(8A)-C(8)-H(8C)	108.3(14)
H(8B)-C(8)-H(8C)	107.8(14)
C(10)-C(9)-C(14)	118.64(12)
C(10)-C(9)-N(2)	119.54(11)
C(14)-C(9)-N(2)	121.80(12)
C(11)-C(10)-C(9)	120.74(13)
C(11)-C(10)-H(10)	119.9(8)
C(9)-C(10)-H(10)	119.4(8)
C(12)-C(11)-C(10)	120.31(14)

C(12)-C(11)-H(11)	121.4(9)
C(10)-C(11)-H(11)	118.3(9)
C(11)-C(12)-C(13)	119.40(13)
C(11)-C(12)-H(12)	121.4(10)
C(13)-C(12)-H(12)	119.2(10)
C(14)-C(13)-C(12)	120.71(14)
C(14)-C(13)-H(13)	119.2(9)
C(12)-C(13)-H(13)	120.1(9)
C(13)-C(14)-C(9)	120.18(13)
C(13)-C(14)-H(14)	120.3(9)
C(9)-C(14)-H(14)	119.5(9)
C(16)-C(15)-C(20)	118.10(11)
C(16)-C(15)-N(2)	119.38(11)
C(20)-C(15)-N(2)	122.52(11)
C(17)-C(16)-C(15)	120.72(12)
C(17)-C(16)-H(16)	120.6(9)
C(15)-C(16)-H(16)	118.7(9)
C(18)-C(17)-C(16)	120.77(13)
C(18)-C(17)-H(17)	120.7(8)
C(16)-C(17)-H(17)	118.5(8)
C(17)-C(18)-C(19)	118.90(12)
C(17)-C(18)-H(18)	120.4(9)
C(19)-C(18)-H(18)	120.7(9)
C(20)-C(19)-C(18)	120.76(13)
C(20)-C(19)-H(19)	118.0(9)
C(18)-C(19)-H(19)	121.2(9)
C(19)-C(20)-C(15)	120.69(12)
C(19)-C(20)-H(20)	119.2(8)
C(15)-C(20)-H(20)	120.0(8)
N(3)-C(21)-C(22)	114.71(11)
N(3)-C(21)-H(21A)	111.1(9)
C(22)-C(21)-H(21A)	107.4(8)
N(3)-C(21)-H(21B)	108.9(9)
C(22)-C(21)-H(21B)	108.9(9)

H(21A)-C(21)-H(21B)	105.3(12)
C(23)-C(22)-C(21)	123.68(14)
C(23)-C(22)-H(22)	121.6(10)
C(21)-C(22)-H(22)	114.6(10)
C(22)-C(23)-C(24)	120.89(14)
C(22)-C(23)-H(23)	118.2(11)
C(24)-C(23)-H(23)	120.9(11)
C(23)-C(24)-B(2)	109.38(12)
C(23)-C(24)-H(24A)	108.4(11)
B(2)-C(24)-H(24A)	110.1(11)
C(23)-C(24)-H(24B)	111.0(11)
B(2)-C(24)-H(24B)	111.3(11)
H(24A)-C(24)-H(24B)	106.6(15)
N(3)-C(25)-C(26)	111.31(11)
N(3)-C(25)-C(27)	110.97(12)
C(26)-C(25)-C(27)	109.82(13)
N(3)-C(25)-C(28)	109.18(11)
C(26)-C(25)-C(28)	106.13(13)
C(27)-C(25)-C(28)	109.29(13)
C(25)-C(26)-H(26A)	109.5(10)
C(25)-C(26)-H(26B)	113.3(11)
H(26A)-C(26)-H(26B)	108.6(14)
C(25)-C(26)-H(26C)	108.7(10)
H(26A)-C(26)-H(26C)	107.8(15)
H(26B)-C(26)-H(26C)	108.8(14)
C(25)-C(27)-H(27A)	111.8(11)
C(25)-C(27)-H(27B)	111.3(10)
H(27A)-C(27)-H(27B)	109.4(15)
C(25)-C(27)-H(27C)	109.1(11)
H(27A)-C(27)-H(27C)	107.3(15)
H(27B)-C(27)-H(27C)	107.7(14)
C(25)-C(28)-H(28A)	112.1(10)
C(25)-C(28)-H(28B)	108.8(10)
H(28A)-C(28)-H(28B)	108.3(14)

C(25)-C(28)-H(28C)	113.2(10)
H(28A)-C(28)-H(28C)	106.7(14)
H(28B)-C(28)-H(28C)	107.5(13)
C(30)-C(29)-C(34)	118.68(13)
C(30)-C(29)-N(4)	119.71(12)
C(34)-C(29)-N(4)	121.59(13)
C(31)-C(30)-C(29)	120.64(14)
C(31)-C(30)-H(30)	120.8(9)
C(29)-C(30)-H(30)	118.6(9)
C(32)-C(31)-C(30)	120.21(16)
C(32)-C(31)-H(31)	122.5(10)
C(30)-C(31)-H(31)	117.3(10)
C(31)-C(32)-C(33)	119.56(15)
C(31)-C(32)-H(32)	120.8(11)
C(33)-C(32)-H(32)	119.6(11)
C(34)-C(33)-C(32)	120.88(15)
C(34)-C(33)-H(33)	118.4(11)
C(32)-C(33)-H(33)	120.6(11)
C(33)-C(34)-C(29)	120.00(15)
C(33)-C(34)-H(34)	121.4(9)
C(29)-C(34)-H(34)	118.6(9)
C(36)-C(35)-C(40)	118.50(12)
C(36)-C(35)-N(4)	118.65(11)
C(40)-C(35)-N(4)	122.82(12)
C(37)-C(36)-C(35)	120.70(13)
C(37)-C(36)-H(36)	119.8(9)
C(35)-C(36)-H(36)	119.5(9)
C(38)-C(37)-C(36)	120.42(14)
C(38)-C(37)-H(37)	120.0(10)
C(36)-C(37)-H(37)	119.5(10)
C(37)-C(38)-C(39)	119.40(14)
C(37)-C(38)-H(38)	119.2(9)
C(39)-C(38)-H(38)	121.4(9)
C(38)-C(39)-C(40)	120.80(14)

C(38)-C(39)-H(39)	120.9(10)
C(40)-C(39)-H(39)	118.3(10)
C(39)-C(40)-C(35)	120.13(14)
C(39)-C(40)-H(40)	119.5(9)
C(35)-C(40)-H(40)	120.4(9)

---

Symmetry transformations used to generate equivalent atoms:

**Table 4. Anisotropic displacement parameters ( $\text{\AA}^2 \times 10^3$ ) for liu14. The anisotropic displacement factor exponent takes the form:  $-2p^2 [ h^2 a^*{}^2 U_{11} + \dots + 2 h k a^* b^* U_{12} ]$**

	U <sub>11</sub>	U <sub>22</sub>	U <sub>33</sub>	U <sub>23</sub>	U <sub>13</sub>	U <sub>12</sub>
N(1)	25(1)	24(1)	27(1)	5(1)	11(1)	3(1)
N(2)	28(1)	22(1)	27(1)	4(1)	13(1)	1(1)
N(3)	22(1)	24(1)	29(1)	0(1)	10(1)	3(1)
N(4)	31(1)	22(1)	30(1)	2(1)	14(1)	3(1)
B(1)	26(1)	28(1)	21(1)	4(1)	9(1)	1(1)
B(2)	25(1)	26(1)	25(1)	2(1)	9(1)	3(1)
C(1)	36(1)	31(1)	34(1)	10(1)	16(1)	10(1)
C(2)	26(1)	49(1)	74(1)	29(1)	12(1)	9(1)
C(3)	24(1)	49(1)	67(1)	22(1)	6(1)	-4(1)
C(4)	30(1)	31(1)	50(1)	2(1)	16(1)	-2(1)
C(5)	33(1)	22(1)	33(1)	0(1)	13(1)	-4(1)
C(6)	31(1)	30(1)	42(1)	-2(1)	6(1)	-4(1)
C(7)	45(1)	32(1)	43(1)	-4(1)	24(1)	-11(1)
C(8)	52(1)	28(1)	35(1)	-2(1)	19(1)	0(1)
C(9)	28(1)	20(1)	27(1)	-1(1)	12(1)	-2(1)
C(10)	28(1)	25(1)	28(1)	0(1)	11(1)	-1(1)
C(11)	39(1)	29(1)	28(1)	3(1)	12(1)	-3(1)
C(12)	45(1)	37(1)	39(1)	4(1)	26(1)	-4(1)
C(13)	33(1)	36(1)	48(1)	4(1)	23(1)	1(1)
C(14)	29(1)	28(1)	32(1)	3(1)	11(1)	1(1)
C(15)	22(1)	21(1)	26(1)	2(1)	7(1)	-2(1)
C(16)	28(1)	24(1)	28(1)	0(1)	11(1)	-1(1)
C(17)	33(1)	28(1)	28(1)	3(1)	11(1)	-4(1)
C(18)	33(1)	22(1)	33(1)	5(1)	6(1)	-2(1)
C(19)	36(1)	23(1)	35(1)	-3(1)	11(1)	1(1)
C(20)	33(1)	26(1)	27(1)	-1(1)	11(1)	-1(1)
C(21)	28(1)	30(1)	35(1)	0(1)	12(1)	7(1)
C(22)	25(1)	42(1)	40(1)	2(1)	10(1)	7(1)

C(23)	27(1)	44(1)	46(1)	-2(1)	13(1)	-3(1)
C(24)	35(1)	30(1)	54(1)	3(1)	22(1)	-1(1)
C(25)	27(1)	24(1)	40(1)	-5(1)	13(1)	-2(1)
C(26)	26(1)	34(1)	58(1)	-13(1)	8(1)	-1(1)
C(27)	48(1)	33(1)	55(1)	0(1)	28(1)	-8(1)
C(28)	38(1)	33(1)	52(1)	-15(1)	16(1)	-4(1)
C(29)	33(1)	20(1)	30(1)	-2(1)	14(1)	-2(1)
C(30)	38(1)	27(1)	32(1)	-1(1)	14(1)	-1(1)
C(31)	58(1)	33(1)	33(1)	2(1)	16(1)	-1(1)
C(32)	75(1)	39(1)	44(1)	2(1)	38(1)	-5(1)
C(33)	53(1)	37(1)	57(1)	-4(1)	37(1)	-4(1)
C(34)	36(1)	29(1)	42(1)	-2(1)	20(1)	-1(1)
C(35)	24(1)	22(1)	33(1)	1(1)	11(1)	1(1)
C(36)	34(1)	29(1)	35(1)	1(1)	16(1)	6(1)
C(37)	39(1)	39(1)	38(1)	10(1)	18(1)	10(1)
C(38)	39(1)	30(1)	53(1)	13(1)	21(1)	9(1)
C(39)	43(1)	23(1)	52(1)	-1(1)	22(1)	5(1)
C(40)	37(1)	25(1)	35(1)	-3(1)	15(1)	1(1)

*Crystallographic data for 4.*

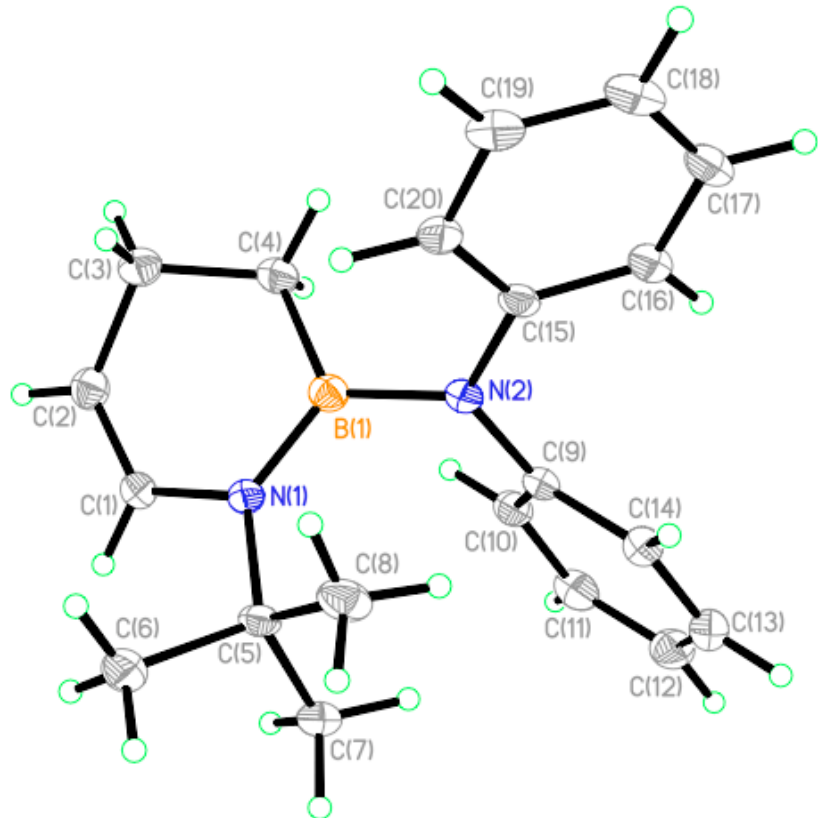


**Table 1. Crystal data and structure refinement for liur21.**

Identification code	liur21
Empirical formula	C <sub>20</sub> H <sub>25</sub> B <sub>1</sub> N <sub>2</sub>
Formula weight	304.23
Temperature	173(2) K
Wavelength	0.71073 Å
Crystal system	Triclinic
Space group	P-1

Unit cell dimensions	$a = 10.1761(11) \text{ \AA}$	$a = 81.469(2)^\circ$
	$b = 11.5744(12) \text{ \AA}$	$b = 83.033(2)^\circ$
	$c = 15.4369(16) \text{ \AA}$	$\gamma = 74.388(2)^\circ$
Volume	$1725.4(3) \text{ \AA}^3$	
Z	4	
Density (calculated)	$1.171 \text{ Mg/m}^3$	
Absorption coefficient	$0.068 \text{ mm}^{-1}$	
F(000)	656	
Crystal size	$0.18 \times 0.15 \times 0.09 \text{ mm}^3$	
Theta range for data collection	1.34 to 25.00°	
Index ranges	$-12 \leq h \leq 12, -13 \leq k \leq 13, -18 \leq l \leq 18$	
Reflections collected	16399	
Independent reflections	6056 [ $R(\text{int}) = 0.0448$ ]	
Completeness to theta = 25.00°	99.7 %	
Absorption correction	Semi-empirical from equivalents	
Max. and min. transmission	0.9939 and 0.9879	
Refinement method	Full-matrix least-squares on $F^2$	
Data / restraints / parameters	6056 / 0 / 599	
Goodness-of-fit on $F^2$	1.028	
Final R indices [ $I > 2\sigma(I)$ ]	$R_1 = 0.0557, wR_2 = 0.1184$	
R indices (all data)	$R_1 = 0.0921, wR_2 = 0.1349$	
Largest diff. peak and hole	0.390 and -0.321 e.Å <sup>-3</sup>	

**Table 2.** Atomic coordinates ( $\times 10^4$ ) and equivalent isotropic displacement parameters ( $\text{\AA}^2 \times 10^3$ ) for liur21. U(eq) is defined as one third of the trace of the orthogonalized  $U^{ij}$  tensor.

	x	y	z	U(eq)
N(1)	1290(2)	10384(2)	1439(1)	26(1)
N(2)	942(2)	12229(2)	2246(1)	29(1)
N(3)	4037(2)	4391(2)	3522(1)	27(1)
N(4)	4396(2)	6387(2)	2744(1)	30(1)
B(1)	1560(3)	11500(2)	1520(2)	29(1)
B(2)	3888(3)	5655(3)	3501(2)	33(1)
C(1)	2255(2)	9619(2)	879(2)	30(1)
C(2)	3041(3)	10016(2)	223(2)	36(1)
C(3)	2938(3)	11338(2)	4(2)	42(1)
C(4)	2684(3)	11915(2)	840(2)	37(1)
C(5)	137(2)	9858(2)	1890(2)	29(1)
C(6)	-292(3)	9137(3)	1270(2)	39(1)
C(7)	589(3)	9023(3)	2723(2)	39(1)
C(8)	-1115(3)	10878(3)	2100(2)	41(1)
C(9)	1187(2)	11707(2)	3127(2)	29(1)
C(10)	2445(3)	10911(2)	3288(2)	33(1)
C(11)	2705(3)	10332(2)	4128(2)	42(1)
C(12)	1717(3)	10573(3)	4816(2)	45(1)
C(13)	471(3)	11374(2)	4666(2)	43(1)
C(14)	191(3)	11935(2)	3825(2)	35(1)
C(15)	247(2)	13462(2)	2066(2)	28(1)
C(16)	155(3)	14306(2)	2645(2)	33(1)
C(17)	-572(3)	15492(2)	2453(2)	38(1)
C(18)	-1200(3)	15882(2)	1680(2)	40(1)
C(19)	-1072(3)	15062(2)	1094(2)	39(1)
C(20)	-381(2)	13864(2)	1279(2)	32(1)

C(21)	3009(3)	3918(2)	4056(2)	32(1)
C(22)	2018(3)	4535(2)	4556(2)	42(1)
C(23)	1858(4)	5835(3)	4629(2)	74(1)
C(24)	3064(4)	6242(3)	4322(2)	65(1)
C(25)	5147(2)	3472(2)	3076(2)	30(1)
C(26)	5622(3)	2361(3)	3742(2)	41(1)
C(27)	4620(3)	3108(3)	2301(2)	40(1)
C(28)	6390(3)	3966(3)	2765(2)	43(1)
C(29)	4053(2)	6346(2)	1885(2)	27(1)
C(30)	2797(3)	6149(2)	1771(2)	32(1)
C(31)	2448(3)	6102(2)	939(2)	37(1)
C(32)	3318(3)	6278(2)	205(2)	40(1)
C(33)	4571(3)	6470(2)	313(2)	37(1)
C(34)	4949(3)	6488(2)	1138(2)	32(1)
C(35)	5074(2)	7261(2)	2882(2)	28(1)
C(36)	4997(3)	8343(2)	2329(2)	31(1)
C(37)	5685(3)	9151(2)	2500(2)	35(1)
C(38)	6419(3)	8933(2)	3225(2)	39(1)
C(39)	6489(3)	7873(2)	3783(2)	41(1)
C(40)	5839(3)	7037(2)	3605(2)	37(1)

---

---

**Table 3.** Bond lengths [Å] and angles [°] for liur21.

N(1)-B(1)	1.417(3)
N(1)-C(1)	1.432(3)
N(1)-C(5)	1.514(3)
N(2)-C(15)	1.414(3)
N(2)-C(9)	1.426(3)
N(2)-B(1)	1.480(3)
N(3)-B(2)	1.426(3)
N(3)-C(21)	1.428(3)
N(3)-C(25)	1.504(3)
N(4)-C(35)	1.420(3)
N(4)-C(29)	1.422(3)
N(4)-B(2)	1.465(3)
B(1)-C(4)	1.579(4)
B(2)-C(24)	1.568(4)
C(1)-C(2)	1.319(3)
C(1)-H(1)	0.94(2)
C(2)-C(3)	1.494(4)
C(2)-H(2)	0.98(2)
C(3)-C(4)	1.504(4)
C(3)-H(3A)	0.97(3)
C(3)-H(3B)	1.08(3)
C(4)-H(4A)	0.98(3)
C(4)-H(4B)	1.08(3)
C(5)-C(8)	1.525(4)
C(5)-C(6)	1.528(3)
C(5)-C(7)	1.529(3)
C(6)-H(6A)	1.00(3)
C(6)-H(6B)	0.98(3)
C(6)-H(6C)	1.00(3)
C(7)-H(7A)	1.00(3)
C(7)-H(7B)	1.01(3)
C(7)-H(7C)	1.02(3)

C(8)-H(8A)	0.97(3)
C(8)-H(8B)	0.97(3)
C(8)-H(8C)	0.98(3)
C(9)-C(10)	1.387(3)
C(9)-C(14)	1.390(3)
C(10)-C(11)	1.389(4)
C(10)-H(10)	0.98(2)
C(11)-C(12)	1.376(4)
C(11)-H(11)	0.95(3)
C(12)-C(13)	1.376(4)
C(12)-H(12)	0.94(3)
C(13)-C(14)	1.389(4)
C(13)-H(13)	0.96(3)
C(14)-H(14)	0.99(2)
C(15)-C(16)	1.397(3)
C(15)-C(20)	1.400(3)
C(16)-C(17)	1.381(3)
C(16)-H(16)	1.00(3)
C(17)-C(18)	1.381(4)
C(17)-H(17)	0.97(3)
C(18)-C(19)	1.377(4)
C(18)-H(18)	0.97(3)
C(19)-C(20)	1.380(3)
C(19)-H(19)	0.96(2)
C(20)-H(20)	1.00(2)
C(21)-C(22)	1.308(3)
C(21)-H(21)	1.01(2)
C(22)-C(23)	1.488(4)
C(22)-H(22)	0.93(3)
C(23)-C(24)	1.435(4)
C(23)-H(23B)	0.9900
C(23)-H(23A)	0.9900
C(24)-H(24A)	0.9900
C(24)-H(24B)	0.9900

C(25)-C(28)	1.523(3)
C(25)-C(27)	1.524(3)
C(25)-C(26)	1.529(3)
C(26)-H(26A)	0.97(3)
C(26)-H(26B)	0.98(3)
C(26)-H(26C)	0.94(3)
C(27)-H(27A)	1.03(3)
C(27)-H(27B)	0.97(3)
C(27)-H(27C)	0.97(3)
C(28)-H(28A)	0.98(3)
C(28)-H(28B)	1.02(3)
C(28)-H(28C)	0.99(3)
C(29)-C(30)	1.393(3)
C(29)-C(34)	1.399(3)
C(30)-C(31)	1.386(3)
C(30)-H(30)	0.98(3)
C(31)-C(32)	1.376(4)
C(31)-H(31)	0.93(2)
C(32)-C(33)	1.386(4)
C(32)-H(32)	0.98(3)
C(33)-C(34)	1.380(3)
C(33)-H(33)	0.98(3)
C(34)-H(34)	0.98(2)
C(35)-C(40)	1.392(3)
C(35)-C(36)	1.396(3)
C(36)-C(37)	1.381(3)
C(36)-H(36)	0.98(3)
C(37)-C(38)	1.375(4)
C(37)-H(37)	0.94(3)
C(38)-C(39)	1.381(3)
C(38)-H(38)	0.98(2)
C(39)-C(40)	1.384(3)
C(39)-H(39)	0.97(3)
C(40)-H(40)	0.96(3)

B(1)-N(1)-C(1)	116.37(19)
B(1)-N(1)-C(5)	128.94(19)
C(1)-N(1)-C(5)	114.65(18)
C(15)-N(2)-C(9)	120.36(19)
C(15)-N(2)-B(1)	120.49(19)
C(9)-N(2)-B(1)	118.80(19)
B(2)-N(3)-C(21)	115.9(2)
B(2)-N(3)-C(25)	129.13(19)
C(21)-N(3)-C(25)	114.99(18)
C(35)-N(4)-C(29)	119.51(18)
C(35)-N(4)-B(2)	119.7(2)
C(29)-N(4)-B(2)	120.26(18)
N(1)-B(1)-N(2)	123.6(2)
N(1)-B(1)-C(4)	117.3(2)
N(2)-B(1)-C(4)	118.9(2)
N(3)-B(2)-N(4)	122.7(2)
N(3)-B(2)-C(24)	115.8(2)
N(4)-B(2)-C(24)	121.3(2)
C(2)-C(1)-N(1)	124.0(2)
C(2)-C(1)-H(1)	118.6(14)
N(1)-C(1)-H(1)	117.4(13)
C(1)-C(2)-C(3)	120.6(2)
C(1)-C(2)-H(2)	118.8(14)
C(3)-C(2)-H(2)	120.6(14)
C(2)-C(3)-C(4)	109.3(2)
C(2)-C(3)-H(3A)	108.1(17)
C(4)-C(3)-H(3A)	112.2(16)
C(2)-C(3)-H(3B)	108.7(15)
C(4)-C(3)-H(3B)	106.1(15)
H(3A)-C(3)-H(3B)	112(2)
C(3)-C(4)-B(1)	113.8(2)
C(3)-C(4)-H(4A)	113.7(15)
B(1)-C(4)-H(4A)	110.2(15)

C(3)-C(4)-H(4B)	104.6(14)
B(1)-C(4)-H(4B)	107.2(14)
H(4A)-C(4)-H(4B)	107(2)
N(1)-C(5)-C(8)	109.68(19)
N(1)-C(5)-C(6)	109.98(19)
C(8)-C(5)-C(6)	106.7(2)
N(1)-C(5)-C(7)	110.57(19)
C(8)-C(5)-C(7)	110.9(2)
C(6)-C(5)-C(7)	108.9(2)
C(5)-C(6)-H(6A)	112.3(16)
C(5)-C(6)-H(6B)	108.7(15)
H(6A)-C(6)-H(6B)	110(2)
C(5)-C(6)-H(6C)	112.0(14)
H(6A)-C(6)-H(6C)	111(2)
H(6B)-C(6)-H(6C)	102(2)
C(5)-C(7)-H(7A)	110.4(15)
C(5)-C(7)-H(7B)	112.7(15)
H(7A)-C(7)-H(7B)	109(2)
C(5)-C(7)-H(7C)	110.2(14)
H(7A)-C(7)-H(7C)	108(2)
H(7B)-C(7)-H(7C)	106(2)
C(5)-C(8)-H(8A)	109.1(16)
C(5)-C(8)-H(8B)	110.8(18)
H(8A)-C(8)-H(8B)	104(2)
C(5)-C(8)-H(8C)	112.8(17)
H(8A)-C(8)-H(8C)	109(2)
H(8B)-C(8)-H(8C)	110(2)
C(10)-C(9)-C(14)	118.9(2)
C(10)-C(9)-N(2)	118.9(2)
C(14)-C(9)-N(2)	122.2(2)
C(9)-C(10)-C(11)	120.9(3)
C(9)-C(10)-H(10)	123.4(14)
C(11)-C(10)-H(10)	115.7(14)
C(12)-C(11)-C(10)	119.8(3)

C(12)-C(11)-H(11)	121.2(16)
C(10)-C(11)-H(11)	119.0(16)
C(13)-C(12)-C(11)	119.8(3)
C(13)-C(12)-H(12)	119.4(16)
C(11)-C(12)-H(12)	120.7(16)
C(12)-C(13)-C(14)	120.7(3)
C(12)-C(13)-H(13)	119.7(16)
C(14)-C(13)-H(13)	119.5(16)
C(13)-C(14)-C(9)	119.9(3)
C(13)-C(14)-H(14)	118.6(13)
C(9)-C(14)-H(14)	121.5(13)
C(16)-C(15)-C(20)	118.1(2)
C(16)-C(15)-N(2)	122.6(2)
C(20)-C(15)-N(2)	119.3(2)
C(17)-C(16)-C(15)	120.6(2)
C(17)-C(16)-H(16)	119.4(15)
C(15)-C(16)-H(16)	120.1(15)
C(16)-C(17)-C(18)	121.1(3)
C(16)-C(17)-H(17)	120.3(15)
C(18)-C(17)-H(17)	118.5(15)
C(19)-C(18)-C(17)	118.5(3)
C(19)-C(18)-H(18)	121.1(15)
C(17)-C(18)-H(18)	120.4(15)
C(18)-C(19)-C(20)	121.5(3)
C(18)-C(19)-H(19)	121.4(15)
C(20)-C(19)-H(19)	117.0(15)
C(19)-C(20)-C(15)	120.2(2)
C(19)-C(20)-H(20)	120.5(14)
C(15)-C(20)-H(20)	119.3(14)
C(22)-C(21)-N(3)	125.1(2)
C(22)-C(21)-H(21)	120.9(13)
N(3)-C(21)-H(21)	113.8(13)
C(21)-C(22)-C(23)	122.3(2)
C(21)-C(22)-H(22)	121.2(17)

C(23)-C(22)-H(22)	116.4(17)
C(24)-C(23)-C(22)	113.8(3)
C(24)-C(23)-H(23B)	108.8
C(22)-C(23)-H(23B)	108.8
C(24)-C(23)-H(23A)	108.8
C(22)-C(23)-H(23A)	108.8
H(23B)-C(23)-H(23A)	107.7
C(23)-C(24)-B(2)	113.9(2)
C(23)-C(24)-H(24A)	108.8
B(2)-C(24)-H(24A)	108.8
C(23)-C(24)-H(24B)	108.8
B(2)-C(24)-H(24B)	108.8
H(24A)-C(24)-H(24B)	107.7
N(3)-C(25)-C(28)	110.65(19)
N(3)-C(25)-C(27)	110.6(2)
C(28)-C(25)-C(27)	110.0(2)
N(3)-C(25)-C(26)	108.9(2)
C(28)-C(25)-C(26)	106.8(2)
C(27)-C(25)-C(26)	109.8(2)
C(25)-C(26)-H(26A)	110.7(16)
C(25)-C(26)-H(26B)	114.8(17)
H(26A)-C(26)-H(26B)	111(2)
C(25)-C(26)-H(26C)	109.3(16)
H(26A)-C(26)-H(26C)	106(2)
H(26B)-C(26)-H(26C)	105(2)
C(25)-C(27)-H(27A)	110.8(15)
C(25)-C(27)-H(27B)	112.1(15)
H(27A)-C(27)-H(27B)	106(2)
C(25)-C(27)-H(27C)	108.2(16)
H(27A)-C(27)-H(27C)	109(2)
H(27B)-C(27)-H(27C)	111(2)
C(25)-C(28)-H(28A)	112.7(18)
C(25)-C(28)-H(28B)	113.1(15)
H(28A)-C(28)-H(28B)	109(2)

C(25)-C(28)-H(28C)	111.1(15)
H(28A)-C(28)-H(28C)	106(2)
H(28B)-C(28)-H(28C)	105(2)
C(30)-C(29)-C(34)	118.2(2)
C(30)-C(29)-N(4)	119.9(2)
C(34)-C(29)-N(4)	121.9(2)
C(31)-C(30)-C(29)	120.7(2)
C(31)-C(30)-H(30)	122.0(15)
C(29)-C(30)-H(30)	117.3(15)
C(32)-C(31)-C(30)	120.9(3)
C(32)-C(31)-H(31)	120.7(15)
C(30)-C(31)-H(31)	118.4(15)
C(31)-C(32)-C(33)	118.8(3)
C(31)-C(32)-H(32)	120.7(16)
C(33)-C(32)-H(32)	120.5(16)
C(34)-C(33)-C(32)	121.0(3)
C(34)-C(33)-H(33)	120.6(15)
C(32)-C(33)-H(33)	118.3(15)
C(33)-C(34)-C(29)	120.4(2)
C(33)-C(34)-H(34)	120.8(13)
C(29)-C(34)-H(34)	118.8(13)
C(40)-C(35)-C(36)	118.3(2)
C(40)-C(35)-N(4)	118.7(2)
C(36)-C(35)-N(4)	123.0(2)
C(37)-C(36)-C(35)	120.0(2)
C(37)-C(36)-H(36)	122.4(15)
C(35)-C(36)-H(36)	117.6(15)
C(38)-C(37)-C(36)	121.3(2)
C(38)-C(37)-H(37)	120.9(15)
C(36)-C(37)-H(37)	117.7(15)
C(37)-C(38)-C(39)	119.2(2)
C(37)-C(38)-H(38)	122.2(15)
C(39)-C(38)-H(38)	118.5(15)
C(38)-C(39)-C(40)	120.1(3)

C(38)-C(39)-H(39)	120.8(15)
C(40)-C(39)-H(39)	119.2(15)
C(39)-C(40)-C(35)	121.0(2)
C(39)-C(40)-H(40)	118.1(15)
C(35)-C(40)-H(40)	120.9(15)

---

Symmetry transformations used to generate equivalent atoms:

**Table 4.** Anisotropic displacement parameters ( $\text{\AA}^2 \times 10^3$ ) for liur21. The anisotropic displacement factor exponent takes the form:  $-2p^2 [ h^2 a^*^2 U_{11} + \dots + 2 h k a^* b^* U_{12} ]$

	U <sub>11</sub>	U <sub>22</sub>	U <sub>33</sub>	U <sub>23</sub>	U <sub>13</sub>	U <sub>12</sub>
N(1)	27(1)	27(1)	26(1)	-3(1)	1(1)	-10(1)
N(2)	36(1)	21(1)	29(1)	-2(1)	0(1)	-9(1)
N(3)	32(1)	25(1)	25(1)	-4(1)	3(1)	-14(1)
N(4)	38(1)	23(1)	34(1)	-6(1)	2(1)	-15(1)
B(1)	30(2)	26(2)	30(2)	0(1)	-7(1)	-6(1)
B(2)	39(2)	29(2)	34(2)	-9(1)	4(1)	-15(1)
C(1)	36(2)	26(1)	30(1)	-5(1)	-2(1)	-8(1)
C(2)	36(2)	36(2)	35(2)	-9(1)	4(1)	-9(1)
C(3)	48(2)	42(2)	38(2)	-5(1)	8(1)	-22(1)
C(4)	43(2)	31(2)	39(2)	-4(1)	3(1)	-17(1)
C(5)	31(1)	26(1)	34(1)	-1(1)	1(1)	-14(1)
C(6)	42(2)	42(2)	39(2)	-5(1)	-5(1)	-20(2)
C(7)	48(2)	34(2)	36(2)	2(1)	0(1)	-20(2)
C(8)	31(2)	34(2)	59(2)	-6(2)	8(1)	-13(1)
C(9)	35(1)	23(1)	30(1)	-4(1)	0(1)	-13(1)
C(10)	37(2)	27(1)	38(2)	-4(1)	-2(1)	-11(1)
C(11)	46(2)	32(2)	49(2)	-3(1)	-14(2)	-12(1)
C(12)	64(2)	39(2)	35(2)	3(1)	-12(2)	-19(2)
C(13)	62(2)	36(2)	33(2)	-7(1)	3(2)	-16(2)
C(14)	41(2)	29(1)	34(2)	-5(1)	2(1)	-9(1)
C(15)	27(1)	24(1)	33(1)	-2(1)	2(1)	-12(1)
C(16)	34(2)	27(1)	38(2)	-3(1)	-2(1)	-11(1)
C(17)	39(2)	25(1)	51(2)	-5(1)	-2(1)	-12(1)
C(18)	33(2)	26(2)	61(2)	4(1)	-4(1)	-9(1)
C(19)	36(2)	37(2)	43(2)	9(1)	-7(1)	-14(1)
C(20)	34(1)	32(1)	33(2)	-1(1)	1(1)	-16(1)
C(21)	41(2)	26(1)	30(1)	-1(1)	1(1)	-16(1)
C(22)	44(2)	36(2)	46(2)	-5(1)	14(1)	-18(1)

C(23)	85(3)	47(2)	90(3)	-31(2)	48(2)	-29(2)
C(24)	94(3)	38(2)	68(2)	-26(2)	39(2)	-35(2)
C(25)	34(1)	23(1)	34(1)	-6(1)	1(1)	-8(1)
C(26)	49(2)	28(2)	45(2)	-2(1)	-4(2)	-6(1)
C(27)	50(2)	34(2)	37(2)	-11(1)	-2(1)	-9(1)
C(28)	38(2)	32(2)	60(2)	-9(2)	9(2)	-11(1)
C(29)	32(1)	20(1)	32(1)	-5(1)	2(1)	-10(1)
C(30)	34(2)	24(1)	40(2)	-6(1)	1(1)	-10(1)
C(31)	32(2)	32(2)	51(2)	-10(1)	-5(1)	-12(1)
C(32)	46(2)	37(2)	41(2)	-12(1)	-5(1)	-13(1)
C(33)	44(2)	35(2)	35(2)	-10(1)	5(1)	-16(1)
C(34)	32(2)	27(1)	39(2)	-10(1)	0(1)	-12(1)
C(35)	30(1)	22(1)	35(1)	-7(1)	2(1)	-10(1)
C(36)	33(1)	24(1)	36(2)	-5(1)	-2(1)	-9(1)
C(37)	40(2)	25(1)	40(2)	0(1)	0(1)	-15(1)
C(38)	47(2)	34(2)	43(2)	-6(1)	-3(1)	-23(1)
C(39)	56(2)	36(2)	39(2)	-2(1)	-13(1)	-21(1)
C(40)	51(2)	28(1)	35(2)	1(1)	-6(1)	-16(1)

---

**Table 5.** Hydrogen coordinates ( $\times 10^4$ ) and isotropic displacement parameters ( $\text{\AA}^2 \times 10^3$ ) for liur21.

	x	y	z	U(eq)
H(23B)	1093	6326	4286	89
H(23A)	1608	5973	5252	89
H(24A)	3672	6059	4806	78
H(24B)	2795	7131	4169	78
H(1)	2330(20)	8780(20)	991(14)	29(6)
H(2)	3680(20)	9430(20)	-122(15)	38(7)
H(3A)	3780(30)	11430(20)	-332(18)	61(9)
H(3B)	2050(30)	11750(30)	-356(18)	62(9)
H(4A)	2480(30)	12800(20)	745(16)	48(8)
H(4B)	3650(30)	11600(20)	1138(17)	59(8)
H(6A)	440(30)	8410(30)	1135(18)	65(9)
H(6B)	-1120(30)	8910(20)	1537(16)	48(8)
H(6C)	-620(30)	9650(20)	716(17)	45(7)
H(7A)	1450(30)	8400(30)	2587(17)	53(8)
H(7B)	740(30)	9470(20)	3198(18)	53(8)
H(7C)	-150(30)	8600(20)	2982(15)	42(7)
H(8A)	-1910(30)	10550(20)	2251(17)	57(8)
H(8B)	-1340(30)	11450(30)	1580(20)	65(10)
H(8C)	-1000(30)	11290(30)	2586(19)	59(9)
H(10)	3200(20)	10720(20)	2831(16)	39(7)
H(11)	3580(30)	9790(20)	4218(16)	47(8)
H(12)	1880(30)	10190(20)	5388(17)	46(8)
H(13)	-220(30)	11530(20)	5144(17)	47(8)
H(14)	-740(20)	12460(20)	3734(15)	34(7)
H(16)	640(30)	14060(20)	3193(17)	48(8)
H(17)	-670(20)	16070(20)	2872(16)	42(7)
H(18)	-1730(30)	16710(20)	1559(16)	42(7)
H(19)	-1480(20)	15290(20)	545(16)	40(7)

H(20)	-310(20)	13280(20)	849(15)	36(7)
H(21)	3060(20)	3050(20)	3982(14)	36(6)
H(22)	1350(30)	4190(20)	4873(17)	55(8)
H(26A)	5880(30)	2590(20)	4264(18)	53(8)
H(26B)	4970(30)	1860(30)	3900(18)	59(9)
H(26C)	6420(30)	1840(20)	3497(17)	49(8)
H(27A)	3750(30)	2810(30)	2498(18)	62(9)
H(27B)	4360(20)	3780(20)	1849(17)	41(7)
H(27C)	5330(30)	2460(30)	2066(18)	57(9)
H(28A)	6200(30)	4640(30)	2290(20)	73(10)
H(28B)	6770(30)	4240(20)	3260(18)	56(9)
H(28C)	7160(30)	3340(20)	2525(16)	47(8)
H(30)	2160(30)	6090(20)	2299(17)	45(7)
H(31)	1600(30)	5960(20)	888(15)	40(7)
H(32)	3070(30)	6240(20)	-381(18)	54(8)
H(33)	5200(30)	6570(20)	-209(17)	45(7)
H(34)	5850(20)	6580(20)	1214(14)	30(6)
H(36)	4430(30)	8500(20)	1833(17)	47(8)
H(37)	5610(30)	9880(20)	2115(16)	45(7)
H(38)	6890(30)	9510(20)	3365(16)	45(7)
H(39)	6990(30)	7700(20)	4304(17)	46(8)
H(40)	5960(30)	6290(20)	3981(17)	48(8)

**Crystallographic data for 5.**

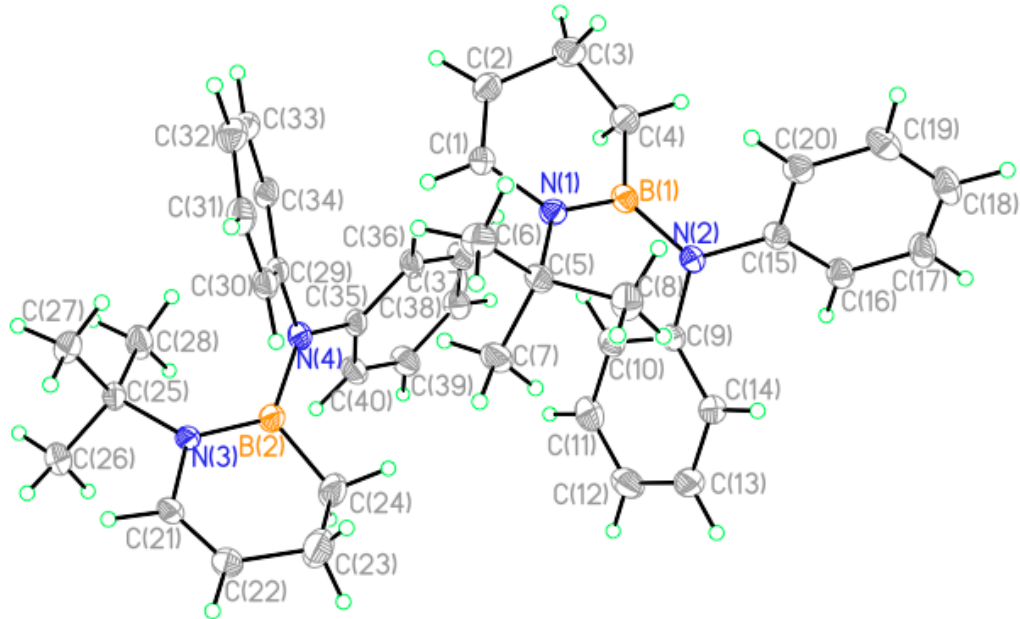


**Table 1. Crystal data and structure refinement for liu20.**

Identification code	liu20		
Empirical formula	C <sub>20</sub> H <sub>25</sub> B <sub>2</sub> N <sub>2</sub>		
Formula weight	304.23		
Temperature	173(2) K		
Wavelength	0.71073 Å		
Crystal system	Monoclinic		
Space group	P2(1)/n		
Unit cell dimensions	a = 9.3902(6) Å	b = 16.6049(11) Å	c = 11.3179(8) Å
			a = 90°. b = 98.3440(10)°. g = 90°.
Volume	1746.0(2) Å <sup>3</sup>		
Z	4		
Density (calculated)	1.157 Mg/m <sup>3</sup>		
Absorption coefficient	0.067 mm <sup>-1</sup>		
F(000)	656		
Crystal size	0.22 x 0.16 x 0.10 mm <sup>3</sup>		
Theta range for data collection	2.19 to 26.99°.		

Index ranges	-11<=h<=11, -21<=k<=21, -14<=l<=14
Reflections collected	19350
Independent reflections	3808 [R(int) = 0.0406]
Completeness to theta = 26.99°	100.0 %
Absorption correction	Semi-empirical from equivalents
Max. and min. transmission	0.9934 and 0.9855
Refinement method	Full-matrix least-squares on F <sup>2</sup>
Data / restraints / parameters	3808 / 0 / 308
Goodness-of-fit on F <sup>2</sup>	1.067
Final R indices [I>2sigma(I)]	R1 = 0.0460, wR2 = 0.0989
R indices (all data)	R1 = 0.0630, wR2 = 0.1090
Largest diff. peak and hole	0.207 and -0.222 e.Å <sup>-3</sup>

**Table 2.** Atomic coordinates ( $\times 10^4$ ) and equivalent isotropic displacement parameters ( $\text{\AA}^2 \times 10^3$ ) for liu20. U(eq) is defined as one third of the trace of the orthogonalized  $U^{ij}$  tensor.

	x	y	z	U(eq)
N(1)	3204(1)	2874(1)	6003(1)	27(1)
N(2)	5846(1)	2473(1)	6090(1)	26(1)
B(1)	4322(2)	2304(1)	6208(1)	26(1)
C(1)	3974(2)	1464(1)	6712(1)	34(1)
C(2)	2959(2)	1427(1)	7427(2)	39(1)
C(3)	2091(2)	2153(1)	7581(2)	41(1)
C(4)	1865(2)	2674(1)	6484(2)	38(1)
C(5)	3075(2)	3615(1)	5234(1)	29(1)
C(6)	1612(2)	3617(1)	4426(2)	44(1)
C(7)	3210(2)	4373(1)	6004(2)	44(1)
C(8)	4201(2)	3624(1)	4392(2)	43(1)
C(9)	6579(1)	3143(1)	6679(1)	26(1)
C(10)	6193(2)	3417(1)	7754(1)	31(1)
C(11)	6850(2)	4090(1)	8318(2)	36(1)
C(12)	7916(2)	4495(1)	7833(2)	38(1)
C(13)	8326(2)	4215(1)	6781(2)	37(1)
C(14)	7665(2)	3549(1)	6203(1)	31(1)
C(15)	6643(1)	1883(1)	5562(1)	26(1)
C(16)	8096(2)	1731(1)	5964(1)	31(1)
C(17)	8830(2)	1148(1)	5413(1)	35(1)
C(18)	8133(2)	696(1)	4476(1)	35(1)
C(19)	6688(2)	827(1)	4096(1)	33(1)
C(20)	5948(2)	1422(1)	4619(1)	29(1)

**Table 3.** Bond lengths [ $\text{\AA}$ ] and angles [ $^\circ$ ] for liu20.

N(1)-B(1)	1.4075(19)
N(1)-C(4)	1.4788(18)
N(1)-C(5)	1.5016(17)
N(2)-C(15)	1.4167(16)
N(2)-C(9)	1.4216(17)
N(2)-B(1)	1.4828(19)
B(1)-C(1)	1.559(2)
C(1)-C(2)	1.338(2)
C(1)-H(1)	0.955(17)
C(2)-C(3)	1.479(2)
C(2)-H(2)	0.985(18)
C(3)-C(4)	1.503(2)
C(3)-H(3A)	0.995(18)
C(3)-H(3B)	1.02(2)
C(4)-H(4A)	1.034(17)
C(4)-H(4B)	1.016(16)
C(5)-C(8)	1.522(2)
C(5)-C(7)	1.526(2)
C(5)-C(6)	1.535(2)
C(6)-H(6A)	0.99(2)
C(6)-H(6B)	1.02(2)
C(6)-H(6C)	1.008(19)
C(7)-H(7A)	1.01(2)
C(7)-H(7B)	0.981(18)
C(7)-H(7C)	1.006(19)
C(8)-H(8A)	1.01(2)
C(8)-H(8B)	0.98(2)
C(8)-H(8C)	1.030(18)
C(9)-C(10)	1.395(2)
C(9)-C(14)	1.3953(19)
C(10)-C(11)	1.388(2)
C(10)-H(10)	0.985(15)

C(11)-C(12)	1.384(2)
C(11)-H(11)	1.001(17)
C(12)-C(13)	1.383(2)
C(12)-H(12)	0.982(16)
C(13)-C(14)	1.386(2)
C(13)-H(13)	0.967(16)
C(14)-H(14)	0.994(15)
C(15)-C(20)	1.3959(19)
C(15)-C(16)	1.3972(19)
C(16)-C(17)	1.388(2)
C(16)-H(16)	0.991(15)
C(17)-C(18)	1.384(2)
C(17)-H(17)	0.995(17)
C(18)-C(19)	1.380(2)
C(18)-H(18)	0.976(17)
C(19)-C(20)	1.388(2)
C(19)-H(19)	0.975(16)
C(20)-H(20)	0.967(16)
B(1)-N(1)-C(4)	116.20(12)
B(1)-N(1)-C(5)	129.96(12)
C(4)-N(1)-C(5)	113.32(11)
C(15)-N(2)-C(9)	119.30(11)
C(15)-N(2)-B(1)	118.86(11)
C(9)-N(2)-B(1)	120.90(11)
N(1)-B(1)-N(2)	124.34(13)
N(1)-B(1)-C(1)	118.08(13)
N(2)-B(1)-C(1)	117.30(13)
C(2)-C(1)-B(1)	117.93(14)
C(2)-C(1)-H(1)	119.6(10)
B(1)-C(1)-H(1)	121.0(10)
C(1)-C(2)-C(3)	119.13(14)
C(1)-C(2)-H(2)	122.8(10)
C(3)-C(2)-H(2)	118.0(10)

C(2)-C(3)-C(4)	112.66(14)
C(2)-C(3)-H(3A)	112.9(10)
C(4)-C(3)-H(3A)	108.6(10)
C(2)-C(3)-H(3B)	107.8(11)
C(4)-C(3)-H(3B)	109.3(11)
H(3A)-C(3)-H(3B)	105.2(14)
N(1)-C(4)-C(3)	114.09(13)
N(1)-C(4)-H(4A)	108.4(9)
C(3)-C(4)-H(4A)	109.3(9)
N(1)-C(4)-H(4B)	109.2(9)
C(3)-C(4)-H(4B)	109.6(9)
H(4A)-C(4)-H(4B)	105.9(12)
N(1)-C(5)-C(8)	111.45(12)
N(1)-C(5)-C(7)	110.58(12)
C(8)-C(5)-C(7)	109.91(14)
N(1)-C(5)-C(6)	109.71(12)
C(8)-C(5)-C(6)	105.70(14)
C(7)-C(5)-C(6)	109.36(14)
C(5)-C(6)-H(6A)	109.6(11)
C(5)-C(6)-H(6B)	114.3(11)
H(6A)-C(6)-H(6B)	107.2(15)
C(5)-C(6)-H(6C)	109.1(10)
H(6A)-C(6)-H(6C)	110.3(15)
H(6B)-C(6)-H(6C)	106.2(14)
C(5)-C(7)-H(7A)	109.8(11)
C(5)-C(7)-H(7B)	109.9(10)
H(7A)-C(7)-H(7B)	106.8(15)
C(5)-C(7)-H(7C)	112.1(11)
H(7A)-C(7)-H(7C)	110.3(15)
H(7B)-C(7)-H(7C)	107.8(15)
C(5)-C(8)-H(8A)	110.0(11)
C(5)-C(8)-H(8B)	112.3(11)
H(8A)-C(8)-H(8B)	110.7(15)
C(5)-C(8)-H(8C)	108.6(10)

H(8A)-C(8)-H(8C)	106.6(14)
H(8B)-C(8)-H(8C)	108.4(14)
C(10)-C(9)-C(14)	118.45(13)
C(10)-C(9)-N(2)	119.66(12)
C(14)-C(9)-N(2)	121.88(12)
C(11)-C(10)-C(9)	120.63(14)
C(11)-C(10)-H(10)	119.6(9)
C(9)-C(10)-H(10)	119.8(9)
C(12)-C(11)-C(10)	120.57(15)
C(12)-C(11)-H(11)	119.5(10)
C(10)-C(11)-H(11)	119.9(10)
C(13)-C(12)-C(11)	119.04(14)
C(13)-C(12)-H(12)	121.3(9)
C(11)-C(12)-H(12)	119.6(9)
C(12)-C(13)-C(14)	120.89(15)
C(12)-C(13)-H(13)	120.0(10)
C(14)-C(13)-H(13)	119.1(10)
C(13)-C(14)-C(9)	120.39(14)
C(13)-C(14)-H(14)	120.6(9)
C(9)-C(14)-H(14)	119.1(9)
C(20)-C(15)-C(16)	118.42(13)
C(20)-C(15)-N(2)	119.01(12)
C(16)-C(15)-N(2)	122.56(12)
C(17)-C(16)-C(15)	120.31(14)
C(17)-C(16)-H(16)	120.1(9)
C(15)-C(16)-H(16)	119.6(9)
C(18)-C(17)-C(16)	120.84(14)
C(18)-C(17)-H(17)	120.9(10)
C(16)-C(17)-H(17)	118.2(10)
C(19)-C(18)-C(17)	119.15(14)
C(19)-C(18)-H(18)	119.2(10)
C(17)-C(18)-H(18)	121.6(10)
C(18)-C(19)-C(20)	120.65(14)
C(18)-C(19)-H(19)	121.3(9)

C(20)-C(19)-H(19)	118.0(9)
C(19)-C(20)-C(15)	120.59(14)
C(19)-C(20)-H(20)	120.4(9)
C(15)-C(20)-H(20)	119.0(9)

Symmetry transformations used to generate equivalent atoms:

**Table 4.** Anisotropic displacement parameters ( $\text{\AA}^2 \times 10^3$ ) for liu20. The anisotropic displacement factor exponent takes the form:  $-2p^2 [ h^2 a^*{}^2 U_{11} + \dots + 2 h k a^* b^* U_{12} ]$

	U <sub>11</sub>	U <sub>22</sub>	U <sub>33</sub>	U <sub>23</sub>	U <sub>13</sub>	U <sub>12</sub>
N(1)	25(1)	25(1)	31(1)	0(1)	7(1)	-2(1)
N(2)	25(1)	23(1)	32(1)	-4(1)	7(1)	-1(1)
B(1)	28(1)	26(1)	26(1)	-5(1)	6(1)	-2(1)
C(1)	32(1)	27(1)	44(1)	3(1)	7(1)	1(1)
C(2)	40(1)	33(1)	46(1)	8(1)	11(1)	-5(1)
C(3)	38(1)	44(1)	46(1)	5(1)	20(1)	-2(1)
C(4)	28(1)	36(1)	52(1)	4(1)	16(1)	0(1)
C(5)	30(1)	26(1)	30(1)	2(1)	3(1)	1(1)
C(6)	38(1)	39(1)	53(1)	6(1)	-6(1)	2(1)
C(7)	66(1)	28(1)	38(1)	0(1)	4(1)	0(1)
C(8)	43(1)	52(1)	36(1)	14(1)	11(1)	6(1)
C(9)	25(1)	21(1)	33(1)	0(1)	3(1)	2(1)
C(10)	30(1)	30(1)	34(1)	-1(1)	5(1)	-2(1)
C(11)	35(1)	34(1)	38(1)	-9(1)	1(1)	1(1)
C(12)	34(1)	26(1)	52(1)	-6(1)	-4(1)	-2(1)
C(13)	30(1)	28(1)	52(1)	4(1)	3(1)	-4(1)
C(14)	31(1)	28(1)	36(1)	1(1)	8(1)	0(1)
C(15)	28(1)	23(1)	28(1)	1(1)	8(1)	0(1)
C(16)	30(1)	28(1)	34(1)	0(1)	4(1)	1(1)
C(17)	29(1)	32(1)	45(1)	3(1)	8(1)	7(1)
C(18)	41(1)	26(1)	42(1)	-1(1)	16(1)	5(1)

C(19)	40(1)	28(1)	32(1)	-4(1)	8(1)	-2(1)
C(20)	28(1)	28(1)	32(1)	-1(1)	6(1)	-1(1)

**Table 5. Hydrogen coordinates ( x 10<sup>4</sup>) and isotropic displacement parameters (Å<sup>2</sup> x 10<sup>3</sup>) for liu20.**

	x	y	z	U(eq)
H(1)	4598(18)	1015(10)	6666(15)	45(5)
H(2)	2773(19)	938(11)	7872(16)	54(5)
H(3A)	1130(20)	2023(10)	7814(16)	52(5)
H(3B)	2620(20)	2477(11)	8281(17)	62(6)
H(4A)	1173(18)	2386(10)	5822(15)	45(5)
H(4B)	1362(17)	3192(10)	6664(14)	39(4)
H(6A)	1490(20)	3107(13)	3975(18)	66(6)
H(6B)	750(20)	3676(11)	4873(17)	63(6)
H(6C)	1572(18)	4088(11)	3862(16)	52(5)
H(7A)	2430(20)	4381(11)	6530(18)	66(6)
H(7B)	3070(18)	4852(11)	5493(16)	53(5)
H(7C)	4180(20)	4418(11)	6505(16)	58(6)
H(8A)	4140(20)	3113(12)	3904(17)	64(6)
H(8B)	5170(20)	3699(11)	4816(17)	57(6)
H(8C)	3973(18)	4092(11)	3797(15)	51(5)
H(10)	5416(17)	3145(9)	8098(13)	37(4)
H(11)	6570(17)	4279(10)	9092(16)	48(5)
H(12)	8371(16)	4971(10)	8242(14)	40(4)
H(13)	9078(17)	4488(10)	6437(14)	43(5)
H(14)	7954(16)	3355(9)	5441(14)	33(4)
H(16)	8598(16)	2039(9)	6651(14)	36(4)
H(17)	9867(19)	1061(10)	5714(15)	49(5)
H(18)	8644(17)	296(10)	4065(14)	44(5)
H(19)	6165(17)	522(10)	3435(14)	39(4)
H(20)	4943(17)	1523(9)	4334(14)	36(4)



**Table 5. Hydrogen coordinates ( x 10<sup>4</sup>) and isotropic displacement parameters (Å<sup>2</sup>x 10<sup>3</sup>) for liu14.**

	x	y	z	U(eq)
H(1A)	5732(10)	-288(14)	1076(10)	45(4)
H(1B)	5639(9)	-505(14)	1877(9)	38(4)
H(2)	6944(14)	252(19)	2197(13)	83(7)
H(3)	7109(13)	2229(17)	2223(11)	71(6)
H(4A)	5885(11)	2934(16)	1053(11)	58(5)
H(4B)	5912(12)	3428(18)	1846(12)	69(6)
H(6A)	3284(11)	1492(15)	544(10)	51(5)
H(6B)	3709(10)	1282(14)	-82(10)	48(5)
H(6C)	3030(10)	375(14)	-30(9)	42(4)
H(7A)	4343(11)	-752(16)	1942(11)	52(5)
H(7B)	3421(11)	-884(15)	1263(10)	48(5)
H(7C)	3687(10)	280(15)	1766(9)	44(4)
H(8A)	3745(12)	-1298(15)	149(10)	53(5)
H(8B)	4653(11)	-1524(15)	798(10)	52(5)
H(8C)	4518(10)	-696(14)	56(10)	42(4)
H(10)	5100(9)	1942(12)	2816(8)	27(4)
H(11)	4578(10)	1421(13)	3744(10)	40(4)
H(12)	3167(10)	1760(14)	3492(10)	44(4)
H(13)	2291(10)	2536(14)	2279(9)	42(4)
H(14)	2789(9)	3004(13)	1310(9)	36(4)
H(16)	4367(9)	3293(13)	74(9)	33(4)
H(17)	3990(9)	5027(12)	-668(9)	30(4)
H(18)	3435(10)	6623(14)	-209(9)	39(4)
H(19)	3369(10)	6477(14)	1053(9)	44(4)
H(20)	3777(8)	4771(12)	1789(8)	26(4)
H(21A)	-337(9)	2127(13)	4300(9)	34(4)
H(21B)	-413(9)	2567(14)	3463(9)	39(4)

H(22)	-1641(11)	1640(15)	3187(10)	49(5)
H(23)	-1739(12)	-358(16)	3186(11)	61(5)
H(24A)	-333(12)	-824(17)	4377(12)	64(6)
H(24B)	-497(12)	-1473(17)	3564(11)	64(6)
H(26A)	1904(11)	837(16)	4911(11)	54(5)
H(26B)	2007(11)	731(16)	4086(11)	56(5)
H(26C)	2382(11)	1845(16)	4640(10)	56(5)
H(27A)	574(13)	3053(17)	3053(12)	69(6)
H(27B)	1187(10)	2051(16)	2962(10)	51(5)
H(27C)	1569(12)	3182(17)	3493(11)	61(5)
H(28A)	1064(10)	2510(15)	5140(10)	51(5)
H(28B)	1641(11)	3320(15)	4854(10)	48(5)
H(28C)	661(11)	3464(15)	4456(10)	49(5)
H(30)	-81(10)	228(13)	2241(9)	36(4)
H(31)	137(11)	762(15)	1122(10)	49(5)
H(32)	1449(11)	352(16)	1080(11)	61(5)
H(33)	2497(11)	-503(15)	2171(10)	55(5)
H(34)	2275(10)	-988(14)	3306(9)	40(4)
H(36)	1292(10)	-1135(14)	5008(9)	42(4)
H(37)	1696(10)	-2909(15)	5704(10)	51(5)
H(38)	1890(10)	-4596(14)	5067(9)	41(4)
H(39)	1668(10)	-4466(15)	3712(10)	51(5)
H(40)	1226(9)	-2745(13)	3012(9)	35(4)

*Crystallographic data for 6.*

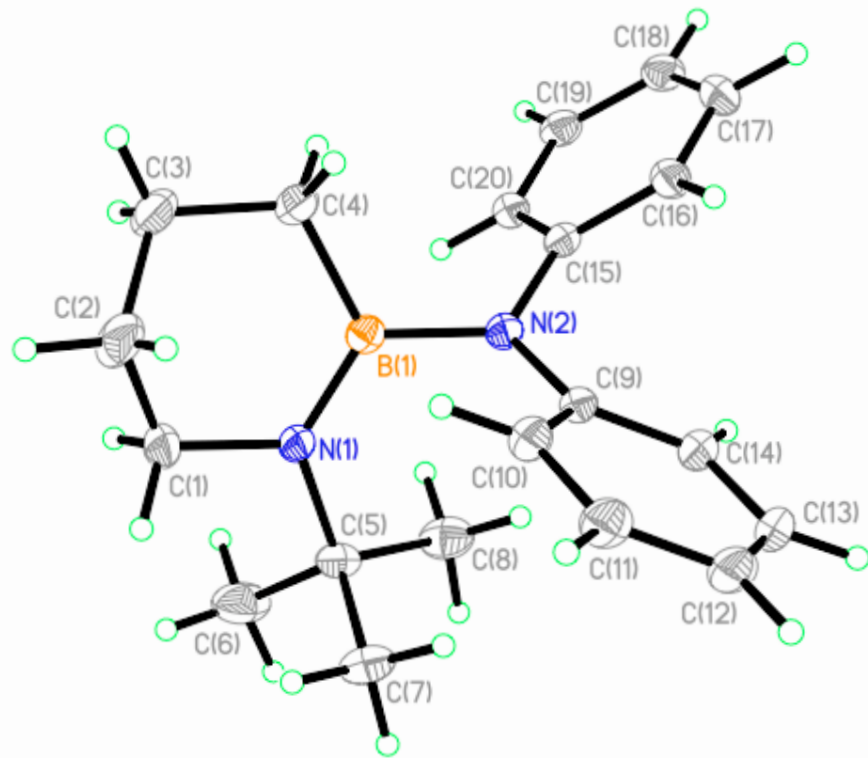


**Table 1. Crystal data and structure refinement for liu23.**

Identification code	liu23	
Empirical formula	C <sub>20</sub> H <sub>27</sub> B N <sub>2</sub>	
Formula weight	306.25	
Temperature	173(2) K	
Wavelength	0.71073 Å	
Crystal system	Monoclinic	
Space group	P2(1)/n	
Unit cell dimensions	a = 9.6233(8) Å b = 16.3666(13) Å c = 11.5544(9) Å	a= 90°. b= 96.654(2)°. g = 90°.
Volume	1807.6(3) Å <sup>3</sup>	
Z	4	

Density (calculated)	1.125 Mg/m <sup>3</sup>
Absorption coefficient	0.065 mm <sup>-1</sup>
F(000)	664
Crystal size	0.17 x 0.14 x 0.09 mm <sup>3</sup>
Theta range for data collection	2.17 to 27.00°.
Index ranges	-12<=h<=12, -20<=k<=20, -14<=l<=14
Reflections collected	19530
Independent reflections	3948 [R(int) = 0.0544]
Completeness to theta = 27.00°	100.0 %
Absorption correction	Semi-empirical from equivalents
Max. and min. transmission	0.9942 and 0.9891
Refinement method	Full-matrix least-squares on F <sup>2</sup>
Data / restraints / parameters	3948 / 0 / 316
Goodness-of-fit on F <sup>2</sup>	1.031
Final R indices [I>2sigma(I)]	R1 = 0.0520, wR2 = 0.1091
R indices (all data)	R1 = 0.0868, wR2 = 0.1282
Largest diff. peak and hole	0.207 and -0.159 e.Å <sup>-3</sup>

**Table 2.** Atomic coordinates ( $\times 10^4$ ) and equivalent isotropic displacement parameters ( $\text{\AA}^2 \times 10^3$ ) for liu23. U(eq) is defined as one third of the trace of the orthogonalized  $U^{ij}$  tensor.

	x	y	z	U(eq)
N(1)	1593(1)	2164(1)	8921(1)	30(1)
N(2)	-985(1)	2523(1)	8859(1)	31(1)
B(1)	484(2)	2717(1)	8675(2)	28(1)
C(1)	2892(2)	2304(1)	8380(2)	48(1)
C(2)	2712(3)	2886(1)	7363(2)	63(1)
C(3)	2167(2)	3701(1)	7728(2)	52(1)
C(4)	731(2)	3578(1)	8107(2)	42(1)
C(5)	1678(2)	1422(1)	9699(2)	35(1)
C(6)	3126(3)	1377(2)	10400(3)	63(1)
C(7)	1418(3)	641(1)	8982(2)	46(1)
C(8)	640(3)	1474(2)	10597(2)	49(1)
C(9)	-1691(2)	1852(1)	8276(2)	31(1)
C(10)	-1323(2)	1593(1)	7205(2)	36(1)
C(11)	-1970(2)	922(1)	6642(2)	44(1)
C(12)	-3004(2)	504(1)	7121(2)	47(1)
C(13)	-3393(2)	762(1)	8171(2)	46(1)
C(14)	-2742(2)	1427(1)	8755(2)	39(1)
C(15)	-1766(2)	3108(1)	9416(2)	30(1)
C(16)	-3178(2)	3261(1)	9066(2)	36(1)
C(17)	-3896(2)	3833(1)	9648(2)	43(1)
C(18)	-3228(2)	4276(1)	10571(2)	41(1)
C(19)	-1823(2)	4144(1)	10902(2)	38(1)
C(20)	-1101(2)	3561(1)	10342(2)	33(1)

**Table 3.** Bond lengths [Å] and angles [°] for liu23.

N(1)-B(1)	1.403(2)
N(1)-C(1)	1.479(2)
N(1)-C(5)	1.508(2)
N(2)-C(15)	1.416(2)
N(2)-C(9)	1.420(2)
N(2)-B(1)	1.488(2)
B(1)-C(4)	1.584(3)
C(1)-C(2)	1.508(3)
C(1)-H(1A)	1.01(2)
C(1)-H(1B)	0.97(2)
C(2)-C(3)	1.511(3)
C(2)-H(2A)	0.98(2)
C(2)-H(2B)	1.02(2)
C(3)-C(4)	1.511(3)
C(3)-H(3A)	1.02(3)
C(3)-H(3B)	0.99(2)
C(4)-H(4A)	1.01(2)
C(4)-H(4B)	0.96(3)
C(5)-C(8)	1.524(3)
C(5)-C(7)	1.527(3)
C(5)-C(6)	1.530(3)
C(6)-H(6A)	1.00(3)
C(6)-H(6B)	1.00(2)
C(6)-H(6C)	1.00(3)
C(7)-H(7A)	1.02(2)
C(7)-H(7B)	1.00(2)
C(7)-H(7C)	1.01(2)
C(8)-H(8A)	1.00(2)
C(8)-H(8B)	0.99(2)
C(8)-H(8C)	1.02(2)
C(9)-C(10)	1.393(2)
C(9)-C(14)	1.394(2)

C(10)-C(11)	1.386(3)
C(10)-H(10)	0.973(18)
C(11)-C(12)	1.376(3)
C(11)-H(11)	0.99(2)
C(12)-C(13)	1.377(3)
C(12)-H(12)	0.98(2)
C(13)-C(14)	1.390(3)
C(13)-H(13)	0.961(19)
C(14)-H(14)	0.980(19)
C(15)-C(20)	1.395(2)
C(15)-C(16)	1.395(2)
C(16)-C(17)	1.383(3)
C(16)-H(16)	0.978(19)
C(17)-C(18)	1.385(3)
C(17)-H(17)	0.97(2)
C(18)-C(19)	1.378(3)
C(18)-H(18)	0.963(19)
C(19)-C(20)	1.385(2)
C(19)-H(19)	0.990(19)
C(20)-H(20)	0.964(17)
B(1)-N(1)-C(1)	118.35(15)
B(1)-N(1)-C(5)	128.88(14)
C(1)-N(1)-C(5)	112.76(14)
C(15)-N(2)-C(9)	119.22(13)
C(15)-N(2)-B(1)	118.97(13)
C(9)-N(2)-B(1)	120.47(13)
N(1)-B(1)-N(2)	123.15(15)
N(1)-B(1)-C(4)	120.73(16)
N(2)-B(1)-C(4)	116.03(15)
N(1)-C(1)-C(2)	113.63(18)
N(1)-C(1)-H(1A)	108.9(12)
C(2)-C(1)-H(1A)	109.0(12)
N(1)-C(1)-H(1B)	108.3(11)

C(2)-C(1)-H(1B)	109.3(11)
H(1A)-C(1)-H(1B)	107.5(16)
C(1)-C(2)-C(3)	110.7(2)
C(1)-C(2)-H(2A)	107.2(13)
C(3)-C(2)-H(2A)	112.0(13)
C(1)-C(2)-H(2B)	109.9(13)
C(3)-C(2)-H(2B)	108.9(13)
H(2A)-C(2)-H(2B)	108.1(18)
C(4)-C(3)-C(2)	108.74(18)
C(4)-C(3)-H(3A)	107.3(14)
C(2)-C(3)-H(3A)	108.9(14)
C(4)-C(3)-H(3B)	112.0(13)
C(2)-C(3)-H(3B)	111.7(13)
H(3A)-C(3)-H(3B)	108.0(19)
C(3)-C(4)-B(1)	115.15(17)
C(3)-C(4)-H(4A)	110.5(14)
B(1)-C(4)-H(4A)	110.1(14)
C(3)-C(4)-H(4B)	108.3(15)
B(1)-C(4)-H(4B)	108.4(15)
H(4A)-C(4)-H(4B)	103.7(19)
N(1)-C(5)-C(8)	111.51(15)
N(1)-C(5)-C(7)	110.86(15)
C(8)-C(5)-C(7)	109.71(17)
N(1)-C(5)-C(6)	109.67(16)
C(8)-C(5)-C(6)	105.7(2)
C(7)-C(5)-C(6)	109.22(18)
C(5)-C(6)-H(6A)	110.9(13)
C(5)-C(6)-H(6B)	110.6(14)
H(6A)-C(6)-H(6B)	108.5(19)
C(5)-C(6)-H(6C)	107.6(14)
H(6A)-C(6)-H(6C)	110.7(19)
H(6B)-C(6)-H(6C)	108.6(19)
C(5)-C(7)-H(7A)	111.1(12)
C(5)-C(7)-H(7B)	110.6(13)

H(7A)-C(7)-H(7B)	108.4(17)
C(5)-C(7)-H(7C)	113.1(12)
H(7A)-C(7)-H(7C)	106.5(17)
H(7B)-C(7)-H(7C)	106.8(17)
C(5)-C(8)-H(8A)	107.3(13)
C(5)-C(8)-H(8B)	112.7(14)
H(8A)-C(8)-H(8B)	109.3(19)
C(5)-C(8)-H(8C)	107.1(11)
H(8A)-C(8)-H(8C)	109.6(17)
H(8B)-C(8)-H(8C)	110.7(18)
C(10)-C(9)-C(14)	118.13(17)
C(10)-C(9)-N(2)	120.02(15)
C(14)-C(9)-N(2)	121.84(16)
C(11)-C(10)-C(9)	120.80(18)
C(11)-C(10)-H(10)	120.5(11)
C(9)-C(10)-H(10)	118.7(11)
C(12)-C(11)-C(10)	120.7(2)
C(12)-C(11)-H(11)	120.6(12)
C(10)-C(11)-H(11)	118.6(12)
C(11)-C(12)-C(13)	119.05(19)
C(11)-C(12)-H(12)	120.2(11)
C(13)-C(12)-H(12)	120.7(11)
C(12)-C(13)-C(14)	120.95(19)
C(12)-C(13)-H(13)	120.8(11)
C(14)-C(13)-H(13)	118.2(11)
C(13)-C(14)-C(9)	120.33(19)
C(13)-C(14)-H(14)	120.3(11)
C(9)-C(14)-H(14)	119.3(11)
C(20)-C(15)-C(16)	118.14(16)
C(20)-C(15)-N(2)	119.15(15)
C(16)-C(15)-N(2)	122.70(15)
C(17)-C(16)-C(15)	120.34(18)
C(17)-C(16)-H(16)	119.9(11)
C(15)-C(16)-H(16)	119.7(11)

C(16)-C(17)-C(18)	121.04(18)
C(16)-C(17)-H(17)	119.1(12)
C(18)-C(17)-H(17)	119.9(12)
C(19)-C(18)-C(17)	119.00(18)
C(19)-C(18)-H(18)	121.4(11)
C(17)-C(18)-H(18)	119.6(11)
C(18)-C(19)-C(20)	120.47(18)
C(18)-C(19)-H(19)	119.4(11)
C(20)-C(19)-H(19)	120.1(11)
C(19)-C(20)-C(15)	120.97(17)
C(19)-C(20)-H(20)	119.9(10)
C(15)-C(20)-H(20)	119.1(10)

---

Symmetry transformations used to generate equivalent atoms:

**Table 4. Anisotropic displacement parameters ( $\text{\AA}^2 \times 10^3$ ) for liu23. The anisotropic displacement factor exponent takes the form:  $-2p^2 [ h^2 a^*{}^2 U_{11} + \dots + 2 h k a^* b^* U_{12} ]$**

	U <sub>11</sub>	U <sub>22</sub>	U <sub>33</sub>	U <sub>23</sub>	U <sub>13</sub>	U <sub>12</sub>
N(1)	28(1)	25(1)	36(1)	-3(1)	6(1)	-2(1)
N(2)	29(1)	23(1)	41(1)	-5(1)	6(1)	-2(1)
B(1)	31(1)	26(1)	27(1)	-4(1)	3(1)	-2(1)
C(1)	37(1)	36(1)	76(2)	-7(1)	27(1)	-2(1)
C(2)	77(2)	45(1)	78(2)	0(1)	54(2)	-7(1)
C(3)	61(1)	33(1)	68(2)	3(1)	29(1)	-10(1)
C(4)	38(1)	34(1)	54(1)	11(1)	2(1)	-4(1)
C(5)	41(1)	26(1)	38(1)	0(1)	-1(1)	3(1)
C(6)	58(2)	40(1)	82(2)	5(1)	-20(1)	6(1)
C(7)	65(2)	26(1)	47(1)	-1(1)	5(1)	-1(1)
C(8)	69(2)	42(1)	36(1)	8(1)	9(1)	5(1)
C(9)	27(1)	23(1)	43(1)	0(1)	2(1)	-1(1)
C(10)	35(1)	32(1)	41(1)	-2(1)	2(1)	-5(1)

C(11)	45(1)	37(1)	48(1)	-10(1)	-3(1)	-3(1)
C(12)	41(1)	31(1)	67(1)	-9(1)	-7(1)	-6(1)
C(13)	32(1)	31(1)	75(2)	3(1)	7(1)	-7(1)
C(14)	34(1)	30(1)	55(1)	-1(1)	10(1)	-2(1)
C(15)	31(1)	23(1)	37(1)	1(1)	7(1)	-2(1)
C(16)	32(1)	31(1)	43(1)	-3(1)	1(1)	0(1)
C(17)	32(1)	37(1)	58(1)	-1(1)	5(1)	6(1)
C(18)	45(1)	28(1)	51(1)	-2(1)	14(1)	5(1)
C(19)	46(1)	27(1)	41(1)	-3(1)	7(1)	-2(1)
C(20)	31(1)	28(1)	42(1)	1(1)	3(1)	-1(1)

---

**Table 5.** Hydrogen coordinates ( $\times 10^4$ ) and isotropic displacement parameters ( $\text{\AA}^2 \times 10^3$ ) for liu23.

	x	y	z	U(eq)
H(1A)	3630(20)	2526(13)	8989(18)	61(7)
H(1B)	3222(19)	1780(12)	8122(16)	46(5)
H(2A)	3620(20)	2937(13)	7072(19)	69(7)
H(2B)	2020(20)	2649(14)	6710(20)	70(8)
H(3A)	2800(30)	3910(15)	8430(20)	83(8)
H(3B)	2160(20)	4114(15)	7100(20)	72(7)
H(4A)	510(20)	4030(15)	8650(20)	77(8)
H(4B)	50(30)	3646(15)	7440(20)	90(9)
H(6A)	3350(20)	1895(16)	10840(20)	76(7)
H(6B)	3860(30)	1280(14)	9870(20)	71(8)
H(6C)	3120(20)	906(16)	10950(20)	79(8)
H(7A)	1560(20)	138(14)	9496(18)	67(7)
H(7B)	2070(20)	607(13)	8372(19)	68(7)
H(7C)	430(20)	606(12)	8563(18)	61(7)
H(8A)	810(20)	2006(15)	11021(19)	72(7)
H(8B)	-340(30)	1452(14)	10240(20)	71(7)
H(8C)	860(20)	1000(13)	11165(18)	61(6)
H(10)	-586(19)	1883(11)	6867(15)	44(5)
H(11)	-1670(20)	748(12)	5893(17)	53(6)
H(12)	-3463(19)	37(12)	6712(17)	52(6)
H(13)	-4120(20)	486(12)	8521(16)	48(6)
H(14)	-2991(19)	1586(11)	9522(17)	45(5)
H(16)	-3666(19)	2955(12)	8413(16)	47(5)
H(17)	-4880(20)	3924(12)	9400(17)	54(6)
H(18)	-3749(19)	4667(12)	10969(15)	45(5)
H(19)	-1334(19)	4467(12)	11551(16)	46(5)
H(20)	-124(18)	3465(10)	10590(14)	28(4)

*Crystallographic data for 7.*

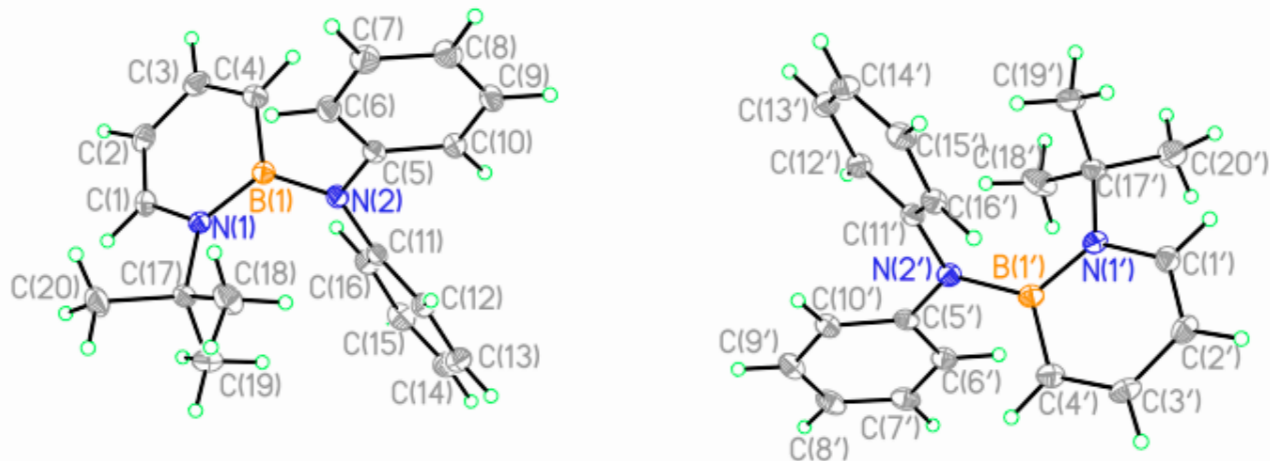


**Table 1. Crystal data and structure refinement for liu6.**

Identification code	liu6		
Empirical formula	C <sub>20</sub> H <sub>23</sub> B N <sub>2</sub>		
Formula weight	302.21		
Temperature	173(2) K		
Wavelength	0.71073 Å		
Crystal system	Monoclinic		
Space group	P2(1)/c		
Unit cell dimensions	a = 17.5145(7) Å	b = 11.3698(4) Å	c = 18.5318(7) Å
	a= 90°.	b= 113.7140(10)°.	g = 90°.
Volume	3378.8(2) Å <sup>3</sup>		
Z	8		
Density (calculated)	1.188 Mg/m <sup>3</sup>		
Absorption coefficient	0.069 mm <sup>-1</sup>		
F(000)	1296		
Crystal size	0.32 x 0.27 x 0.18 mm <sup>3</sup>		
Theta range for data collection	2.16 to 27.50°.		
Index ranges	-22<=h<=22, -14<=k<=14, -24<=l<=23		

Reflections collected	37892
Independent reflections	7737 [R(int) = 0.0337]
Completeness to theta = 27.50°	99.7 %
Absorption correction	Semi-empirical from equivalents
Max. and min. transmission	0.9877 and 0.9783
Refinement method	Full-matrix least-squares on F <sup>2</sup>
Data / restraints / parameters	7737 / 0 / 599
Goodness-of-fit on F <sup>2</sup>	1.003
Final R indices [I>2sigma(I)]	R1 = 0.0506, wR2 = 0.1328
R indices (all data)	R1 = 0.0612, wR2 = 0.1450
Largest diff. peak and hole	0.378 and -0.203 e.Å <sup>-3</sup>

**Table 2.** Atomic coordinates ( $\times 10^4$ ) and equivalent isotropic displacement parameters ( $\text{\AA}^2 \times 10^3$ ) for liu6. U(eq) is defined as one third of the trace of the orthogonalized  $U_{ij}$  tensor.

	x	y	z	U(eq)
B(1)	4864(1)	127(1)	1414(1)	23(1)
N(1)	4782(1)	-1112(1)	1220(1)	22(1)
N(2)	4196(1)	811(1)	1525(1)	23(1)
C(1)	5504(1)	-1738(1)	1362(1)	27(1)
C(2)	6265(1)	-1235(1)	1570(1)	30(1)
C(3)	6364(1)	-3(1)	1650(1)	33(1)
C(4)	5701(1)	692(1)	1569(1)	31(1)
C(5)	3926(1)	1888(1)	1129(1)	23(1)
C(6)	3935(1)	2038(1)	382(1)	28(1)
C(7)	3692(1)	3101(1)	-12(1)	33(1)
C(8)	3424(1)	4019(1)	314(1)	33(1)
C(9)	3409(1)	3878(1)	1051(1)	31(1)
C(10)	3663(1)	2830(1)	1462(1)	26(1)
C(11)	3955(1)	480(1)	2142(1)	23(1)
C(12)	3137(1)	625(1)	2076(1)	27(1)
C(13)	2918(1)	274(1)	2684(1)	34(1)
C(14)	3498(1)	-244(1)	3356(1)	36(1)
C(15)	4306(1)	-405(1)	3422(1)	34(1)
C(16)	4538(1)	-36(1)	2824(1)	28(1)
C(17)	3981(1)	-1826(1)	862(1)	26(1)
C(18)	3238(1)	-1029(1)	421(1)	38(1)
C(19)	3845(1)	-2508(1)	1510(1)	39(1)
C(20)	4046(1)	-2678(2)	243(1)	40(1)
B(1')	0(1)	7745(1)	3526(1)	23(1)
N(1')	97(1)	8992(1)	3704(1)	23(1)
N(2')	685(1)	7003(1)	3488(1)	24(1)
C(1')	-618(1)	9654(1)	3519(1)	27(1)
C(2')	-1398(1)	9189(1)	3264(1)	30(1)

C(3')	-1521(1)	7956(1)	3181(1)	32(1)
C(4')	-860(1)	7231(1)	3311(1)	29(1)
C(5')	931(1)	5957(1)	3933(1)	23(1)
C(6')	834(1)	5867(1)	4646(1)	27(1)
C(7')	1078(1)	4857(1)	5101(1)	31(1)
C(8')	1433(1)	3923(1)	4873(1)	33(1)
C(9')	1522(1)	3997(1)	4161(1)	32(1)
C(10')	1263(1)	4988(1)	3689(1)	27(1)
C(11')	987(1)	7274(1)	2903(1)	23(1)
C(12')	1825(1)	7114(1)	3029(1)	26(1)
C(13')	2101(1)	7429(1)	2453(1)	31(1)
C(14')	1562(1)	7927(1)	1747(1)	33(1)
C(15')	735(1)	8109(1)	1625(1)	30(1)
C(16')	448(1)	7769(1)	2191(1)	26(1)
C(17')	916(1)	9663(1)	4089(1)	26(1)
C(18')	1578(1)	8843(2)	4658(1)	45(1)
C(19')	1182(1)	10148(1)	3457(1)	36(1)
C(20')	828(1)	10703(1)	4577(1)	36(1)

---

**Table 3. Bond lengths [Å] and angles [°] for liu6.**

B(1)-N(1)	1.4460(17)
B(1)-N(2)	1.4856(16)
B(1)-C(4)	1.5182(18)
N(1)-C(1)	1.3826(15)
N(1)-C(17)	1.5221(15)
N(2)-C(5)	1.4092(15)
N(2)-C(11)	1.4192(15)
C(1)-C(2)	1.3561(18)
C(1)-H(1)	0.991(16)
C(2)-C(3)	1.412(2)
C(2)-H(2)	0.982(17)
C(3)-C(4)	1.3626(19)
C(3)-H(3)	0.983(17)
C(4)-H(4)	0.991(19)
C(5)-C(6)	1.4007(17)
C(5)-C(10)	1.4019(17)
C(6)-C(7)	1.3877(19)
C(6)-H(6)	0.978(16)
C(7)-C(8)	1.380(2)
C(7)-H(7)	0.990(17)
C(8)-C(9)	1.386(2)
C(8)-H(8)	1.009(16)
C(9)-C(10)	1.3880(18)
C(9)-H(9)	1.002(18)
C(10)-H(10)	0.976(14)
C(11)-C(16)	1.3947(17)
C(11)-C(12)	1.3990(17)
C(12)-C(13)	1.3872(18)
C(12)-H(12)	0.991(16)
C(13)-C(14)	1.383(2)
C(13)-H(13)	0.976(16)
C(14)-C(15)	1.382(2)

C(14)-H(14)	0.971(18)
C(15)-C(16)	1.3888(19)
C(15)-H(15)	0.961(18)
C(16)-H(16)	0.992(16)
C(17)-C(19)	1.5256(19)
C(17)-C(18)	1.5260(19)
C(17)-C(20)	1.5399(19)
C(18)-H(18A)	0.996(18)
C(18)-H(18B)	1.02(2)
C(18)-H(18C)	0.98(2)
C(19)-H(19A)	1.02(2)
C(19)-H(19B)	0.997(18)
C(19)-H(19C)	0.987(19)
C(20)-H(20A)	0.995(18)
C(20)-H(20B)	1.00(2)
C(20)-H(20C)	0.975(19)
B(1')-N(1')	1.4500(17)
B(1')-N(2')	1.4915(17)
B(1')-C(4')	1.5129(18)
N(1')-C(1')	1.3804(16)
N(1')-C(17')	1.5248(15)
N(2')-C(5')	1.4117(15)
N(2')-C(11')	1.4193(15)
C(1')-C(2')	1.3597(18)
C(1')-H(1')	0.981(17)
C(2')-C(3')	1.417(2)
C(2')-H(2')	0.991(17)
C(3')-C(4')	1.3603(19)
C(3')-H(3')	0.968(16)
C(4')-H(4')	0.976(18)
C(5')-C(6')	1.4024(17)
C(5')-C(10')	1.4035(18)
C(6')-C(7')	1.3870(18)
C(6')-H(6')	0.990(16)

C(7')-C(8')	1.379(2)
C(7')-H(7')	0.998(17)
C(8')-C(9')	1.393(2)
C(8')-H(8')	0.974(18)
C(9')-C(10')	1.3860(18)
C(9')-H(9')	0.978(17)
C(10')-H(10')	0.960(15)
C(11')-C(16')	1.3950(17)
C(11')-C(12')	1.4015(17)
C(12')-C(13')	1.3844(18)
C(12')-H(12')	0.975(15)
C(13')-C(14')	1.389(2)
C(13')-H(13')	0.971(16)
C(14')-C(15')	1.387(2)
C(14')-H(14')	0.970(16)
C(15')-C(16')	1.3885(18)
C(15')-H(15')	0.997(17)
C(16')-H(16')	0.990(14)
C(17')-C(19')	1.5254(19)
C(17')-C(18')	1.530(2)
C(17')-C(20')	1.5343(19)
C(18')-H(18D)	0.989(19)
C(18')-H(18E)	0.98(2)
C(18')-H(18F)	1.00(2)
C(19')-H(19D)	1.034(19)
C(19')-H(19E)	0.995(19)
C(19')-H(19F)	0.954(18)
C(20')-H(20D)	1.04(2)
C(20')-H(20E)	0.975(18)
C(20')-H(20F)	0.96(2)
N(1)-B(1)-N(2)	122.60(11)
N(1)-B(1)-C(4)	116.82(11)
N(2)-B(1)-C(4)	120.38(11)

C(1)-N(1)-B(1)	117.56(10)
C(1)-N(1)-C(17)	114.84(10)
B(1)-N(1)-C(17)	127.59(10)
C(5)-N(2)-C(11)	120.24(10)
C(5)-N(2)-B(1)	120.04(10)
C(11)-N(2)-B(1)	118.63(10)
C(2)-C(1)-N(1)	123.85(12)
C(2)-C(1)-H(1)	119.9(9)
N(1)-C(1)-H(1)	116.3(9)
C(1)-C(2)-C(3)	120.85(12)
C(1)-C(2)-H(2)	117.0(10)
C(3)-C(2)-H(2)	122.1(10)
C(4)-C(3)-C(2)	120.05(12)
C(4)-C(3)-H(3)	122.3(10)
C(2)-C(3)-H(3)	117.6(10)
C(3)-C(4)-B(1)	119.42(12)
C(3)-C(4)-H(4)	117.2(10)
B(1)-C(4)-H(4)	123.3(10)
C(6)-C(5)-C(10)	118.54(11)
C(6)-C(5)-N(2)	119.08(11)
C(10)-C(5)-N(2)	122.37(11)
C(7)-C(6)-C(5)	120.24(12)
C(7)-C(6)-H(6)	122.2(9)
C(5)-C(6)-H(6)	117.5(9)
C(8)-C(7)-C(6)	120.93(13)
C(8)-C(7)-H(7)	118.6(10)
C(6)-C(7)-H(7)	120.5(10)
C(7)-C(8)-C(9)	119.29(12)
C(7)-C(8)-H(8)	119.6(9)
C(9)-C(8)-H(8)	121.1(9)
C(8)-C(9)-C(10)	120.68(12)
C(8)-C(9)-H(9)	119.7(10)
C(10)-C(9)-H(9)	119.6(10)
C(9)-C(10)-C(5)	120.30(12)

C(9)-C(10)-H(10)	120.0(9)
C(5)-C(10)-H(10)	119.7(9)
C(16)-C(11)-C(12)	118.65(12)
C(16)-C(11)-N(2)	119.68(11)
C(12)-C(11)-N(2)	121.64(11)
C(13)-C(12)-C(11)	120.23(12)
C(13)-C(12)-H(12)	121.2(9)
C(11)-C(12)-H(12)	118.6(9)
C(14)-C(13)-C(12)	120.70(13)
C(14)-C(13)-H(13)	120.4(9)
C(12)-C(13)-H(13)	118.9(10)
C(15)-C(14)-C(13)	119.43(13)
C(15)-C(14)-H(14)	121.9(10)
C(13)-C(14)-H(14)	118.7(10)
C(14)-C(15)-C(16)	120.48(13)
C(14)-C(15)-H(15)	120.5(10)
C(16)-C(15)-H(15)	119.1(10)
C(15)-C(16)-C(11)	120.49(13)
C(15)-C(16)-H(16)	120.7(9)
C(11)-C(16)-H(16)	118.8(9)
N(1)-C(17)-C(19)	109.62(11)
N(1)-C(17)-C(18)	110.76(10)
C(19)-C(17)-C(18)	110.71(12)
N(1)-C(17)-C(20)	109.26(10)
C(19)-C(17)-C(20)	110.34(12)
C(18)-C(17)-C(20)	106.08(12)
C(17)-C(18)-H(18A)	108.2(10)
C(17)-C(18)-H(18B)	111.5(11)
H(18A)-C(18)-H(18B)	106.1(15)
C(17)-C(18)-H(18C)	113.9(11)
H(18A)-C(18)-H(18C)	107.0(15)
H(18B)-C(18)-H(18C)	109.9(17)
C(17)-C(19)-H(19A)	111.9(11)
C(17)-C(19)-H(19B)	110.4(10)

H(19A)-C(19)-H(19B)	109.9(16)
C(17)-C(19)-H(19C)	112.9(11)
H(19A)-C(19)-H(19C)	106.9(15)
H(19B)-C(19)-H(19C)	104.6(14)
C(17)-C(20)-H(20A)	107.8(10)
C(17)-C(20)-H(20B)	112.6(11)
H(20A)-C(20)-H(20B)	109.6(15)
C(17)-C(20)-H(20C)	113.8(10)
H(20A)-C(20)-H(20C)	102.9(14)
H(20B)-C(20)-H(20C)	109.6(15)
N(1')-B(1')-N(2')	122.76(11)
N(1')-B(1')-C(4')	116.80(11)
N(2')-B(1')-C(4')	120.26(12)
C(1')-N(1')-B(1')	117.69(10)
C(1')-N(1')-C(17')	115.64(10)
B(1')-N(1')-C(17')	126.66(10)
C(5')-N(2')-C(11')	120.62(10)
C(5')-N(2')-B(1')	120.72(10)
C(11')-N(2')-B(1')	117.89(10)
C(2')-C(1')-N(1')	123.95(12)
C(2')-C(1')-H(1')	119.1(9)
N(1')-C(1')-H(1')	117.0(9)
C(1')-C(2')-C(3')	120.66(12)
C(1')-C(2')-H(2')	119.0(10)
C(3')-C(2')-H(2')	120.4(10)
C(4')-C(3')-C(2')	119.92(12)
C(4')-C(3')-H(3')	122.7(10)
C(2')-C(3')-H(3')	117.4(10)
C(3')-C(4')-B(1')	119.89(13)
C(3')-C(4')-H(4')	118.1(10)
B(1')-C(4')-H(4')	121.9(10)
C(6')-C(5')-C(10')	118.02(11)
C(6')-C(5')-N(2')	119.18(11)
C(10')-C(5')-N(2')	122.79(11)

C(7')-C(6')-C(5')	120.59(12)
C(7')-C(6')-H(6')	121.8(9)
C(5')-C(6')-H(6')	117.6(9)
C(8')-C(7')-C(6')	121.20(13)
C(8')-C(7')-H(7')	119.9(10)
C(6')-C(7')-H(7')	118.9(10)
C(7')-C(8')-C(9')	118.68(12)
C(7')-C(8')-H(8')	122.7(10)
C(9')-C(8')-H(8')	118.6(10)
C(10')-C(9')-C(8')	120.95(13)
C(10')-C(9')-H(9')	120.9(10)
C(8')-C(9')-H(9')	118.2(10)
C(9')-C(10')-C(5')	120.50(12)
C(9')-C(10')-H(10')	118.6(9)
C(5')-C(10')-H(10')	120.9(9)
C(16')-C(11')-C(12')	118.41(11)
C(16')-C(11')-N(2')	119.44(11)
C(12')-C(11')-N(2')	122.08(11)
C(13')-C(12')-C(11')	120.28(12)
C(13')-C(12')-H(12')	120.8(9)
C(11')-C(12')-H(12')	118.9(9)
C(12')-C(13')-C(14')	121.00(12)
C(12')-C(13')-H(13')	120.2(10)
C(14')-C(13')-H(13')	118.8(10)
C(15')-C(14')-C(13')	119.02(12)
C(15')-C(14')-H(14')	121.4(9)
C(13')-C(14')-H(14')	119.5(9)
C(14')-C(15')-C(16')	120.37(12)
C(14')-C(15')-H(15')	119.5(9)
C(16')-C(15')-H(15')	120.1(10)
C(15')-C(16')-C(11')	120.89(12)
C(15')-C(16')-H(16')	120.3(8)
C(11')-C(16')-H(16')	118.8(8)
N(1')-C(17')-C(19')	110.04(10)

N(1')-C(17')-C(18')	109.08(10)
C(19')-C(17')-C(18')	111.69(13)
N(1')-C(17')-C(20')	111.21(10)
C(19')-C(17')-C(20')	107.91(11)
C(18')-C(17')-C(20')	106.88(13)
C(17')-C(18')-H(18D)	108.0(11)
C(17')-C(18')-H(18E)	110.6(12)
H(18D)-C(18')-H(18E)	107.8(16)
C(17')-C(18')-H(18F)	111.8(14)
H(18D)-C(18')-H(18F)	106.9(17)
H(18E)-C(18')-H(18F)	111.5(19)
C(17')-C(19')-H(19D)	111.1(10)
C(17')-C(19')-H(19E)	110.9(11)
H(19D)-C(19')-H(19E)	107.2(15)
C(17')-C(19')-H(19F)	111.7(11)
H(19D)-C(19')-H(19F)	108.2(14)
H(19E)-C(19')-H(19F)	107.5(14)
C(17')-C(20')-H(20D)	113.7(10)
C(17')-C(20')-H(20E)	109.1(10)
H(20D)-C(20')-H(20E)	106.5(14)
C(17')-C(20')-H(20F)	111.8(13)
H(20D)-C(20')-H(20F)	110.2(16)
H(20E)-C(20')-H(20F)	105.1(15)

---

Symmetry transformations used to generate equivalent atoms:

**Table 4. Anisotropic displacement parameters ( $\text{\AA}^2 \times 10^3$ ) for liu6. The anisotropic displacement factor exponent takes the form:  $-2p^2 [ h^2 a^*{}^2 U_{11} + \dots + 2 h k a^* b^* U_{12} ]$**

	U <sub>11</sub>	U <sub>22</sub>	U <sub>33</sub>	U <sub>23</sub>	U <sub>13</sub>	U <sub>12</sub>
B(1)	24(1)	23(1)	21(1)	2(1)	9(1)	2(1)
N(1)	21(1)	23(1)	22(1)	1(1)	9(1)	0(1)
N(2)	26(1)	20(1)	25(1)	2(1)	12(1)	2(1)
C(1)	27(1)	26(1)	27(1)	-1(1)	11(1)	4(1)
C(2)	25(1)	38(1)	27(1)	-1(1)	10(1)	6(1)
C(3)	23(1)	43(1)	33(1)	-3(1)	12(1)	-5(1)
C(4)	30(1)	28(1)	37(1)	-4(1)	14(1)	-6(1)
C(5)	21(1)	20(1)	25(1)	1(1)	7(1)	0(1)
C(6)	34(1)	25(1)	27(1)	1(1)	14(1)	2(1)
C(7)	38(1)	33(1)	30(1)	7(1)	14(1)	4(1)
C(8)	33(1)	26(1)	41(1)	9(1)	14(1)	6(1)
C(9)	30(1)	22(1)	41(1)	-1(1)	16(1)	3(1)
C(10)	27(1)	24(1)	28(1)	-2(1)	12(1)	0(1)
C(11)	26(1)	18(1)	24(1)	-2(1)	11(1)	-1(1)
C(12)	28(1)	26(1)	29(1)	2(1)	12(1)	2(1)
C(13)	35(1)	33(1)	40(1)	1(1)	22(1)	-1(1)
C(14)	50(1)	34(1)	33(1)	3(1)	24(1)	-5(1)
C(15)	43(1)	31(1)	24(1)	3(1)	8(1)	0(1)
C(16)	28(1)	26(1)	27(1)	1(1)	7(1)	1(1)
C(17)	24(1)	23(1)	31(1)	-4(1)	11(1)	-3(1)
C(18)	25(1)	32(1)	44(1)	-7(1)	1(1)	-1(1)
C(19)	39(1)	35(1)	45(1)	3(1)	21(1)	-9(1)
C(20)	36(1)	36(1)	48(1)	-19(1)	16(1)	-7(1)
B(1')	23(1)	26(1)	21(1)	3(1)	8(1)	-1(1)
N(1')	20(1)	26(1)	22(1)	2(1)	9(1)	0(1)
N(2')	25(1)	24(1)	24(1)	5(1)	10(1)	2(1)
C(1')	28(1)	27(1)	26(1)	3(1)	11(1)	3(1)
C(2')	24(1)	38(1)	29(1)	5(1)	11(1)	6(1)

C(3')	21(1)	43(1)	31(1)	5(1)	10(1)	-4(1)
C(4')	26(1)	30(1)	30(1)	2(1)	10(1)	-3(1)
C(5')	20(1)	23(1)	22(1)	2(1)	5(1)	-4(1)
C(6')	27(1)	27(1)	25(1)	0(1)	9(1)	-3(1)
C(7')	33(1)	31(1)	25(1)	4(1)	8(1)	-7(1)
C(8')	35(1)	25(1)	30(1)	6(1)	2(1)	-4(1)
C(9')	32(1)	23(1)	34(1)	-1(1)	7(1)	-1(1)
C(10')	28(1)	24(1)	26(1)	0(1)	9(1)	-2(1)
C(11')	25(1)	20(1)	23(1)	1(1)	10(1)	-1(1)
C(12')	25(1)	26(1)	27(1)	4(1)	9(1)	2(1)
C(13')	28(1)	31(1)	38(1)	4(1)	16(1)	1(1)
C(14')	39(1)	32(1)	32(1)	5(1)	21(1)	-2(1)
C(15')	35(1)	28(1)	25(1)	5(1)	9(1)	-1(1)
C(16')	24(1)	25(1)	26(1)	2(1)	8(1)	0(1)
C(17')	24(1)	24(1)	30(1)	0(1)	10(1)	-5(1)
C(18')	28(1)	34(1)	52(1)	6(1)	-5(1)	-6(1)
C(19')	41(1)	33(1)	44(1)	-5(1)	27(1)	-12(1)
C(20')	37(1)	39(1)	33(1)	-9(1)	14(1)	-9(1)

---

**Table 5.** Hydrogen coordinates ( $\times 10^4$ ) and isotropic displacement parameters ( $\text{\AA}^2 \times 10^3$ ) for liu6.

	x	y	z	U(eq)
H(1)	5446(9)	-2604(15)	1308(9)	35(4)
H(2)	6737(10)	-1765(15)	1656(10)	41(4)
H(3)	6926(11)	319(15)	1789(10)	44(5)
H(4)	5805(10)	1548(17)	1650(10)	46(5)
H(6)	4111(9)	1369(14)	154(9)	32(4)
H(7)	3697(10)	3210(15)	-541(10)	47(5)
H(8)	3247(10)	4782(15)	15(10)	37(4)
H(9)	3215(10)	4541(16)	1291(10)	44(4)
H(10)	3666(8)	2749(13)	1986(9)	27(4)
H(12)	2721(9)	984(13)	1588(9)	34(4)
H(13)	2341(10)	374(14)	2623(9)	39(4)
H(14)	3326(10)	-473(16)	3773(10)	47(5)
H(15)	4713(10)	-780(16)	3879(11)	43(4)
H(16)	5121(10)	-130(14)	2875(9)	38(4)
H(18A)	2744(11)	-1537(16)	136(10)	46(5)
H(18B)	3330(12)	-548(19)	1(13)	65(6)
H(18C)	3087(12)	-507(18)	765(11)	59(5)
H(19A)	4349(12)	-3011(18)	1831(12)	60(6)
H(19B)	3338(11)	-3011(17)	1279(11)	51(5)
H(19C)	3735(11)	-1991(17)	1885(11)	50(5)
H(20A)	3488(11)	-3041(16)	-42(10)	47(5)
H(20B)	4226(11)	-2280(17)	-140(11)	55(5)
H(20C)	4402(11)	-3356(17)	470(10)	46(5)
H(1')	-548(10)	10508(15)	3587(9)	39(4)
H(2')	-1878(11)	9724(15)	3152(10)	44(5)
H(3')	-2087(10)	7669(15)	3011(9)	39(4)
H(4')	-967(10)	6389(16)	3229(10)	41(4)
H(6')	592(9)	6550(14)	4812(9)	32(4)

H(7')	992(10)	4810(15)	5601(10)	42(4)
H(8')	1638(10)	3224(16)	5197(10)	43(4)
H(9')	1772(10)	3330(16)	4002(10)	42(4)
H(10')	1325(9)	5002(13)	3197(9)	29(4)
H(12')	2210(9)	6793(14)	3532(9)	31(4)
H(13')	2681(10)	7312(14)	2540(9)	38(4)
H(14')	1771(9)	8153(15)	1356(9)	37(4)
H(15')	348(10)	8492(15)	1128(10)	42(4)
H(16')	-145(9)	7880(13)	2097(8)	28(4)
H(18D)	2078(11)	9318(16)	4959(11)	49(5)
H(18E)	1381(12)	8495(19)	5035(12)	61(6)
H(18F)	1753(14)	8230(20)	4374(14)	84(7)
H(19D)	711(11)	10645(17)	3049(11)	52(5)
H(19E)	1678(11)	10668(17)	3695(11)	52(5)
H(19F)	1325(10)	9534(16)	3183(10)	44(5)
H(20D)	477(11)	11397(17)	4237(11)	54(5)
H(20E)	1380(11)	11020(15)	4892(10)	42(4)
H(20F)	611(12)	10462(18)	4951(12)	63(6)

---

APPENDIX B  
SUPPORTING INFORMATION FOR CHAPTER III

***General***

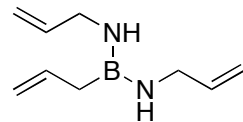
All oxygen- and moisture-sensitive manipulations were carried out under an inert atmosphere using either standard Schlenk techniques or a glove box.

$\text{Et}_2\text{O}$ ,  $\text{CH}_2\text{Cl}_2$ , THF and pentane were purified by passing through a neutral alumina column under argon. Acetonitrile was distilled from molecular sieves ( $3\text{\AA}$ ), Potassium hydride was washed with pentane three times prior to use. 10% Pd/C was purchased from Strem and dried by heating under reduced pressure overnight. All other chemicals and solvents were purchased (Aldrich, TCI, or Strem) and used as received.

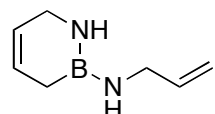
$^{11}\text{B}$  NMR spectra were recorded on a Varian Unity/Inova 600 or a Varian Unity/Inova 300 spectrometer at ambient temperature.  $^1\text{H}$  NMR spectra were recorded on a Varian Unity/Inova 300 or Varian Unity/Inova 600 spectrometer.  $^{13}\text{C}$  NMR spectra were recorded on a Varian Unity/Inova 300 or Varian Unity/Inova 500 spectrometer. All chemical shifts are externally referenced:  $^{11}\text{B}$  NMR to  $\text{BF}_3 \cdot \text{Et}_2\text{O}$  ( $\delta$  0).

IR spectra were recorded on a Nicolet Magna 550 FT-IR instrument with OMNIC software. High-resolution mass spectroscopy data were obtained at the Mass Spectroscopy Facilities and Services Core of the Environmental Health Sciences Center at Oregon State University. Financial support for this facility has been furnished in part by the National Institute of Environmental Health Sciences, NIH (P30 ES00210).

**Compound 6:** In a 2 L RBF equipped with a reflux condenser fitted with a septum, and a stir bar, potassium allyltrifluoroborate (45.00 g, 304.1 mmol) was suspended in acetonitrile (800 mL) under N<sub>2</sub>. Allylamine (113.7 mL, 1.52 mol) was added quickly to the suspension while stirring under N<sub>2</sub>, followed by dropwise addition of TMSCl (115.8 mL, 912.3 mmol). The reaction was heated to reflux for 16 h, and cooled to room temperature. Approximately half the solvent was removed under reduced pressure and the mixture was filtered through a filter stick containing a glass frit. The remainder or the solvent was removed under reduced pressure and the crude product was purified by fractional vacuum distillation (55 °C, 350 mTorr) to afford the clear colorless product **6** (30.7 g, 61%). <sup>1</sup>H NMR (500 MHz, CDCl<sub>3</sub>): δ 5.77 (m, 2H), 4.97 (m, 4H), 4.84 (m, 2H), 3.39 (s br, 4H), 2.48 (s br, 2H), 1.54 (d <sup>3</sup>J<sub>HH</sub> = 7.6 Hz, 2H). <sup>13</sup>C NMR (125 MHz, CD<sub>2</sub>Cl<sub>2</sub>): δ 140.4 (br), 138.5, 113.8, 113.4, 45.1 (br), 22.5 (br). FTIR (thin film) 3424, 3021, 2977, 2851, 1659, 1519, 1473, 1395, 998, 914, 669. HRMS (EI) calcd. for C<sub>9</sub>H<sub>16</sub>BN<sub>2</sub> (M<sup>+</sup>) 163.14066, found 163.13923.

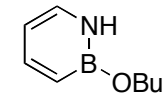


**Compound 7:** In a 250 mL RBF equipped with a stir bar in a glove box, **6** (3.30 g, 20.1 mmol) was dissolved in CH<sub>2</sub>Cl<sub>2</sub> (80 mL.) Schrock's Mo catalyst (462 mg, 0.600 mmol) was dissolved in CH<sub>2</sub>Cl<sub>2</sub> (20 mL) and added quickly to the stirred solution, and stirred for 90 min under N<sub>2</sub>. The reaction was judged to be complete by <sup>1</sup>H NMR, and the solvent was removed under reduced pressure. The crude mixture was purified by fractional vacuum distillation (45 °C, 400 mTorr) to afford **7** (2.40 g, 88%) as a clear colorless liquid. <sup>1</sup>H NMR (500 MHz, CDCl<sub>3</sub>): δ 5.89 (m,



1H), 5.77 (s br, 1H), 5.58 (m, 1H), 5.13 (app d  $^3J_{HH}$  = 17.1 Hz, 1H), 5.01 (app d  $^3J_{HH}$  = 11.2 Hz, 1H), 3.67 (s, 2H), 3.45 (m, 2H), 2.93 (s br, 1H), 2.42 (s br, 1H), 1.30 (s, 2H).  $^{13}C$  NMR (125 MHz, CD<sub>2</sub>Cl<sub>2</sub>):  $\delta$  140.1, 126.1, 125.9, 113.4, 44.1, 42.8, 12.0 (br).  $^{11}B$  NMR (96.3 MHz, CD<sub>2</sub>Cl<sub>2</sub>)  $\delta$  FTIR (thin film) 3426, 3076, 2980, 2912, 2853, 1633, 1503, 1463, 1309, 1270, 995, 915. HRMS (EI) calcd. for C<sub>7</sub>H<sub>12</sub>N<sub>2</sub>B (M<sup>+</sup>) 135.10936, found 135.10942.

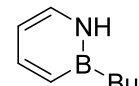
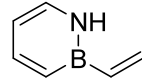
**Compound 5:** A 100 mL Parr bomb equipped with a stir bar in a glove box was charged with a solution of **7** (1.00 g, 7.35 mmol) in CH<sub>2</sub>Cl<sub>2</sub> (20 mL.) *n*-Butanol (545 mg, 7.35 mmol) in CH<sub>2</sub>Cl<sub>2</sub> (2 mL) was added dropwise to the solution while stirring vigorously. The reaction was stirred for 16 h, followed by solvent removal under reduced pressure. Cyclohexene (40 mL) followed by 10% Pd/C (1.56 g, 1.47 mmol) was added, and the vessel was sealed and heated to 60 °C for 24 h. After cooling to room temperature, the mixture was filtered through a glass frit and washed with CH<sub>2</sub>Cl<sub>2</sub> (30 mL.) The solvent was removed under reduced pressure and the crude product was purified with a short plug of silica (3:1 pentane/Et<sub>2</sub>O) to afford **5** (443 mg, 40%) as light yellow liquid.  $^1H$  NMR (500 MHz, CD<sub>2</sub>Cl<sub>2</sub>):  $\delta$  7.54, (m, 1H), 7.05 ( $t$   $^3J_{HH}$  = 7.6 Hz, 1H), 6.89 (s br, 1H), 6.29 (d  $^3J_{HH}$  = 11.7 Hz, 1H), 5.91 (d  $^3J_{HH}$  = 7.0 Hz, 1H), 3.95 ( $t$   $^3J_{HH}$  = 6.7 Hz, 2H), 1.65 (m, 2H), 1.43 (m, 2H), 0.95 (m, 3H).  $^{11}B$  NMR (96.3 MHz, CD<sub>2</sub>Cl<sub>2</sub>)  $\delta$  29.1. FTIR (thin film) HRMS (EI) calcd. for C<sub>8</sub>H<sub>14</sub>NBO (M<sup>+</sup>) 151.11685, found 151.11686.



**Compound 10:** In a glove box, a 4 mL vial was charged with a solution of **5** (0.054 g, 0.35 mmol), and ether (1 mL). The vessel was sealed and cooled to -30 °C. Vinylmagnesium bromide (1.0 M in Et<sub>2</sub>O; 0.710 mL, 0.71 mmol) was added to the vessel and reacted for 3 h. Cold HCl (2.0 M in Et<sub>2</sub>O; 0.354 mL, 0.71 mmol) was slowly added to the reaction mixture and reacted for 1 h at -30 °C, then allowed to warm to room temperature and reacted an additional hour. The mixture was concentrated under reduced pressure and the crude mixture was subjected to silica gel chromatography using pentane as eluent, yielding **10** (0.023g, 62%) as a clear colorless oil. Characterization is consistent with previous work.<sup>1</sup>

<sup>1</sup>H NMR (300 MHz, CD<sub>2</sub>Cl<sub>2</sub>): δ 8.03 (s, 1H), 7.77 (dd, <sup>3</sup>J<sub>HH</sub> = 6.4, 11 Hz, 1H) 7.39 (t, <sup>3</sup>J<sub>HH</sub> = 7.0 Hz, 1H), 6.94 (d, <sup>3</sup>J<sub>HH</sub> = 7.0 Hz, 1H) 6.48 (m, 1H), 6.37 (t, <sup>3</sup>J<sub>HH</sub> = 19.8, 13.4 Hz, 1H), 6.05(d, <sup>3</sup>J<sub>HH</sub> = 12.4 Hz, 1H), 5.93 (d, <sup>3</sup>J<sub>HH</sub> = 6.4 Hz, 1H), <sup>11</sup>B NMR (96.3 MHz, CD<sub>2</sub>Cl<sub>2</sub>): δ 33.9.

**Compound 11:** In a glove box, a 4 mL vial was charged with a solution of **5** (0.047 g, 0.31 mmol) and ether (2 mL). The vessel was sealed and cooled to -30 °C. BuLi (2.5 M in hexane; 0.250 mL, 0.62 mmol) was added to the vessel and reacted for 3 h. Cold HCl (2.0 M in Et<sub>2</sub>O; 0.241 mL, 0.48 mmol) was slowly added to the reaction mixture and reacted for 1 h at -30 °C, then allowed to warm to room temperature and reacted an additional hour. The mixture was concentrated under reduced pressure and the crude mixture was subjected to silica gel chromatography using pentane as eluent, yielding the desired compound **11** (0.035g, 83%) as a clear colorless liquid. Characterization is consistent with previous work.<sup>2</sup>



<sup>1</sup>H NMR (300 MHz, CD<sub>2</sub>Cl<sub>2</sub>): δ 7.81 (s, 1 H), 7.63 (dd, <sup>3</sup>J<sub>HH</sub> = 6.4, 4.7 Hz, 1H), 7.16 (t, <sup>3</sup>J<sub>HH</sub> = 6.7 Hz, 1H), 6.63 (d, <sup>3</sup>J<sub>HH</sub> = 11.1 Hz, 1H), 6.15 (t, <sup>3</sup>J<sub>HH</sub> = 6.4 Hz, 1H), 1.43 (m, 4H), 1.13 (m, 2H), 0.96 (t, <sup>3</sup>J<sub>HH</sub> = 7.0 Hz, 3H). <sup>11</sup>B NMR (96.3 MHz, CD<sub>2</sub>Cl<sub>2</sub>): d 38.3.

**Compound 12:** Compound **5** (10 mg, 0.07 mmol) was dissolved in CD<sub>3</sub>OD (0.6 mL) and heated at 80 °C overnight in a sealed 1 dram vial. Evidence for methoxide substitution was provided by a shift in the <sup>1</sup>H NMR. *n*-Butanol was also visible in the <sup>1</sup>H NMR. The same experiment was repeated in MeOH and the product was analyzed by HRMS. HRMS (EI) for C<sub>5</sub>H<sub>8</sub>BNO: Calculated 109.0699 found 109.0513.

**Compound 13:** In a glove box, a 4 mL vial was charged with a solution of **5** (0.051 g, 0.34 mmol) and ether (2 mL). The vessel was sealed and cooled to -30 °C. MeLi (1.6 M in hexane; 0.420 mL, 0.67 mmol) was added to the vessel and reacted for 3 h. Cold TMSCl (0.0731 mL, 0.67 mmol) was slowly added to the reaction mixture and reacted for 1 h at -30 °C, then allowed to warm to room temperature and reacted an additional hour. The mixture was concentrated under reduced pressure and the crude mixture was subjected to silica gel chromatography using pentane as eluent, yielding the desired compound (0.035g, 63%) as a clear colorless liquid.

<sup>1</sup>H NMR (300 MHz, CD<sub>2</sub>Cl<sub>2</sub>): δ 7.48 (dd, <sup>3</sup>J<sub>HH</sub> = 6.4, 4.4 Hz, 1H), 7.34 (d, <sup>3</sup>J<sub>HH</sub> = 6.4 Hz, 1H), 6.63 (d, <sup>3</sup>J<sub>HH</sub> = 10.7 Hz, 1H), 6.24 (t, <sup>3</sup>J<sub>HH</sub> = 6.4 Hz, 1H), 0.84 (s, 3H), 0.48 (s, 9H). <sup>13</sup>C NMR (125 MHz, CD<sub>2</sub>Cl<sub>2</sub>): δ 143.0, 137.8, 132 (br), 111.1 20 (br), 1.7. <sup>11</sup>B NMR (96.3 MHz, CD<sub>2</sub>Cl<sub>2</sub>): δ 40.4. FTIR (thin film) 3068, 3024, 2962, 1607, 1509, 1452, 1393,

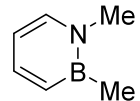
1310, 1268, 1256, 1202, 1150, 1084, 1017, 994, 884, 845, 760, 737, 629 cm<sup>-1</sup>. HRMS (EI) calcd for C<sub>8</sub>H<sub>16</sub>BNSi (M+) 165.11451, found 151.11798.

**Compound 14:** In a glove box, a 4 mL vial was charged with a solution of **5** (0.052 g, 0.34 mmol) and ether (2 mL). The vessel was sealed and cooled to -30 °C. MeLi (1.6 M in hexane; 0.430 mL, 0.68 mmol) was added to the vessel and reacted for 3 h. Cold MeI (0.097 g, 0.68 mmol) was slowly added to the reaction mixture and reacted for 1 h at -30 °C, then allowed to warm to room temperature and reacted an additional hour. The mixture was concentrated under reduced pressure and the crude mixture was subjected to silica gel chromatography using pentane as eluent, yielding the desired compound (0.018g, 49%) as a clear colorless liquid.

<sup>1</sup>H NMR (300 MHz, CD<sub>2</sub>Cl<sub>2</sub>): δ 7.47 (dd, <sup>3</sup>J<sub>HH</sub> = 6.2, 5.3, 1H), 7.19 (d, <sup>3</sup>J<sub>HH</sub> = 6.5 Hz, 1H), 6.63 (d, <sup>3</sup>J<sub>HH</sub> = 10.8 Hz, 1H), 6.19 (t, <sup>3</sup>J<sub>HH</sub> = 6.73 Hz, 1H), 3.51 (s, 3H), 1.31 (s, 3H).

<sup>11</sup>B NMR (96.3 MHz, CD<sub>2</sub>Cl<sub>2</sub>): δ 37.4. FTIR (thin film) 2964, 2951, 2939, 1610, 1517, 1463, 1417, 1402, 1266, 1123, 701, 626 cm<sup>-1</sup>.

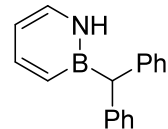
**Compound 4:** In a glove box, a 4 mL vial was charged with a solution of **5** (0.154 g, 1.02 mmol) and dihexyl ether (2 mL). The vessel was sealed and cooled to -30 °C. LiAlH<sub>4</sub> (0.020 g, 0.50 mmol) was added to the vessel and reacted for 3 h. Ammonium chloride (0.110, 2.04 mmol) was slowly added to the reaction mixture and reacted for 1 h at -30 °C, then allowed to warm to room temperature and reacted an additional hour. The mixture was passed through a plug of silica gel with dihexyl ether



and subjected to vacuum transfer yielding the desired compound **4** (0.018 g, 22%) as a clear colorless liquid. Characterization is consistent with previous work.<sup>3</sup>

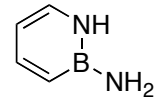
<sup>1</sup>H NMR (300 MHz, CD<sub>2</sub>Cl<sub>2</sub>): δ 8.44 (t, <sup>1</sup>J<sub>NH</sub> = 57 Hz, 1H), 7.70 (t, <sup>3</sup>J<sub>HH</sub> = 6.2 Hz, 1H), 7.40 (t, <sup>3</sup>J<sub>HH</sub> = 6.5 Hz, 1H), 6.92 (d, <sup>3</sup>J<sub>HH</sub> = 10.7 Hz, 1H), 6.43 (t, <sup>3</sup>J<sub>HH</sub> = 6.5 Hz, 1H), 4.9 (br, q, <sup>1</sup>J<sub>HH</sub> = 128 Hz, 1 H). <sup>11</sup>B NMR (96.3 MHz, CD<sub>2</sub>Cl<sub>2</sub>): d 31.0 (<sup>1</sup>J<sub>BH</sub> = 130 Hz).

**Compound 16:** In a glove box, a 4 mL vial was charged with a solution of **5** (0.018 g, 0.12 mmol) and pentane (1 mL). The vessel was sealed and cooled to -30 °C. Diphenylmethane lithiate (0.062 mL, 0.36 mmol) in 2 mL THF was added to the vessel and reacted for 3 h at -30 °C. Cold HCl (2.0 M in Et<sub>2</sub>O; 0.180 mL, 0.36 mmol) was slowly added to the reaction mixture and reacted for 1 h at -30 °C, then allowed to warm to room temperature and reacted an additional hour. The mixture was concentrated under reduced pressure and the crude mixture was subjected to silica gel chromatography using pentane/CH<sub>2</sub>Cl<sub>2</sub> as eluent, yielding the desired compound **16** (0.021g, 75%) as a solid.



<sup>1</sup>H NMR (300 MHz, CD<sub>2</sub>Cl<sub>2</sub>): <sup>1</sup>H NMR (300 MHz, CD<sub>2</sub>Cl<sub>2</sub>): δ 7.72 (s, 1H), 7.59 (dd, <sup>3</sup>J<sub>HH</sub> = 6.8, 4.4 Hz, 1H), 7.24 (m, 11H), 6.63 (d, <sup>3</sup>J<sub>HH</sub> = 11.7 Hz, 1H), 6.29 (t, <sup>3</sup>J<sub>HH</sub> = 6.8 Hz 1H), 4.33 (s, 1H). <sup>13</sup>C NMR (125 MHz, CD<sub>2</sub>Cl<sub>2</sub>): δ 145.8, 144.3, 134.0, 130.1, 130 (br), 129.0, 128.9, 128.3, 125.8, 110.7, 47 (br). <sup>11</sup>B NMR (96.3 MHz, CD<sub>2</sub>Cl<sub>2</sub>): δ 36.9. FTIR (thin film) 3378, 3058, 3022, 2927, 1615, 1598, 1576, 1533, 1492, 1460, 1419, 1154, 1154, 1072, 1030, 990, 789, 741, 722, 700, 608, 582 cm<sup>-1</sup>. HRMS (EI) calcd for C<sub>17</sub>H<sub>16</sub>BN (M+) 245.13758,

**Compound 17:** Compound **5** (20 mg, 0.13 mmol) was dissolved in pentane and cooled to  $-20^{\circ}\text{C}$ . A solution of 1 M  $\text{BCl}_3$  in hexanes (0.066 mL, 0.066 mmol) was added via syringe and allowed to react cold for 30 min. Excess  $\text{NaNH}_2$  (15 mg, 0.40 mmol) was added and the reaction was kept in the freezer overnight. The reaction was worked up with  $\text{Me}_3\text{NHCl}$  (55 mg, 0.040 mmol.) The mixture was filtered and solvent was removed. The residue (a mixture of pdt and *n*-BuOH) was dissolved in  $\text{CD}_2\text{Cl}_2$ . Evidence for  $\text{NH}_2$  substitution was provided by shift in the  $^{11}\text{B}$  NMR (from 29 ppm to 36 ppm, consistent with other N-substituted 1,2-azaborines) and a peak consistent with  $\text{NH}_2$  protons in the  $^1\text{H}$  NMR.



APPENDIX C  
SUPPORTING INFORMATION FOR CHAPTER IV

***General***

All oxygen- and moisture-sensitive manipulations were carried out under an inert atmosphere using either standard Schlenk techniques or a glove box.

$\text{Et}_2\text{O}$ ,  $\text{CH}_2\text{Cl}_2$ , and pentane were purified by passing through a neutral alumina column under argon. All other chemicals and solvents were purchased (Aldrich or Strem) and used as received.

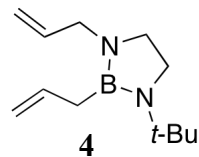
Preparative TLC (1000  $\mu\text{m}$  thickness) plates were purchased from Silicycle and heated to 120° C for 2 h in an oven before being brought into the glove box.

$^{11}\text{B}$  NMR spectra were recorded on a Varian Unity/Inova 600 or a Varian Unity/Inova 300 spectrometer at ambient temperature.  $^1\text{H}$  NMR spectra were recorded on a Varian Unity/Inova 300 or Varian Unity/Inova 600 spectrometer.  $^{13}\text{C}$  NMR spectra were recorded on a Varian Unity/Inova 300 or Varian Unity/Inova 500 spectrometer. All chemical shifts are externally referenced:  $^{11}\text{B}$  NMR to  $\text{BF}_3 \cdot \text{Et}_2\text{O}$  ( $\delta$  0).

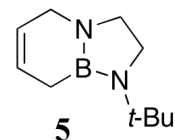
IR spectra were recorded on a Nicolet Magna 550 FT-IR instrument with OMNIC software.

High-resolution mass spectroscopy data were obtained at the Mass Spectroscopy Facilities and Services Core of the Environmental Health Sciences Center at Oregon State University. Financial support for this facility has been furnished in part by the National Institute of Environmental Health Sciences, NIH (P30 ES00210).

**Compound 4:** In a glove box, a 1 L RBF containing a stir bar was charged with allyltriphenyltin (38.89 g, 99.47 mmol) and CH<sub>2</sub>Cl<sub>2</sub> (250 mL). The stirred solution was cooled to -78 °C in a dry ice/acetone bath under N<sub>2</sub>, and a solution of BCl<sub>3</sub> in hexanes (1.0 M, 100 mL) was added dropwise via cannula. The reaction was stirred for 3.5 h at -78 °C, and a solution of *N*-allyl-*N*-*t*-Bu-ethylenediamine (15.56 g, 99.57 mmol) and triethylamine (29.2 mL, 209 mmol) in CH<sub>2</sub>Cl<sub>2</sub> (20 mL) was added dropwise via cannula. The reaction mixture was allowed to slowly warm to 25 °C for 16 h, and ~75% of the solvent was removed under reduced pressure. Pentane (150 mL) was added to precipitate the side products, and the mixture was filtered through a frit in a glove box. The precipitate was washed with pentane (~100 mL) and the mother liquor solvent was removed under reduced pressure. The oily residue was purified via fractional vacuum distillation (b.p. 45 °C, 200 mTorr) to afford the clear colorless liquid **4** (10.45 g, 50%). Spectral data for **4**: <sup>1</sup>H NMR (CD<sub>2</sub>Cl<sub>2</sub>, 300 MHz): δ 5.85 (m, 1H), 5.75 (m, 1H), 5.06 (dd <sup>3</sup>J<sub>HH</sub> = 17.1, 30.1 Hz, 2H), 4.89 (dd <sup>3</sup>J<sub>HH</sub> = 17.1, 39.6 Hz, 2H), 3.53 (d <sup>3</sup>J<sub>HH</sub> = 5.7 Hz, 2H), 3.23 (t <sup>3</sup>J<sub>HH</sub> = 8.8 Hz, 2H), 3.03 (t <sup>3</sup>J<sub>HH</sub> = 7.6 Hz, 2H), 1.81 (d <sup>3</sup>J<sub>HH</sub> = 7.1 Hz, 2H), 1.23 (s, 9H). <sup>13</sup>C NMR (CD<sub>2</sub>Cl<sub>2</sub>, 125 MHz): δ 138.2, 137.6, 115.1, 114.3, 51.8, 49.9, 48.1, 45.7, 30.8, 20.7 (br.). <sup>11</sup>B NMR (CD<sub>2</sub>Cl<sub>2</sub>, 192.5 MHz): δ 31.1. FTIR (thin film) 3075, 2970, 2925, 1632, 1478, 1411, 1361, 1319, 1292, 1260, 1021, 914, 801 cm<sup>-1</sup>.



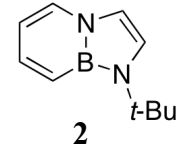
**Compound 5 (*via Grubbs' catalyst b*):** In a glove box, a 500 mL RBF containing a stir bar was charged with **4** (4.48 g, 21.4 mmol) in CH<sub>2</sub>Cl<sub>2</sub> (90 mL.) In a 20 mL scintillation vial, Grubbs Gen. 1 catalyst (bis(tricyclohexylphosphine) benzylidene ruthenium(IV) chloride) (1.05 g, 1.28 mmol) was suspended in CH<sub>2</sub>Cl<sub>2</sub> (10 mL) and quickly poured into the stirred solution of **4**. The reaction was stirred for 2 h under N<sub>2</sub> and the solvent was removed under reduced pressure. The crude material was purified by fractional vacuum distillation (45 °C, 200 mTorr) to afford the clear colorless liquid **5** (2.01 g, 51%). Spectral data for



**5:**  $^1\text{H}$  NMR ( $\text{CD}_2\text{Cl}_2$ , 300 MHz):  $\delta$  5.73 (m, 1H), 5.65 (m, 1H), 3.45 (m, 2H), 3.26 ( $t$   $^3J_{\text{HH}} = 9.1$  Hz, 2H), 3.14 ( $t$   $^3J_{\text{HH}} = 10.3$  Hz, 2H), 1.53 (br d  $^3J_{\text{HH}} = 2.35$  Hz, 2H), 1.16 (s, 9H).  $^{13}\text{C}$  NMR ( $\text{CD}_2\text{Cl}_2$ , 125 MHz):  $\delta$  126.2, 125.5, 49.8, 47.4, 45.0, 30.3, 14.4 (br.)  $^{11}\text{B}$  NMR ( $\text{CD}_2\text{Cl}_2$ , 192.5 MHz):  $\delta$  30.5. FTIR (thin film) 3021, 2968, 2876, 2818, 1500, 1484, 1436, 1418, 1399, 1360, 1351, 1294, 1251, 1212, 1164, 1053, 669  $\text{cm}^{-1}$ .

**Compound 5(via Schrock's catalyst b):** In a glove box, a 100 mL RBF containing a stir bar was charged with a solution of **4** (1.40 g, 6.70 mmol) in  $\text{CH}_2\text{Cl}_2$  (35 mL.) A solution of Schrock's catalyst (2,6-diisopropylphenylimidophenylidene molybdenum(VI) bis(hexafluoro-t-butoxide) (103 mg, 0.134 mmol) in  $\text{CH}_2\text{Cl}_2$  (10 mL) was added quickly to the stirred solution. The reaction was stirred for 5 h under  $\text{N}_2$ , and an additional aliquot of catalyst (100 mg, 0.131 mmol) was added in  $\text{CH}_2\text{Cl}_2$  (5 mL.) The reaction was stirred for an additional 14 h. The solvent was removed under reduced pressure, and the residue was purified by fractional vacuum distillation (b.p. 45 °C, 200 mTorr) to afford the clear colorless liquid **5** (960 mg, 79%). Spectral data matched that of the previous synthesis of **5**.

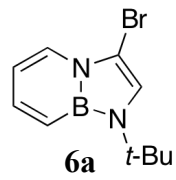
**N-t-Bu-BN-indole (2):** In a glove box, a 500 mL RBF containing a stir bar was charged with Pd/C (10 wt.% Pd, 4.84 g, 4.60 mmol) and a solution of **5** (2.80 g, 15.4 mmol) in anhydrous decane (250 mL.) The RBF was fitted with a reflux condenser equipped with a gas adapter and refluxed while stirring under an atmosphere of  $\text{N}_2$  for 3 h, then allowed to cool to 25 °C. The reaction mixture was filtered through a frit, then stirred under air for 1 h, until the side product at 25 ppm was no longer visible by  $^{11}\text{B}$  NMR. The reaction mixture was again filtered through a frit, and the solvent was removed under reduced pressure. The oily residue was purified via silica gel chromatography to afford the clear colorless oil **2** (885 mg, 32%). Spectral data for **2**:  $^1\text{H}$  NMR ( $\text{CD}_2\text{Cl}_2$ , 300 MHz):  $\delta$  7.73 (d  $^3J_{\text{HH}} = 6.5$  Hz, 1H), (m, 1H), 6.91 (s, 2H), 6.80 (d  $^3J_{\text{HH}} = 11.7$  Hz, 1H), 6.27 (app t  $^3J_{\text{HH}} = 7.0$  Hz, 1H), 1.56 (s, 9H).  $^{13}\text{C}$  NMR ( $\text{C}_6\text{D}_6$ , 75.5 MHz):  $\delta$  138.2, 130.2, 121.1, 120.5 (br,) 111.6, 109.3, 53.9, 32.5.  $^{11}\text{B}$  NMR ( $\text{CD}_2\text{Cl}_2$ , 192.5 MHz):  $\delta$  23.4. FTIR (thin film) 2973, 2931,



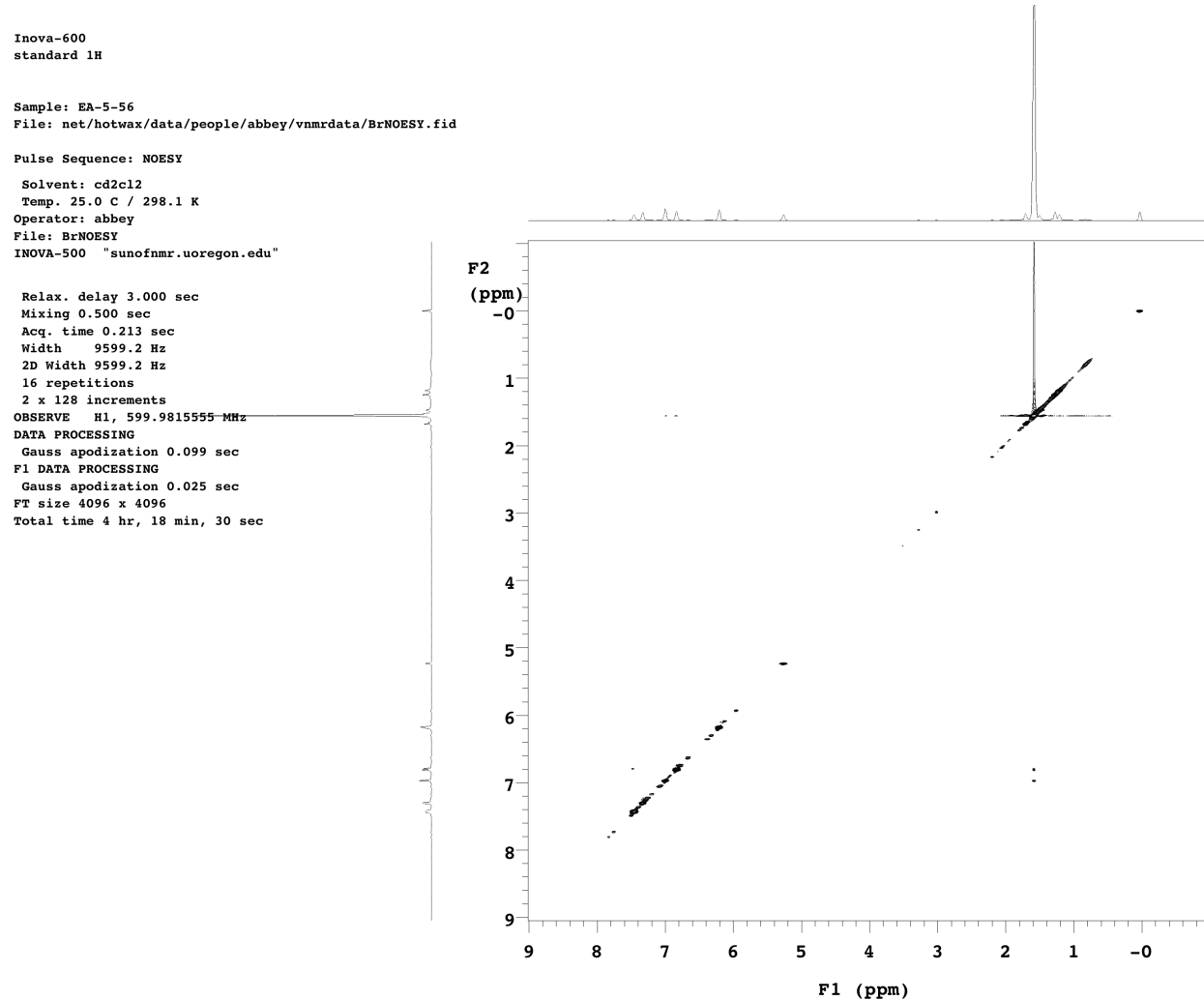
2870, 1606, 1561, 1500, 1456, 1442, 1368, 1310, 1258, 1221, 1152, 993, 976, 868, 728, 676 cm.<sup>-1</sup>

***Electrophilic Aromatic Substitution Reactions of 2:***

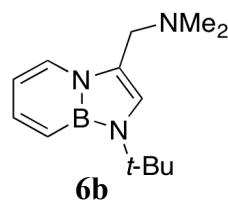
**Compound 6a:** A 20 mL scintillation vial containing a stir bar was charged with **2** (50 mg, 0.28 mmol,) and CH<sub>2</sub>Cl<sub>2</sub> (2 mL) in a glove box, then cooled to -20 °C in the freezer. A solution of Br<sub>2</sub> (48 mg, 0.30 mmol) in CH<sub>2</sub>Cl<sub>2</sub> (1 mL) was cooled to -20 °C and added dropwise to the stirred solution of **2**. The brown solution was stirred for 2 h and quenched by dropwise addition of triethylamine (43 µL, 0.31 mmol.) The solvent was removed under reduced pressure, and the solid residue was extracted with Et<sub>2</sub>O (2 x 1.5 mL) then filtered through and Acrodisc. The brown extract was purified by silica gel chromatography (5% Et<sub>2</sub>O in pentane) to yield the light brown oil **6a** (28 mg, 39%). Spectral data for **6a**: <sup>1</sup>H NMR (CD<sub>2</sub>Cl<sub>2</sub>, 300 MHz): δ 7.51 (q <sup>3</sup>J<sub>HH</sub> = 11.7, 6.7 Hz, 1H), 7.39 (d <sup>3</sup>J<sub>HH</sub> = 6.7 Hz, 1H), 7.06 (s, 1H), 6.89 (d <sup>3</sup>J<sub>HH</sub> = 11.4 Hz, 1H), 6.27 (app t <sup>3</sup>J<sub>HH</sub> = 6.7 Hz, 1 H), 1.64 (s, 9H). <sup>13</sup>C NMR (CD<sub>2</sub>Cl<sub>2</sub>, 125 MHz): δ 137.9, 128.0, 123.2, 120.3 (br,) 113.1, 108.7, 32.2, *ipso* carbon not observed. <sup>11</sup>B NMR (CD<sub>2</sub>Cl<sub>2</sub>, 96.3 MHz): δ 23.1. FTIR (thin film) 2973, 2932, 2869, 1641, 1604, 1595, 1558, 1500, 1428, 1394, 1367, 1250, 1225, 1176, 803, 730, 698 cm.<sup>-1</sup>



**<sup>1</sup>H NOESY (6a):** Cross peaks were observed between the indole C-2 and *t*-Bu singlets, confirming C-3 substitution. Cross peaks were also observed between C-7 and *t*-Bu.

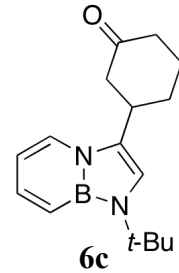


**Compound 6b:** A 1 dram vial in a containing a stir bar was charged with **2** (50 mg, 0.28 mmol,) followed by CH<sub>2</sub>Cl<sub>2</sub> (1 mL) in a glove box. Solid dimethyliminium chloride (31 mg, 0.30 mmol) was added

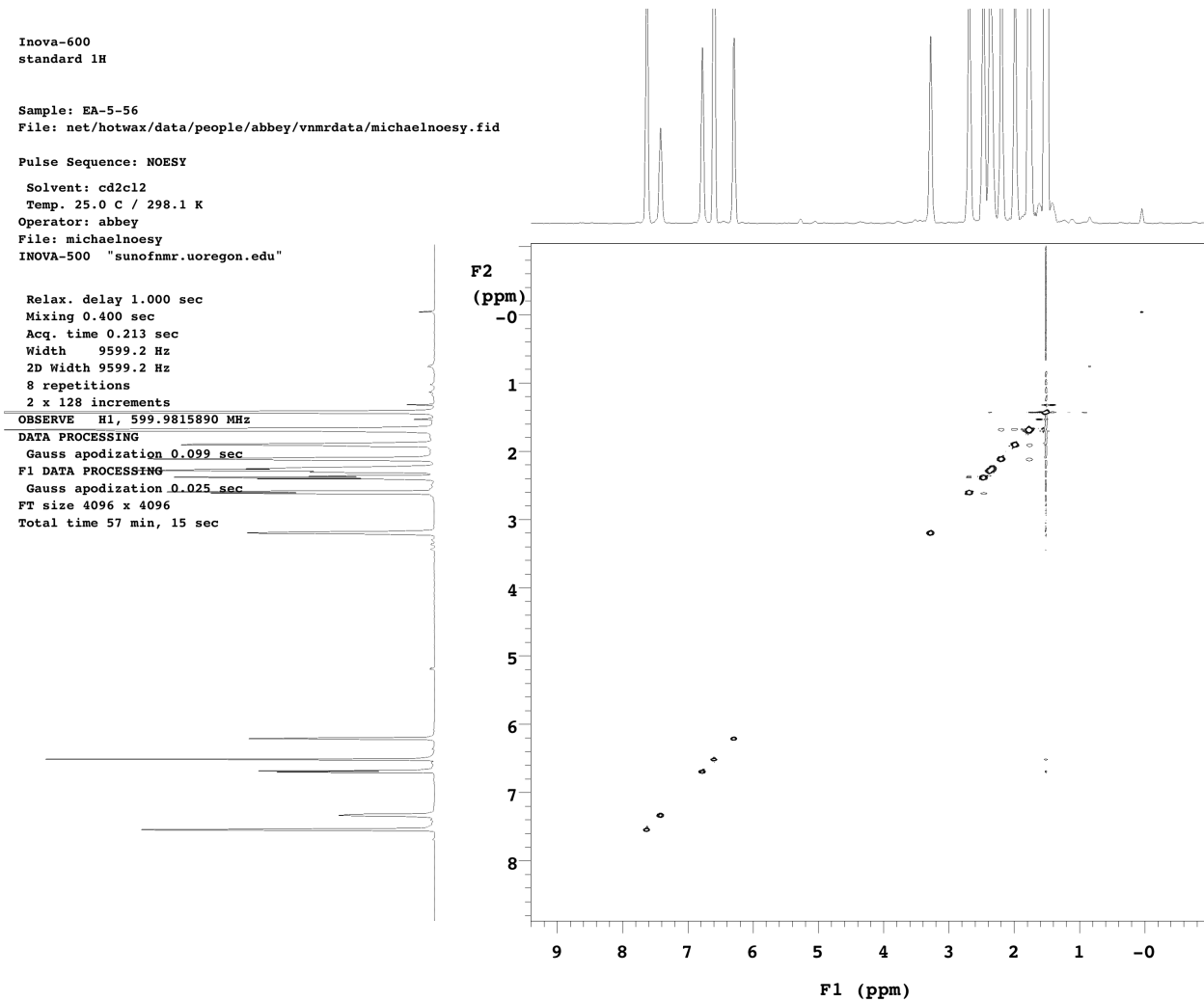


and the reaction mixture was stirred for 3 h, turning from colorless to gold. The reaction was quenched by dropwise addition of triethylamine (43  $\mu$ L, 0.31 mmol), and the solvent was removed under reduced pressure. The solid residue was extracted with Et<sub>2</sub>O (2 x 1.5 mL) and filtered through an Acrodisc. The solvent was removed under reduced pressure and the amber oil was purified by silica gel chromatography (10% Et<sub>2</sub>O, 3% triethylamine in pentane) to yield the colorless oil **6b** (35 mg, 53%). Spectral data for **6b**: <sup>1</sup>H NMR (CD<sub>2</sub>Cl<sub>2</sub>, 300 MHz):  $\delta$  7.94 (d, <sup>3</sup>J<sub>HH</sub> = 6.7 Hz, 1H), 7.46 (m, 1H), 6.78 (d, <sup>3</sup>J<sub>HH</sub> = 11.7 Hz, 1H), 6.77 (s, 1H), 6.30 (app t, <sup>3</sup>J<sub>HH</sub> = 6.7 Hz, 1H), 3.47 (s, 2H), 2.19 (s, 6H), 1.56 (s, 9H). <sup>13</sup>C NMR (CD<sub>2</sub>Cl<sub>2</sub>, 125 MHz):  $\delta$  137.4, 128.3, 120.7, 120.0 (br,), 119.4, 108.0, 55.3, 45.3, 32.2, *ipso* carbon not observed. <sup>11</sup>B NMR (CD<sub>2</sub>Cl<sub>2</sub>, 96.3 MHz):  $\delta$  22.8. FTIR (thin film) 2972, 2934, 2871, 2562, 2456, 1728, 1623, 1587, 1500, 1443, 1433, 1367, 1341, 1317, 1276, 1224, 1163, 1018, 786, 730, 696 cm.<sup>-1</sup> HRMS (EI) calcd. for C<sub>13</sub>H<sub>22</sub>BN<sub>3</sub> (M<sup>+</sup>) 231.1907, found 231.1914.

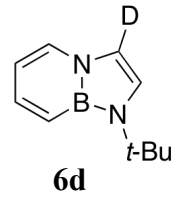
**Compound 6c:** A 20 mL vial containing a stir bar was charged with **2** (100 mg, 0.565 mmol) followed by CH<sub>2</sub>Cl<sub>2</sub> (3 mL) in a glove box. A solution of 2-cyclohexenone (54 mg, .57 mmol) in CH<sub>2</sub>Cl<sub>2</sub> (2 mL) was added to the stirred solution of **2**, followed by solid ZrCl<sub>4</sub> (5.3 mg, 0.023 mmol). The solution turned green after 15 min, then turned red after stirring for 18 h. The solvent was removed under reduced pressure, and the residue was purified by silica gel chromatography (10% Et<sub>2</sub>O, followed by 30% Et<sub>2</sub>O in pentane) to afford the clear colorless oil **6c** (88 mg, 57%, 68% based on recovered starting material) and starting material **2** (17 mg, 0.096 mmol.) Spectral data for **6c**: <sup>1</sup>H NMR (CD<sub>2</sub>Cl<sub>2</sub>, 300 MHz):  $\delta$  7.68 (d, <sup>3</sup>J<sub>HH</sub> = 6.7, 1H), 7.47 (q, <sup>3</sup>J<sub>HH</sub> = 11.4, 6.5 Hz, 1H), 6.83 (d, <sup>3</sup>J<sub>HH</sub> = 11.7 Hz, 1H), 6.65 (s, 1H), 6.35 (app t, <sup>3</sup>J<sub>HH</sub> = 6.4 Hz, 1H), 3.34 (m, 1H), 2.74 (dd, <sup>3</sup>J<sub>HH</sub> = 4.4, 1.8 Hz, 1H), 2.54 (d, <sup>3</sup>J<sub>HH</sub> = 10.8 Hz, 1H), 2.40 (m, 2H), 2.24 (m, 1H), 2.03 (m, 1H), 1.83 (m, 2H), 1.56 (s, 9H.) <sup>13</sup>C NMR (CD<sub>2</sub>Cl<sub>2</sub>, 125 MHz):  $\delta$  210.5, 137.3, 126.4, 122.4, 120.3 (br,), 117.3, 108.5, 53.9, 46.8, 42.0, 35.4, 32.2, 30.4, 25.2. <sup>11</sup>B NMR (CD<sub>2</sub>Cl<sub>2</sub>, 96.3 MHz):  $\delta$  22.5. FTIR (thin film) 2972, 2866, 1711, 1617, 1584, 1500, 1432, 1367, 1318, 1276, 1223, 1164, 729, 698 cm.<sup>-1</sup>



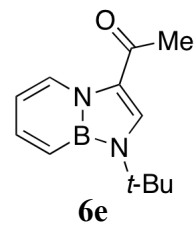
**$^1\text{H NOESY}$  (6c):** Cross peaks were observed between the indole C-2 and *t*-Bu singlets, confirming C-3 substitution. Cross peaks were also observed between C-7 and *t*-Bu.



**Compound 6d:** A 25 mL storage tube containing a stir bar charged with **2** (46 mg, 0.026 mmol), followed by degassed CD<sub>3</sub>OD (1 mL) and degassed D<sub>2</sub>O (1 mL) in a glove box. The tube was sealed and heated to 100 °C for 24 h while stirring vigorously, then cooled and extracted with Et<sub>2</sub>O (3x, 3 mL.) The solvent was removed under reduced pressure and the brown residue was purified by silica gel chromatography (5% Et<sub>2</sub>O in pentane) to afford the deuterium-enriched (~80% by <sup>1</sup>H NMR) product **6d** (18 mg, 39%). Spectral data for **6d**: <sup>1</sup>H NMR (CD<sub>2</sub>Cl<sub>2</sub>, 300 MHz): δ 7.73 (d <sup>3</sup>J<sub>HH</sub> = 6.5 Hz, 1H), 7.46 (m, 1H), 6.91 (s, 1H), δ 6.80 (d <sup>3</sup>J<sub>HH</sub> = 11.7 Hz, 1H), 6.29 (app t <sup>3</sup>J<sub>HH</sub> = 6.4 Hz, 1H) 1.57 (s, 9H) <sup>13</sup>C NMR (CD<sub>2</sub>Cl<sub>2</sub>, 125 MHz): δ 137.5, 129.8, 121.1, 121.0, 120.0 (br,) 111.0, 108.6, 32.2. <sup>11</sup>B NMR (CD<sub>2</sub>Cl<sub>2</sub>, 192.5 MHz): δ 23.4. FTIR (thin film) 2972, 2931, 2871, 1605, 1500, 1441, 1368, 1341, 1257, 1223, 1152, 1094, 1022, 801, 728, 698, 678 cm.<sup>-1</sup> HRMS (EI) calcd. for C<sub>10</sub>H<sub>15</sub>BN<sub>2</sub>D (M<sup>+</sup>) 175.1391, found 175.1383.

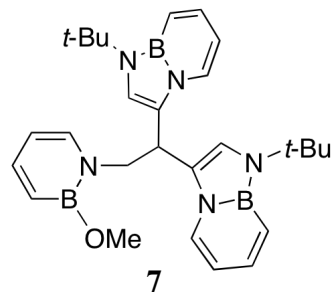


**Compound 6e:** A 20 mL vial containing a stir bar was charged with **2** (50 mg, 0.28 mmol) followed by CH<sub>2</sub>Cl<sub>2</sub> (2 mL) in a glove box. The vial was removed from the glove box and cooled to 0 °C in an ice bath. A solution of diethylaluminum chloride (1.0 M, 42 μL) in hexanes was added dropwise via syringe to the stirred solution of **2**, and stirred at 0 °C for 30 min. A solution of acetyl chloride (31 mg, 0.42 mmol) in CH<sub>2</sub>Cl<sub>2</sub> (2 mL) was added dropwise via syringe, and the reaction was stirred for an additional 2 h at 0 °C. The reaction was allowed to warm to 25 °C and stirred for 20 h. Triethylamine (60 μL, 0.42 mmol) was added dropwise via syringe, and ~75% of the solvent was removed under reduced pressure. The crude mixture was purified via prep plate TLC (5% Et<sub>2</sub>O in pentane) to afford the white solid **6e** (14 mg, 23%, 28% brsm) and starting material **2** (9 mg, 0.051 mmol.) X-ray quality crystals were grown by slow vapor diffusion of pentane into CH<sub>2</sub>Cl<sub>2</sub> in a glovebox freezer. Spectral data for **6e**: <sup>1</sup>H NMR (CD<sub>2</sub>Cl<sub>2</sub>, 300 MHz): δ 9.24 (d <sup>3</sup>J<sub>HH</sub> = 6.6 Hz, 1H), 7.83 (s, 1H), 7.62 (dd <sup>3</sup>J<sub>HH</sub> = 11.4, 7.0 Hz, 1H), 6.89 (d <sup>3</sup>J<sub>HH</sub> = 11.4 Hz, 1H), 6.43 (app t <sup>3</sup>J<sub>HH</sub> = 6.7 Hz, 1H), 2.42 (s, 3H), 1.64 (s, 9H.) <sup>13</sup>C NMR (CD<sub>2</sub>Cl<sub>2</sub>, 125 MHz): δ 188.3, 140.1, 134.7, 131.3, 122.5, 120.0 (br,) 110.1, 55.4, 31.9, 26.8. <sup>11</sup>B NMR (CD<sub>2</sub>Cl<sub>2</sub>, 96.3 MHz): δ 24.2. FTIR (thin film) 3048, 2971, 2931, 2874,



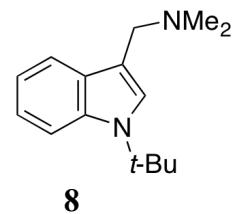
1642, 1596, 1551, 1506, 1430, 1369, 1316, 1230, 1193, 1020, 968, 918, 750, 705 cm<sup>-1</sup>  
 HRMS (EI) calcd. for C<sub>12</sub>H<sub>17</sub>BN<sub>2</sub>O (M<sup>+</sup>) 216.1434, found 216.1433.

**N-t-Bu-BN indole trimer (7):** A 1 dram vial containing a stir bar was charged with **2** (10 mg, 0.056 mmol) in CD<sub>3</sub>OD (0.5 mL), in a glove box. Acetic acid *d*4 (3 x 2 μL) was added dropwise via syringe while stirring over 4 h. The solvent was removed and the crude mixture was purified via silica gel chromatography to yield an impure mixture containing **7**. A single X-ray quality crystal was obtained by slow evaporation of the impure mixture from methanol. Spectral data for **7**: <sup>11</sup>B NMR (THF, 192.5 MHz): δ 30.2 (br,) 23.4.

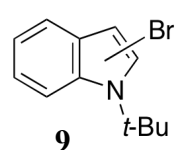


#### **EAS Competition Reference Compounds:**

**N-t-Bu-grammine (8):** A 1 dram vial was charged with a solution of *N*-t-Bu-indole (20.0 mg, 0.113 mmol) in CD<sub>2</sub>Cl<sub>2</sub> (1 mL) in a glove box. Solid dimethyliminium chloride (11.7 mg, 0.113 mmol) was added, and the reaction was stirred for 2.5 h, followed by dropwise addition of triethylamine (19 μL, 0.14 mmol.) A single product consistent with **8** was visible along with Et<sub>3</sub>NHCl in the <sup>1</sup>H NMR spectrum. Spectral data for **8**: <sup>1</sup>H NMR (CD<sub>2</sub>Cl<sub>2</sub>, 300 MHz): δ 7.64 (app t <sup>3</sup>J<sub>HH</sub> = 9.4 Hz, 2H), 7.27 (s, 1H), 7.13 (app t <sup>3</sup>J<sub>HH</sub> = 8.5 Hz, 1H), 7.05 (app t, <sup>3</sup>J<sub>HH</sub> = 8.5 Hz, 1H), 3.63 (s, 2H), 2.27 (s, 6H), 1.72 (s, 9H).



**Bromo-N-t-Bu-indole (9):** A 1 dram vial containing a stir bar was charged with a solution of *N*-t-Bu-indole (20.0 mg, 0.113 mmol) in



$\text{CH}_2\text{Cl}_2$  (0.5 mL) in a glove box. A solution of  $\text{Br}_2$  (20 mg, 0.13 mmol) in  $\text{CH}_2\text{Cl}_2$  (0.5 mL) was added dropwise via pipet, and the reaction was stirred for 3 h, then quenched with triethylamine (19  $\mu\text{L}$ , 0.14 mmol.) The solvent was removed under reduced pressure and the residue was purified (2x) by preparative TLC (5%  $\text{Et}_2\text{O}$  in pentane) to yield an inseparable mixture of two different indole products. Spectral data for mixture **9**:  $^1\text{H}$  NMR ( $\text{CD}_2\text{Cl}_2$ , 300 MHz):  $\delta$  8.43 (br s, 1H), 8.02 ( $d$   $^3J_{\text{HH}} = 7.6$  Hz, 1H),  $\delta$  7.79 (s, 1H), 7.72 ( $d$   $^3J_{\text{HH}} = 7.0$  Hz, 1H), 7.57 ( $d$   $^3J_{\text{HH}} = 7.0$  Hz, 1H), 7.44 ( $d$   $^3J_{\text{HH}} = 7.0$  Hz, 1H), 7.25 (m, 2H), 7.08 (m, 2H),  $\delta$  6.73 ( $d$   $^3J_{\text{HH}} = 2.1$  Hz, 1H), 1.79 (s, 9H).

#### **EAS Competition Studies:**

**Mannich Reaction:** Equal amounts of **2** (13 mg, 0.074 mmol) and *N*-*t*-Bu-indole (13 mg, 0.075 mmol) were combined in a 1 dram vial containing a stir bar in a glove box. Hexamethylbenzene (8 mg, 0.05 mmol) in  $\text{CD}_2\text{Cl}_2$  (1 mL) was added to the vial, and the  $^1\text{H}$  NMR spectrum of the starting material was recorded with  $t_1 = 10$  s. The peak integrations were referenced to the hexamethylbenzene internal standard. Solid dimethyliminium chloride (4.3 mg, 0.042 mmol) was added, and the reaction was stirred for 90 m, followed by dropwise addition of triethylamine (6.4  $\mu\text{L}$ , 0.046 mmol.) Analysis showed only the BN-substituted product **6b**, and unconsumed starting materials **2** and *N*-*t*-Bu-indole, with minor side peaks inconsistent with **6b** or **8**.

**Bromination:** Equal amounts of **2** (11.5 mg, 0.0650 mmol) and *N*-*t*-Bu-indole (11.5 mg, 0.0650 mmol) were combined in a 1 dram vial containing a stir bar in a glove box. Hexamethylbenzene (7.0 mg, 0.43 mmol) in  $\text{CD}_2\text{Cl}_2$  (0.5 mL) was added to the vial, and the  $^1\text{H}$  NMR spectrum of the starting material was recorded with  $t_1 = 10$  s. The solution was cooled to -20 °C in a glove box freezer, and a solution of  $\text{Br}_2$  (6.0 mg, 0.033 mmol) in  $\text{CD}_2\text{Cl}_2$  (0.5 mL) cooled to -20 °C was added dropwise via pipet. The reaction was stirred for 3.25 h, followed by dropwise addition of triethylamine (6.4  $\mu\text{L}$ , 0.046 mmol.) Analysis showed only the BN-substituted product **6a**, and unconsumed starting materials **2** and *N*-*t*-Bu-indole, with side peaks inconsistent with **6a** or **9**.

### **X-ray Crystal Structure Determination.**

Diffraction intensity data were collected with a Bruker Smart Apex CCD diffractometer at 173(2) K using MoK $\alpha$  - radiation (0.71073 Å). The structure was solved using direct methods, completed by subsequent difference Fourier syntheses, and refined by full matrix least-squares procedures on F<sup>2</sup>. All non-H atoms were refined with anisotropic thermal parameters. H atoms were found on the residual density map and refined with isotropic thermal parameters. The Flack parameter is 0.00(8). All software and sources scattering factors are contained in the SHELXTL (6.10) program package (G.Sheldrick, Bruker XRD, Madison, WI). Crystallographic data and some details of data collection and crystal structure refinement are given in the following tables.

**Crystallographic data for 6e.**

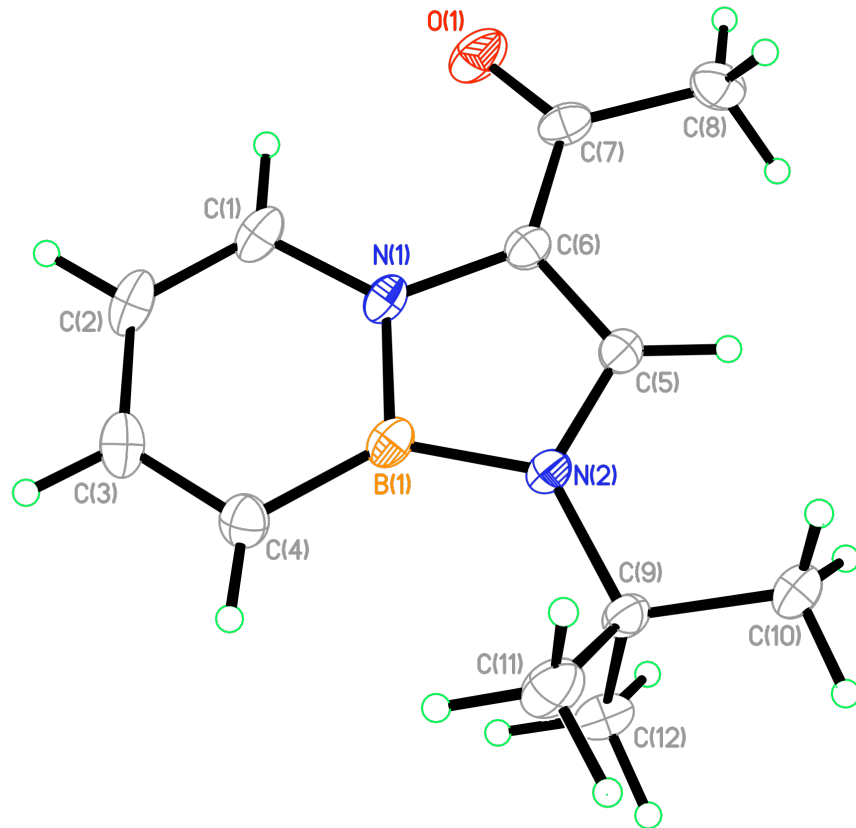


Table 1. Crystal data and structure refinement for liu69.

Identification code	liu69
Empirical formula	C <sub>12</sub> H <sub>17</sub> B N <sub>2</sub> O
Formula weight	216.09
Temperature	173(2) K
Wavelength	0.71073 Å
Crystal system	Triclinic
Space group	P-1
Unit cell dimensions	
a = 7.961(2) Å	α = 80.769(5)°.
b = 8.703(3) Å	β = 75.052(5)°.
c = 9.587(3) Å	γ = 68.094(4)°.

Volume	593.9(3) Å <sup>3</sup>
Z	2
Density (calculated)	1.208 Mg/m <sup>3</sup>
Absorption coefficient	0.076 mm <sup>-1</sup>
F(000)	232
Crystal size	0.39 x 0.08 x 0.04 mm <sup>3</sup>
Theta range for data collection	2.20 to 26.99°.
Index ranges	-10<=h<=10, -11<=k<=11, -12<=l<=12
Reflections collected	6615
Independent reflections	2569 [R(int) = 0.0223]
Completeness to theta = 26.99°	99.1 %
Absorption correction	Semi-empirical from equivalents
Max. and min. transmission	0.9969 and 0.9708
Refinement method	Full-matrix least-squares on F <sup>2</sup>
Data / restraints / parameters	2569 / 0 / 213
Goodness-of-fit on F <sup>2</sup>	1.049
Final R indices [I>2sigma(I)]	R1 = 0.0477, wR2 = 0.1080
R indices (all data)	R1 = 0.0673, wR2 = 0.1206
Largest diff. peak and hole	0.192 and -0.154 e.Å <sup>-3</sup>

Table 2. Atomic coordinates ( $\times 10^4$ ) and equivalent isotropic displacement parameters ( $\text{\AA}^2 \times 10^3$ ) for liu69. U(eq) is defined as one third of the trace of the orthogonalized  $U^{ij}$  tensor.

x	y	z	U(eq)
N(1)	1564(2)	11271(2)	8861(1)
N(2)	2862(2)	8650(2)	8047(1)
O(1)	2163(2)	12050(2)	11513(1)
B(1)	1809(2)	10364(2)	7642(2)
C(1)	602(2)	12950(2)	8903(2)
C(2)	-126(2)	13798(2)	7760(2)
C(3)	94(2)	13010(2)	6507(2)
C(4)	1012(2)	11345(2)	6382(2)
C(5)	3184(2)	8616(2)	9382(2)
C(6)	2437(2)	10155(2)	9919(2)
C(7)	2670(2)	10596(2)	11226(2)
C(8)	3584(3)	9215(2)	12242(2)
C(9)	3708(2)	7192(2)	7141(2)
C(10)	4379(3)	5584(2)	8064(2)
C(11)	2243(3)	7119(3)	6421(2)
C(12)	5339(3)	7438(3)	6008(2)

Table 3. Bond lengths [ $\text{\AA}$ ] and angles [ $^\circ$ ] for liu69.

N(1)-C(1)	1.375(2)
N(1)-C(6)	1.414(2)
N(1)-B(1)	1.446(2)
N(2)-C(5)	1.363(2)
N(2)-B(1)	1.459(2)
N(2)-C(9)	1.4938(19)
O(1)-C(7)	1.2301(19)
B(1)-C(4)	1.500(3)
C(1)-C(2)	1.353(3)
C(1)-H(1)	0.97(2)
C(2)-C(3)	1.418(3)
C(2)-H(2)	0.98(2)
C(3)-C(4)	1.367(2)
C(3)-H(3)	0.968(19)
C(4)-H(4)	0.922(17)
C(5)-C(6)	1.372(2)
C(5)-H(5)	0.978(16)
C(6)-C(7)	1.442(2)
C(7)-C(8)	1.504(3)
C(8)-H(8A)	0.97(3)
C(8)-H(8B)	0.97(3)
C(8)-H(8C)	1.04(3)
C(9)-C(10)	1.522(2)
C(9)-C(12)	1.522(2)
C(9)-C(11)	1.525(2)
C(10)-H(10A)	0.99(2)
C(10)-H(10B)	0.99(2)
C(10)-H(10C)	1.04(2)
C(11)-H(11A)	0.99(2)
C(11)-H(11B)	1.01(2)
C(11)-H(11C)	1.01(2)
C(12)-H(12A)	0.989(19)
C(12)-H(12B)	1.02(2)
C(12)-H(12C)	1.012(19)

C(1)-N(1)-C(6)	128.70(14)
C(1)-N(1)-B(1)	122.38(14)
C(6)-N(1)-B(1)	108.92(13)
C(5)-N(2)-B(1)	107.49(13)
C(5)-N(2)-C(9)	123.46(13)
B(1)-N(2)-C(9)	128.53(13)
N(1)-B(1)-N(2)	104.56(14)
N(1)-B(1)-C(4)	117.04(15)
N(2)-B(1)-C(4)	138.39(16)
C(2)-C(1)-N(1)	119.24(17)
C(2)-C(1)-H(1)	123.1(12)
N(1)-C(1)-H(1)	117.6(12)
C(1)-C(2)-C(3)	121.92(16)
C(1)-C(2)-H(2)	116.9(12)
C(3)-C(2)-H(2)	121.1(12)
C(4)-C(3)-C(2)	122.61(17)
C(4)-C(3)-H(3)	119.4(11)
C(2)-C(3)-H(3)	118.0(11)
C(3)-C(4)-B(1)	116.78(16)
C(3)-C(4)-H(4)	117.3(11)
B(1)-C(4)-H(4)	125.9(11)
N(2)-C(5)-C(6)	112.38(14)
N(2)-C(5)-H(5)	120.6(9)
C(6)-C(5)-H(5)	127.0(9)
C(5)-C(6)-N(1)	106.64(13)
C(5)-C(6)-C(7)	126.96(15)
N(1)-C(6)-C(7)	126.04(14)
O(1)-C(7)-C(6)	122.01(16)
O(1)-C(7)-C(8)	120.05(15)
C(6)-C(7)-C(8)	117.94(15)
C(7)-C(8)-H(8A)	108.4(15)
C(7)-C(8)-H(8B)	112.9(15)
H(8A)-C(8)-H(8B)	113(2)
C(7)-C(8)-H(8C)	112.5(13)
H(8A)-C(8)-H(8C)	107(2)
H(8B)-C(8)-H(8C)	103.0(19)
N(2)-C(9)-C(10)	110.91(14)

N(2)-C(9)-C(12)	107.85(13)
C(10)-C(9)-C(12)	109.70(15)
N(2)-C(9)-C(11)	108.48(13)
C(10)-C(9)-C(11)	109.24(16)
C(12)-C(9)-C(11)	110.65(15)
C(9)-C(10)-H(10A)	110.7(12)
C(9)-C(10)-H(10B)	107.5(12)
H(10A)-C(10)-H(10B)	109.4(17)
C(9)-C(10)-H(10C)	112.1(11)
H(10A)-C(10)-H(10C)	110.8(16)
H(10B)-C(10)-H(10C)	106.3(16)
C(9)-C(11)-H(11A)	109.1(11)
C(9)-C(11)-H(11B)	110.9(11)
H(11A)-C(11)-H(11B)	109.5(16)
C(9)-C(11)-H(11C)	110.4(12)
H(11A)-C(11)-H(11C)	108.5(16)
H(11B)-C(11)-H(11C)	108.3(16)
C(9)-C(12)-H(12A)	110.4(11)
C(9)-C(12)-H(12B)	112.5(12)
H(12A)-C(12)-H(12B)	108.3(15)
C(9)-C(12)-H(12C)	110.8(10)
H(12A)-C(12)-H(12C)	106.5(15)
H(12B)-C(12)-H(12C)	108.1(16)

---

Symmetry transformations used to generate equivalent atoms:

Table 4. Anisotropic displacement parameters ( $\text{\AA}^2 \times 10^3$ ) for liu69. The anisotropic displacement factor exponent takes the form:  $-2p^2 [ h^2 a^{*2} U^{11} + \dots + 2 h k a^{*} b^{*} U^{12} ]$

$U^{11}$	$U^{22}$	$U^{33}$	$U^{23}$	$U^{13}$	$U^{12}$
N(1)	22(1)	25(1)	40(1)	-6(1)	-6(1)
N(2)	27(1)	25(1)	31(1)	-7(1)	-6(1)
O(1)	48(1)	42(1)	62(1)	-26(1)	-16(1)
B(1)	22(1)	27(1)	41(1)	-5(1)	-4(1)
C(1)	28(1)	26(1)	58(1)	-11(1)	-9(1)
C(2)	32(1)	25(1)	72(1)	-4(1)	-17(1)
C(3)	36(1)	35(1)	58(1)	8(1)	-20(1)
C(4)	34(1)	37(1)	40(1)	-2(1)	-12(1)
C(5)	27(1)	27(1)	30(1)	-3(1)	-4(1)
C(6)	25(1)	29(1)	33(1)	-5(1)	-3(1)
C(7)	26(1)	40(1)	38(1)	-13(1)	0(1)
C(8)	50(1)	46(1)	34(1)	-4(1)	-8(1)
C(9)	33(1)	25(1)	33(1)	-8(1)	-7(1)
C(10)	65(1)	26(1)	46(1)	-8(1)	-12(1)
C(11)	43(1)	41(1)	60(1)	-19(1)	-16(1)
C(12)	39(1)	43(1)	42(1)	-16(1)	0(1)
					-13(1)

Table 5. Hydrogen coordinates ( $\times 10^4$ ) and isotropic displacement parameters ( $\text{\AA}^2 \times 10^3$ ) for liu69.

x	y	z	U(eq)
H(1)	520(30)	13470(20)	9750(20)
H(2)	-800(30)	14990(30)	7830(20)
H(3)	-390(30)	13700(20)	5700(20)
H(4)	1110(20)	10930(20)	5528(19)
H(5)	3900(20)	7580(20)	9845(16)
H(8A)	3890(30)	9700(30)	12950(30)
H(8B)	2850(30)	8510(30)	12680(30)
H(8C)	4820(30)	8380(30)	11720(30)
H(10A)	3350(30)	5450(20)	8850(20)
H(10B)	4850(30)	4650(30)	7420(20)
H(10C)	5500(30)	5510(20)	8480(20)
H(11A)	2790(30)	6140(30)	5830(20)
H(11B)	1790(30)	8160(30)	5780(20)
H(11C)	1140(30)	6990(20)	7180(20)
H(12A)	5900(20)	6520(20)	5350(20)
H(12B)	6340(30)	7480(20)	6460(20)
H(12C)	4920(30)	8500(20)	5380(20)

Table 6. Torsion angles [°] for liu69.

C(1)-N(1)-B(1)-N(2)	-179.08(12)
C(6)-N(1)-B(1)-N(2)	0.39(15)
C(1)-N(1)-B(1)-C(4)	1.9(2)
C(6)-N(1)-B(1)-C(4)	-178.64(13)
C(5)-N(2)-B(1)-N(1)	-0.36(15)
C(9)-N(2)-B(1)-N(1)	-172.18(13)
C(5)-N(2)-B(1)-C(4)	178.35(19)
C(9)-N(2)-B(1)-C(4)	6.5(3)
C(6)-N(1)-C(1)-C(2)	179.73(15)
B(1)-N(1)-C(1)-C(2)	-0.9(2)
N(1)-C(1)-C(2)-C(3)	-0.8(3)
C(1)-C(2)-C(3)-C(4)	1.6(3)
C(2)-C(3)-C(4)-B(1)	-0.5(2)
N(1)-B(1)-C(4)-C(3)	-1.1(2)
N(2)-B(1)-C(4)-C(3)	-179.73(17)
B(1)-N(2)-C(5)-C(6)	0.20(17)
C(9)-N(2)-C(5)-C(6)	172.54(13)
N(2)-C(5)-C(6)-N(1)	0.05(17)
N(2)-C(5)-C(6)-C(7)	-173.40(14)
C(1)-N(1)-C(6)-C(5)	179.14(14)
B(1)-N(1)-C(6)-C(5)	-0.29(16)
C(1)-N(1)-C(6)-C(7)	-7.3(2)
B(1)-N(1)-C(6)-C(7)	173.24(14)
C(5)-C(6)-C(7)-O(1)	169.52(15)
N(1)-C(6)-C(7)-O(1)	-2.7(2)
C(5)-C(6)-C(7)-C(8)	-9.8(2)
N(1)-C(6)-C(7)-C(8)	177.98(14)
C(5)-N(2)-C(9)-C(10)	19.6(2)
B(1)-N(2)-C(9)-C(10)	-169.76(16)
C(5)-N(2)-C(9)-C(12)	-100.54(17)
B(1)-N(2)-C(9)-C(12)	70.10(19)
C(5)-N(2)-C(9)-C(11)	139.57(16)
B(1)-N(2)-C(9)-C(11)	-49.8(2)

Symmetry transformations used to generate equivalent atoms:

*Crystallographic data for 7.*

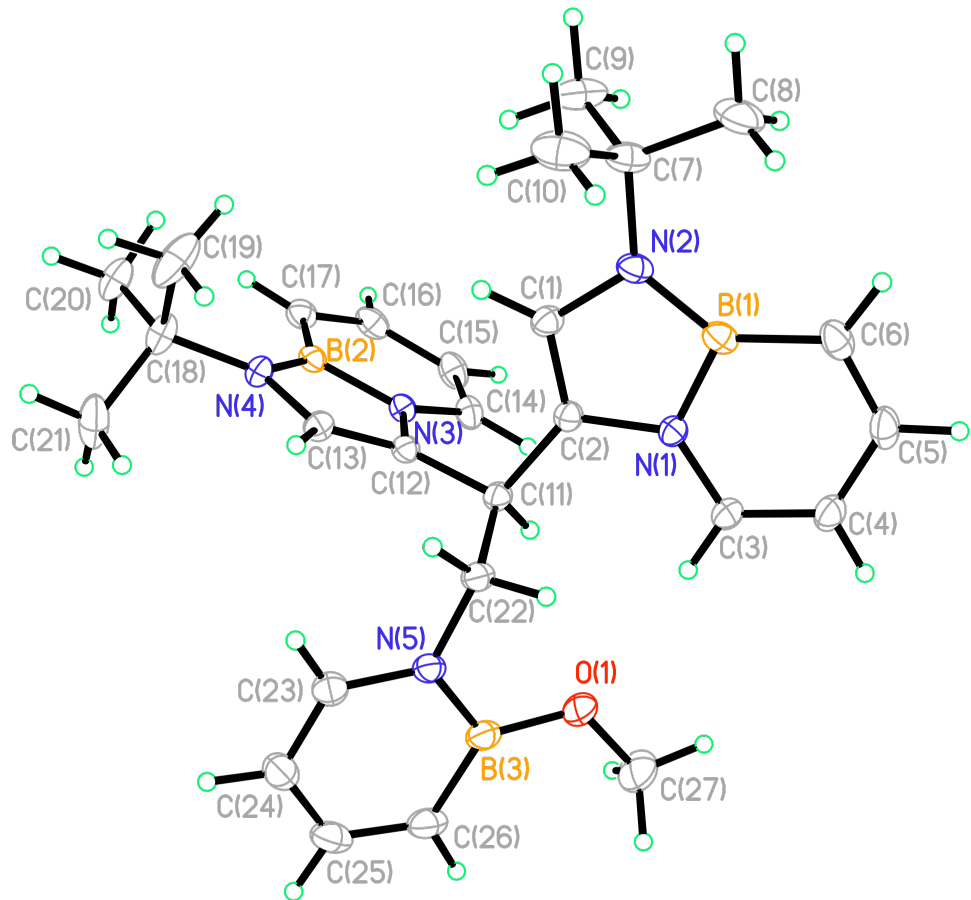


Table 1. Crystal data and structure refinement for liu10a.

Identification code	liu10a
Empirical formula	C <sub>27</sub> H <sub>38</sub> B <sub>3</sub> N <sub>5</sub> O
Formula weight	481.05
Temperature	173(2) K
Wavelength	0.71073 Å

Crystal system	Orthorhombic
Space group	Pbcn
Unit cell dimensions	
$a = 17.5388(17)$ Å	$\alpha = 90^\circ$ .
$b = 17.3342(17)$ Å	$\beta = 90^\circ$ .
$c = 18.8857(18)$ Å	$\gamma = 90^\circ$ .
Volume	5741.7(10) Å <sup>3</sup>
Z	8
Density (calculated)	1.113 Mg/m <sup>3</sup>
Absorption coefficient	0.068 mm <sup>-1</sup>
F(000)	2064
Crystal size	0.39 x 0.34 x 0.28 mm <sup>3</sup>
Theta range for data collection	1.65 to 27.00°.
Index ranges	-22<=h<=22, -20<=k<=22, -24<=l<=24
Reflections collected	51080
Independent reflections	6278 [R(int) = 0.0603]
Completeness to theta = 27.00°	100.0 %
Absorption correction	Semi-empirical from equivalents
Max. and min. transmission	0.9813 and 0.9741
Refinement method	Full-matrix least-squares on F <sup>2</sup>
Data / restraints / parameters	6278 / 0 / 477
Goodness-of-fit on F <sup>2</sup>	1.025
Final R indices [I>2sigma(I)]	R1 = 0.0465, wR2 = 0.1025
R indices (all data)	R1 = 0.0745, wR2 = 0.1188
Largest diff. peak and hole	0.204 and -0.174 e.Å <sup>-3</sup>

Table 2. Atomic coordinates ( $\times 10^4$ ) and equivalent isotropic displacement parameters ( $\text{\AA}^2 \times 10^3$ ) for liu10a. U(eq) is defined as one third of the trace of the orthogonalized  $U^{ij}$  tensor.

x	y	z	U(eq)
B(1)	3210(1)	5817(1)	1557(1)
B(2)	1795(1)	7988(1)	-831(1)
B(3)	-200(1)	6960(1)	1538(1)
N(1)	2394(1)	5953(1)	1458(1)
N(2)	3570(1)	6469(1)	1224(1)
N(3)	1613(1)	7323(1)	-388(1)
N(4)	1868(1)	8613(1)	-338(1)
N(5)	379(1)	7551(1)	1552(1)
O(1)	68(1)	6215(1)	1577(1)
C(1)	2993(1)	6936(1)	956(1)
C(2)	2294(1)	6646(1)	1086(1)
C(3)	1843(1)	5448(1)	1682(1)
C(4)	2053(1)	4783(1)	2008(1)
C(5)	2831(1)	4601(1)	2130(1)
C(6)	3415(1)	5076(1)	1931(1)
C(7)	4383(1)	6701(1)	1146(1)
C(8)	4877(1)	6059(2)	1454(2)
C(9)	4580(1)	6797(2)	369(1)
C(10)	4517(1)	7446(2)	1549(1)
C(11)	1523(1)	6991(1)	926(1)
C(12)	1594(1)	7555(1)	326(1)
C(13)	1747(1)	8315(1)	339(1)
C(14)	1491(1)	6602(1)	-659(1)
C(15)	1545(1)	6484(1)	-1367(1)
C(16)	1724(1)	7095(1)	-1841(1)
C(17)	1845(1)	7833(1)	-1621(1)
C(18)	2088(1)	9429(1)	-423(1)
C(19)	2845(2)	9556(2)	-37(1)
C(20)	2187(1)	9608(1)	-1208(1)
C(21)	1461(2)	9944(1)	-123(1)
C(22)	1191(1)	7352(1)	1606(1)
C(23)	179(1)	8313(1)	1544(1)

C(24)	-556(1)	8551(1)	1511(1)	44(1)
C(25)	-1153(1)	8007(1)	1476(1)	47(1)
C(26)	-1018(1)	7237(1)	1489(1)	43(1)
C(27)	-457(1)	5589(1)	1606(2)	62(1)

Table 3. Bond lengths [Å] and angles [°] for liu10a.

B(1)-N(2)	1.440(2)
B(1)-N(1)	1.463(2)
B(1)-C(6)	1.509(3)
B(2)-N(4)	1.433(2)
B(2)-N(3)	1.460(2)
B(2)-C(17)	1.519(2)
B(3)-O(1)	1.377(2)
B(3)-N(5)	1.442(2)
B(3)-C(26)	1.516(3)
N(1)-C(3)	1.370(2)
N(1)-C(2)	1.4038(19)
N(2)-C(1)	1.392(2)
N(2)-C(7)	1.4879(19)
N(3)-C(14)	1.367(2)
N(3)-C(12)	1.4065(18)
N(4)-C(13)	1.3945(18)
N(4)-C(18)	1.476(2)
N(5)-C(23)	1.366(2)
N(5)-C(22)	1.4682(19)
O(1)-C(27)	1.424(2)
C(1)-C(2)	1.348(2)
C(1)-H(1)	0.958(17)
C(2)-C(11)	1.509(2)
C(3)-C(4)	1.357(2)
C(3)-H(3)	0.980(17)
C(4)-C(5)	1.420(3)
C(4)-H(4)	0.988(19)
C(5)-C(6)	1.367(3)
C(5)-H(5)	0.963(18)
C(6)-H(6)	0.984(18)

C(7)-C(9)	1.517(2)
C(7)-C(10)	1.517(3)
C(7)-C(8)	1.525(3)
C(8)-H(8A)	1.03(3)
C(8)-H(8B)	1.01(2)
C(8)-H(8C)	0.96(2)
C(9)-H(9A)	1.00(3)
C(9)-H(9B)	1.02(2)
C(9)-H(9C)	1.01(2)
C(10)-H(10A)	0.98(2)
C(10)-H(10B)	0.98(2)
C(10)-H(10C)	0.99(2)
C(11)-C(12)	1.501(2)
C(11)-C(22)	1.542(2)
C(11)-H(11)	0.992(16)
C(12)-C(13)	1.344(2)
C(13)-H(13)	0.976(15)
C(14)-C(15)	1.356(2)
C(14)-H(14)	0.990(18)
C(15)-C(16)	1.423(3)
C(15)-H(15)	0.96(2)
C(16)-C(17)	1.362(2)
C(16)-H(16)	1.011(18)
C(17)-H(17)	0.989(18)
C(18)-C(21)	1.525(3)
C(18)-C(20)	1.526(2)
C(18)-C(19)	1.530(3)
C(19)-H(19A)	1.01(3)
C(19)-H(19B)	0.96(3)
C(19)-H(19C)	1.00(2)
C(20)-H(20A)	0.980(19)
C(20)-H(20B)	1.03(2)
C(20)-H(20C)	0.98(2)
C(21)-H(21A)	1.03(2)
C(21)-H(21B)	0.96(2)
C(21)-H(21C)	0.99(2)
C(22)-H(22A)	1.000(16)

C(22)-H(22B)	1.000(16)
C(23)-C(24)	1.356(2)
C(23)-H(23)	0.958(18)
C(24)-C(25)	1.412(3)
C(24)-H(24)	1.00(2)
C(25)-C(26)	1.356(3)
C(25)-H(25)	0.970(19)
C(26)-H(26)	1.008(18)
C(27)-H(27A)	1.02(3)
C(27)-H(27B)	0.99(3)
C(27)-H(27C)	0.98(2)
N(2)-B(1)-N(1)	104.29(13)
N(2)-B(1)-C(6)	140.20(15)
N(1)-B(1)-C(6)	115.48(15)
N(4)-B(2)-N(3)	104.13(12)
N(4)-B(2)-C(17)	140.03(15)
N(3)-B(2)-C(17)	115.84(14)
O(1)-B(3)-N(5)	115.19(14)
O(1)-B(3)-C(26)	128.52(17)
N(5)-B(3)-C(26)	116.28(17)
C(3)-N(1)-C(2)	127.82(13)
C(3)-N(1)-B(1)	123.17(14)
C(2)-N(1)-B(1)	108.97(13)
C(1)-N(2)-B(1)	107.26(12)
C(1)-N(2)-C(7)	120.24(14)
B(1)-N(2)-C(7)	132.49(13)
C(14)-N(3)-C(12)	128.03(13)
C(14)-N(3)-B(2)	122.78(13)
C(12)-N(3)-B(2)	109.19(12)
C(13)-N(4)-B(2)	107.53(12)
C(13)-N(4)-C(18)	119.65(12)
B(2)-N(4)-C(18)	132.66(12)
C(23)-N(5)-B(3)	120.38(14)
C(23)-N(5)-C(22)	118.46(14)
B(3)-N(5)-C(22)	121.12(14)
B(3)-O(1)-C(27)	119.76(15)

C(2)-C(1)-N(2)	112.28(14)
C(2)-C(1)-H(1)	125.8(10)
N(2)-C(1)-H(1)	121.9(10)
C(1)-C(2)-N(1)	107.20(13)
C(1)-C(2)-C(11)	129.17(14)
N(1)-C(2)-C(11)	123.50(12)
C(4)-C(3)-N(1)	119.47(16)
C(4)-C(3)-H(3)	124.4(10)
N(1)-C(3)-H(3)	116.1(10)
C(3)-C(4)-C(5)	121.49(17)
C(3)-C(4)-H(4)	116.8(11)
C(5)-C(4)-H(4)	121.8(11)
C(6)-C(5)-C(4)	122.79(17)
C(6)-C(5)-H(5)	119.2(10)
C(4)-C(5)-H(5)	118.0(11)
C(5)-C(6)-B(1)	117.59(16)
C(5)-C(6)-H(6)	117.5(11)
B(1)-C(6)-H(6)	124.9(11)
N(2)-C(7)-C(9)	110.15(13)
N(2)-C(7)-C(10)	109.17(14)
C(9)-C(7)-C(10)	110.82(19)
N(2)-C(7)-C(8)	108.06(16)
C(9)-C(7)-C(8)	108.67(18)
C(10)-C(7)-C(8)	109.93(19)
C(7)-C(8)-H(8A)	109.8(15)
C(7)-C(8)-H(8B)	108.3(13)
H(8A)-C(8)-H(8B)	112(2)
C(7)-C(8)-H(8C)	107.6(14)
H(8A)-C(8)-H(8C)	111(2)
H(8B)-C(8)-H(8C)	108.4(17)
C(7)-C(9)-H(9A)	111.7(14)
C(7)-C(9)-H(9B)	111.0(12)
H(9A)-C(9)-H(9B)	108.9(18)
C(7)-C(9)-H(9C)	108.3(12)
H(9A)-C(9)-H(9C)	111.0(19)
H(9B)-C(9)-H(9C)	105.8(17)
C(7)-C(10)-H(10A)	109.2(14)

C(7)-C(10)-H(10B)	111.1(13)
H(10A)-C(10)-H(10B)	110.6(19)
C(7)-C(10)-H(10C)	112.2(12)
H(10A)-C(10)-H(10C)	109.4(18)
H(10B)-C(10)-H(10C)	104.3(18)
C(12)-C(11)-C(2)	109.53(12)
C(12)-C(11)-C(22)	113.31(13)
C(2)-C(11)-C(22)	109.41(12)
C(12)-C(11)-H(11)	108.1(9)
C(2)-C(11)-H(11)	108.6(9)
C(22)-C(11)-H(11)	107.8(9)
C(13)-C(12)-N(3)	106.98(12)
C(13)-C(12)-C(11)	129.85(13)
N(3)-C(12)-C(11)	122.63(13)
C(12)-C(13)-N(4)	112.16(13)
C(12)-C(13)-H(13)	126.6(9)
N(4)-C(13)-H(13)	121.2(9)
C(15)-C(14)-N(3)	119.81(16)
C(15)-C(14)-H(14)	123.4(10)
N(3)-C(14)-H(14)	116.8(10)
C(14)-C(15)-C(16)	121.55(16)
C(14)-C(15)-H(15)	118.6(11)
C(16)-C(15)-H(15)	119.9(11)
C(17)-C(16)-C(15)	122.79(15)
C(17)-C(16)-H(16)	120.5(10)
C(15)-C(16)-H(16)	116.7(10)
C(16)-C(17)-B(2)	117.22(15)
C(16)-C(17)-H(17)	119.3(10)
B(2)-C(17)-H(17)	123.5(10)
N(4)-C(18)-C(21)	109.40(15)
N(4)-C(18)-C(20)	109.28(14)
C(21)-C(18)-C(20)	108.92(16)
N(4)-C(18)-C(19)	108.18(15)
C(21)-C(18)-C(19)	111.4(2)
C(20)-C(18)-C(19)	109.61(17)
C(18)-C(19)-H(19A)	109.3(17)
C(18)-C(19)-H(19B)	105.9(14)

H(19A)-C(19)-H(19B)	116(2)
C(18)-C(19)-H(19C)	111.7(12)
H(19A)-C(19)-H(19C)	110(2)
H(19B)-C(19)-H(19C)	103.5(18)
C(18)-C(20)-H(20A)	109.3(11)
C(18)-C(20)-H(20B)	112.3(12)
H(20A)-C(20)-H(20B)	110.4(16)
C(18)-C(20)-H(20C)	106.1(11)
H(20A)-C(20)-H(20C)	111.3(16)
H(20B)-C(20)-H(20C)	107.5(16)
C(18)-C(21)-H(21A)	111.8(13)
C(18)-C(21)-H(21B)	106.5(14)
H(21A)-C(21)-H(21B)	109.8(19)
C(18)-C(21)-H(21C)	112.2(12)
H(21A)-C(21)-H(21C)	106.6(18)
H(21B)-C(21)-H(21C)	109.8(18)
N(5)-C(22)-C(11)	113.80(12)
N(5)-C(22)-H(22A)	108.5(8)
C(11)-C(22)-H(22A)	107.7(9)
N(5)-C(22)-H(22B)	108.2(9)
C(11)-C(22)-H(22B)	109.6(8)
H(22A)-C(22)-H(22B)	108.9(12)
C(24)-C(23)-N(5)	122.66(17)
C(24)-C(23)-H(23)	120.9(10)
N(5)-C(23)-H(23)	116.4(10)
C(23)-C(24)-C(25)	120.23(19)
C(23)-C(24)-H(24)	118.3(11)
C(25)-C(24)-H(24)	121.5(11)
C(26)-C(25)-C(24)	121.87(17)
C(26)-C(25)-H(25)	120.7(12)
C(24)-C(25)-H(25)	117.4(11)
C(25)-C(26)-B(3)	118.55(17)
C(25)-C(26)-H(26)	118.2(10)
B(3)-C(26)-H(26)	123.3(10)
O(1)-C(27)-H(27A)	113.8(16)
O(1)-C(27)-H(27B)	109.1(14)
H(27A)-C(27)-H(27B)	108(2)

O(1)-C(27)-H(27C)	110.4(14)
H(27A)-C(27)-H(27C)	109(2)
H(27B)-C(27)-H(27C)	105.6(19)

---

Symmetry transformations used to generate equivalent atoms:

Table 4. Anisotropic displacement parameters ( $\text{\AA}^2 \times 10^3$ ) for liu10a. The anisotropic displacement factor exponent takes the form:  $-2p^2[h^2a^*{}^2U^{11} + \dots + 2hk a^* b^* U^{12}]$

	U <sup>11</sup>	U <sup>22</sup>	U <sup>33</sup>	U <sup>23</sup>	U <sup>13</sup>	U <sup>12</sup>
B(1)	31(1)	43(1)	23(1)	-2(1)	1(1)	7(1)
B(2)	23(1)	28(1)	29(1)	2(1)	-1(1)	4(1)
B(3)	31(1)	45(1)	32(1)	7(1)	4(1)	-2(1)
N(1)	31(1)	30(1)	25(1)	5(1)	3(1)	3(1)
N(2)	24(1)	45(1)	28(1)	2(1)	-1(1)	3(1)
N(3)	25(1)	26(1)	26(1)	0(1)	-2(1)	3(1)
N(4)	32(1)	26(1)	25(1)	3(1)	1(1)	-2(1)
N(5)	27(1)	37(1)	28(1)	4(1)	3(1)	2(1)
O(1)	31(1)	40(1)	63(1)	12(1)	4(1)	-7(1)
C(1)	28(1)	36(1)	28(1)	5(1)	-1(1)	-3(1)
C(2)	28(1)	29(1)	26(1)	4(1)	0(1)	0(1)
C(3)	37(1)	35(1)	29(1)	6(1)	7(1)	1(1)
C(4)	50(1)	36(1)	33(1)	8(1)	9(1)	3(1)
C(5)	63(1)	37(1)	29(1)	8(1)	5(1)	16(1)
C(6)	47(1)	48(1)	27(1)	2(1)	0(1)	18(1)
C(7)	24(1)	61(1)	33(1)	-4(1)	-1(1)	-2(1)
C(8)	26(1)	95(2)	74(2)	15(1)	-3(1)	8(1)
C(9)	33(1)	98(2)	39(1)	0(1)	6(1)	-14(1)
C(10)	37(1)	82(2)	65(2)	-22(1)	-3(1)	-11(1)
C(11)	24(1)	28(1)	29(1)	4(1)	-2(1)	-2(1)
C(12)	23(1)	27(1)	26(1)	2(1)	-1(1)	1(1)
C(13)	29(1)	30(1)	23(1)	1(1)	0(1)	-1(1)
C(14)	37(1)	25(1)	40(1)	-1(1)	-4(1)	3(1)
C(15)	45(1)	31(1)	41(1)	-9(1)	-7(1)	7(1)
C(16)	37(1)	44(1)	30(1)	-7(1)	-4(1)	11(1)
C(17)	31(1)	39(1)	30(1)	2(1)	0(1)	5(1)

C(18)	56(1)	28(1)	33(1)	5(1)	-3(1)	-11(1)
C(19)	85(2)	62(2)	51(1)	17(1)	-21(1)	-44(1)
C(20)	64(1)	38(1)	36(1)	10(1)	-2(1)	-14(1)
C(21)	108(2)	29(1)	42(1)	2(1)	6(1)	10(1)
C(22)	26(1)	36(1)	29(1)	4(1)	1(1)	-2(1)
C(23)	40(1)	39(1)	32(1)	0(1)	4(1)	1(1)
C(24)	47(1)	46(1)	39(1)	2(1)	4(1)	13(1)
C(25)	32(1)	70(2)	37(1)	8(1)	4(1)	14(1)
C(26)	28(1)	61(1)	40(1)	9(1)	4(1)	-2(1)
C(27)	45(1)	50(2)	90(2)	16(1)	-2(1)	-16(1)

Table 5. Hydrogen coordinates ( $\times 10^4$ ) and isotropic displacement parameters ( $\text{\AA}^2 \times 10^3$ ) for liu10a.

x	y	z	U(eq)
H(1)	3101(9)	7405(10)	707(9)
H(3)	1314(10)	5605(10)	1598(8)
H(4)	1638(10)	4430(11)	2151(10)
H(5)	2947(10)	4122(11)	2365(9)
H(6)	3937(10)	4912(10)	2048(9)
H(8A)	4791(15)	5558(17)	1175(15)
H(8B)	4741(12)	5996(13)	1969(13)
H(8C)	5397(14)	6223(13)	1423(11)
H(9A)	4494(14)	6311(15)	97(13)
H(9B)	5135(13)	6965(12)	307(11)
H(9C)	4263(12)	7231(13)	172(11)
H(10A)	4389(13)	7367(13)	2047(13)
H(10B)	4215(13)	7869(13)	1348(12)
H(10C)	5051(13)	7625(12)	1511(10)
H(11)	1174(9)	6572(9)	774(8)
H(13)	1777(8)	8643(9)	757(8)
H(14)	1379(9)	6187(10)	-315(9)
H(15)	1459(10)	5973(12)	-1547(9)
H(16)	1761(9)	6957(10)	-2360(10)
H(17)	1972(9)	8234(10)	-1974(9)

H(19A)	3243(17)	9191(18)	-236(16)	124(12)
H(19B)	2954(13)	10093(15)	-80(12)	84(8)
H(19C)	2791(11)	9478(12)	488(12)	69(6)
H(20A)	1706(11)	9509(11)	-1456(10)	50(5)
H(20B)	2624(12)	9293(13)	-1435(11)	67(6)
H(20C)	2329(10)	10152(12)	-1236(10)	53(5)
H(21A)	951(14)	9870(14)	-389(13)	88(8)
H(21B)	1633(12)	10466(14)	-177(12)	77(7)
H(21C)	1357(11)	9835(12)	383(12)	66(6)
H(22A)	1256(8)	6969(9)	1998(8)	28(4)
H(22B)	1480(9)	7831(9)	1726(8)	26(4)
H(23)	589(10)	8677(10)	1565(8)	39(5)
H(24)	-659(11)	9117(12)	1497(9)	56(6)
H(25)	-1669(11)	8204(11)	1436(9)	52(5)
H(26)	-1468(10)	6876(11)	1466(9)	47(5)
H(27A)	-838(15)	5628(16)	2009(14)	108(9)
H(27B)	-170(13)	5100(15)	1660(12)	83(8)
H(27C)	-733(13)	5543(13)	1156(12)	76(7)

---

APPENDIX D  
SUPPORTING INFORMATION FOR CHAPTER V

***General***

All oxygen- and moisture-sensitive manipulations were carried out under an inert atmosphere using either standard Schlenk techniques or a glove box.

$\text{Et}_2\text{O}$ ,  $\text{CH}_2\text{Cl}_2$ , THF and pentane were purified by passing through a neutral alumina column under argon. Potassium hydride was washed with pentane three times prior to use. 10% Pd/C was purchased from Strem and dried by heating under reduced pressure overnight. All other chemicals and solvents were purchased (Aldrich, TCI, or Strem) and used as received.

$^{11}\text{B}$  NMR spectra were recorded on a Varian Unity/Inova 600 or a Varian Unity/Inova 300 spectrometer at ambient temperature.  $^1\text{H}$  NMR spectra were recorded on a Varian Unity/Inova 300 or Varian Unity/Inova 600 spectrometer.  $^{13}\text{C}$  NMR spectra were recorded on a Varian Unity/Inova 300 or Varian Unity/Inova 500 spectrometer. All chemical shifts are externally referenced:  $^{11}\text{B}$  NMR to  $\text{BF}_3 \cdot \text{Et}_2\text{O}$  ( $\delta$  0).

IR spectra were recorded on a Nicolet Magna 550 FT-IR instrument with OMNIC software. Fluorescence emission spectra were collected on a Jobin Yvon Horiba Fluoromax 4 spectrometer in dry degassed acetonitrile. Photoluminescence quantum yields were calculated using tryptophan and tyrosine standards by standard procedures.<sup>1</sup> UV-Vis spectra were collected on an Agilent 8453 spectrophotometer with ChemStation software. Extinction coefficients were calculated by finding the slope of the absorbance plot used for quantum yield measurements at five different concentrations ranging from  $4.35 \times 10^{-6} \text{ M}$  to  $2.76 \times 10^{-5} \text{ M}$ .

Cyclic voltammetry was conducted using a traditional 3-electrode configuration using a glassy carbon working electrode (Bioanalytical Systems, Inc, 3mm diameter), Pt coil counter electrode, and  $\text{Ag}/\text{Ag}^+$  (0.08M TBAOTf / 0.005M  $\text{AgNO}_3$  filling solution) reference. The reference was standardized against a saturated calomel electrode (+339mV vs SCE). Experiments were performed using 0.08M TBAOTf (Fluka, >99%) in high purity acetonitrile (Burdick & Jackson), distilled from molecular sieves (3 $\text{\AA}$ ), and

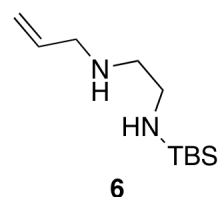
conducted under an N<sub>2</sub> atmosphere. CVs were collected at a sweep rate of 50mV/s with the first cycle being used for determination of E<sub>pa</sub> (E<sub>pa</sub> = Anodic peak potential) due to polymerization or fouling on subsequent cycles. Analyte concentration was ~0.005M. Measurements were performed in duplicate.

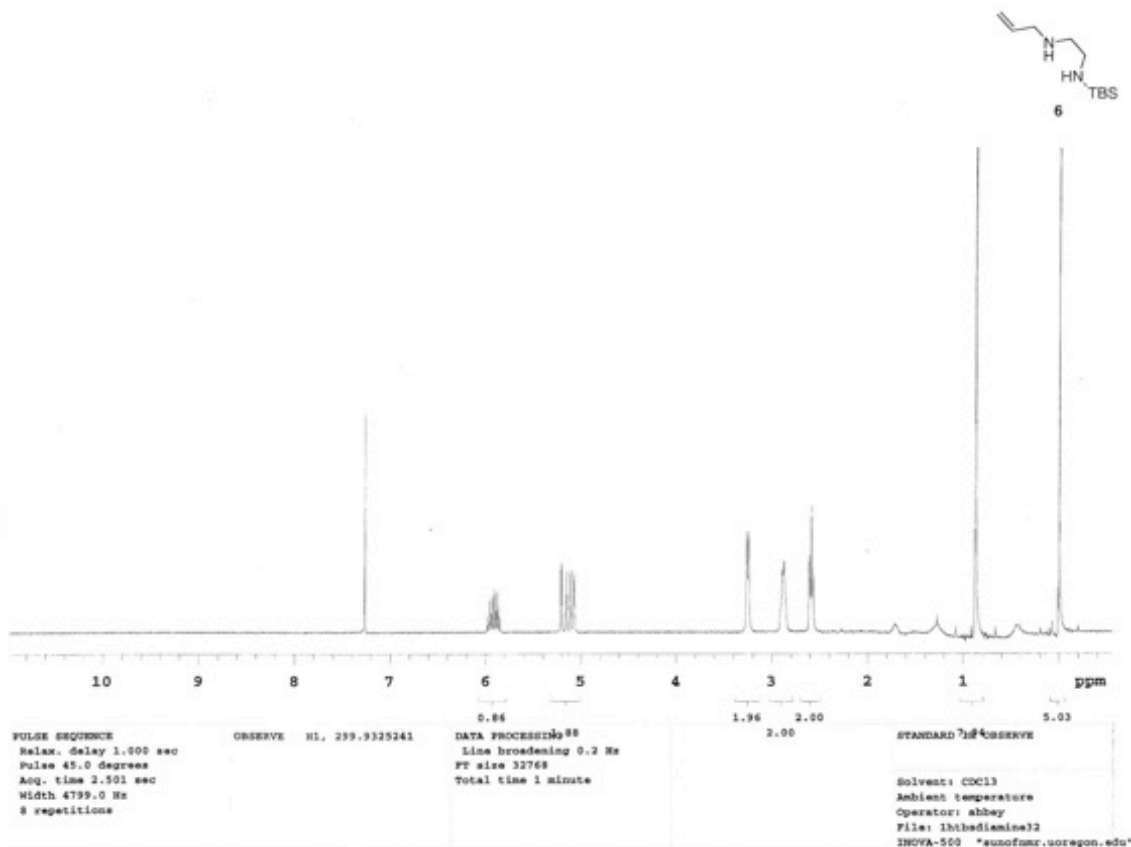
High-resolution mass spectroscopy data were obtained at the Mass Spectroscopy Facilities and Services Core of the Environmental Health Sciences Center at Oregon State University. Financial support for this facility has been furnished in part by the National Institute of Environmental Health Sciences, NIH (P30 ES00210).

Air and water stability measurements were performed using the protocol of Lamm et al.<sup>2</sup>

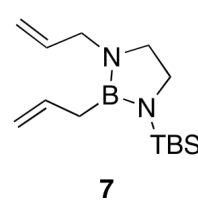
**Compound 6:** A 500 mL RBF equipped with a magnetic stir bar was charged with a solution of *N*-allylenediamine<sup>3</sup> (7.35 g, 73.3 mmol) in THF (220 mL) and cooled to -78 °C under N<sub>2</sub> in a dry ice/acetone bath. *n*-BuLi (46.0 mL, 74.0 mmol, 1.6 M in pentane) was added dropwise via syringe, and the solution was stirred at -78 °C for 90 minutes. A solution of TBSCl (11.05 g, 73.3 mmol) in THF (70 mL) was added dropwise via cannula while stirring at -78 °C. The solution was allowed to slowly warm to room temperature overnight, and the solvent was removed under reduced pressure. Pentane (100 mL) was added via syringe, and the reaction mixture was filtered through a glass frit. The solvent was again removed under reduced pressure and the crude product was purified by fractional vacuum distillation (b.p. 55 °C, 50 mTorr) to yield **6** as a clear colorless liquid (13.67 g, 87%).

<sup>1</sup>H NMR (CDCl<sub>3</sub>, 300 MHz): δ 5.92 (m, 1H), 5.13 (m, 2H), 3.25 (d, *J*<sub>HH</sub>= 5.9 Hz, 2H), 2.88 (m, 2H), 2.59 (t, *J*<sub>HH</sub>= 5.9 Hz, 2H), 1.71 (s, br, 1H), 1.28 (s, br, 1H), 0.88 (s, 9H), 0.00 (s, 6H). <sup>13</sup>C NMR (CDCl<sub>3</sub>, 125.75 MHz): δ 137.4, 115.8, 53.2, 52.6, 42.4, 26.7, 18.6, -4.7. FTIR (thin film) 2954, 2929, 2856, 1471, 1101, 909, 833, 734. HRMS (EI) calcd. for C<sub>11</sub>H<sub>26</sub>N<sub>2</sub>Si (M<sup>+</sup>) 214.18653, found 214.18588.



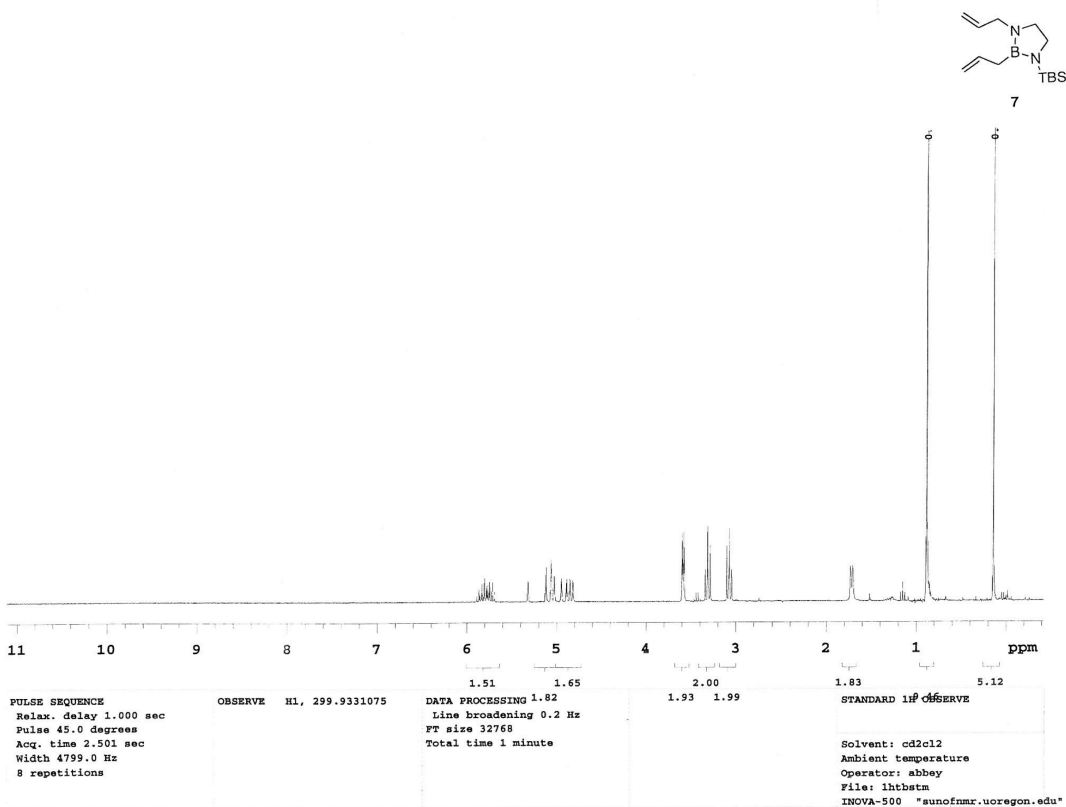


**Compound 7:** A solution of allyltriphenyltin (25.83 g, 66.04 mmol) in CH<sub>2</sub>Cl<sub>2</sub> (220 mL) in a 500 mL RBF equipped with a magnetic stir bar was cooled to -78 °C under N<sub>2</sub> in a dry ice/acetone bath. BCl<sub>3</sub> (64.0 mL, 64.0 mmol, 1.0 M in hexanes) was added via cannula, and the reaction mixture was stirred at -78 °C for 4 h. A solution of **6** (13.11 g, 61.15 mmol) and Et<sub>3</sub>N (18.75 mL, 134.53 mmol) in pentane (30 mL) was added dropwise via cannula, and the reaction was allowed to slowly warm to room temperature and stirred at room temperature for 8 hours. At the conclusion of the reaction, approximately 75% of the solvent was removed under reduced pressure. Pentane (120 mL) was then added, and the

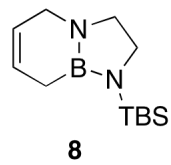


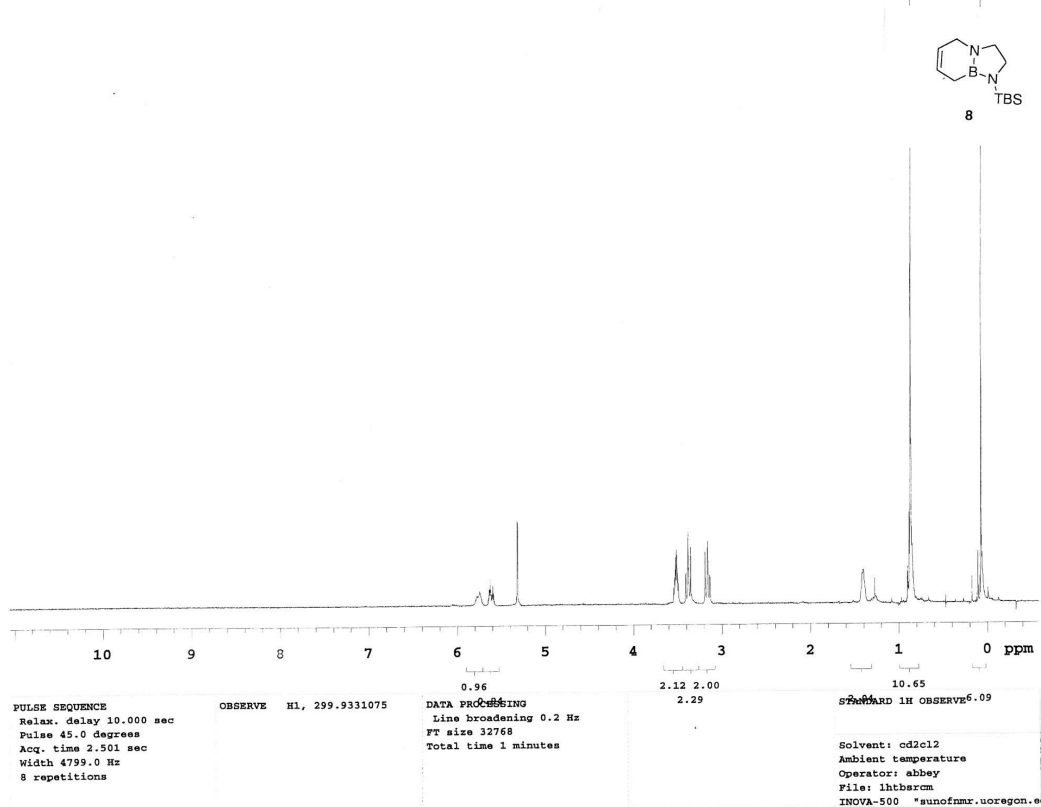
reaction mixture was filtered through a glass frit in a glove box. The solvent was again removed under reduced pressure and the crude oil was purified by fractional vacuum distillation (b.p. 85 °C, 300 mTorr) to afford 7 as a clear colorless liquid (9.27 g, 57%).

<sup>1</sup>H NMR (CD<sub>2</sub>Cl<sub>2</sub>, 300 MHz): δ 5.81 (m, 2H), 5.07 (m, 2H), 4.91 (m, 2H), 3.59 (d, *J*<sub>HH</sub>=7.0 Hz, 2H), 3.31 (t, *J*<sub>HH</sub>=8.0 Hz, 2H), 3.08 (t, *J*<sub>HH</sub>=8.0 Hz, 2H), 1.72 (d, *J*<sub>HH</sub>=8.3 Hz, 2H), 0.88 (s, 9H), 0.14 (s, 6H). <sup>13</sup>C NMR (CD<sub>2</sub>Cl<sub>2</sub>, 125.75 MHz): δ 137.9, 137.5, 115.0, 114.1, 50.1, 49.4, 48.0, 27.2, 20.1, 20.0 (br), -3.5. <sup>11</sup>B NMR (CD<sub>2</sub>Cl<sub>2</sub>, 192.5 MHz): δ 34.1. FTIR (thin film) 3076, 2928, 2855, 1632, 1436, 1372, 1256, 1190, 1044, 897, 831, 773, 671. HRMS (EI) calcd. for C<sub>14</sub>H<sub>29</sub>BN<sub>2</sub>Si (M<sup>+</sup>) 264.21932, found 264.21916.

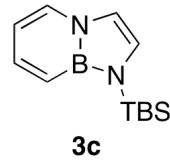


**Compound 8:** In a glove box, a 500 mL RBF equipped with a magnetic stir bar was charged with a solution of **7** (4.70 g, 17.6 mmol) in CH<sub>2</sub>Cl<sub>2</sub> (130 mL). In a 20 mL scintillation vial, Grubbs Gen. 1 catalyst (bis(tricyclohexylphosphine) benzylidene ruthenium(IV) chloride) (0.600 g, 0.729 mmol) was suspended in CH<sub>2</sub>Cl<sub>2</sub> (10 mL) and quickly poured into the stirring solution of **7**. The reaction was stirred for 2 hours under N<sub>2</sub> at room temperature and was monitored by <sup>1</sup>H NMR. At the conclusion of the reaction, the solvent was removed under reduced pressure. The crude material was purified by fractional vacuum distillation (b.p. 69 °C, 80 mTorr) to afford the clear colorless liquid **8** (2.01 g, 55%). <sup>1</sup>H NMR (CD<sub>2</sub>Cl<sub>2</sub>, 300 MHz): δ 5.75 (m, 1H), 5.62 (m, 1H), 3.52 (m, 2H), 3.37 (t, *J*<sub>HH</sub>= 7.0 Hz, 2H), 3.16 (t, *J*<sub>HH</sub>= 7.0 Hz, 2H), 1.41 (m, 2H), 0.87 (s, 9H), 0.08 (s, 6H). <sup>13</sup>C NMR (CD<sub>2</sub>Cl<sub>2</sub>, 125.75 MHz): δ 126.3, 125.6, 51.3, 47.4, 47.2, 27.2, 20.2, 13.0 (br), -4.4. <sup>11</sup>B NMR (CD<sub>2</sub>Cl<sub>2</sub>, 192.5 MHz): δ 32.5. FTIR (thin film) 3022, 2954, 2925, 2853, 1380, 1255, 1161, 1087, 1032, 831, 669. HRMS (EI) calcd. for C<sub>12</sub>H<sub>25</sub>BN<sub>2</sub>Si (M<sup>+</sup>) 236.18802, found 236.18722.

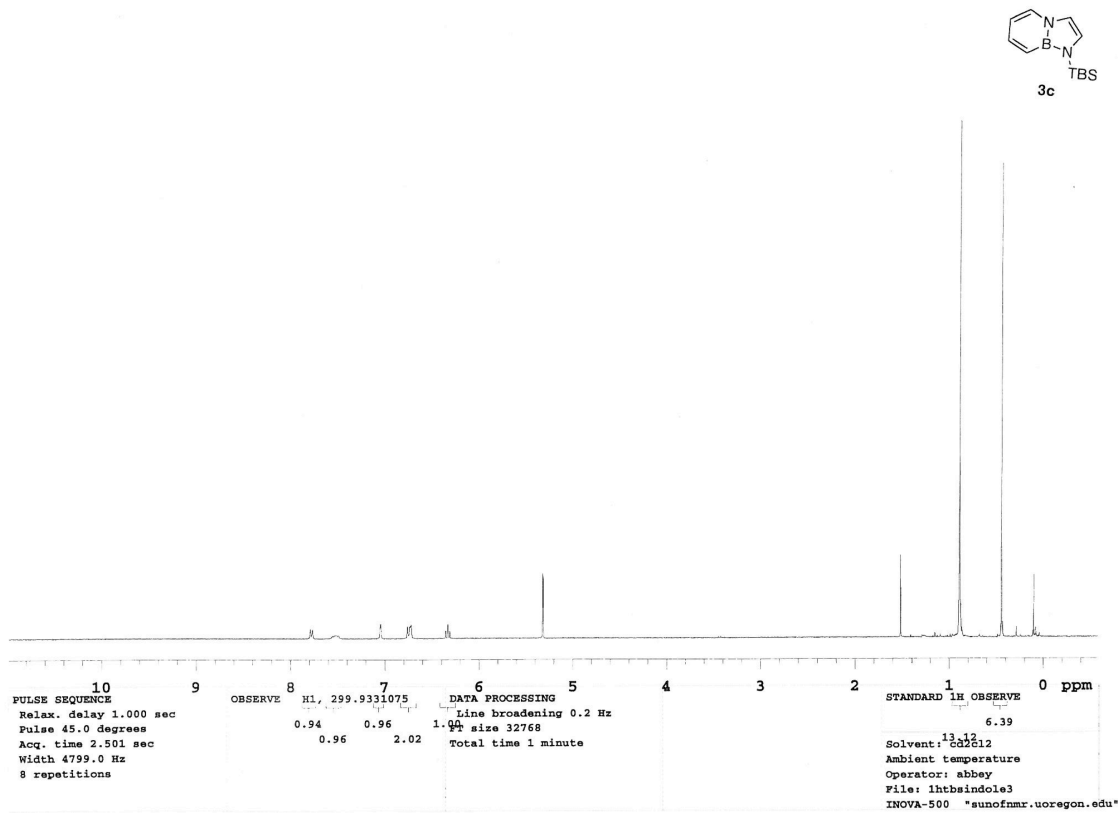




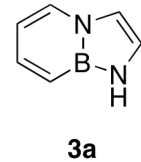
**N-TBS BN indole 3c:** In a glove box, a 420 mL high-pressure bomb equipped with a magnetic stir bar was charged with 10 wt% Pd/C (3.50 g, 3.15 mmol), perfluorodecalin (50 mL) and **8** (2.50 g, 10.5 mmol). The vessel was sealed and heated to 185 °C while stirring vigorously for 100 minutes. At the conclusion of the reaction, the reaction mixture was cooled to room temperature and filtered through a glass frit. The filtrate was washed with THF (100 mL), and the organic phase was separated from the fluorous phase with a separatory funnel. The fluorous phase was washed with THF (2x, 50 mL), and the organic phase was stirred under air for approximately 2 hours until only the product peak at ~25 ppm was visible by <sup>11</sup>B NMR. The solvent was removed under reduced pressure, and the crude product was purified by silica gel chromatography (5% Et<sub>2</sub>O in pentane) under N<sub>2</sub> to afford **3c** as a yellowish oil (0.660 g, 26%). Perfluorodecalin can be redistilled and reused in further reactions.



<sup>1</sup>H NMR (CD<sub>2</sub>Cl<sub>2</sub>, 500 MHz): δ 7.78 (d, <sup>3</sup>J<sub>HH</sub>= 6.4 Hz, 1H), 7.50 (m, 1H), 7.05 (d, <sup>3</sup>J<sub>HH</sub>= 2.1 Hz, 1H), 6.74 (m, 2H), 6.33 (t, <sup>3</sup>J<sub>HH</sub>= 0.9 Hz, 1H), 0.89 (s, 9H), 0.46 (s, 6H). <sup>13</sup>C NMR (CD<sub>2</sub>Cl<sub>2</sub>, 125.75 MHz): δ 138.8, 129.8, 124.0, 119.5, 115.1, 109.0, 26.3, 19.1, -4.2. <sup>11</sup>B NMR (THF, 192.5 MHz): δ 25.2. FTIR (thin film) 2954, 2928, 2857, 1604, 1498, 1436, 1254, 1151, 1128, 836, 782, 687 cm<sup>-1</sup>. HRMS (EI) calcd. for C<sub>12</sub>H<sub>21</sub>BN<sub>2</sub>Si (M<sup>+</sup>) 232.15672, found 232.15639.



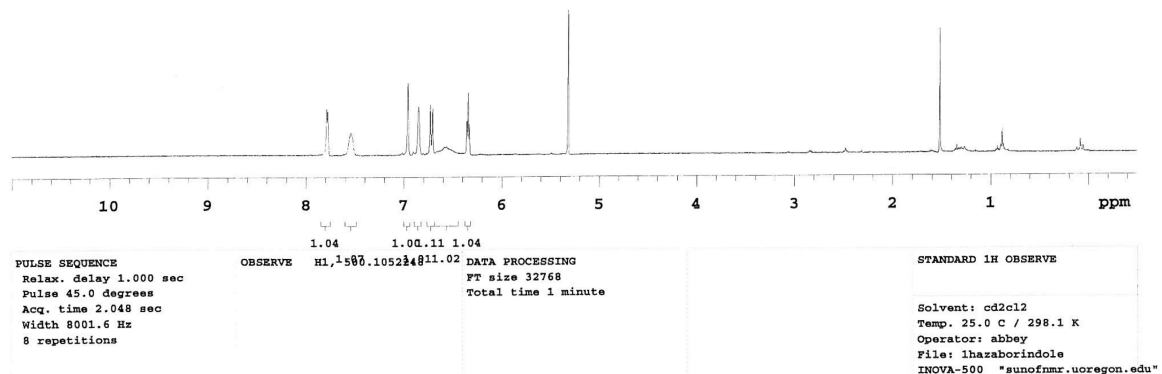
**N-H BN indole 3a:** A 250 mL RBF equipped with a stir bar was charged with a solution of **3c** (3.61g, 15.5 mmol) in THF (60 mL) in a glove box. TBAF hydrate (4.34 g, 15.5 mmol) in THF (20 mL) was added dropwise via pipet. The reaction was stirred for 30 min at room temperature, and then the solvent was removed under reduced pressure. The crude mixture was run through a plug of silica gel (25% Et<sub>2</sub>O in pentane), and the solvent was removed under reduced pressure. The resulting oil was purified by silica gel chromatography (25% Et<sub>2</sub>O in pentane) to afford **3a** as a yellowish oil (0.998 g, 55%).



<sup>1</sup>H NMR (CD<sub>2</sub>Cl<sub>2</sub>, 300 MHz): δ 7.78 (d, <sup>3</sup>J<sub>HH</sub>= 5.9 Hz, 1H), 7.54 (m, 1H), 6.96 (s, 1H), 6.85 (s, 1H), 6.72 (d, <sup>3</sup>J<sub>HH</sub>= 11.7 Hz, 1H), 6.57 (s, br, 1H), 6.34 (t, <sup>3</sup>J<sub>HH</sub> = 6.4 Hz, 1H). <sup>13</sup>C NMR (CD<sub>2</sub>Cl<sub>2</sub>, 125.75 MHz): δ 139.0, 129.7, 119.8, 117.1 (br), 112.4, 109.0. <sup>11</sup>B NMR (CD<sub>2</sub>Cl<sub>2</sub>, 192.5 MHz): δ 23.7. m.p. 28 °C. FTIR (thin film) 3463, 2962, 1607, 1493, 1453, 1346, 1305, 1063, 798, 733, 684 cm<sup>-1</sup>. HRMS (EI) calcd. for C<sub>6</sub>H<sub>7</sub>BN<sub>2</sub>(M<sup>+</sup>) 118.07024, found 118.06960.

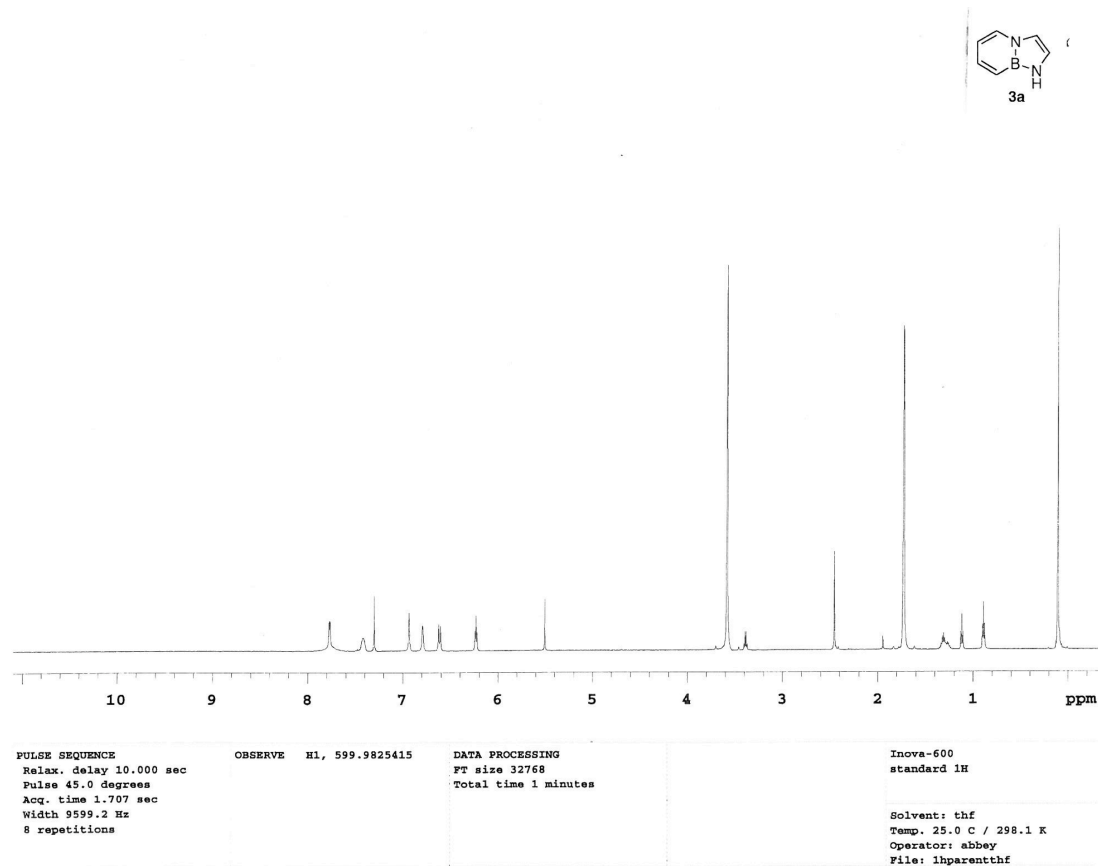


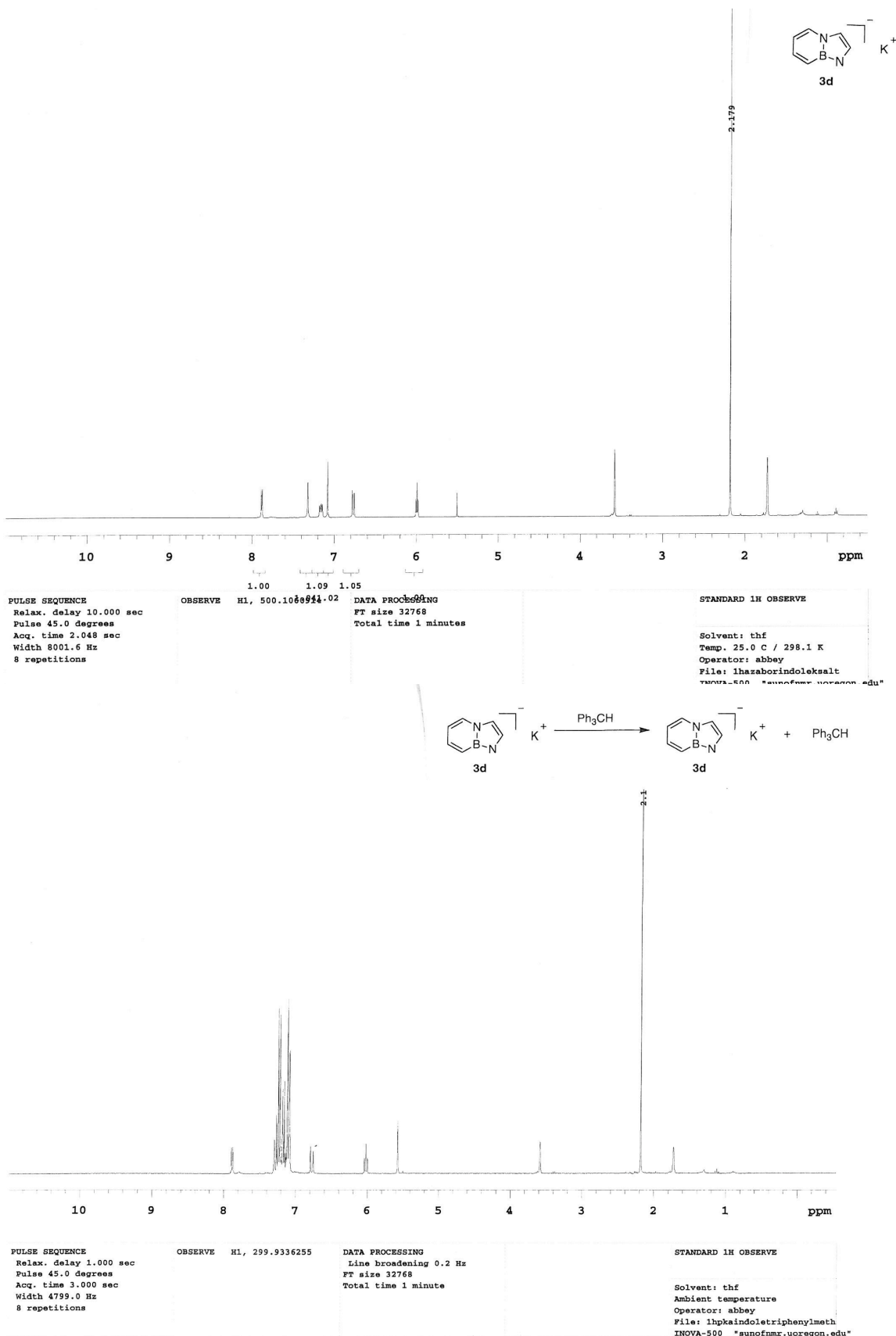
3a



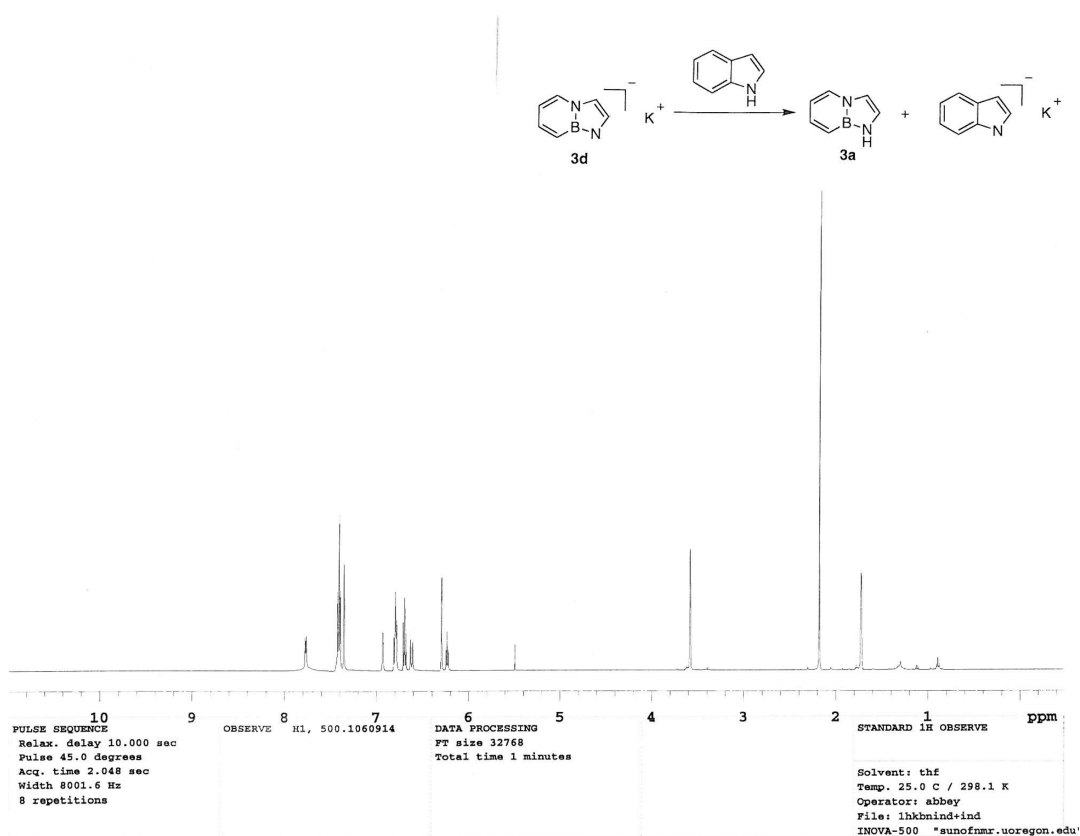
### **General Procedure for $pK_a$ Bracketing Experiments:**

BN indole **3a** (5.7 mg, 0.048mmol) and a hexamethylbenzene (1.0 mg, 0.0062 mmol) internal standard were dissolved in THF-*d*8 (0.5 mL) and added to a 1-dram vial equipped with a stir bar containing KH (2.2 mg, 0.055 mmol.) The reaction was stirred for 2 hours at room temperature in a glove box, generating the potassium salt **3d**. The reaction mixture was filtered through an Acrodisc (0.45  $\mu$ m, PTFE). A solution of the proton source, triphenylmethane (10.8 mg, 0.044 mmol) in THF-*d*8 (0.2 mL) was added dropwise to the solution of **3d** via pipet while stirring. The  $^1\text{H}$  NMR spectrum was taken immediately after addition. If the starting material **3a** was observed, then BN indole **3a** was judged to be more basic than the proton source. If the salt **3d** was observed, then BN indole **3a** was judged to be more acidic than the proton source. Result: **3d** was observed unchanged by  $^1\text{H}$  NMR, the reaction turned light pink, indicating slight deprotonation of triphenylmethane.

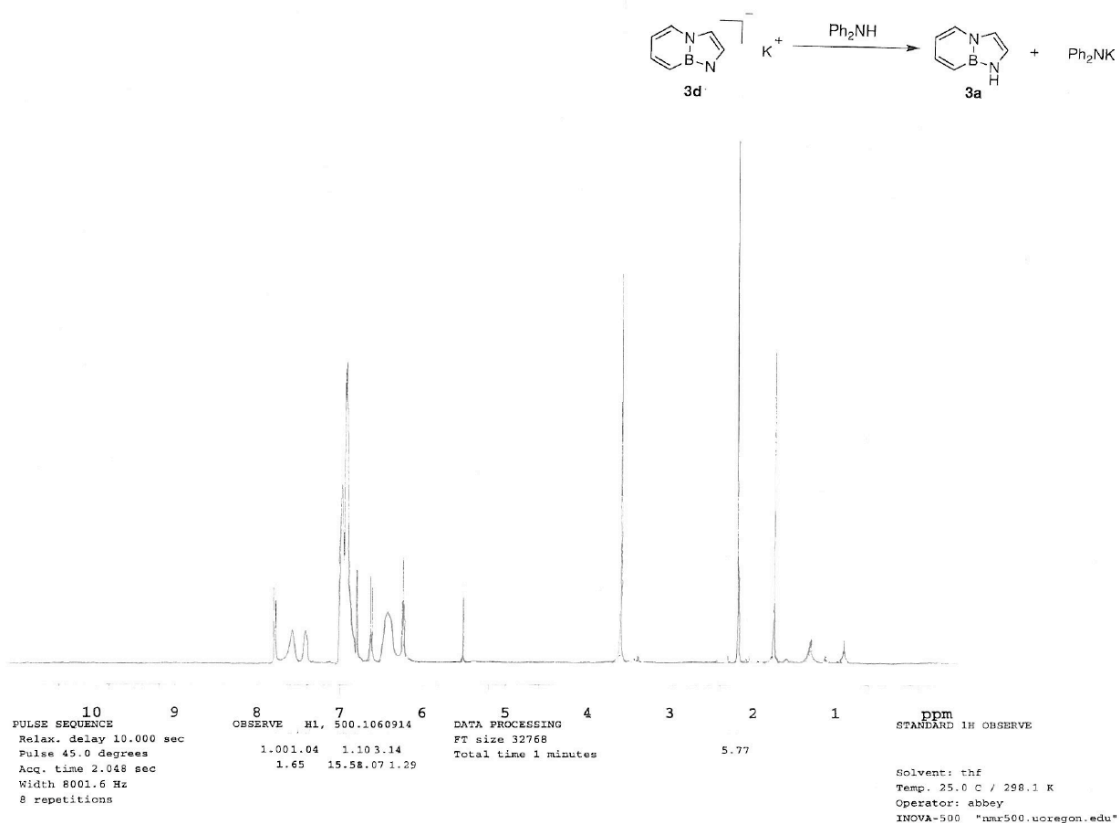




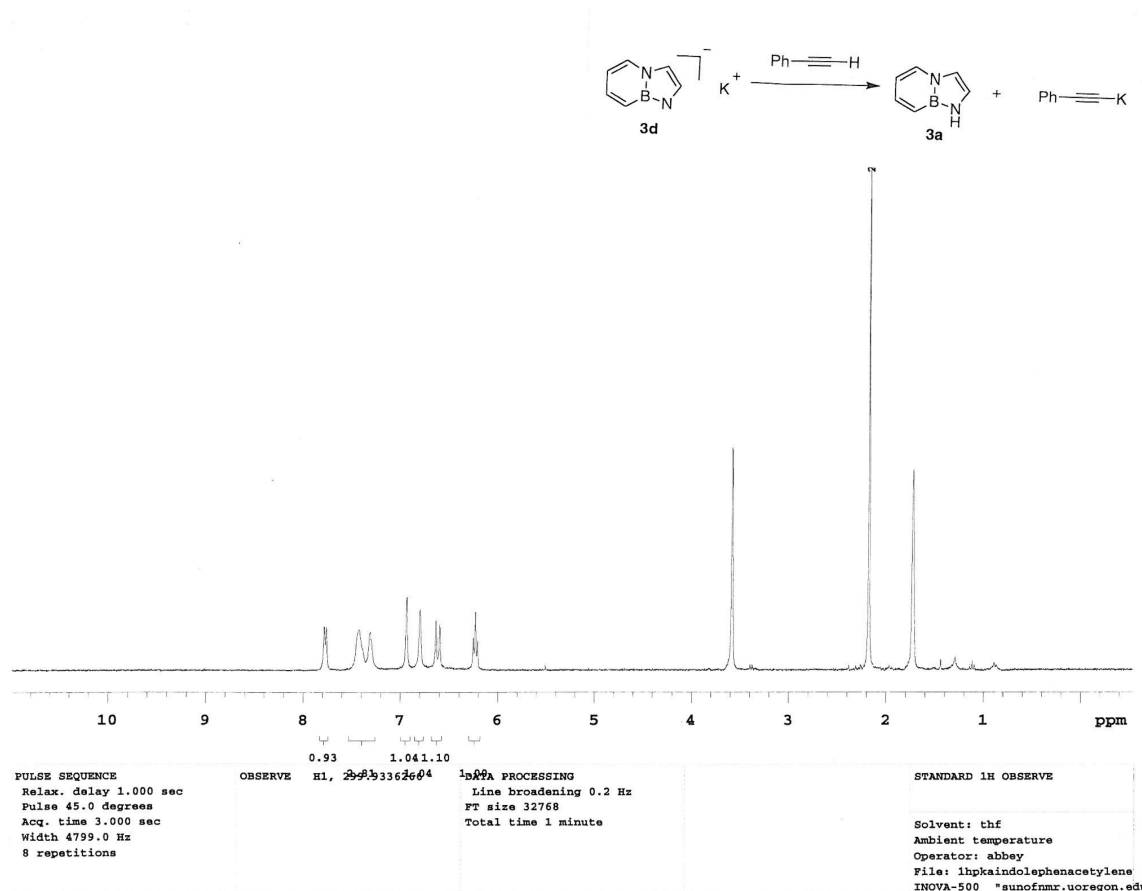
**Proton source = indole:** **3a** (4.9 mg, 0.041 mmol), hexamethylbenzene (1.4 mg, 0.0086 mmol), KH (2.0 mg, 0.050 mmol), and indole (4.9 mg, 0.041 mmol) were reacted following the general procedure. Indole was cleanly deprotonated, yielding **3a** as observed by <sup>1</sup>H NMR.

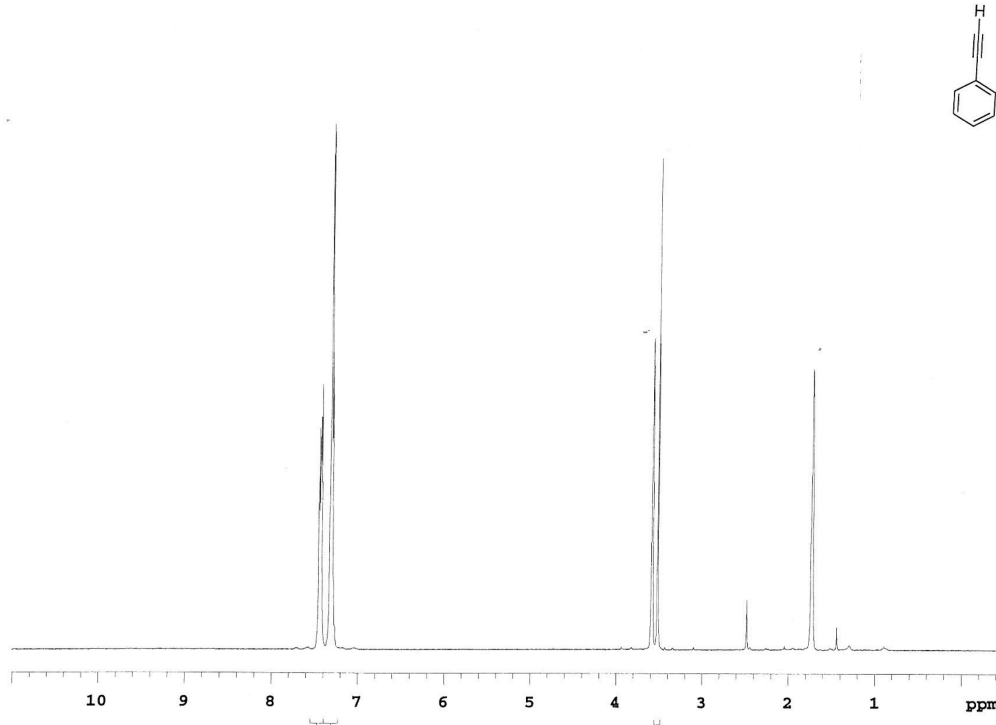


**Proton source = diphenylamine:** **3a** (4.9 mg, 0.041 mmol), hexamethylbenzene (1.4 mg, 0.0086 mmol), KH (2.0 mg, 0.050 mmol), and diphenylamine (6.9 mg, 0.041 mmol) were reacted following the general procedure. Diphenylamine was cleanly deprotonated, yielding **3a** as observed by <sup>1</sup>H NMR.



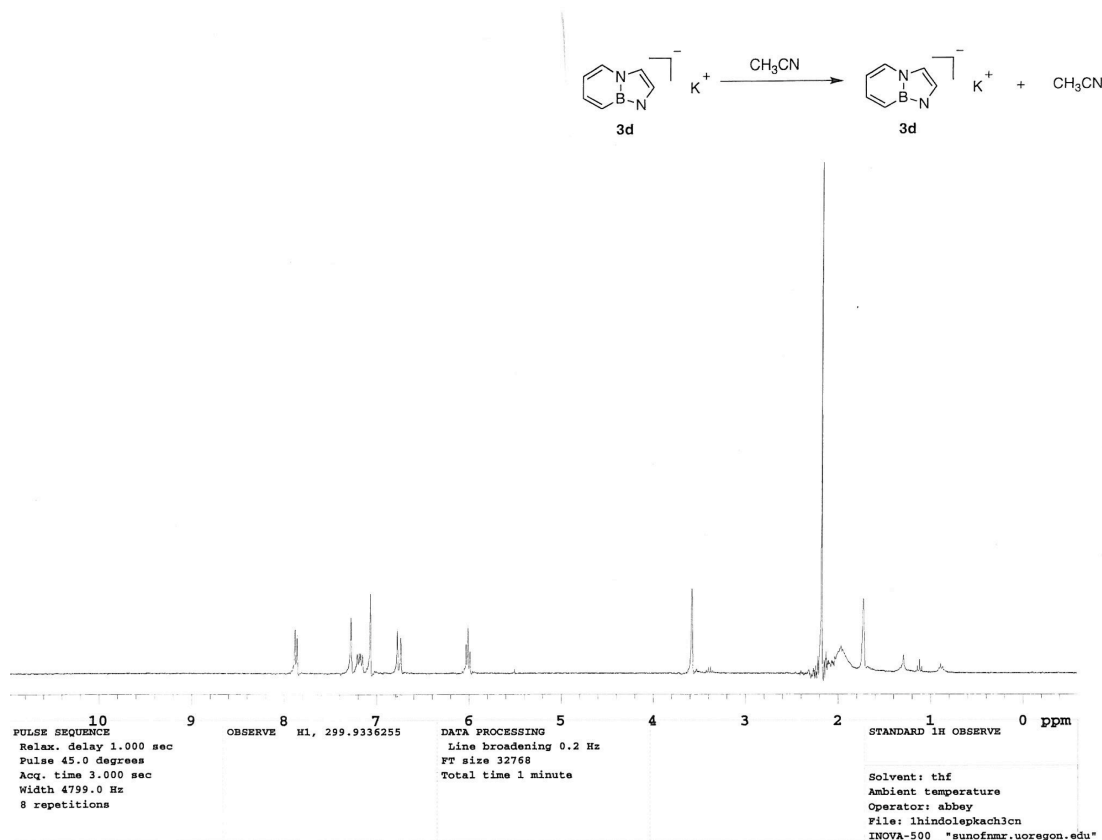
**Proton source = phenylacetylene:** **3a** (5.7 mg, 0.048 mmol), hexamethylbenzene (1.0 mg, 0.0062 mmol), KH (2.2 mg, 0.055 mmol), and phenylacetylene (4.5 mg, 0.044 mmol) were reacted following the general procedure. Phenylacetylene was cleanly deprotonated, yielding **3a** as observed by  $^1\text{H}$  NMR.





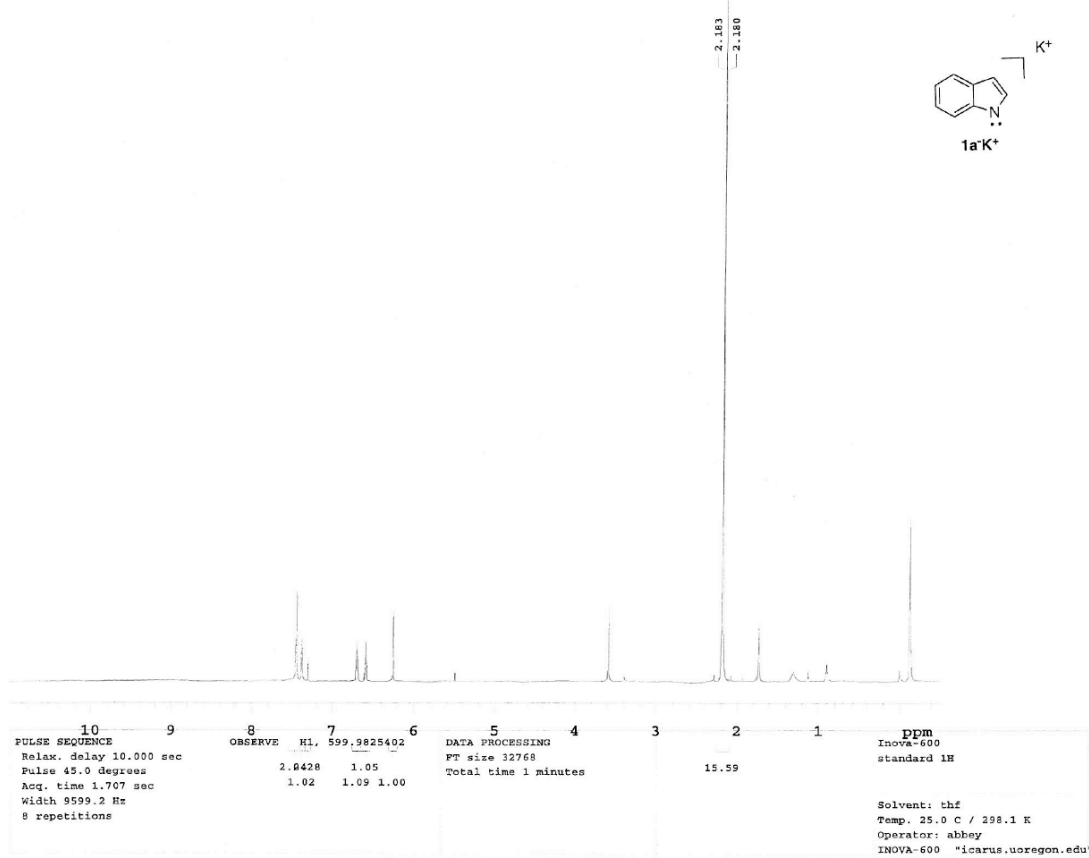
PULSE SEQUENCE	OBSERVE <sup>3</sup> H <sup>14</sup> 299.9341824	DATA PROCESSING	UO Inova-300 Standard-1H
Relax, delay 1.000 sec		Line broadening 0.2 Hz	
Pulse 45.0 degrees		FT size 32768	
Acq. time 3.000 sec		Total time 1 minute	
Width 4799.0 Hz			Solvent: thf
8 repetitions			Temp. 25.0 C / 298.1 K
			Operator: abbey
			INOVA-300 "carbon.uoregon.edu"

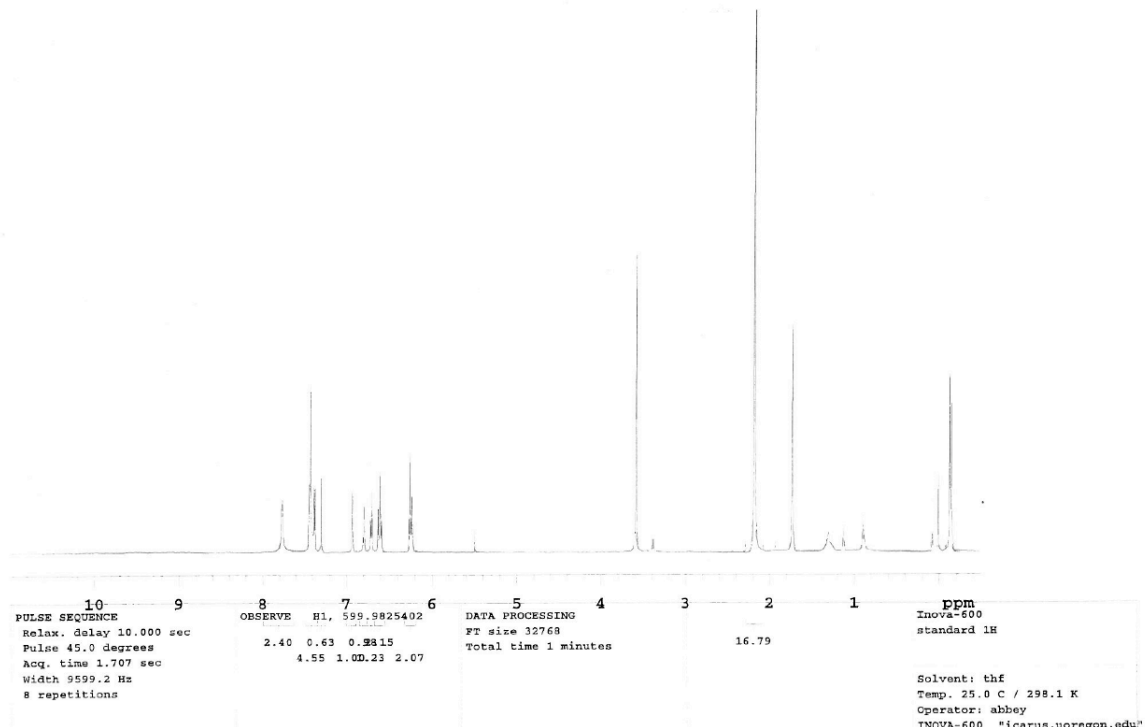
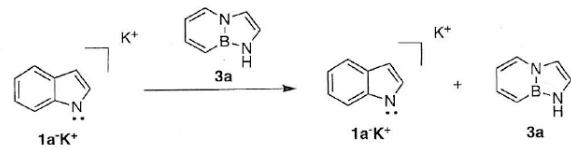
**Proton source = acetonitrile:** **3a** (4.9 mg, 0.041 mmol), hexamethylbenzene (1.6 mg, 0.0099 mmol), KH (2.2 mg, 0.055 mmol), and acetonitrile (1.7 mg, 0.041 mmol) were reacted following the general procedure. Acetonitrile was not deprotonated, leaving **3d** intact as observed by  $^1\text{H}$  NMR.



**pK<sub>a</sub> Control Experiment:**

Indole **1a** (9.4 mg, 0.080 mmol) and a hexamethylbenzene (2.8 mg, 0.017 mmol) internal standard were dissolved in THF-*d*8 (0.7 mL) and added to a 1-dram vial equipped with a stir bar containing KH (4.6 mg, 0.011 mmol). The reaction was stirred for 2 hours at room temperature in a glove box, generating the potassium salt **1a-K<sup>+</sup>**. The reaction mixture was filtered through an Acrodisc (0.45 µm, PTFE). A solution of the proton source, BN indole **3a** (10.4 mg, 0.088 mmol) in THF-*d*8 (0.3 mL) was added dropwise to the solution of **1a-K<sup>+</sup>** via pipet while stirring. The <sup>1</sup>H NMR spectrum was taken immediately after addition. The starting material **1a-K<sup>+</sup>** was observed, and BN indole **3a** remained intact. Therefore, **3a** was judged to be more basic than **1a**.





### **X-ray Crystal Structure Determination.**

Diffraction intensity data were collected with a Bruker Smart Apex CCD diffractometer at 173(2) K using MoK $\alpha$  - radiation (0.71073 Å). The structure was solved using direct methods, completed by subsequent difference Fourier syntheses, and refined by full matrix least-squares procedures on F<sup>2</sup>. All non-H atoms were refined with anisotropic thermal parameters. All software and sources scattering factors are contained in the SHELXTL (6.10) program package (G.Sheldrick, Bruker XRD, Madison, WI). Crystallographic data and some details of data collection and crystal structure refinement are given in the following tables.

**Crystallographic data for 3c•Fnap:** X-ray quality crystals were found in the crude product after removal of the solvent under reduced pressure.

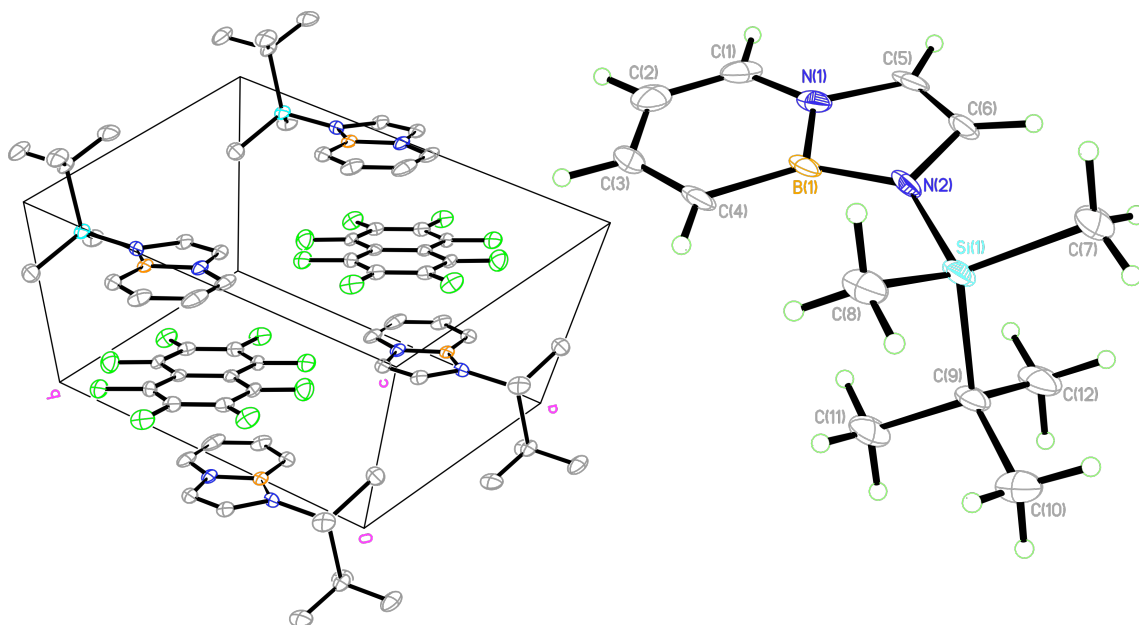


Table 1. Crystal data and structure refinement for **3c•Fnap** (liu80)

Identification code	liu80	
Empirical formula	C17 H21 B F4 N2 Si	
Formula weight	368.26	
Temperature	173(2) K	
Wavelength	0.71073 Å	
Crystal system	Triclinic	
Space group	P-1	
Unit cell dimensions	a = 7.091(4) Å b = 11.046(6) Å c = 13.008(7) Å	a= 104.199(9)°. b= 99.358(9)°. g = 107.318(8)°.
Volume	912.0(9) Å <sup>3</sup>	
Z	2	
Density (calculated)	1.341 Mg/m <sup>3</sup>	
Absorption coefficient	0.169 mm <sup>-1</sup>	
F(000)	384	
Crystal size	0.38 x 0.26 x 0.02 mm <sup>3</sup>	
Theta range for data collection	1.67 to 23.99°.	
Index ranges	-8<=h<=8, -12<=k<=12, -14<=l<=14	
Reflections collected	6335	
Independent reflections	2835 [R(int) = 0.0775]	
Completeness to theta = 23.99°	99.4 %	
Absorption correction	Semi-empirical from equivalents	
Max. and min. transmission	0.9966 and 0.9386	
Refinement method	Full-matrix least-squares on F <sup>2</sup>	
Data / restraints / parameters	2835 / 0 / 310	
Goodness-of-fit on F <sup>2</sup>	0.986	
Final R indices [I>2sigma(I)]	R1 = 0.0807, wR2 = 0.1779	
R indices (all data)	R1 = 0.1497, wR2 = 0.2160	
Largest diff. peak and hole	0.551 and -0.568 e.Å <sup>-3</sup>	

Table 2. Atomic coordinates ( $\times 10^4$ ) and equivalent isotropic displacement parameters ( $\text{\AA}^2 \times 10^3$ ) for liu80. U(eq) is defined as one third of the trace of the orthogonalized  $U_{ij}$  tensor.

	x	y	z	U(eq)
Si(1)	2185(2)	9973(2)	7268(1)	29(1)
N(1)	2399(7)	6569(5)	7837(4)	32(1)
N(2)	2415(6)	8465(4)	7367(4)	27(1)
B(1)	1385(10)	7528(6)	7875(5)	27(2)
C(1)	1891(12)	5535(7)	8239(5)	42(2)
C(2)	232(13)	5365(8)	8692(5)	53(2)
C(3)	-844(12)	6238(7)	8775(5)	42(2)
C(4)	-398(9)	7301(7)	8409(5)	34(2)
C(5)	3964(10)	6939(7)	7315(5)	37(2)
C(6)	3956(9)	8007(7)	7058(5)	33(2)
C(7)	3112(13)	10329(8)	6074(5)	45(2)
C(8)	-553(11)	9780(8)	7038(7)	43(2)
C(9)	3747(9)	11360(6)	8570(5)	33(2)
C(10)	3540(15)	12672(7)	8510(7)	56(2)
C(11)	3019(13)	11030(8)	9551(6)	49(2)
C(12)	5989(12)	11483(9)	8736(7)	51(2)
C(1S)	5(9)	6435(6)	4511(5)	32(2)
C(2S)	1587(9)	6549(6)	4000(5)	32(2)
C(3S)	2610(9)	5672(6)	3973(5)	35(2)
C(4S)	2115(9)	4683(6)	4414(5)	34(2)
C(5S)	536(8)	4547(5)	4981(4)	28(1)
F(1S)	-1004(6)	7293(4)	4486(3)	55(1)
F(2S)	2046(6)	7476(4)	3502(3)	52(1)
F(3S)	4161(5)	5813(3)	3469(3)	49(1)
F(4S)	3158(5)	3843(3)	4366(3)	46(1)

Table 3. Bond lengths [ $\text{\AA}$ ] and angles [ $^\circ$ ] for liu80.

Si(1)-N(2)	1.753(5)
Si(1)-C(8)	1.854(7)
Si(1)-C(7)	1.865(7)
Si(1)-C(9)	1.883(6)
N(1)-C(1)	1.349(8)
N(1)-C(5)	1.403(8)
N(1)-B(1)	1.442(8)
N(2)-C(6)	1.408(7)
N(2)-B(1)	1.444(8)
B(1)-C(4)	1.525(9)
C(1)-C(2)	1.384(10)
C(1)-H(6)	1.00(8)
C(2)-C(3)	1.392(11)
C(2)-H(15)	0.79(5)
C(3)-C(4)	1.343(9)
C(3)-H(19)	0.89(7)
C(4)-H(1)	0.91(6)
C(5)-C(6)	1.304(9)
C(5)-H(3)	0.83(5)
C(6)-H(4)	0.93(5)
C(7)-H(16)	0.94(7)
C(7)-H(17)	1.05(9)
C(7)-H(29)	1.00(7)
C(8)-H(2)	1.07(9)
C(8)-H(25)	0.79(7)
C(8)-H(32)	1.03(11)
C(9)-C(10)	1.519(9)
C(9)-C(12)	1.529(10)
C(9)-C(11)	1.535(9)
C(10)-H(11)	1.11(8)
C(10)-H(13)	1.03(8)
C(10)-H(21)	0.89(6)
C(11)-H(9)	1.10(7)
C(11)-H(10)	0.98(6)

C(11)-H(24)	0.96(8)
C(12)-H(8)	1.06(7)
C(12)-H(18)	0.81(6)
C(12)-H(20)	0.99(9)
C(1S)-F(1S)	1.350(7)
C(1S)-C(2S)	1.384(8)
C(1S)-C(5S)#1	1.395(8)
C(2S)-F(2S)	1.330(6)
C(2S)-C(3S)	1.370(8)
C(3S)-C(4S)	1.338(8)
C(3S)-F(3S)	1.359(6)
C(4S)-F(4S)	1.344(7)
C(4S)-C(5S)	1.429(8)
C(5S)-C(1S)#1	1.395(8)
C(5S)-C(5S)#1	1.423(11)

N(2)-Si(1)-C(8)	108.3(3)
N(2)-Si(1)-C(7)	108.9(3)
C(8)-Si(1)-C(7)	109.2(4)
N(2)-Si(1)-C(9)	109.5(2)
C(8)-Si(1)-C(9)	110.8(3)
C(7)-Si(1)-C(9)	110.1(3)
C(1)-N(1)-C(5)	128.5(6)
C(1)-N(1)-B(1)	124.9(6)
C(5)-N(1)-B(1)	106.6(5)
C(6)-N(2)-B(1)	104.2(5)
C(6)-N(2)-Si(1)	123.9(4)
B(1)-N(2)-Si(1)	131.5(4)
N(1)-B(1)-N(2)	106.9(5)
N(1)-B(1)-C(4)	115.2(6)
N(2)-B(1)-C(4)	137.9(6)
N(1)-C(1)-C(2)	117.1(7)
N(1)-C(1)-H(6)	126(5)
C(2)-C(1)-H(6)	117(5)
C(1)-C(2)-C(3)	122.4(8)
C(1)-C(2)-H(15)	103(4)

C(3)-C(2)-H(15)	134(4)
C(4)-C(3)-C(2)	123.5(7)
C(4)-C(3)-H(19)	119(4)
C(2)-C(3)-H(19)	116(4)
C(3)-C(4)-B(1)	116.7(7)
C(3)-C(4)-H(1)	121(4)
B(1)-C(4)-H(1)	122(4)
C(6)-C(5)-N(1)	109.2(6)
C(6)-C(5)-H(3)	134(4)
N(1)-C(5)-H(3)	116(4)
C(5)-C(6)-N(2)	113.1(6)
C(5)-C(6)-H(4)	132(3)
N(2)-C(6)-H(4)	114(3)
Si(1)-C(7)-H(16)	110(4)
Si(1)-C(7)-H(17)	115(5)
H(16)-C(7)-H(17)	118(6)
Si(1)-C(7)-H(29)	117(4)
H(16)-C(7)-H(29)	96(5)
H(17)-C(7)-H(29)	98(6)
Si(1)-C(8)-H(2)	111(4)
Si(1)-C(8)-H(25)	107(5)
H(2)-C(8)-H(25)	122(7)
Si(1)-C(8)-H(32)	110(5)
H(2)-C(8)-H(32)	105(7)
H(25)-C(8)-H(32)	102(7)
C(10)-C(9)-C(12)	109.7(6)
C(10)-C(9)-C(11)	109.6(6)
C(12)-C(9)-C(11)	108.3(6)
C(10)-C(9)-Si(1)	110.4(5)
C(12)-C(9)-Si(1)	109.3(4)
C(11)-C(9)-Si(1)	109.6(4)
C(9)-C(10)-H(11)	119(4)
C(9)-C(10)-H(13)	112(4)
H(11)-C(10)-H(13)	92(5)
C(9)-C(10)-H(21)	105(4)
H(11)-C(10)-H(21)	113(6)

H(13)-C(10)-H(21)	115(6)
C(9)-C(11)-H(9)	110(4)
C(9)-C(11)-H(10)	106(3)
H(9)-C(11)-H(10)	118(5)
C(9)-C(11)-H(24)	117(5)
H(9)-C(11)-H(24)	98(6)
H(10)-C(11)-H(24)	109(6)
C(9)-C(12)-H(8)	109(4)
C(9)-C(12)-H(18)	116(5)
H(8)-C(12)-H(18)	116(6)
C(9)-C(12)-H(20)	117(5)
H(8)-C(12)-H(20)	93(6)
H(18)-C(12)-H(20)	103(6)
F(1S)-C(1S)-C(2S)	117.7(5)
F(1S)-C(1S)-C(5S)#1	121.5(5)
C(2S)-C(1S)-C(5S)#1	120.8(6)
F(2S)-C(2S)-C(3S)	120.6(6)
F(2S)-C(2S)-C(1S)	119.6(6)
C(3S)-C(2S)-C(1S)	119.7(6)
C(4S)-C(3S)-F(3S)	119.5(6)
C(4S)-C(3S)-C(2S)	122.2(6)
F(3S)-C(3S)-C(2S)	118.3(6)
C(3S)-C(4S)-F(4S)	120.2(5)
C(3S)-C(4S)-C(5S)	120.4(6)
F(4S)-C(4S)-C(5S)	119.4(6)
C(1S)#1-C(5S)-C(5S)#1	118.8(6)
C(1S)#1-C(5S)-C(4S)	123.1(5)
C(5S)#1-C(5S)-C(4S)	118.1(7)

---

Symmetry transformations used to generate equivalent atoms:

#1 -x,-y+1,-z+1

Table 4. Anisotropic displacement parameters ( $\text{\AA}^2 \times 10^3$ ) for liu80. The anisotropic displacement factor exponent takes the form:  $-2p^2 [ h^2 a^{*2} U^{11} + \dots + 2 h k a^{*} b^{*} U^{12} ]$

	U11	U22	U33	U23	U13	U12
Si(1)	32(1)	33(1)	18(1)	-1(1)	11(1)	11(1)
N(1)	36(3)	29(3)	22(3)	-6(2)	5(2)	11(2)
N(2)	21(2)	39(3)	18(3)	-1(2)	11(2)	13(2)
B(1)	29(4)	32(4)	14(3)	-6(3)	6(3)	11(3)
C(1)	60(5)	28(4)	23(4)	-3(3)	1(3)	9(4)
C(2)	89(7)	32(4)	19(4)	0(3)	1(4)	6(4)
C(3)	52(5)	39(4)	22(4)	-2(3)	17(3)	3(4)
C(4)	31(4)	44(4)	20(3)	-6(3)	10(3)	17(3)
C(5)	33(4)	44(4)	23(4)	-14(3)	6(3)	18(4)
C(6)	30(4)	35(4)	26(4)	-4(3)	17(3)	6(3)
C(7)	55(5)	53(5)	17(4)	1(3)	12(3)	14(4)
C(8)	43(4)	53(5)	31(4)	5(4)	10(4)	21(4)
C(9)	48(4)	32(3)	18(3)	-1(3)	13(3)	16(3)
C(10)	79(7)	36(4)	41(5)	-3(4)	11(5)	19(4)
C(11)	59(5)	59(5)	21(4)	-5(4)	14(4)	20(4)
C(12)	47(5)	58(5)	28(4)	-9(4)	9(4)	10(4)
C(1S)	35(4)	25(3)	26(4)	-5(3)	3(3)	12(3)
C(2S)	35(4)	29(3)	24(3)	5(3)	4(3)	3(3)
C(3S)	27(3)	38(4)	31(4)	0(3)	13(3)	6(3)
C(4S)	25(3)	38(4)	33(4)	-6(3)	12(3)	14(3)
C(5S)	26(3)	30(3)	18(3)	-5(3)	3(3)	7(2)
F(1S)	56(3)	53(2)	61(3)	12(2)	25(2)	26(2)
F(2S)	61(3)	44(2)	48(2)	10(2)	25(2)	10(2)
F(3S)	42(2)	59(2)	38(2)	0(2)	29(2)	7(2)
F(4S)	39(2)	51(2)	39(2)	-7(2)	19(2)	18(2)

Table 5. Hydrogen coordinates ( $\times 10^4$ ) and isotropic displacement parameters ( $\text{\AA}^2 \times 10^3$ ) for liu80.

	x	y	z	U(eq)
H(1)	-1250(90)	7770(60)	8390(50)	36(18)
H(2)	-830(110)	10540(80)	6740(70)	90(30)
H(3)	4760(80)	6520(50)	7310(40)	20(16)
H(4)	4790(80)	8530(50)	6730(40)	21(14)
H(6)	2620(120)	4890(80)	8260(70)	90(30)
H(8)	6150(100)	10630(70)	8920(60)	70(20)
H(9)	3160(100)	10080(70)	9600(60)	70(20)
H(10)	1660(90)	11100(50)	9470(40)	26(16)
H(11)	3840(110)	13010(70)	7790(70)	90(30)
H(13)	2040(120)	12600(70)	8320(60)	80(30)
H(15)	220(80)	4770(50)	8930(40)	14(16)
H(16)	4380(100)	10220(60)	6100(50)	50(20)
H(17)	2930(120)	11170(90)	5900(70)	110(30)
H(18)	6550(90)	11700(60)	8280(60)	40(20)
H(19)	-1980(100)	6000(60)	8990(60)	60(20)
H(20)	6940(120)	12100(80)	9440(70)	90(30)
H(21)	4300(90)	13270(60)	9150(50)	41(19)
H(24)	3850(110)	11590(80)	10270(70)	90(30)
H(25)	-900(100)	9640(70)	7560(60)	60(30)
H(29)	2390(100)	9660(70)	5330(60)	60(20)
H(32)	-1440(150)	8900(100)	6420(90)	140(40)

Table 6. Torsion angles [°] for liu80.

C(8)-Si(1)-N(2)-C(6)	150.5(5)
C(7)-Si(1)-N(2)-C(6)	31.9(5)
C(9)-Si(1)-N(2)-C(6)	-88.6(5)
C(8)-Si(1)-N(2)-B(1)	-38.8(6)
C(7)-Si(1)-N(2)-B(1)	-157.4(5)
C(9)-Si(1)-N(2)-B(1)	82.1(5)
C(1)-N(1)-B(1)-N(2)	179.5(5)
C(5)-N(1)-B(1)-N(2)	-0.3(6)
C(1)-N(1)-B(1)-C(4)	-0.6(8)
C(5)-N(1)-B(1)-C(4)	179.6(5)
C(6)-N(2)-B(1)-N(1)	0.2(6)
Si(1)-N(2)-B(1)-N(1)	-171.9(4)
C(6)-N(2)-B(1)-C(4)	-179.7(7)
Si(1)-N(2)-B(1)-C(4)	8.3(10)
C(5)-N(1)-C(1)-C(2)	-178.2(6)
B(1)-N(1)-C(1)-C(2)	2.0(9)
N(1)-C(1)-C(2)-C(3)	-2.3(9)
C(1)-C(2)-C(3)-C(4)	1.2(10)
C(2)-C(3)-C(4)-B(1)	0.3(9)
N(1)-B(1)-C(4)-C(3)	-0.6(8)
N(2)-B(1)-C(4)-C(3)	179.2(7)
C(1)-N(1)-C(5)-C(6)	-179.5(5)
B(1)-N(1)-C(5)-C(6)	0.3(7)
N(1)-C(5)-C(6)-N(2)	-0.2(7)
B(1)-N(2)-C(6)-C(5)	0.0(7)
Si(1)-N(2)-C(6)-C(5)	172.9(4)
N(2)-Si(1)-C(9)-C(10)	-179.0(5)
C(8)-Si(1)-C(9)-C(10)	-59.6(6)
C(7)-Si(1)-C(9)-C(10)	61.2(6)
N(2)-Si(1)-C(9)-C(12)	60.3(6)
C(8)-Si(1)-C(9)-C(12)	179.7(6)
C(7)-Si(1)-C(9)-C(12)	-59.5(6)
N(2)-Si(1)-C(9)-C(11)	-58.2(5)
C(8)-Si(1)-C(9)-C(11)	61.2(6)

C(7)-Si(1)-C(9)-C(11)	-178.0(5)
F(1S)-C(1S)-C(2S)-F(2S)	-0.5(8)
C(5S)#1-C(1S)-C(2S)-F(2S)	178.7(5)
F(1S)-C(1S)-C(2S)-C(3S)	-177.9(5)
C(5S)#1-C(1S)-C(2S)-C(3S)	1.3(8)
F(2S)-C(2S)-C(3S)-C(4S)	-176.3(5)
C(1S)-C(2S)-C(3S)-C(4S)	1.0(9)
F(2S)-C(2S)-C(3S)-F(3S)	2.9(8)
C(1S)-C(2S)-C(3S)-F(3S)	-179.8(5)
F(3S)-C(3S)-C(4S)-F(4S)	0.6(8)
C(2S)-C(3S)-C(4S)-F(4S)	179.8(5)
F(3S)-C(3S)-C(4S)-C(5S)	177.8(5)
C(2S)-C(3S)-C(4S)-C(5S)	-3.0(9)
C(3S)-C(4S)-C(5S)-C(1S)#1	-177.8(6)
F(4S)-C(4S)-C(5S)-C(1S)#1	-0.6(8)
C(3S)-C(4S)-C(5S)-C(5S)#1	2.7(9)
F(4S)-C(4S)-C(5S)-C(5S)#1	179.9(6)

---

Symmetry transformations used to generate equivalent atoms:

#1 -x,-y+1,-z+1

**Crystallographic data for 3a•Ar:** X-ray quality crystals were grown by slow vapor diffusion of pentane into a 1:1 solution of **3a** and **Ar** in CH<sub>2</sub>Cl<sub>2</sub> at room temperature.

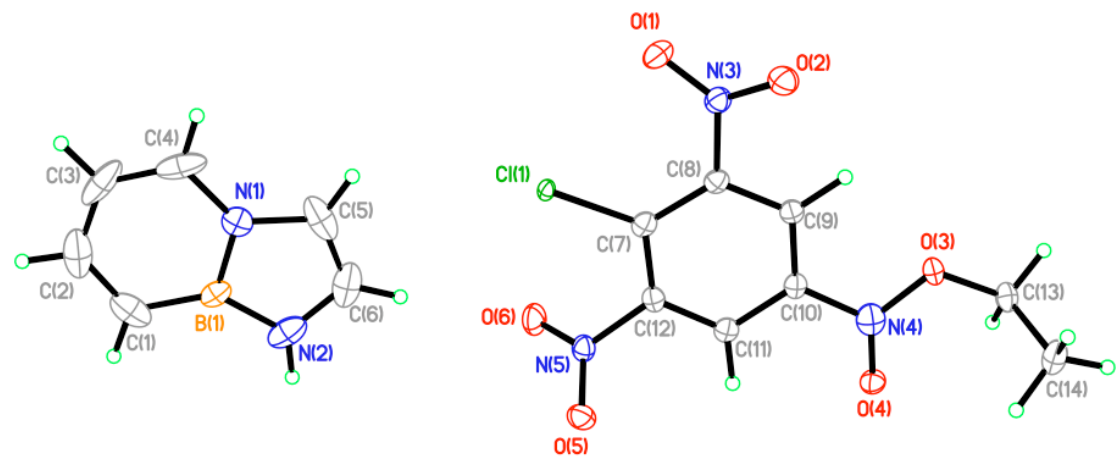


Table 1. Crystal data and structure refinement for **3a•Ar** (lirr85)

Identification code	lirr85	
Empirical formula	C14 H14 B Cl N5 O6	
Formula weight	394.56	
Temperature	110(2) K	
Wavelength	0.71073 Å	
Crystal system	Triclinic	
Space group	P-1	
Unit cell dimensions	a = 6.6731(19) Å	a = 77.830(4)°.
	b = 11.562(3) Å	b = 76.546(4)°.
	c = 11.907(3) Å	g = 80.917(4)°.
Volume	867.6(4) Å <sup>3</sup>	
Z	2	
Density (calculated)	1.510 Mg/m <sup>3</sup>	
Absorption coefficient	0.264 mm <sup>-1</sup>	
F(000)	406	
Crystal size	0.23 x 0.12 x 0.05 mm <sup>3</sup>	
Theta range for data collection	1.79 to 25.00°.	
Index ranges	-7<=h<=7, -13<=k<=13, -14<=l<=14	
Reflections collected	8243	
Independent reflections	3051 [R(int) = 0.0268]	
Completeness to theta = 25.00°	99.7 %	
Absorption correction	Semi-empirical from equivalents	
Max. and min. transmission	0.9869 and 0.9417	
Refinement method	Full-matrix least-squares on F <sup>2</sup>	
Data / restraints / parameters	3051 / 0 / 272	
Goodness-of-fit on F <sup>2</sup>	1.080	
Final R indices [I>2sigma(I)]	R1 = 0.0634, wR2 = 0.1731	
R indices (all data)	R1 = 0.0777, wR2 = 0.1850	
Largest diff. peak and hole	0.980 and -0.644 e.Å <sup>-3</sup>	

Table 2. Atomic coordinates ( $\times 10^4$ ) and equivalent isotropic displacement parameters ( $\text{\AA}^2 \times 10^3$ ) for lirr85. U(eq) is defined as one third of the trace of the orthogonalized  $U^{ij}$  tensor.

	x	y	z	U(eq)
Cl(1)	1808(1)	8448(1)	104(1)	19(1)
O(1)	3251(5)	5981(3)	207(3)	43(1)
O(2)	2485(5)	5114(3)	-1054(3)	41(1)
O(3)	4974(4)	6646(2)	-5125(3)	31(1)
O(4)	4581(5)	8638(3)	-5773(2)	31(1)
O(5)	905(5)	11017(3)	-2509(3)	37(1)
O(6)	3325(5)	10719(3)	-1507(3)	43(1)
N(1)	1702(5)	11769(4)	2779(4)	39(1)
N(2)	2096(6)	13022(5)	1032(4)	55(1)
N(3)	2933(5)	5986(3)	-761(3)	31(1)
N(4)	4480(6)	7780(4)	-4980(4)	42(1)
N(5)	2288(5)	10389(3)	-2078(3)	31(1)
B(1)	1536(7)	12998(5)	2259(4)	34(1)
C(1)	868(8)	13891(5)	3048(7)	59(2)
C(2)	484(8)	13446(8)	4220(7)	73(2)
C(3)	679(8)	12226(10)	4666(5)	78(3)
C(4)	1276(8)	11392(6)	3969(6)	64(2)
C(5)	2365(7)	11094(5)	1883(7)	61(2)
C(6)	2605(8)	11868(7)	865(6)	62(2)
C(7)	2656(6)	8203(4)	-1352(4)	28(1)
C(8)	3113(6)	7074(4)	-1654(4)	26(1)
C(9)	3696(6)	6908(4)	-2816(4)	26(1)
C(10)	3819(6)	7886(4)	-3719(3)	25(1)
C(11)	3316(6)	9026(4)	-3458(4)	27(1)
C(12)	2777(6)	9160(4)	-2297(4)	26(1)
C(13)	5790(7)	6468(4)	-6335(4)	35(1)
C(14)	4081(8)	6530(5)	-6972(5)	46(1)

Table 3. Bond lengths [ $\text{\AA}$ ] and angles [ $^\circ$ ] for lirr85.

Cl(1)-C(7)	1.763(4)
O(1)-N(3)	1.218(5)
O(2)-N(3)	1.233(5)
O(3)-N(4)	1.337(5)
O(3)-C(13)	1.463(5)
O(4)-N(4)	1.215(5)
O(5)-N(5)	1.223(5)
O(6)-N(5)	1.224(5)
N(1)-C(4)	1.367(7)
N(1)-C(5)	1.402(7)
N(1)-B(1)	1.423(7)
N(2)-C(6)	1.369(8)
N(2)-B(1)	1.417(7)
N(2)-H(2B)	0.8800
N(3)-C(8)	1.468(5)
N(4)-C(10)	1.490(6)
N(5)-C(12)	1.471(5)
B(1)-C(1)	1.487(8)
C(1)-C(2)	1.361(10)
C(1)-H(1A)	0.9500
C(2)-C(3)	1.395(11)
C(2)-H(2A)	0.9500
C(3)-C(4)	1.357(10)
C(3)-H(3A)	0.9500
C(4)-H(4A)	0.9500
C(5)-C(6)	1.339(9)
C(5)-H(5A)	0.9500
C(6)-H(6A)	0.9500
C(7)-C(8)	1.395(6)
C(7)-C(12)	1.399(6)
C(8)-C(9)	1.392(6)
C(9)-C(10)	1.384(6)
C(9)-H(9)	1.04(5)
C(10)-C(11)	1.390(6)

C(11)-C(12)	1.380(6)
C(11)-H(11)	1.01(5)
C(13)-C(14)	1.494(7)
C(13)-H(13B)	1.01(5)
C(13)-H(13A)	1.03(6)
C(14)-H(14C)	1.10(6)
C(14)-H(14B)	1.04(6)
C(14)-H(14A)	1.00(6)
N(4)-O(3)-C(13)	115.7(3)
C(4)-N(1)-C(5)	129.2(6)
C(4)-N(1)-B(1)	122.1(5)
C(5)-N(1)-B(1)	108.7(5)
C(6)-N(2)-B(1)	107.4(5)
C(6)-N(2)-H(2B)	126.3
B(1)-N(2)-H(2B)	126.3
O(1)-N(3)-O(2)	123.8(4)
O(1)-N(3)-C(8)	119.5(4)
O(2)-N(3)-C(8)	116.7(3)
O(4)-N(4)-O(3)	124.9(4)
O(4)-N(4)-C(10)	122.9(4)
O(3)-N(4)-C(10)	112.2(4)
O(6)-N(5)-O(5)	124.7(4)
O(6)-N(5)-C(12)	118.0(3)
O(5)-N(5)-C(12)	117.3(3)
N(2)-B(1)-N(1)	105.2(5)
N(2)-B(1)-C(1)	136.6(5)
N(1)-B(1)-C(1)	118.3(5)
C(2)-C(1)-B(1)	116.1(5)
C(2)-C(1)-H(1A)	122.0
B(1)-C(1)-H(1A)	122.0
C(1)-C(2)-C(3)	122.4(6)
C(1)-C(2)-H(2A)	118.8
C(3)-C(2)-H(2A)	118.8
C(4)-C(3)-C(2)	122.8(6)
C(4)-C(3)-H(3A)	118.6

C(2)-C(3)-H(3A)	118.6
C(3)-C(4)-N(1)	118.3(6)
C(3)-C(4)-H(4A)	120.9
N(1)-C(4)-H(4A)	120.9
C(6)-C(5)-N(1)	106.7(5)
C(6)-C(5)-H(5A)	126.6
N(1)-C(5)-H(5A)	126.6
C(5)-C(6)-N(2)	111.9(5)
C(5)-C(6)-H(6A)	124.0
N(2)-C(6)-H(6A)	124.0
C(8)-C(7)-C(12)	115.4(4)
C(8)-C(7)-Cl(1)	123.7(3)
C(12)-C(7)-Cl(1)	120.7(3)
C(9)-C(8)-C(7)	122.4(4)
C(9)-C(8)-N(3)	115.9(4)
C(7)-C(8)-N(3)	121.6(4)
C(10)-C(9)-C(8)	119.8(4)
C(10)-C(9)-H(9)	121(3)
C(8)-C(9)-H(9)	119(3)
C(9)-C(10)-C(11)	119.6(4)
C(9)-C(10)-N(4)	122.9(4)
C(11)-C(10)-N(4)	117.5(4)
C(12)-C(11)-C(10)	119.0(4)
C(12)-C(11)-H(11)	124(3)
C(10)-C(11)-H(11)	117(3)
C(11)-C(12)-C(7)	123.6(4)
C(11)-C(12)-N(5)	116.4(4)
C(7)-C(12)-N(5)	120.0(4)
O(3)-C(13)-C(14)	111.4(4)
O(3)-C(13)-H(13B)	109(3)
C(14)-C(13)-H(13B)	105(3)
O(3)-C(13)-H(13A)	111(3)
C(14)-C(13)-H(13A)	108(3)
H(13B)-C(13)-H(13A)	113(4)
C(13)-C(14)-H(14C)	109(3)
C(13)-C(14)-H(14B)	106(3)

H(14C)-C(14)-H(14B)	116(4)
C(13)-C(14)-H(14A)	111(3)
H(14C)-C(14)-H(14A)	102(4)
H(14B)-C(14)-H(14A)	111(5)

---

Symmetry transformations used to generate equivalent atoms:

Table 4. Anisotropic displacement parameters ( $\text{\AA}^2 \times 10^3$ ) for lirr85. The anisotropic displacement factor exponent takes the form:  $-2p^2 [ h^2 a^{*2} U^{11} + \dots + 2 h k a^{*} b^{*} U^{12} ]$

	U11	U22	U33	U23	U13	U12
Cl(1)	14(1)	26(1)	16(1)	-9(1)	-4(1)	4(1)
O(1)	53(2)	49(2)	27(2)	-3(1)	-13(2)	-2(2)
O(2)	48(2)	34(2)	42(2)	-4(1)	-14(2)	-7(1)
O(3)	33(2)	28(2)	33(2)	-13(1)	-5(1)	-2(1)
O(4)	36(2)	29(2)	26(2)	0(1)	-4(1)	-8(1)
O(5)	33(2)	35(2)	39(2)	-6(1)	-8(1)	4(1)
O(6)	46(2)	45(2)	46(2)	-22(2)	-15(2)	-5(2)
N(1)	23(2)	46(2)	49(2)	-8(2)	-10(2)	-6(2)
N(2)	34(2)	89(4)	41(3)	6(2)	-13(2)	-18(2)
N(3)	30(2)	35(2)	29(2)	-6(2)	-7(2)	-1(2)
N(4)	31(2)	49(3)	49(2)	-15(2)	-8(2)	-6(2)
N(5)	28(2)	34(2)	29(2)	-11(2)	-3(2)	-2(2)
B(1)	18(2)	53(3)	33(3)	0(2)	-10(2)	-10(2)
C(1)	31(3)	43(3)	111(6)	-19(3)	-29(3)	-3(2)
C(2)	31(3)	123(6)	88(5)	-71(5)	-18(3)	3(3)
C(3)	26(3)	182(9)	28(3)	-12(4)	-7(2)	-17(4)
C(4)	27(3)	89(5)	65(4)	36(4)	-23(3)	-18(3)
C(5)	20(2)	60(4)	119(6)	-53(4)	-15(3)	-2(2)
C(6)	29(3)	111(6)	60(4)	-44(4)	-4(3)	-15(3)
C(7)	18(2)	37(2)	28(2)	-8(2)	-7(2)	-2(2)
C(8)	20(2)	32(2)	28(2)	-5(2)	-8(2)	-2(2)
C(9)	20(2)	30(2)	32(2)	-8(2)	-9(2)	-1(2)
C(10)	17(2)	32(2)	29(2)	-9(2)	-5(2)	-4(2)
C(11)	18(2)	33(2)	31(2)	-7(2)	-6(2)	-3(2)
C(12)	20(2)	29(2)	32(2)	-10(2)	-5(2)	-2(2)
C(13)	37(2)	37(3)	32(2)	-15(2)	-1(2)	-3(2)
C(14)	45(3)	59(3)	40(3)	-22(3)	-11(2)	-7(3)

Table 5. Hydrogen coordinates ( $\times 10^4$ ) and isotropic displacement parameters ( $\text{\AA}^2 \times 10^3$ ) for lirr85.

	x	y	z	U(eq)
H(2B)	2113	13662	479	66
H(1A)	718	14722	2750	71
H(2A)	67	13986	4754	88
H(3A)	382	11969	5494	94
H(4A)	1395	10568	4298	77
H(5A)	2599	10250	1979	73
H(6A)	3073	11643	116	75
H(9)	4020(70)	6040(40)	-3000(40)	38(13)
H(11)	3320(80)	9710(50)	-4140(50)	47(14)
H(13B)	6510(70)	5630(40)	-6320(40)	35(12)
H(13A)	6740(90)	7110(50)	-6780(50)	67(18)
H(14C)	3150(90)	7400(50)	-6980(50)	54(15)
H(14B)	4780(90)	6310(50)	-7780(50)	66(17)
H(14A)	3040(100)	5980(50)	-6520(50)	65(18)

Table 6. Torsion angles [°] for lirr85.

C(13)-O(3)-N(4)-O(4)	3.3(6)
C(13)-O(3)-N(4)-C(10)	-175.6(3)
C(6)-N(2)-B(1)-N(1)	-1.5(5)
C(6)-N(2)-B(1)-C(1)	178.8(5)
C(4)-N(1)-B(1)-N(2)	180.0(4)
C(5)-N(1)-B(1)-N(2)	0.7(5)
C(4)-N(1)-B(1)-C(1)	-0.2(6)
C(5)-N(1)-B(1)-C(1)	-179.5(4)
N(2)-B(1)-C(1)-C(2)	-179.8(5)
N(1)-B(1)-C(1)-C(2)	0.6(6)
B(1)-C(1)-C(2)-C(3)	-0.6(8)
C(1)-C(2)-C(3)-C(4)	0.4(9)
C(2)-C(3)-C(4)-N(1)	0.0(8)
C(5)-N(1)-C(4)-C(3)	179.0(4)
B(1)-N(1)-C(4)-C(3)	-0.1(7)
C(4)-N(1)-C(5)-C(6)	-178.9(4)
B(1)-N(1)-C(5)-C(6)	0.3(5)
N(1)-C(5)-C(6)-N(2)	-1.3(6)
B(1)-N(2)-C(6)-C(5)	1.8(6)
C(12)-C(7)-C(8)-C(9)	1.4(6)
Cl(1)-C(7)-C(8)-C(9)	177.2(3)
C(12)-C(7)-C(8)-N(3)	-176.4(3)
Cl(1)-C(7)-C(8)-N(3)	-0.5(5)
O(1)-N(3)-C(8)-C(9)	151.0(4)
O(2)-N(3)-C(8)-C(9)	-28.1(5)
O(1)-N(3)-C(8)-C(7)	-31.1(6)
O(2)-N(3)-C(8)-C(7)	149.8(4)
C(7)-C(8)-C(9)-C(10)	-0.6(6)
N(3)-C(8)-C(9)-C(10)	177.3(3)
C(8)-C(9)-C(10)-C(11)	-1.4(6)
C(8)-C(9)-C(10)-N(4)	178.5(3)
O(4)-N(4)-C(10)-C(9)	179.7(4)
O(3)-N(4)-C(10)-C(9)	-1.4(5)
O(4)-N(4)-C(10)-C(11)	-0.4(6)

O(3)-N(4)-C(10)-C(11)	178.4(3)
C(9)-C(10)-C(11)-C(12)	2.4(6)
N(4)-C(10)-C(11)-C(12)	-177.4(3)
C(10)-C(11)-C(12)-C(7)	-1.6(6)
C(10)-C(11)-C(12)-N(5)	179.2(3)
C(8)-C(7)-C(12)-C(11)	-0.3(6)
Cl(1)-C(7)-C(12)-C(11)	-176.3(3)
C(8)-C(7)-C(12)-N(5)	178.9(3)
Cl(1)-C(7)-C(12)-N(5)	2.9(5)
O(6)-N(5)-C(12)-C(11)	-121.2(4)
O(5)-N(5)-C(12)-C(11)	57.0(5)
O(6)-N(5)-C(12)-C(7)	59.6(5)
O(5)-N(5)-C(12)-C(7)	-122.2(4)
N(4)-O(3)-C(13)-C(14)	-82.4(5)

---

Symmetry transformations used to generate equivalent atoms:

Table 7. Hydrogen bonds for lirr85 [Å and °].

D-H...A	d(D-H)	d(H...A)	d(D...A)	<(DHA)
N(2)-H(2B)...O(2)#1	0.88	2.20	3.075(6)	172.1

Symmetry transformations used to generate equivalent atoms:

#1 x,y+1,z

## REFERENCES CITED

### Chapter I

- (1) For a recent review surveying all BN arenes, see: Bosdet, M. J. D.; Piers, W. E. *Can. J. Chem.* **2009**, *87*, 8-29.
- (2) Marwitz, A. J. V. *Doctoral Thesis*, **2010**, University of Oregon.
- (3) Ulmschneider, D.; Goubeau, J. *Chem. Ber.* **1957**, *90*, 2733-2738.
- (4) Abbey, E.R.; Zakharov, L. N.; Liu, S. -Y. *J. Am. Chem. Soc.* **2010**, *132*, 16340-16342.
- (5) Cacchi, S.; Fabrizi, G. *Chem. Rev.* **2005**, *105*, 2873-2920.
- (6) Dewar, M. J. S.; Kubba, V., P.; Pettit, R. *J. Chem. Soc.* **1958**, 3076-3079.
- (7) Soloway, A. H.; Nyalis, E. *J. Am. Chem. Soc.* **1959**, *81*, 2681-2683.
- (8) Letsinger, R. L.; Hamilton, S. B. *J. Am. Chem. Soc.* **1959**, *81*, 3009-3012.
- (9) Letsinger, R. L.; Nazy, J. R. *J. Am. Chem. Soc.* **1959**, *81*, 3013-3017.
- (10) Hawthorne, M. F. *J. Am. Chem. Soc.* **1961**, *83*, 831-833.
- (11) Goubeau, J.; Snyder, H. *Liebigs Ann. Chem.* **1964**, *675*, 1-9.
- (12) Weber, L.; Wartig, H. B.; Stammler, H. -G.; Neumann, B. *Z. Anorg. Allg. Chem.* **2001**, *627*, 2663-2668.
- (13) Braun, U.; Habereder, T.; Noth, H.; Piotrowski, H.; Warchold, H. *Eur. J. Inorg. Chem.* **2002**, 1132-1145.
- (14) Clark, G. R.; Irvine, J.; Roper, W. R.; Wright, J. *J. Organomet. Chem.* **2003**, *12*, 2245.
- (15) Habereder, T.; Noth, H. *Appl. Organometal. Chem.* **2003**, *17*, 525.
- (16) Weber, L.; Wartig, H. B.; Stammler, H. -G.; Neumann, B. *Organometallics*, **2001**, 5248.
- (17) Segawa, Y.; Suzuki, Y. Yamashita, M.; Nozaki, K. *J. Am. Chem. Soc.* **2008**, *130*, 16069-16079.

- (18) Hadebe, S. W.; Robinson, R. S. *Eur. J. Org. Chem.* **2006**, 4898-4904.
- (19) Suginome, M.; Yamamoto, A.; Murakami, M. *Angew. Chem. Int. Ed.* **2005**, *44*, 2380-2382.
- (20) Daini, M.; Suginome, M. *Chem. Commun.* **2008**, 5224-5226.
- (21) Segawa, Y.; Yamashita, M.; Nozaki, K. *J. Am. Chem. Soc.* **2009**, *131*, 9201-9203.
- (22) Weber, L.; Werner, V.; Fox, M. A.; Marder, T. B.; Scwedler, S.; Brockhinke, A.; Stammler, H. -G.; Neumann, B. *Dalton Trans.* **2009**, 1339-1351.
- (23) Weber, L.; Werner, V.; Fox, M. A.; Marder, T. B.; Scwedler, S.; Brockhinke, A.; Stammler, H. -G.; Neumann, B. *Dalton Trans.* **2009**, 2823-2831.
- (24) Maruyama, S.; Kawanishi, Y. *J. Mater. Chem.* **2002**, *12*, 2245-2249.
- (25) Kubo, Y.; Tsuruzoe, K; Okuyama, S.; Nishiyabu, R.; Fujihara, T. *Chem. Commun.* **2010**, *46*, 3604-3606.

## Chapter II

- (1) Schleyer, P. v. R.; Jiao, H. *Pure Appl. Chem.* **1996**, *68*, 209-218.
- (2) Schleyer, P. v. R. *Chem. Rev.* **2001**, *101*, 1115-1117.
- (3) Astruc, D. In *Modern Arene Chemistry*, Astruc, D., Ed.; Wiley-VCH: Weinheim, 2002; pp 1-19.
- (4) *Carbon-Rich Compounds*; Haley, M. M, Tykwincky, R. R., Eds.; Wiley-VCH: Weinheim, 2006.
- (5) Liu, Z.; Marder, T. B. *Angew. Chem. Int. Ed.* **2008**, *47*, 242-244.
- (6) Dewar, M. J. S.; Marr, P. A. *J. Am. Chem. Soc.* **1962**, *84*, 3782-3783.
- (7) Davies, K. M.; Dewar, M. J. S.; Rona, P. *J. Am. Chem. Soc.* **1967**, *89*, 6294-6297.
- (8) White, D. G. *J. Am. Chem. Soc.* **1963**, *85*, 3634-3636.
- (9) For a review, see: Fritsch, A. J. *Chem. Heterocycl. Compd.* **1977**, *30*, 381- 440.
- (10) For pioneering contributions, see: (a) Ashe, A. J., III; Fang, C. *Org. Lett.* **2000**, *2*, 2089-2091. (b) Ashe, A. J., III; Fang, X.; Fang, X.; Kampf, J. W. *Organometallics* **2001**, *20*, 5413-5418.

- (11) Ashe, A. J., III; Yang, H.; Fang, X.; Kampf, J. W. *Organometallics* **2002**, *21*, 4578-4580.
- (12) Pan, J.; Kampf, J. W.; Ashe, A. J., III. *Organometallics* **2004**, *23*, 5626-5629.
- (13) Pan, J.; Kampf, J. W.; Ashe, A. J., III. *Organometallics* **2006**, *25*, 197-202.
- (14) Fang, X.; Yang, H.; Kampf, J. W.; Holl, M. M. B.; Ashe, A. J., III. *Organometallics* **2006**, *25*, 513-518.
- (15) Pan, J.; Wang, J.; Holl, M. M. B.; Kampf, J. W.; Ashe, A. J., III. *Organometallics* **2006**, *25*, 3463-3467.
- (16) Pan, J.; Kampf, J. W.; Ashe, A. J., III. *Org. Lett.* **2007**, *9*, 679-681.
- (17) Pan, J.; Kampf, J. W.; Ashe, A. J., III. *Organometallics* **2008**, *27*, 1345-1347.
- (18) Emslie, D. J. H.; Piers, W. E.; Parvez, M. *Angew. Chem. Int. Ed.* **2003**, *42*, 1252-1255.
- (19) Ghesner, I.; Piers, W. E.; Parvez, M.; McDonald, R. *Organometallics* **2004**, *23*, 3085-3087.
- (20) Jaska, C. A.; Emslie, D. J. H.; Bosdet, M. J. D.; Piers, W. E.; Sorensen, T. S.; Parvez, M. *J. Am. Chem. Soc.* **2006**, *128*, 10885-10896.
- (21) Bosdet, M. J. D.; Jaska, C. A.; Piers, W. E.; Sorensen, T. S.; Parvez, M. *Org. Lett.* **2007**, *9*, 1395-1398.
- (22) Bosdet, M. J. D.; Piers, W. E.; Sorensen, T. S.; Parvez, M. *Angew. Chem. Int. Ed.* **2007**, *46*, 4940-4943.
- (23) Jaska, C. A.; Piers, W. E.; McDonald, R.; Parvez, M. *J. Org. Chem.* **2007**, *72*, 5234-5243.
- (24) Paetzold, P.; Stanescu, C.; Stubenrauch, J. R.; Bienmüller, M.; Englert, U. Z. *Anorg. Allg. Chem.* **2004**, *630*, 2632-2640.
- (25) Marwitz, A. J. V.; Abbey, E. R.; Jenkins, J. T.; Zakharov, L. N.; Liu, S.-Y. *Org. Lett.* **2007**, *9*, 4905-4908.
- (26) Massey, S. T.; Zoellner, R. W. *Int. J. Quantum Chem.* **1991**, *39*, 784-804.
- (27) Doerksen, R. J.; Thakkar, A. J. *J. Phys. Chem. A* **1998**, *102*, 4679-4686.

- (28) Kranz, M.; Clark, T. *J. Org. Chem.* **1992**, *57*, 5492-5500.
- (29) Fazen, P. J.; Burke, L. A. *Inorg. Chem.* **2006**, *45*, 2494-2500.
- (30) Krygowski, T. M.; Cyranski, M. K. *Chem. Rev.* **2001**, *101*, 1385-1419.
- (31) Katritzky, A. R.; Jug, K.; Oniciu, D. C. *Chem. Rev.* **2001**, *101*, 1421-1449.
- (32) Based on a search of the Cambridge Crystallographic Database (Version 2007).
- (33) Brown, R. C. D.; Satcharoen, V. *Heterocycles* **2006**, *70*, 705-736.
- (34) Krompiec, S.; Pigulla, M.; Krompiec, M.; Baj, S.; Mrowiec-Bialon, J.; Kasperczyk, J. *Tetrahedron Lett.* **2004**, *45*, 5257-5261.
- (35) Hiraki, K.; Matasunaga, T.; Kawano, H. *Organometallics* **1994**, *13*, 1878-1885.
- (36) Stille, J. K.; Becker, Y. *J. Org. Chem.* **1980**, *45*, 2139-2145.
- (37) Allen, F. H.; Kennard, O.; Watson, D. G.; Brammer, L.; Orpen, A. G.; Taylor, R. *J. Chem. Soc., Perkin Trans. 2* **1987**, S1-S17.
- (38) Based on a search of the Cambridge Crystallographic Database (Version 2007). For example, see: von Essen, R.; Frank, D.; Sünnemann, H. W.; Vidovic, D.; Magull, J.; de Meijere, A. *Chem. Eur. J.* **2005**, *11*, 6583-6592.
- (39) Based on a search of the Cambridge Crystallographic Database (Version 2007). For example, see: Lee, S. I.; Park, S. Y.; Park, J. H.; Jung, I. G.; Choi, S. Y.; Chung, Y. K.; Lee, B. Y. *J. Org. Chem.* **2006**, *71*, 91-96.
- (40) Ashe, A. J., III.; Kampf, J. W.; Müller, C.; Schneider, M. *Organometallics* **1996**, *15*, 387-393.
- (41) For a comparison with a diphenylamino-substituted boratabenzene, see: Hoic, D. A.; DiMare, M.; Fu, G. C. *J. Am. Chem. Soc.* **1997**, *119*, 7155-7156.

### Chapter III

- (1) Campbell, P. G.; Abbey, E. R.; Zakharov, L. N.; Grant, D. J.; Dixon, D. A.; Liu, S. -Y. *J. Am. Chem. Soc.* **2010**, *132*, 18048-18050.
- (2) Pan, J.; Kampf, J. W.; Ashe, A. J. *Org. Lett.* **2007**, *9*, 679-681.
- (3) Lamm, A. N.; Liu, S. -Y. *Angew. Chem. Int. Ed.* **2011**, accepted.

- (4) (a) Pan, J.; Kampf, J. W.; Ashe, A. J. III *Organometallics*, **2004**, *23*, 5626-5629.  
(b) Abbey, E. R.; Zakharov, L. N.; Liu, S. -Y. *J. Am. Chem. Soc.* **2008**, *130*, 7250-7252.
- (5) Taniguchi, T.; Yamaguchi, T. *Organometallics* **2010**, *29*, 5732-5735.
- (6) Campbell, P. G.; Zakharov, L. N.; Grant, D. J.; Dixon, D. A.; Liu, S. -Y. *J. Am. Chem. Soc.* **2010**, *132*, 3289-3291.
- (7) Liu, L.; Marwitz, A. J. V.; Mathews, B. W.; Liu, S. -Y. *Angew. Chem. Int. Ed.* **2009**, *48*, 6817-6819.
- (8) Marwitz, A. J.; Abbey, E. R.; Jenkins, J. T.; Zakharov, L. N.; Liu, S.-Y. *Org. Lett.* **2007**, *9*, 4905-4908.
- (9) (a) Dewar, M. J. S.; Marr, P. A. *J. Am. Chem. Soc.* **1962**, *84*, 3782-3783.  
(b) Culling, G. C.; Dewar, M. J. S.; Marr, P. A. *J. Am. Chem. Soc.* **1964**, *86*, 1125-1127.
- (10) White, D. G.; *J. Am. Chem. Soc.* **1963**, *85*, 3634-3636.
- (11)(a) Ashe, A. J. III; Fang, X.; Fang, X.; Kampf, J. W. *Organometallics* **2001**, *20*, 5413-5418. (b) Ashe, A. J. III; Fang, X. *Org. Lett.* **2000**, *2*, 2089-2091.
- (12)(a) Bosdet, M. J. D.; Jaska, C. A.; Piers, W. E.; Sorensen, T. S.; Parvez, M. *Org. Lett.* **2007**, *9*, 1395-1398. (b) Bosdet, M. J. D.; Piers, W. E.; Sorensen, T. S.; Parvez, M. *Angew. Chem., Int. Ed.* **2007**, *46*, 4940- 4943.
- (13)(a) Marwitz, A. J. V.; Jenkins, J. T.; Zakharov, L. N.; Liu, S. -Y. *Angew. Chem. Int. Ed.* **2010**, *49*, 7444-7447. (b) Marwitz, A. J. V.; Jenkins, J. T.; Zakharov, L. N.; Liu, S. -Y. *Organometallics*, **2011**, *30*, 52-54. (c) Marwitz, A. J. V.; McClintock, S. P.; Zakharov, L. N.; Liu, S. -Y. *Chem. Commun.* **2010**, *46*, 779-781.
- (14) Pan, J.; Kampf, J. W.; Ashe, A. J. III *Organometallics*, **2006**, *23*, 5626-5629.
- (15) Marwitz, A. J. V.; Matus, M. H.; Zakharov, L. N.; Dixon, D. A.; Liu, S. -Y. *Angew. Chem. Int. Ed.* **2009**, *48*, 973-977.
- (16) The strategies of increasing atom economy, reducing derivatives such as protecting groups, and relying on catalytic methods when possible are consistent with three of the Twelve Principles of Green Chemistry" see: Anastas, P. T.; Warner, J. C.; *Green Chemistry: Theory and Practice*, Oxford University Press: New York, **1998**, pp. 30.

- (17) Chavant, P. Y.; Vaultier, M. *J. Organomet. Chem.* **1993**, *455*, 37-46.
- (18) Davies, K. M.; Dewar, M. J. S.; Rona, P. *J. Am. Chem. Soc.* **1967**, *89*, 6294-6297.
- (19) Pan, J.; Kampf, J. W.; Ashe, A. J. III *J. Organomet. Chem.* **2009**, *694*, 1036-1040.

## Chapter IV

- (1) (a) Baeyer, A. *Liebigs. Ann. Chem.* **1866**, *140*, 295-296. (b) Baeyer, A.; Emmerling, A. *Chem. Ber.* **1869**, *2*, 679-683.
- (2) For leading references, see: (a) O'Connor, S. E.; Maresh, J. J. *Nat. Prod. Rep.* **2006**, *23*, 532-547. (b) Gul, W.; Hamann, M. T. *Life Sci.* **2005**, *78*, 442-453.
- (3) (a) Cacchi, S.; Fabrizi, G. *Chem. Rev.* **2005**, *105*, 2873-2920. (b) Humphrey, G. R.; Kuethe, J. T. *Chem. Rev.* **2006**, *106*, 2875-2911.
- (4) (a) Zhou, H. B.; Nettles, K. W.; Bruning, J. B.; Kim, Y.; Joachimiak, A.; Sharma, S.; Carlson, K. E.; Stossi, F.; Katzenellenbogen, B. S.; Greene, G. L.; Katzenellenbogen, J. A. *Chem. Biol.* **2007**, *14*, 659-669. (b) Ito, H.; Yumura, K.; Saigo, K. *Org. Lett.* **2010**, *12*, 3386-3389.
- (5) Liu, L.; Marwitz, A. J. V.; Matthews, B. W.; Liu, S. -Y. *Angew. Chem. Int. Ed.* **2009**, *48*, 6817-6819.
- (6) Ashe, A. J., III; Yang, H.; Fang, X.; Kampf, J. W. *Organometallics* **2002**, *22*, 4578-4580. (b) Fang, X.; Yang, H.; Kampf, J. W.; Holl, M. M. B.; Ashe, A. J., III *Organometallics* **2006**, *25*, 513-518.
- (7) For pioneering work in this area, see: (a) Ulmschneider, D.; Goubeau, J. *Chem. Ber.* **1957**, *90*, 2733-2738. (b) Goubeau, J.; Schneider, H. *Liebigs Ann. Chem.* **1964**, *675*, 1-9.
- (8) For an overview, see: Weber, L. *Coord. Chem. Rev.* **2008**, *252*, 1-31.
- (9) For a review of tryptophan biosynthesis, see: Raboni, S.; Bettati, S.; Mozzarelli, A. *Cell. Mol. Life Sci.* **2009**, *66*, 2391-2403.
- (10) Fletcher, A. J.; Bax, M. N.; Willis, M. C. *Chem. Comm.* **2007**, *45*, 4764-4766.
- (11) Ashe, A. J., III; Fang, X. A *Org. Lett.* **2000**, *2*, 2089-2091.
- (12) Marwitz, A. J. V.; Abbey, E. R.; Jenkins, J. T.; Zakharov, L. N.; Liu, S.-Y. *Org. Lett.* **2007**, *9*, 4905-4908.

- (13) Sundberg, R. J. In *Best Synthetic Methods, Indoles*; Academic Press: San Diego, 1996; pp 1-6.
- (14) For an overview, see: (a) Bosdet, M. J. D.; Piers, W. E. *Can. J. Chem.* **2009**, *87*, 8-29. (b) Liu, Z.; Marder, T. B. *Angew. Chem. Int. Ed.* **2008**, *47*, 242-244.
- (15) Marwitz, A. J. V.; Matus, M. H.; Zakharov, L. N.; Dixon, D. A.; Liu, S.-Y. *Angew. Chem. Int. Ed. Engl.* **2009**, *48*, 973-977.
- (16) For an overview on 2,3-dihydro-1*H*-1,3,2-diazaboroles, see: Weber, L. *Coord. Chem. Rev.* **2001**, *215*, 39-77.
- (17) Pan, J.; Kampf, J. W.; Ashe, A. J., III *Org. Lett.* **2007**, *9*, 679-681.
- (18) Kumar, V; Kaur, S.; Kumar, S. *Tetrahedron Lett.* **2006**, *47*, 7001-7005.
- (19) Lane, B. S.; Brown, M.; Sames, D. *J. Am. Chem. Soc.* **2005**, *127*, 8050-8057.
- (20) Okauchi, T; Itonaga, M.; Minami, T.; Owa, T.; Kitoh, K.; Yoshino, H. *Org. Lett.* **2000**, *2*, 1485-1487.
- (21) Smith, G. F. *Adv. Heterocycl. Chem.* **1963**, *2*, 300-309.
- (22) Ishii, H.; Murakami, K.; Sakurada, E.; Hosoya, K.; Murakami, Y. *J. Chem. Soc. Perkin Trans. 1* **1988**, 2377-2385.
- (23) Abbey, E. R.; Zakharov, L. N.; Liu, S.-Y. *J. Am. Chem. Soc.* **2008**, *130*, 7250-7252.
- (24) For a representative example, see the structure published in: Evans, D. A.; Scheidt, K. A.; Fandrick, K. R.; Lam, H. W.; Wu, J. *J. Am. Chem. Soc.* **2003**, *125*, 10780-10781.
- (25) Pyykkö, P.; Atsumi, M. *Chem. Eur. J.* **2009**, *15*, 12770-12779.

## Chapter V

- (1) (a) Shih, C; Museth, A. K.; Abrahamsson, M.; Blanco-Rodriguez, A. M.; Di Bilio, A. J.; Sudhamsu, J.; Crane, B. R.; Ronayne, K. L.; Towrie, M.; Vlcek, Jr., A.; Richards, J. H.; Winkler, J. R.; Gray, H. B. *Science* **2008**, *320*, 1760-1762.
- (2) Lippitz, M.; Erker, W.; Decker, H.; van Holde, K. E.; Basche, T. *Proc. Nat. Acad. Sci. USA* **2002**, *99*, 2772-2777.

- (3) Fernstrom, J. D. *Physiol. Rev.* **1983**, *63*, 484-546.
- (4) Klein, D. C.; Berg, G. R.; Weller, J.; Glinsmann, W. *Science* **1970**, *167*, 1738-1740.
- (5) Radwanski, E. R.; Last, R. L. *Plant Cell*, **1995**, *7*, 921-934.
- (6) Humphrey, G. R.; Kuethe, J. T. *Chem. Rev.* **2005**, *106*, 2875-2911.
- (7) For pioneering work in this area, see: (a) Ulmschneider, D.; Goubeau, J. *Chem. Ber.* **1957**, *90*, 2733-2738. (b) Goubeau, J.; Schneider, H. *Liebigs Ann. Chem.* **1964**, *675*, 1-9.
- (8) For an overview, see: Weber, L. *Coord. Chem. Rev.* **2008**, *252*, 1-31.
- (9) Abbey, E.R.; Zakharov, L. N.; Liu, S. -Y. *J. Am. Chem. Soc.* **2010**, *132*, 16340-16342.
- (10) (a) Sun, H.; Greathouse, D. V.; Andersen, O., S.,; Koeppe II, R. E. *J. Biol. Chem.* **2008**, *283*, 22233-22243. (b) Chauhan, N.; Thackray, S. J.; Rafice, S. A.; Eaton, G.; Lee, M.; Efimov, I.; Basran, J.; Jenkins, P. R.; Mowat, C. G.; Chapman, S. K.; Raven, E. L. *J. Am. Chem. Soc.* **2009**, *131*, 4186-4187.
- (11) Spielvogel, B. F.; Das, M. K.; McPhail, A. T.; Onan, K. D.; Hall, I. H. *J. Am. Chem. Soc.* **1980**, *102*, 6344-6346.
- (12) Soloway, A. H.; Zhuo, J. -C.; Rong, F. -G.; Lunato, A. J.; Ives, D. H.; Barth, R. F.; Anisuzzaman, A. K. M.; Barth, C. D.; Barnum, B. A. *J. Organomet. Chem.* **1999**, *581*, 150-155.
- (13) Lamm, A. N.; Liu, S. -Y. *Mol. BioSyst.* **2009**, *5*, 1303-1305.
- (14) Roychowdhury, P; Basak, B. S. *Acta Cryst., Sect. B: Struct. Crystallogr. Cryst. Chem.* **1975**, *31*, 1559
- (15) Gartland, G. L.; Freeman, G. R.; Bugg, C. E. *Acta Cryst.* **1974**, *B30*, 1841-1849.
- (16) (a) Tourillon, G.; Garnier, F. *J. Electroanal. Chem. Interfacial Electrochem.* **1982**, *135*, 173-178. (b) Keech, P. G.; Chartrand, M. M. G.; Bunce, N. J. *J. Electroanal. Chem.* **2002**, *534*, 75-78.
- (17) For a comparison of BN and CC conjugated systems, see: Taniguchi, T.; Yamaguchi, T. *Organometallics* **2010**, *29*, 5732-5735.
- (18) For a comparison of BN pyrene to pyrene, see: Bosdet, M. J. D.; Piers, W. E.; Sorensen T. S.; Parvez, M. *Angew. Chem. Int. Ed.* **2007**, *46*, 4940-4943.

- (19) Muranaka, A.; Yasuike, S.; Liu, C.-Y.; Kurita, J.; Kakusawa, N.; Tsuchiya, T.; Okuda, M.; Kobayashi, N.; Matsumoto, Y.; Yoshida, K.; Hashizumi, D.; Uchiyama, M. *J. Phys. Chem. A*, **2009**, *113*, 464-473.
- (20) Tatischeff, I.; Klein, R. *Photochem. and Photobiol.* **1975**, *22*, 221-229.
- (21) For a review of pK<sub>a</sub> measurements in DMSO see: Bordwell, F. G. *Acc. Chem. Res.* **1988**, *21*, 456-463.

## Appendix B

- (1) J. Pan, J. W. Kampf, A. J. Ashe III *J. Organomet. Chem.* **2009**, *694*, 1036–1040.
- (2) A. N. Lamm, E. B. Garner III, D. A. Dixon, S. Y. Liu *Angew. Chem. Int. Ed. Manuscript accepted.*
- (3) A. J. Marwitz, M. H. Matus, L. N. Zakharov, D. A. Dixon, S. -Y. Liu, *Angew. Chem. Int. Ed.* **2009**, *48*, 973-977.

## Appendix D

- (1) Rhys Williams, A. T.; Winfield, S. A.; Miller, J. A. *Analyst*, **1983**, *108*, 1067-1071.
- (2) Lamm, A. N.; Liu, S. -Y. *Mol. BioSyst.* **2009**, *5*, 1303-1305.
- (3) Linsker, F.; Evans, R. L. *J. Am. Chem. Soc.* **1945**, *67*, 1581-1582.